

Chapter 19 Thermal Properties



This photograph shows a white-hot cube of a silica fiber insulation material, which, only seconds after having been removed from a hot furnace, can be held by its edges with the bare hands. Initially, the heat transfer from the surface is relatively rapid; however, the thermal conductivity of this material is so small that heat conduction from the interior [maximum temperature approximately 1250°C] is extremely slow.

This material was developed especially for the tiles that cover the Space Shuttle Orbiters and protect and insulate them during their fiery reentry into the atmosphere. Other attractive features of this *high-temperature reusable surface insulation (HRSI)* include low density and a low coefficient of thermal expansion. (Photograph courtesy of Lockheed Missiles & Space Company, Inc.)

Learning Objectives

After careful study of this chapter you should be able to do the following:

1. Define *heat capacity* and *specific heat*.
2. Note the primary mechanism by which thermal energy is assimilated in solid materials.
3. Determine the linear coefficient of thermal expansion given the length alteration that accompanies a specified temperature change.
4. Briefly explain the phenomenon of thermal expansion from an atomic perspective using a potential energy-versus-interatomic separation plot.
5. Define *thermal conductivity*.
6. Note the two principal mechanisms of heat conduction in solids, and compare the relative magnitudes of these contributions for each of metals, ceramics, and polymeric materials.

19.1 INTRODUCTION

By “thermal property” is meant the response of a material to the application of heat. As a solid absorbs energy in the form of heat, its temperature rises and its dimensions increase. The energy may be transported to cooler regions of the specimen if temperature gradients exist, and ultimately, the specimen may melt. Heat capacity, thermal expansion, and thermal conductivity are properties that are often critical in the practical utilization of solids.

19.2 HEAT CAPACITY

A solid material, when heated, experiences an increase in temperature signifying that some energy has been absorbed. **Heat capacity** is a property that is indicative of a material’s ability to absorb heat from the external surroundings; it represents the amount of energy required to produce a unit temperature rise. In mathematical terms, the heat capacity C is expressed as follows:

$$C = \frac{dQ}{dT} \quad (19.1)$$

where dQ is the energy required to produce a dT temperature change. Ordinarily, heat capacity is specified per mole of material (e.g., J/mol-K, or cal/mol-K). **Specific heat** (often denoted by a lowercase c) is sometimes used; this represents the heat capacity per unit mass and has various units (J/kg-K, cal/g-K, Btu/lb_m-°F).

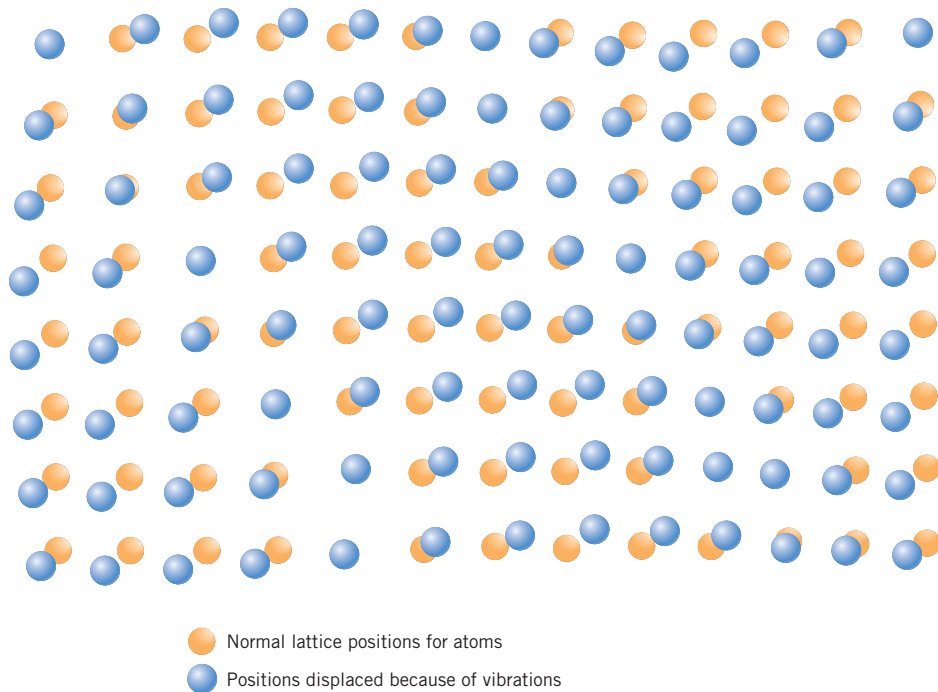
There are really two ways in which this property may be measured, according to the environmental conditions accompanying the transfer of heat. One is the heat capacity while maintaining the specimen volume constant, C_v ; the other is for constant external pressure, which is denoted C_p . The magnitude of C_p is almost always greater than C_v ; however, this difference is very slight for most solid materials at room temperature and below.

Vibrational Heat Capacity

In most solids the principal mode of thermal energy assimilation is by the increase in vibrational energy of the atoms. Again, atoms in solid materials are constantly vibrating at very high frequencies and with relatively small amplitudes. Rather than being independent of one another, the vibrations of adjacent atoms are coupled by virtue of the atomic bonding. These vibrations are coordinated in such a way that traveling lattice waves are produced, a phenomenon represented in Figure 19.1.

720 • Chapter 19 / Thermal Properties

Figure 19.1
Schematic representation of the generation of lattice waves in a crystal by means of atomic vibrations. (Adapted from “The Thermal Properties of Materials” by J. Ziman. Copyright © 1967 by Scientific American, Inc. All rights reserved.)



These may be thought of as elastic waves or simply sound waves, having short wavelengths and very high frequencies, which propagate through the crystal at the velocity of sound. The vibrational thermal energy for a material consists of a series of these elastic waves, which have a range of distributions and frequencies. Only certain energy values are allowed (the energy is said to be quantized), and a single quantum of vibrational energy is called a **phonon**. (A phonon is analogous to the quantum of electromagnetic radiation, the **photon**.) On occasion, the vibrational waves themselves are termed phonons.

The thermal scattering of free electrons during electronic conduction (Section 17.7) is by these vibrational waves, and these elastic waves also participate in the transport of energy during thermal conduction (see Section 19.4).

Temperature Dependence of the Heat Capacity

The variation with temperature of the vibrational contribution to the heat capacity at constant volume for many relatively simple crystalline solids is shown in Figure 19.2. The C_v is zero at 0 K, but it rises rapidly with temperature; this corresponds to an increased ability of the lattice waves to enhance their average energy with ascending temperature. At low temperatures the relationship between C_v and the absolute temperature T is

$$C_v = AT^3 \quad (19.2)$$

where A is a temperature-independent constant. Above what is called the *Debye temperature* θ_D , C_v levels off and becomes essentially independent of temperature at a value of approximately $3R$, R being the gas constant. Thus even though the total energy of the material is increasing with temperature, the quantity of energy required to produce a one-degree temperature change is constant. The value of θ_D is

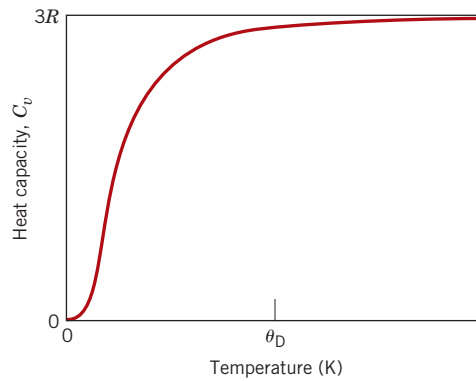


Figure 19.2 The temperature dependence of the heat capacity at constant volume; θ_D is the Debye temperature.

below room temperature for many solid materials, and 25 J/mol-K is a reasonable room-temperature approximation for C_v . Table 19.1 presents experimental specific heats for a number of materials; c_p values for still more materials are tabulated in Table B.8 of Appendix B.

Other Heat Capacity Contributions

Other energy-absorptive mechanisms also exist that can add to the total heat capacity of a solid. In most instances, however, these are minor relative to the magnitude of the vibrational contribution. There is an electronic contribution in that electrons absorb energy by increasing their kinetic energy. However, this is possible only for free electrons—those that have been excited from filled states to empty states above the Fermi energy (Section 17.6). In metals, only electrons at states near the Fermi energy are capable of such transitions, and these represent only a very small fraction of the total number. An even smaller proportion of electrons experiences excitations in insulating and semiconducting materials. Hence, this electronic contribution is ordinarily insignificant, except at temperatures near 0 K.

Furthermore, in some materials other energy-absorptive processes occur at specific temperatures—for example, the randomization of electron spins in a ferromagnetic material as it is heated through its Curie temperature. A large spike is produced on the heat capacity-versus-temperature curve at the temperature of this transformation.

19.3 THERMAL EXPANSION

Most solid materials expand upon heating and contract when cooled. The change in length with temperature for a solid material may be expressed as follows:

$$\frac{l_f - l_0}{l_0} = \alpha_l(T_f - T_0) \quad (19.3a)$$

or

$$\frac{\Delta l}{l_0} = \alpha_l \Delta T \quad (19.3b)$$

where l_0 and l_f represent, respectively, initial and final lengths with the temperature change from T_0 to T_f . The parameter α_l is called the **linear coefficient of**

722 • Chapter 19 / Thermal Properties

Table 19.1 Tabulation of the Thermal Properties for a Variety of Materials

<i>Material</i>	c_p (J/kg-K) ^a	α_l [(°C) ⁻¹ × 10 ⁻⁶] ^b	k (W/m-K) ^c	L [Ω·W/(K) ² × 10 ⁻⁸]
Metals				
Aluminum	900	23.6	247	2.20
Copper	386	17.0	398	2.25
Gold	128	14.2	315	2.50
Iron	448	11.8	80	2.71
Nickel	443	13.3	90	2.08
Silver	235	19.7	428	2.13
Tungsten	138	4.5	178	3.20
1025 Steel	486	12.0	51.9	—
316 Stainless steel	502	16.0	15.9	—
Brass (70Cu–30Zn)	375	20.0	120	—
Kovar (54Fe–29Ni–17Co)	460	5.1	17	2.80
Invar (64Fe–36Ni)	500	1.6	10	2.75
Super Invar (63Fe–32Ni–5Co)	500	0.72	10	2.68
Ceramics				
Alumina (Al ₂ O ₃)	775	7.6	39	—
Magnesia (MgO)	940	13.5 ^d	37.7	—
Spinel (MgAl ₂ O ₄)	790	7.6 ^d	15.0 ^e	—
Fused silica (SiO ₂)	740	0.4	1.4	—
Soda–lime glass	840	9.0	1.7	—
Borosilicate (Pyrex TM) glass	850	3.3	1.4	—
Polymers				
Polyethylene (high density)	1850	106–198	0.46–0.50	—
Polypropylene	1925	145–180	0.12	—
Polystyrene	1170	90–150	0.13	—
Polytetrafluoroethylene (Teflon TM)	1050	126–216	0.25	—
Phenol-formaldehyde, phenolic	1590–1760	122	0.15	—
Nylon 6,6	1670	144	0.24	—
Polyisoprene	—	220	0.14	—

^a To convert to cal/g-K, multiply by 2.39×10^{-4} ; to convert to Btu/lb_m-°F, multiply by 2.39×10^{-4} .

^b To convert to (°F)⁻¹, multiply by 0.56.

^c To convert to cal/s-cm-K, multiply by 2.39×10^{-3} ; to convert to Btu/ft-h-°F, multiply by 0.578.

^d Value measured at 100°C.

^e Mean value taken over the temperature range 0–1000°C.

thermal expansion; it is a material property that is indicative of the extent to which a material expands upon heating, and has units of reciprocal temperature [(°C)⁻¹ or (°F)⁻¹]. Of course, heating or cooling affects all the dimensions of a body, with a resultant change in volume. Volume changes with temperature may be computed from

$$\frac{\Delta V}{V_0} = \alpha_v \Delta T \quad (19.4)$$

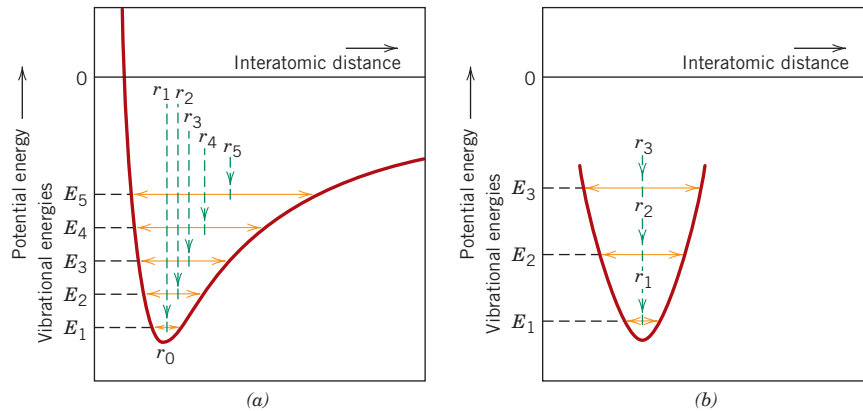


Figure 19.3 (a) Plot of potential energy versus interatomic distance, demonstrating the increase in interatomic separation with rising temperature. With heating, the interatomic separation increases from r_0 to r_1 to r_2 , and so on. (b) For a symmetric potential energy-versus-interatomic distance curve, there is no increase in interatomic separation with rising temperature (i.e., $r_1 = r_2 = r_3$). (Adapted from R. M. Rose, L. A. Shepard, and J. Wulff, *The Structure and Properties of Materials*, Vol. 4, *Electronic Properties*. Copyright © 1966 by John Wiley & Sons, New York. Reprinted by permission of John Wiley & Sons, Inc.)

where ΔV and V_0 are the volume change and the original volume, respectively, and α_v symbolizes the volume coefficient of thermal expansion. In many materials, the value of α_v is anisotropic; that is, it depends on the crystallographic direction along which it is measured. For materials in which the thermal expansion is isotropic, α_v is approximately $3\alpha_l$.

From an atomic perspective, thermal expansion is reflected by an increase in the average distance between the atoms. This phenomenon can best be understood by consultation of the potential energy-versus-interatomic spacing curve for a solid material introduced previously (Figure 2.8b), and reproduced in Figure 19.3a. The curve is in the form of a potential energy trough, and the equilibrium interatomic spacing at 0 K, r_0 , corresponds to the trough minimum. Heating to successively higher temperatures (T_1 , T_2 , T_3 , etc.) raises the vibrational energy from E_1 to E_2 to E_3 , and so on. The average vibrational amplitude of an atom corresponds to the trough width at each temperature, and the average interatomic distance is represented by the mean position, which increases with temperature from r_0 to r_1 to r_2 , and so on.

Thermal expansion is really due to the asymmetric curvature of this potential energy trough, rather than the increased atomic vibrational amplitudes with rising temperature. If the potential energy curve were symmetric (Figure 19.3b), there would be no net change in interatomic separation and, consequently, no thermal expansion.

For each class of materials (metals, ceramics, and polymers), the greater the atomic bonding energy, the deeper and more narrow this potential energy trough. As a result, the increase in interatomic separation with a given rise in temperature will be lower, yielding a smaller value of α_l . Table 19.1 lists the linear coefficients of thermal expansion for several materials. With regard to temperature dependence, the magnitude of the coefficient of expansion increases with rising temperature. The values in Table 19.1 are taken at room temperature unless indicated otherwise. A more comprehensive list of coefficients of thermal expansion is provided in Table B.6 of Appendix B.

Metals

As noted in Table 19.1, linear coefficients of thermal expansion for some of the common metals range between about 5×10^{-6} and $25 \times 10^{-6} (\text{°C})^{-1}$; these values are intermediate in magnitude between those for ceramic and polymeric materials. As the following Materials of Importance piece explains, several low-expansion and controlled-expansion metal alloys have been developed, which are used in applications requiring dimensional stability with temperature variations.

Ceramics

Relatively strong interatomic bonding forces are found in many ceramic materials as reflected in comparatively low coefficients of thermal expansion; values typically range between about 0.5×10^{-6} and $15 \times 10^{-6} (\text{°C})^{-1}$. For noncrystalline ceramics and also those having cubic crystal structures, α_l is isotropic. Otherwise, it is anisotropic; and, in fact, some ceramic materials, upon heating, contract in some crystallographic directions while expanding in others. For inorganic glasses, the coefficient of expansion is dependent on composition. Fused silica (high-purity SiO_2 glass) has a small expansion coefficient, $0.4 \times 10^{-6} (\text{°C})^{-1}$. This is explained by a low atomic packing density such that interatomic expansion produces relatively small macroscopic dimensional changes.

Ceramic materials that are to be subjected to temperature changes must have coefficients of thermal expansion that are relatively low, and in addition, isotropic. Otherwise, these brittle materials may experience fracture as a consequence of nonuniform dimensional changes in what is termed **thermal shock**, as discussed later in the chapter.

Polymers

Some polymeric materials experience very large thermal expansions upon heating as indicated by coefficients that range from approximately 50×10^{-6} to $400 \times 10^{-6} (\text{°C})^{-1}$. The highest α_l values are found in linear and branched polymers because the secondary intermolecular bonds are weak, and there is a minimum of crosslinking. With increased crosslinking, the magnitude of the expansion coefficient diminishes; the lowest coefficients are found in the thermosetting network polymers such as phenol-formaldehyde, in which the bonding is almost entirely covalent.



Concept Check 19.1

- (a) Explain why a brass lid ring on a glass canning jar will loosen when heated.
- (b) Suppose the ring is made of tungsten instead of brass. What will be the effect of heating the lid and jar? Why?

[The answer may be found in enclosed CD.]

19.4 THERMAL CONDUCTIVITY

Thermal conduction is the phenomenon by which heat is transported from high- to low-temperature regions of a substance. The property that characterizes the ability of a material to transfer heat is the **thermal conductivity**. It is best defined in terms of the expression

$$q = -k \frac{dT}{dx} \quad (19.5)$$

MATERIALS OF IMPORTANCE

Invar and Other Low-Expansion Alloys

In 1896, Charles-Edouard Guillaume of France made an interesting and important discovery that earned him the 1920 Nobel Prize in Physics; his discovery: an iron–nickel alloy that has a very low (near-zero) coefficient of thermal expansion between room temperature and approximately 230°C. This material became the forerunner of a family of “low-expansion” (also sometimes called “controlled-expansion”) metal alloys. Its composition is 64 wt% Fe–36 wt% Ni, and it has been given the trade-name of “Invar” since the length of a specimen of this material is virtually invariable with changes in temperature. Its coefficient of thermal expansion near room temperature is $1.6 \times 10^{-6} (\text{°C})^{-1}$.

One might surmise that this near zero expansion is explained by a symmetrical potential energy-versus-interatomic distance curve [Figure 19.3(b)]. Such is not so; rather, this behavior relates to the magnetic characteristics of Invar. Both iron and nickel are ferromagnetic materials (Section 20.4). A ferromagnetic material may be made to form a permanent and strong magnet; upon heating, this property disappears at a specific temperature, called the “Curie temperature,” which temperature varies from one ferromagnetic material to another (Section 20.6). As a specimen of Invar is heated, its tendency to expand is counteracted by a contraction phenomenon that is associated with its ferromagnetic properties (which is termed “magnetostriction”). Above its Curie temperature (approximately 230°C), Invar expands in a normal manner, and its coefficient of thermal expansion assumes a much greater value.

Heat treating and processing of Invar will also affect its thermal expansion characteristics. The lowest α_f values result for specimens quenched from elevated temperatures (near 800°C) that are then cold worked. Annealing leads to an increase in α_f .

Other low-expansion alloys have been developed. One of these is called “Super-Invar” because its thermal expansion coefficient [$0.72 \times 10^{-6} (\text{°C})^{-1}$] is lower than the value for Invar. However, the temperature range over which its low expansion characteristics persist is relatively narrow. Compositionally, for Super-Invar some of the nickel in Invar is replaced by another ferromagnetic metal, cobalt; Super-Invar contains 63 wt% Fe, 32 wt% Ni, and 5 wt% Co.

Another such alloy, with the trade-name of “Kovar,” has been designed to have expansion characteristics close to those of borosilicate (or Pyrex) glass; when joined to Pyrex and subjected to temperature variations, thermal stresses and possible fracture at the junction are avoided. The composition of Kovar is 54 wt% Fe, 29 wt% Ni, and 17 wt% Co.

These low-expansion alloys are employed in applications that require dimensional stability with temperature fluctuations; these include the following:

- Compensating pendulums and balance wheels for mechanical clocks and watches.
- Structural components in optical and laser measuring systems that require dimensional stabilities on the order of a wavelength of light.
- Bimetallic strips that are used to actuate microswitches in water heating systems.
- Shadow masks on cathode ray tubes that are used for television and display screens; higher contrast, improved brightness, and sharper definition are possible using low-expansion materials.
- Vessels and piping for the storage and piping of liquefied natural gas.



Photograph showing tubular products that have glass-to-metal junctions. The thermal expansion coefficient of the metal alloy (Kovar) is approximately the same as that of the Pyrex glass. Thus, with changes in temperature, the likelihood of the establishment of thermal stresses and fracture at the junction are minimized. [Photograph courtesy of Moores (EVIC) Glassworks, Ltd., Walton-on-Thames, England.]

726 • Chapter 19 / Thermal Properties

where q denotes the *heat flux*, or heat flow, per unit time per unit area (area being taken as that perpendicular to the flow direction), k is the thermal conductivity, and dT/dx is the *temperature gradient* through the conducting medium.

The units of q and k are W/m^2 and $\text{W}/\text{m}\cdot\text{K}$, respectively. Equation 19.5 is valid only for steady-state heat flow—that is, for situations in which the heat flux does not change with time. Also, the minus sign in the expression indicates that the direction of heat flow is from hot to cold, or down the temperature gradient.

Equation 19.5 is similar in form to Fick's first law (Equation 6.3) for steady-state diffusion. For these expressions, k is analogous to the diffusion coefficient D , and the temperature gradient parallels the concentration gradient, dC/dx .

Mechanisms of Heat Conduction

Heat is transported in solid materials by both lattice vibration waves (phonons) and free electrons. A thermal conductivity is associated with each of these mechanisms, and the total conductivity is the sum of the two contributions, or

$$k = k_l + k_e \quad (19.6)$$

where k_l and k_e represent the lattice vibration and electron thermal conductivities, respectively; usually one or the other predominates. The thermal energy associated with phonons or lattice waves is transported in the direction of their motion. The k_l contribution results from a net movement of phonons from high- to low-temperature regions of a body across which a temperature gradient exists.

Free or conducting electrons participate in electronic thermal conduction. To the free electrons in a hot region of the specimen is imparted a gain in kinetic energy. They then migrate to colder areas, where some of this kinetic energy is transferred to the atoms themselves (as vibrational energy) as a consequence of collisions with phonons or other imperfections in the crystal. The relative contribution of k_e to the total thermal conductivity increases with increasing free electron concentrations, since more electrons are available to participate in this heat transfer process.

Metals

In high-purity metals, the electron mechanism of heat transport is much more efficient than the phonon contribution because electrons are not as easily scattered as phonons and have higher velocities. Furthermore, metals are extremely good conductors of heat because relatively large numbers of free electrons exist that participate in thermal conduction. The thermal conductivities of several of the common metals are given in Table 19.1; values generally range between about 20 and 400 $\text{W}/\text{m}\cdot\text{K}$.

Since free electrons are responsible for both electrical and thermal conduction in pure metals, theoretical treatments suggest that the two conductivities should be related according to the *Wiedemann–Franz law*:

$$L = \frac{k}{\sigma T} \quad (19.7)$$

where σ is the electrical conductivity, T is the absolute temperature, and L is a constant. The theoretical value of L , $2.44 \times 10^{-8} \Omega\cdot\text{W}/(\text{K})^2$, should be independent of temperature and the same for all metals if the heat energy is transported entirely by free electrons. Included in Table 19.1 are the experimental L values for these

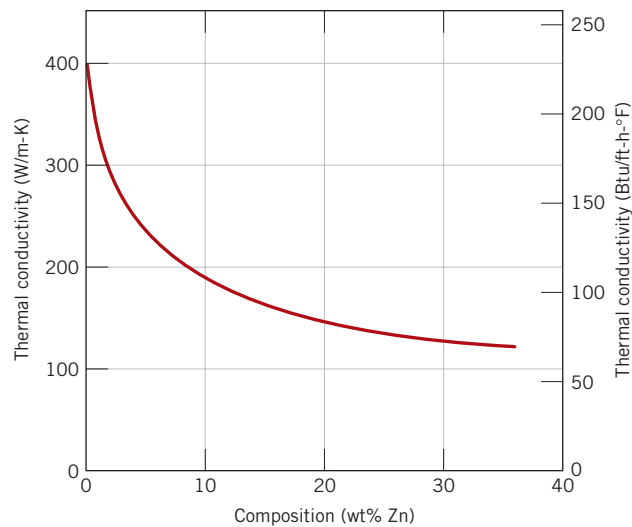


Figure 19.4 Thermal conductivity versus composition for copper–zinc alloys. [Adapted from *Metals Handbook: Properties and Selection: Nonferrous Alloys and Pure Metals*, Vol. 2, 9th edition, H. Baker (Managing Editor), American Society for Metals, 1979, p. 315.]

several metals; note that the agreement between these and the theoretical value is quite reasonable (well within a factor of 2).

Alloying metals with impurities results in a reduction in the thermal conductivity, for the same reason that the electrical conductivity is diminished (Section 18.8); namely, the impurity atoms, especially if in solid solution, act as scattering centers, lowering the efficiency of electron motion. A plot of thermal conductivity versus composition for copper–zinc alloys (Figure 19.4) displays this effect.

Concept Check 19.2

The thermal conductivity of a plain carbon steel is greater than for a stainless steel. Why is this so? *Hint:* you may want to consult Section 9.2.

[The answer may be found in enclosed CD.]

Ceramics

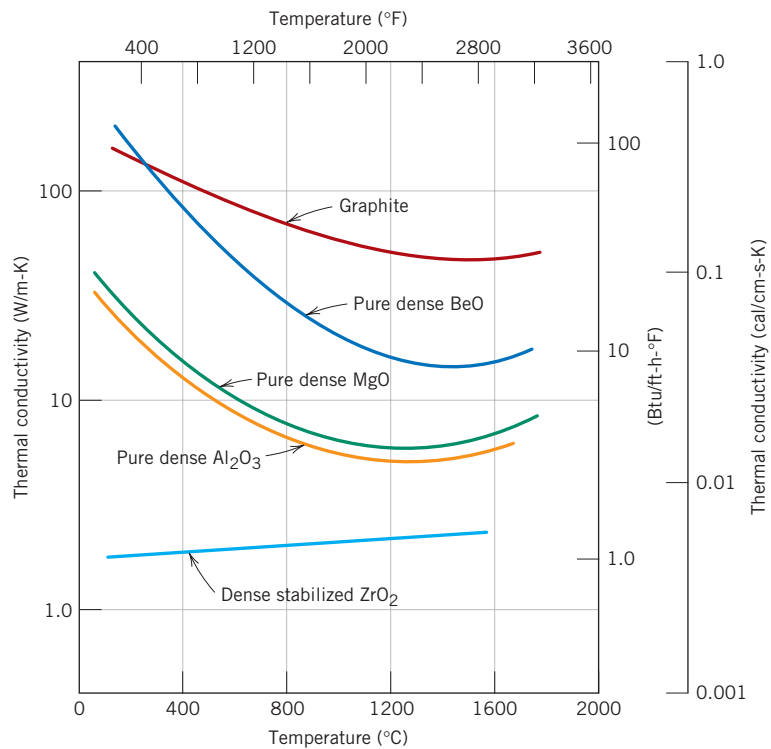
Nonmetallic materials are thermal insulators inasmuch as they lack large numbers of free electrons. Thus the phonons are primarily responsible for thermal conduction: k_e is much smaller than k_i . Again, the phonons are not as effective as free electrons in the transport of heat energy as a result of the very efficient phonon scattering by lattice imperfections.

Thermal conductivity values for a number of ceramic materials are contained in Table 19.1; room-temperature thermal conductivities range between approximately 2 and 50 W/m-K. Glass and other amorphous ceramics have lower conductivities than crystalline ceramics, since the phonon scattering is much more effective when the atomic structure is highly disordered and irregular.

The scattering of lattice vibrations becomes more pronounced with rising temperature; hence, the thermal conductivity of most ceramic materials normally diminishes with increasing temperature, at least at relatively low temperatures (Figure 19.5). As Figure 19.5 indicates, the conductivity begins to increase at higher temperatures, which is due to radiant heat transfer: significant quantities of infrared radiant heat may be transported through a transparent ceramic material. The efficiency of this process increases with temperature.

728 • Chapter 19 / Thermal Properties

Figure 19.5
Dependence of thermal conductivity on temperature for several ceramic materials. (Adapted from W. D. Kingery, H. K. Bowen, and D. R. Uhlmann, *Introduction to Ceramics*, 2nd edition. Copyright © 1976 by John Wiley & Sons, New York. Reprinted by permission of John Wiley & Sons, Inc.)



Porosity in ceramic materials may have a dramatic influence on thermal conductivity; increasing the pore volume will, under most circumstances, result in a reduction of the thermal conductivity. In fact, many ceramics that are used for thermal insulation are porous. Heat transfer across pores is ordinarily slow and inefficient. Internal pores normally contain still air, which has an extremely low thermal conductivity—approximately 0.02 W/m-K. Furthermore, gaseous convection within the pores is also comparatively ineffective.

✓ Concept Check 19.3

The thermal conductivity of a single-crystal ceramic specimen is slightly greater than a polycrystalline one of the same material. Why is this so?

[The answer may be found in enclosed CD.]

Polymers

As noted in Table 19.1, thermal conductivities for most polymers are on the order of 0.3 W/m-K. For these materials, energy transfer is accomplished by the vibration and rotation of the chain molecules. The magnitude of the thermal conductivity depends on the degree of crystallinity; a polymer with a highly crystalline and ordered structure will have a greater conductivity than the equivalent amorphous material. This is due to the more effective coordinated vibration of the molecular chains for the crystalline state.

Polymers are often utilized as thermal insulators because of their low thermal conductivities. As with ceramics, their insulative properties may be further enhanced by the introduction of small pores, which are ordinarily introduced by foaming

during polymerization (Section 14.18). Foamed polystyrene (Styrofoam) is commonly used for drinking cups and insulating chests.

✓ Concept Check 19.4

Which of a linear polyethylene ($\bar{M}_n = 450,000$ g/mol) and a lightly branched polyethylene ($\bar{M}_n = 650,000$ g/mol) has the higher thermal conductivity? Why? *Hint:* you may want to consult Section 4.18.

[The answer may be found in enclosed CD.]

✓ Concept Check 19.5

Explain why, on a cold day, the metal door handle of an automobile feels colder to the touch than a plastic steering wheel, even though both are at the same temperature.

[The answer may be found in enclosed CD.]

19.5 THERMAL STRESSES

Thermal stresses are stresses induced in a body as a result of changes in temperature. An understanding of the origins and nature of thermal stresses is important because these stresses can lead to fracture or undesirable plastic deformation.

Stresses Resulting From Restrained Thermal Expansion and Contraction

Let us first consider a homogeneous and isotropic solid rod that is heated or cooled uniformly; that is, no temperature gradients are imposed. For free expansion or contraction, the rod will be stress free. If, however, axial motion of the rod is restrained by rigid end supports, thermal stresses will be introduced. The magnitude of the stress σ resulting from a temperature change from T_0 to T_f is

$$\sigma = E\alpha_l(T_0 - T_f) = E\alpha_l\Delta T \quad (19.8)$$

where E is the modulus of elasticity and α_l is the linear coefficient of thermal expansion. Upon heating ($T_f > T_0$), the stress is compressive ($\sigma < 0$), since rod expansion has been constrained. Of course, if the rod specimen is cooled ($T_f < T_0$), a tensile stress will be imposed ($\sigma > 0$). Also, the stress in Equation 19.8 is the same as the stress that would be required to elastically compress (or elongate) the rod specimen back to its original length after it had been allowed to freely expand (or contract) with the $T_0 - T_f$ temperature change.

EXAMPLE PROBLEM 19.1

Thermal Stress Created Upon Heating

A brass rod is to be used in an application requiring its ends to be held rigid. If the rod is stress free at room temperature [20°C (68°F)], what is the maximum temperature to which the rod may be heated without exceeding a compressive stress of 172 MPa (25,000 psi)? Assume a modulus of elasticity of 100 GPa (14.6×10^6 psi) for brass.

Solution

Use Equation 19.8 to solve this problem, where the stress of 172 MPa is taken to be negative. Also, the initial temperature T_0 is 20°C, and the magnitude of the linear coefficient of thermal expansion from Table 19.1 is $20.0 \times 10^{-6} (\text{°C})^{-1}$. Thus, solving for the final temperature T_f yields

$$\begin{aligned} T_f &= T_0 - \frac{\sigma}{E\alpha_l} \\ &= 20^\circ\text{C} - \frac{-172 \text{ MPa}}{(100 \times 10^3 \text{ MPa})[20 \times 10^{-6} (\text{°C})^{-1}]} \\ &= 20^\circ\text{C} + 86^\circ\text{C} = 106^\circ\text{C} \end{aligned}$$

Stresses Resulting From Temperature Gradients

When a solid body is heated or cooled, the internal temperature distribution will depend on its size and shape, the thermal conductivity of the material, and the rate of temperature change. Thermal stresses may be established as a result of temperature gradients across a body, which are frequently caused by rapid heating or cooling, in that the outside changes temperature more rapidly than the interior; differential dimensional changes serve to restrain the free expansion or contraction of adjacent volume elements within the piece. For example, upon heating, the exterior of a specimen is hotter and, therefore, will have expanded more than the interior regions. Hence, compressive surface stresses are induced and are balanced by tensile interior stresses. The interior–exterior stress conditions are reversed for rapid cooling such that the surface is put into a state of tension.

Thermal Shock of Brittle Materials

For ductile metals and polymers, alleviation of thermally induced stresses may be accomplished by plastic deformation. However, the nonductility of most ceramics enhances the possibility of brittle fracture from these stresses. Rapid cooling of a brittle body is more likely to inflict such thermal shock than heating, since the induced surface stresses are tensile. Crack formation and propagation from surface flaws are more probable when an imposed stress is tensile (Section 12.10).

The capacity of a material to withstand this kind of failure is termed its *thermal shock resistance*. For a ceramic body that is rapidly cooled, the resistance to thermal shock depends not only on the magnitude of the temperature change, but also on the mechanical and thermal properties of the material. The thermal shock resistance is best for ceramics that have high fracture strengths σ_f and high thermal conductivities, as well as low moduli of elasticity and low coefficients of thermal expansion. The resistance of many materials to this type of failure may be approximated by a thermal shock resistance parameter *TSR*:

$$TSR \cong \frac{\sigma_f k}{E\alpha_l} \quad (19.9)$$

Thermal shock may be prevented by altering the external conditions to the degree that cooling or heating rates are reduced and temperature gradients across a body are minimized. Modification of the thermal and/or mechanical characteristics in Equation 19.9 may also enhance the thermal shock resistance of a material. Of

these parameters, the coefficient of thermal expansion is probably most easily changed and controlled. For example, common soda–lime glasses, which have an α_l of approximately $9 \times 10^{-6} (\text{°C})^{-1}$, are particularly susceptible to thermal shock, as anyone who has baked can probably attest. Reducing the CaO and Na₂O contents while at the same time adding B₂O₃ in sufficient quantities to form borosilicate (or Pyrex) glass will reduce the coefficient of expansion to about $3 \times 10^{-6} (\text{°C})^{-1}$; this material is entirely suitable for kitchen oven heating and cooling cycles. The introduction of some relatively large pores or a ductile second phase may also improve the thermal shock characteristics of a material; both serve to impede the propagation of thermally induced cracks.

It is often necessary to remove thermal stresses in ceramic materials as a means of improving their mechanical strengths and optical characteristics. This may be accomplished by an annealing heat treatment, as discussed for glasses in Section 12.16.

SUMMARY

Heat Capacity

This chapter discussed heat absorption, thermal expansion, and thermal conduction—three important thermal phenomena. Heat capacity represents the quantity of heat required to produce a unit rise in temperature for one mole of a substance; on a per-unit mass basis, it is termed specific heat. Most of the energy assimilated by many solid materials is associated with increasing the vibrational energy of the atoms; contributions to the total heat capacity by other energy-absorptive mechanisms (i.e., increased free-electron kinetic energies) are normally insignificant.

For many crystalline solids and at temperatures within the vicinity of 0 K, the heat capacity measured at constant volume varies as the cube of the absolute temperature; in excess of the Debye temperature, C_v becomes temperature independent, assuming a value of approximately $3R$.

Thermal Expansion

Solid materials expand when heated and contract when cooled. The fractional change in length is proportional to the temperature change, the constant of proportionality being the coefficient of thermal expansion. Thermal expansion is reflected by an increase in the average interatomic separation, which is a consequence of the asymmetric nature of the potential energy versus interatomic spacing curve trough. The larger the interatomic bonding energy, the lower is the coefficient of thermal expansion.

Thermal Conductivity

The transport of thermal energy from high- to low-temperature regions of a material is termed thermal conduction. For steady-state heat transport, the flux is proportional to the temperature gradient along the direction of flow; the proportionality constant is the thermal conductivity.

For solid materials, heat is transported by free electrons and by vibrational lattice waves, or phonons. The high thermal conductivities for relatively pure metals are due to the large numbers of free electrons, and also the efficiency with which these electrons transport thermal energy. By way of contrast, ceramics and polymers are poor thermal conductors because free-electron concentrations are low and phonon conduction predominates.

Thermal Stresses

Thermal stresses, which are introduced in a body as a consequence of temperature changes, may lead to fracture or undesirable plastic deformation. The two prime sources of thermal stresses are restrained thermal expansion (or contraction) and temperature gradients established during heating or cooling.

Thermal shock is the fracture of a body resulting from thermal stresses induced by rapid temperature changes. Because ceramic materials are brittle, they are especially susceptible to this type of failure. The thermal shock resistance of many materials is proportional to the fracture strength and thermal conductivity, and inversely proportional to both the modulus of elasticity and the coefficient of thermal expansion.

REFERENCES

- Kingery, W. D., H. K. Bowen, and D. R. Uhlmann, *Introduction to Ceramics*, 2nd edition, Wiley, New York, 1976. Chapters 12 and 16.
- Rose, R. M., L. A. Shepard, and J. Wulff, *The Structure and Properties of Materials*, Vol. IV, *Electronic Properties*, Wiley, New York, 1966. Chapters 3 and 8.
- Ziman, J., "The Thermal Properties of Materials," *Scientific American*, Vol. 217, No. 3, September 1967, pp. 180–188.

QUESTIONS AND PROBLEMS**Heat Capacity**

- 19.1** Estimate the energy required to raise the temperature of 5 kg of the following materials from 20 to 150°C: aluminum, brass, aluminum oxide (alumina), and polypropylene.
- 19.2** To what temperature would 4.5 kg of a brass specimen at 25°C be raised if 67500 J of heat is supplied?
- 19.3** (a) Determine the room temperature heat capacities at constant pressure for the following materials: copper, iron, gold, and nickel. (b) How do these values compare with one another? How do you explain this?
- 19.4** For copper, the heat capacity at constant volume C_v at 20 K is 0.38 J/mol-K, and the Debye temperature is 340 K. Estimate the specific heat (a) at 40 K and (b) at 400 K.
- 19.5** The constant A in Equation 19.2 is $12\pi^4 R/5\theta_D^3$, where R is the gas constant and θ_D is the Debye temperature (K). Estimate θ_D for aluminum, given that the specific heat is 4.60 J/kg-K at 15 K.
- 19.6** (a) Briefly explain why C_v rises with increasing temperature at temperatures near 0 K. (b) Briefly explain why C_v becomes vir-

tually independent of temperature at temperatures far removed from 0 K.

Thermal Expansion

- 19.7** A bimetallic strip is constructed from strips of two different metals that are bonded along their lengths. Explain how such a device may be used in a thermostat to regulate temperature.
- 19.8** A copper wire 15 m long is cooled from 40 to -9°C. How much change in length will it experience?
- 19.9** A 0.4 m rod of a metal elongates 0.48 mm on heating from 20 to 100°C. Determine the value of the linear coefficient of thermal expansion for this material.
- 19.10** Briefly explain thermal expansion using the potential energy-versus-interatomic spacing curve.
- 19.11** Compute the density for iron at 700°C, given that its room-temperature density is 7.870 g/cm³. Assume that the volume coefficient of thermal expansion, α_v , is equal to $3\alpha_l$.
- 19.12** When a metal is heated its density decreases. There are two sources that give rise

to this diminishment of ρ : (1) the thermal expansion of the solid, and (2) the formation of vacancies (Section 5.2). Consider a specimen of gold at room temperature (20°C) that has a density of 19.320 g/cm³. **(a)** Determine its density upon heating to 800°C when only thermal expansion is considered. **(b)** Repeat the calculation when the introduction of vacancies is taken into account. Assume that the energy of vacancy formation is 0.98 eV/atom, and that the volume coefficient of thermal expansion, α_v is equal to $3\alpha_l$.

- 19.13** The difference between the specific heats at constant pressure and volume is described by the expression

$$c_p - c_v = \frac{\alpha_v^2 v_0 T}{\beta} \quad (19.10)$$

where α_v is the volume coefficient of thermal expansion, v_0 is the specific volume (i.e., volume per unit mass, or the reciprocal of density), β is the compressibility, and T is the absolute temperature. Compute the values of c_v at room temperature (293 K) for aluminum and iron using the data in Table 19.1, assuming that $\alpha_v = 3\alpha_l$ and given that the values of β for Al and Fe are 1.77×10^{-11} and 2.65×10^{-12} (Pa)⁻¹, respectively.

- 19.14** To what temperature must a cylindrical rod of tungsten 15.025 mm in diameter and a plate of 1025 steel having a circular hole 15.000 mm in diameter have to be heated for the rod to just fit into the hole? Assume that the initial temperature is 25°C.

Thermal Conductivity

- 19.15 (a)** Calculate the heat flux through a sheet of brass 7.5 mm (0.30 in.) thick if the temperatures at the two faces are 150 and 50°C (302 and 122°F); assume steady-state heat flow. **(b)** What is the heat loss per hour if the area of the sheet is 0.5 m² (5.4 ft²)? **(c)** What will be the heat loss per hour if soda–lime glass instead of brass is used? **(d)** Calculate the heat loss per hour if brass is used and the thickness is increased to 15 mm (0.59 in.).
- 19.16 (a)** Would you expect Equation 19.7 to be valid for ceramic and polymeric materials? Why or why not? **(b)** Estimate the value

for the Wiedemann–Franz constant L [in $\Omega\text{-W}/(\text{K})^2$] at room temperature (293 K) for the following nonmetals: zirconia (3 mol% Y₂O₃), diamond (synthetic), gallium arsenide (intrinsic), poly(ethylene terephthalate) (PET), and silicone. Consult Tables B.7 and B.9 in Appendix B.

- 19.17** Briefly explain why the thermal conductivities are higher for crystalline than noncrystalline ceramics.
- 19.18** Briefly explain why metals are typically better thermal conductors than ceramic materials.
- 19.19 (a)** Briefly explain why porosity decreases the thermal conductivity of ceramic and polymeric materials, rendering them more thermally insulative. **(b)** Briefly explain how the degree of crystallinity affects the thermal conductivity of polymeric materials and why.
- 19.20** For some ceramic materials, why does the thermal conductivity first decrease and then increase with rising temperature?
- 19.21** For each of the following pairs of materials, decide which has the larger thermal conductivity. Justify your choices.
- (a)** Pure silver; sterling silver (92.5 wt% Ag–7.5 wt% Cu).
- (b)** Fused silica; polycrystalline silica.
- (c)** Linear and syndiotactic poly(vinyl chloride) ($DP = 1000$); linear and syndiotactic polystyrene ($DP = 1000$).
- (d)** Atactic polypropylene ($\bar{M}_w = 10^6$ g/mol); isotactic polypropylene ($\bar{M}_w = 5 \times 10^5$ g/mol).

- 19.22** We might think of a porous material as being a composite wherein one of the phases is a pore phase. Estimate upper and lower limits for the room-temperature thermal conductivity of an aluminum oxide material having a volume fraction of 0.25 of pores that are filled with still air.

- 19.23** Nonsteady-state heat flow may be described by the following partial differential equation:

$$\frac{\partial T}{\partial t} = D_T \frac{\partial^2 T}{\partial x^2}$$

where D_T is the thermal diffusivity; this expression is the thermal equivalent of

734 • Chapter 19 / Thermal Properties

Fick's second law of diffusion (Equation 6.4b). The thermal diffusivity is defined according to

$$D_T = \frac{k}{\rho c_p}$$

In this expression, k , ρ , and c_p represent the thermal conductivity, the mass density, and the specific heat at constant pressure, respectively.

- (a) What are the SI units for D_T ?
 (b) Determine values of D_T for copper, brass, magnesia, fused silica, polystyrene, and polypropylene using the data in Table 19.1. Density values are included in Table B.1, Appendix B. (*Note:* the density of magnesia (MgO) is 3.58 g/cm^3 .)

Thermal Stresses

- 19.24** Beginning with Equation 19.3, show that Equation 19.8 is valid.
19.25 (a) Briefly explain why thermal stresses may be introduced into a structure by rapid heating or cooling. (b) For cooling, what is the nature of the surface stresses? (c) For heating, what is the nature of the surface stresses?
19.26 (a) If a rod of brass 0.35 m long is heated from 15 to 85°C while its ends are main-

tained rigid, determine the type and magnitude of stress that develops. Assume that at 15°C the rod is stress free.

- (b) What will be the stress magnitude if a rod 1 m long is used?
 (c) If the rod in part (a) is cooled from 15°C to -15°C , what type and magnitude of stress will result?
19.27 A steel wire is stretched with a stress of 70 MPa at 20°C . If the length is held constant, to what temperature must the wire be heated to reduce the stress to 17 MPa?
19.28 If a cylindrical rod of brass 150.00 mm long and 10.000 mm in diameter is heated from 20°C to 160°C while its ends are maintained rigid, determine its change in diameter. You may want to consult Table 9.10.
19.29 The two ends of a cylindrical rod of nickel 120.00 mm long and 12.000 mm in diameter are maintained rigid. If the rod is initially at 70°C , to what temperature must it be cooled in order to have a 0.023-mm reduction in diameter?
19.30 What measures may be taken to reduce the likelihood of thermal shock of a ceramic piece?

DESIGN PROBLEMS

Thermal Expansion

- 19.D1** Railroad tracks made of 1025 steel are to be laid during the time of year when the temperature averages 4°C . If a joint space of 5.4 mm is allowed between the standard 11.9-m long rails, what is the hottest possible temperature that can be tolerated without the introduction of thermal stresses?

Thermal Stresses

- 19.D2** The ends of a cylindrical rod 6.4 mm in diameter and 250 mm long are mounted between rigid supports. The rod is stress free at room temperature [20°C]; and upon cooling to -60°C , a maximum thermally induced

tensile stress of 138 MPa is possible. Of which of the following metals or alloys may the rod be fabricated: aluminum, copper, brass, 1025 steel, and tungsten? Why?

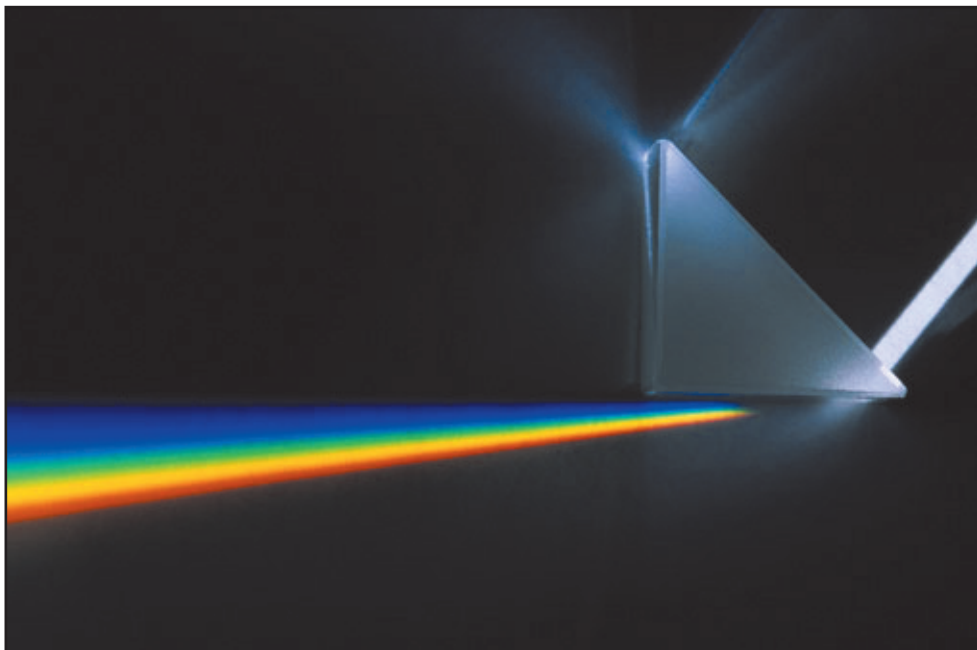
- 19.D3** (a) What are the units for the thermal shock resistance parameter (TSR)? (b) Rank the following ceramic materials according to their thermal shock resistance: soda-lime glass, fused silica, and silicon [$\langle 100 \rangle$ direction and $\{100\}$ orientation, as-cut surface]. Appropriate data may be found in Tables B.2, B.4, B.6, and B.7 of Appendix B.

19.D4 Equation 19.9, for the thermal shock resistance of a material, is valid for relatively low rates of heat transfer. When the rate is high, then, upon cooling of a body, the maximum temperature change allowable without thermal shock, ΔT_f , is approximately

$$\Delta T_f \cong \frac{\sigma_f}{E\alpha_l}$$

where σ_f is the fracture strength. Using the data in Tables B.2, B.4, and B.6 (Appendix B), determine ΔT_f for a soda–lime glass, borosilicate (Pyrex) glass, aluminum oxide (96% pure), and gallium arsenide [$\langle 100 \rangle$ direction and $\{100\}$ orientation, as-cut surface].

Chapter 20 Optical Properties



A white light beam experiences both refraction and dispersion as it passes through the triangular glass prism. Refraction—in that the direction of the light beam is bent at both glass-air prism interfaces (i.e., as it passes into and out of the prism). And dispersion (chromatic)—in that the degree of bending depends on wavelength (i.e., the beam is separated into its component colors). (© PhotoDisc/Getty Images.)



Learning Objectives

After careful study of this chapter you should be able to do the following:

1. Compute the energy of a photon given its frequency and the value of Planck's constant.
2. Briefly describe electronic polarization that results from electromagnetic radiation-atomic interactions. Cite two consequences of electronic polarization.
3. Briefly explain why metallic materials are opaque to visible light.
4. Define *index of refraction*.
5. Describe the mechanism of photon absorption for (a) high-purity insulators and semiconductors, and (b) insulators and semiconductors that contain electrically active defects.
6. For inherently transparent dielectric materials, note three sources of internal scattering that can lead to translucency and opacity.
7. Briefly describe the construction and operation of ruby and semiconductor lasers.

20.1 INTRODUCTION

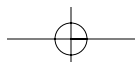
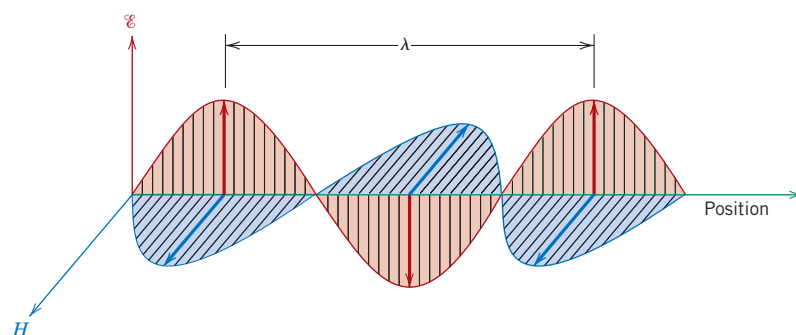
By “optical property” is meant a material’s response to exposure to electromagnetic radiation and, in particular, to visible light. This chapter first discusses some of the basic principles and concepts relating to the nature of electromagnetic radiation and its possible interactions with solid materials. Next to be explored are the optical behaviors of metallic and nonmetallic materials in terms of their absorption, reflection, and transmission characteristics. The final sections outline luminescence, photoconductivity, and light amplification by stimulated emission of radiation (laser), the practical utilization of these phenomena, and optical fibers in communications.

Basic Concepts

20.2 ELECTROMAGNETIC RADIATION

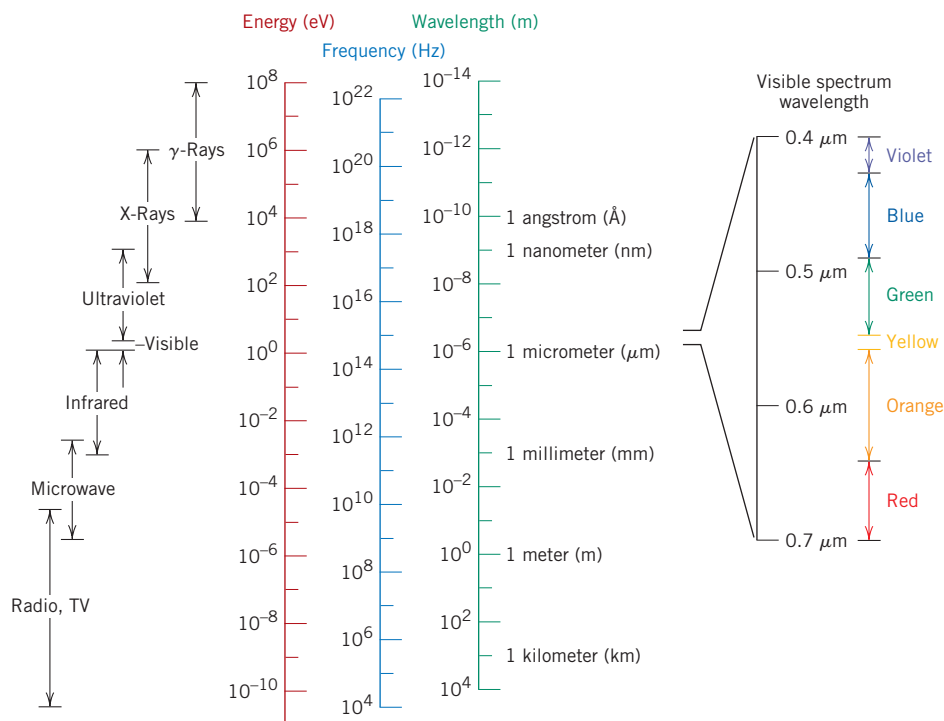
In the classical sense, electromagnetic radiation is considered to be wave-like, consisting of electric and magnetic field components that are perpendicular to each other and also to the direction of propagation (Figure 20.1). Light, heat (or radiant energy), radar, radio waves, and x-rays are all forms of electromagnetic radiation. Each is characterized primarily by a specific range of wavelengths, and also according to the technique by which it is generated. The *electromagnetic spectrum* of radiation spans the wide range from γ -rays (emitted by radioactive materials) having wavelengths on the order of 10^{-12} m (10^{-3} nm), through x-rays, ultraviolet, visible, infrared, and finally radio waves with wavelengths as long as 10^5 m. This spectrum, on a logarithmic scale, is shown in Figure 20.2.

Figure 20.1 An electromagnetic wave showing electric field \mathcal{E} and magnetic field H components, and the wavelength λ .



738 • Chapter 20 / Optical Properties

Figure 20.2 The spectrum of electromagnetic radiation, including wavelength ranges for the various colors in the visible spectrum.



Visible light lies within a very narrow region of the spectrum, with wavelengths ranging between about $0.4 \mu\text{m}$ ($4 \times 10^{-7} \text{ m}$) and $0.7 \mu\text{m}$. The perceived color is determined by wavelength; for example, radiation having a wavelength of approximately $0.4 \mu\text{m}$ appears violet, whereas green and red occur at about 0.5 and $0.65 \mu\text{m}$, respectively. The spectral ranges for the several colors are included in Figure 20.2. White light is simply a mixture of all colors. The ensuing discussion is concerned primarily with this visible radiation, by definition the only radiation to which the eye is sensitive.

All electromagnetic radiation traverses a vacuum at the same velocity, that of light—namely, $3 \times 10^8 \text{ m/s}$ (186,000 miles/s). This velocity, c , is related to the electric permittivity of a vacuum ϵ_0 and the magnetic permeability of a vacuum μ_0 through

$$c = \frac{1}{\sqrt{\epsilon_0 \mu_0}} \quad (20.1)$$

Thus, there is an association between the electromagnetic constant c and these electrical and magnetic constants.

Furthermore, the frequency ν and the wavelength λ of the electromagnetic radiation are a function of velocity according to

$$c = \lambda \nu \quad (20.2)$$

Frequency is expressed in terms of hertz (Hz), and $1 \text{ Hz} = 1 \text{ cycle per second}$. Ranges of frequency for the various forms of electromagnetic radiation are also included in the spectrum (Figure 20.2).

20.3 Light Interactions with Solids • 739

Sometimes it is more convenient to view electromagnetic radiation from a quantum-mechanical perspective, in which the radiation, rather than consisting of waves, is composed of groups or packets of energy, which are called **photons**. The energy E of a photon is said to be quantized, or can only have specific values, defined by the relationship

$$E = h\nu = \frac{hc}{\lambda} \quad (20.3)$$

where h is a universal constant called **Planck's constant**, which has a value of 6.63×10^{-34} J-s. Thus, photon energy is proportional to the frequency of the radiation, or inversely proportional to the wavelength. Photon energies are also included in the electromagnetic spectrum (Figure 20.2).

When describing optical phenomena involving the interactions between radiation and matter, an explanation is often facilitated if light is treated in terms of photons. On other occasions, a wave treatment is more appropriate; at one time or another, both approaches are used in this discussion.

 **Concept Check 20.1**

Briefly discuss the similarities and differences between photons and phonons. *Hint:* you may want to consult Section 19.2.

[The answer may be found in enclosed CD.]

 **Concept Check 20.2**

Electromagnetic radiation may be treated from the classical or the quantum-mechanical perspective. Briefly compare these two viewpoints.

[The answer may be found in enclosed CD.]

20.3 LIGHT INTERACTIONS WITH SOLIDS

When light proceeds from one medium into another (e.g., from air into a solid substance), several things happen. Some of the light radiation may be transmitted through the medium, some will be absorbed, and some will be reflected at the interface between the two media. The intensity I_0 of the beam incident to the surface of the solid medium must equal the sum of the intensities of the transmitted, absorbed, and reflected beams, denoted as I_T , I_A , and I_R , respectively, or

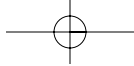
$$I_0 = I_T + I_A + I_R \quad (20.4)$$

Radiation intensity, expressed in watts per square meter, corresponds to the energy being transmitted per unit of time across a unit area that is perpendicular to the direction of propagation.

An alternate form of Equation 20.4 is

$$T + A + R = 1 \quad (20.5)$$

where T , A , and R represent, respectively, the transmissivity (I_T/I_0), absorptivity (I_A/I_0), and reflectivity (I_R/I_0), or the fractions of incident light that are transmitted,



740 • Chapter 20 / Optical Properties

absorbed, and reflected by a material; their sum must equal unity, since all the incident light is either transmitted, absorbed, or reflected.

Materials that are capable of transmitting light with relatively little absorption and reflection are **transparent**—one can see through them. **Translucent** materials are those through which light is transmitted diffusely; that is, light is scattered within the interior, to the degree that objects are not clearly distinguishable when viewed through a specimen of the material. Materials that are impervious to the transmission of visible light are termed **opaque**.

Bulk metals are opaque throughout the entire visible spectrum; that is, all light radiation is either absorbed or reflected. On the other hand, electrically insulating materials can be made to be transparent. Furthermore, some semiconducting materials are transparent whereas others are opaque.

20.4 ATOMIC AND ELECTRONIC INTERACTIONS

The optical phenomena that occur within solid materials involve interactions between the electromagnetic radiation and atoms, ions, and/or electrons. Two of the most important of these interactions are electronic polarization and electron energy transitions.

Electronic Polarization

One component of an electromagnetic wave is simply a rapidly fluctuating electric field (Figure 20.1). For the visible range of frequencies, this electric field interacts with the electron cloud surrounding each atom within its path in such a way as to induce electronic polarization, or to shift the electron cloud relative to the nucleus of the atom with each change in direction of electric field component, as demonstrated in Figure 17.32*a*. Two consequences of this polarization are: (1) some of the radiation energy may be absorbed, and (2) light waves are retarded in velocity as they pass through the medium. The second consequence is manifested as refraction, a phenomenon to be discussed in Section 20.5.

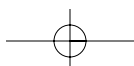
Electron Transitions

The absorption and emission of electromagnetic radiation may involve electron transitions from one energy state to another. For the sake of this discussion, consider an isolated atom, the electron energy diagram for which is represented in Figure 20.3. An electron may be excited from an occupied state at energy E_2 to a vacant and higher-lying one, denoted E_4 , by the absorption of a photon of energy. The change in energy experienced by the electron, ΔE , depends on the radiation frequency as follows:

$$\Delta E = h\nu \quad (20.6)$$

where, again, h is Planck's constant. At this point it is important that several concepts be understood. First, since the energy states for the atom are discrete, only specific ΔE 's exist between the energy levels; thus, only photons of frequencies corresponding to the possible ΔE 's for the atom can be absorbed by electron transitions. Furthermore, all of a photon's energy is absorbed in each excitation event.

A second important concept is that a stimulated electron cannot remain in an **excited state** indefinitely; after a short time, it falls or decays back into its **ground state**, or unexcited level, with a reemission of electromagnetic radiation. Several decay paths are possible, and these are discussed later. In any case, there must be a conservation of energy for absorption and emission electron transitions.



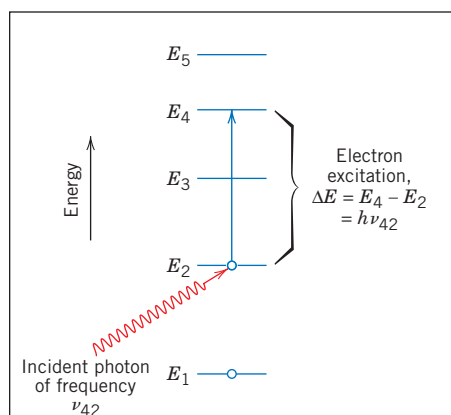


Figure 20.3 For an isolated atom, a schematic illustration of photon absorption by the excitation of an electron from one energy state to another. The energy of the photon ($h\nu_{42}$) must be exactly equal to the difference in energy between the two states ($E_4 - E_2$).

As the ensuing discussions show, the optical characteristics of solid materials that relate to absorption and emission of electromagnetic radiation are explained in terms of the electron band structure of the material (possible band structures were discussed in Section 17.5) and the principles relating to electron transitions, as outlined in the preceding two paragraphs.

Optical Properties of Metals

Consider the electron energy band schemes for metals as illustrated in Figures 17.4a and 18.4b; in both cases a high-energy band is only partially filled with electrons. Metals are opaque because the incident radiation having frequencies within the visible range excites electrons into unoccupied energy states above the Fermi energy, as demonstrated in Figure 20.4a; as a consequence, the incident radiation is absorbed, in accordance with Equation 20.6. Total absorption is within a very thin outer layer, usually less than $0.1 \mu\text{m}$; thus only metallic films thinner than $0.1 \mu\text{m}$ are capable of transmitting visible light.

All frequencies of visible light are absorbed by metals because of the continuously available empty electron states, which permit electron transitions as in Figure 20.4a.

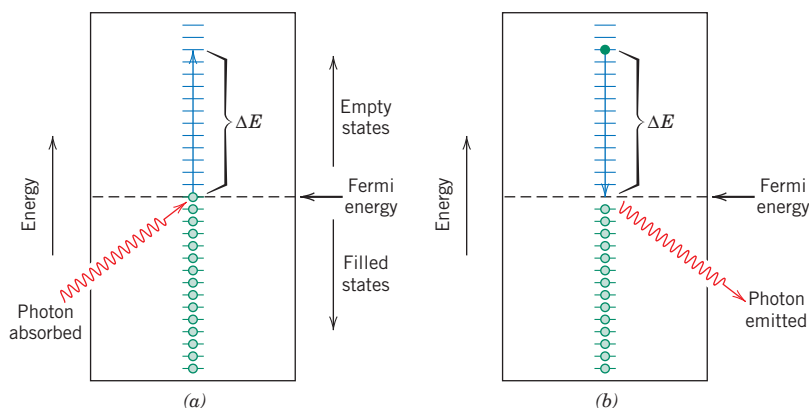


Figure 20.4 (a) Schematic representation of the mechanism of photon absorption for metallic materials in which an electron is excited into a higher-energy unoccupied state. The change in energy of the electron ΔE is equal to the energy of the photon. (b) Reemission of a photon of light by the direct transition of an electron from a high to a low energy state.

742 • Chapter 20 / Optical Properties

In fact, metals are opaque to all electromagnetic radiation on the low end of the frequency spectrum, from radio waves, through infrared, the visible, and into about the middle of the ultraviolet radiation. Metals are transparent to high-frequency (x- and γ -ray) radiation.

Most of the absorbed radiation is reemitted from the surface in the form of visible light of the same wavelength, which appears as reflected light; an electron transition accompanying reradiation is shown in Figure 20.4*b*. The reflectivity for most metals is between 0.90 and 0.95; some small fraction of the energy from electron decay processes is dissipated as heat.

Since metals are opaque and highly reflective, the perceived color is determined by the wavelength distribution of the radiation that is reflected and not absorbed. A bright silvery appearance when exposed to white light indicates that the metal is highly reflective over the entire range of the visible spectrum. In other words, for the reflected beam, the composition of these reemitted photons, in terms of frequency and number, is approximately the same as for the incident beam. Aluminum and silver are two metals that exhibit this reflective behavior. Copper and gold appear red-orange and yellow, respectively, because some of the energy associated with light photons having short wavelengths is not reemitted as visible light.

**Concept Check 20.3**

Why are metals transparent to high-frequency X-ray and γ -ray radiation?

[The answer may be found in enclosed CD.]

Optical Properties of Nonmetals

By virtue of their electron energy band structures, nonmetallic materials may be transparent to visible light. Therefore, in addition to reflection and absorption, refraction and transmission phenomena also need to be considered.

20.5 REFRACTION

Light that is transmitted into the interior of transparent materials experiences a decrease in velocity, and, as a result, is bent at the interface; this phenomenon is termed **refraction**. The **index of refraction** n of a material is defined as the ratio of the velocity in a vacuum c to the velocity in the medium v , or

$$n = \frac{c}{v} \quad (20.7)$$

The magnitude of n (or the degree of bending) will depend on the wavelength of the light. This effect is graphically demonstrated by the familiar dispersion or separation of a beam of white light into its component colors by a glass prism. Each color is deflected by a different amount as it passes into and out of the glass, which results in the separation of the colors. Not only does the index of refraction affect the optical path of light, but also, as explained below, it influences the fraction of incident light that is reflected at the surface.

Just as Equation 20.1 defines the magnitude of c , an equivalent expression gives the velocity of light v in a medium as

$$v = \frac{1}{\sqrt{\epsilon\mu}} \quad (20.8)$$

where ϵ and μ are, respectively, the permittivity and permeability of the particular substance. From Equation 20.7, we have

$$n = \frac{c}{v} = \frac{\sqrt{\epsilon\mu}}{\sqrt{\epsilon_0\mu_0}} = \sqrt{\epsilon_r\mu_r} \quad (20.9)$$

where ϵ_r and μ_r are the dielectric constant and the relative magnetic permeability, respectively. Since most substances are only slightly magnetic, $\mu_r \cong 1$, and

$$n \cong \sqrt{\epsilon_r} \quad (20.10)$$

Thus, for transparent materials, there is a relation between the index of refraction and the dielectric constant. As already mentioned, the phenomenon of refraction is related to electronic polarization (Section 20.4) at the relatively high frequencies for visible light; thus, the electronic component of the dielectric constant may be determined from index of refraction measurements using Equation 20.10.

Since the retardation of electromagnetic radiation in a medium results from electronic polarization, the size of the constituent atoms or ions has a considerable influence on the magnitude of this effect—generally, the larger an atom or ion, the greater will be the electronic polarization, the slower the velocity, and the greater the index of refraction. The index of refraction for a typical soda–lime glass is approximately 1.5. Additions of large barium and lead ions (as BaO and PbO) to a glass will increase n significantly. For example, highly leaded glasses containing 90 wt% PbO have an index of refraction of approximately 2.1.

For crystalline ceramics that have cubic crystal structures, and for glasses, the index of refraction is independent of crystallographic direction (i.e., it is isotropic). Noncubic crystals, on the other hand, have an anisotropic n ; that is, the index is greatest along the directions that have the highest density of ions. Table 20.1 gives refractive indices for several glasses, transparent ceramics, and polymers. Average values are provided for the crystalline ceramics in which n is anisotropic.

Table 20.1 Refractive Indices for Some Transparent Materials

<i>Material</i>	<i>Average Index of Refraction</i>
Ceramics	
Silica glass	1.458
Borosilicate (Pyrex) glass	1.47
Soda–lime glass	1.51
Quartz (SiO ₂)	1.55
Dense optical flint glass	1.65
Spinel (MgAl ₂ O ₄)	1.72
Periclase (MgO)	1.74
Corundum (Al ₂ O ₃)	1.76
Polymers	
Polytetrafluoroethylene	1.35
Polymethyl methacrylate	1.49
Polypropylene	1.49
Polyethylene	1.51
Polystyrene	1.60



Concept Check 20.4

Which of the following oxide materials when added to fused silica (SiO_2) will increase its index of refraction: Al_2O_3 , TiO_2 , NiO , MgO ? Why? You may find Table 4.4 helpful.

[The answer may be found in enclosed CD.]

20.6 REFLECTION

When light radiation passes from one medium into another having a different index of refraction, some of the light is scattered at the interface between the two media even if both are transparent. The reflectivity R represents the fraction of the incident light that is reflected at the interface, or

$$R = \frac{I_R}{I_0} \quad (20.11)$$

where I_0 and I_R are the intensities of the incident and reflected beams, respectively. If the light is normal (or perpendicular) to the interface, then

$$R = \left(\frac{n_2 - n_1}{n_2 + n_1} \right)^2 \quad (20.12)$$

where n_1 and n_2 are the indices of refraction of the two media. If the incident light is not normal to the interface, R will depend on the angle of incidence. When light is transmitted from a vacuum or air into a solid s , then

$$R = \left(\frac{n_s - 1}{n_s + 1} \right)^2 \quad (20.13)$$

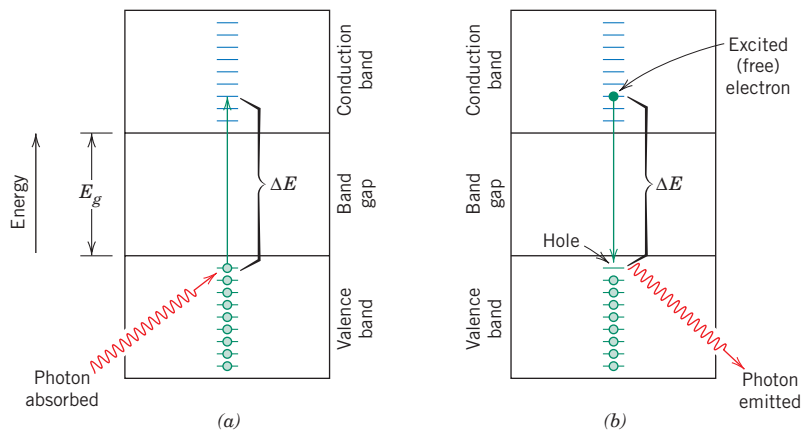
since the index of refraction of air is very nearly unity. Thus, the higher the index of refraction of the solid, the greater is the reflectivity. For typical silicate glasses, the reflectivity is approximately 0.05. Just as the index of refraction of a solid depends on the wavelength of the incident light, so also does the reflectivity vary with wavelength. Reflection losses for lenses and other optical instruments are minimized significantly by coating the reflecting surface with very thin layers of dielectric materials such as magnesium fluoride (MgF_2).

20.7 ABSORPTION

Nonmetallic materials may be opaque or transparent to visible light; and, if transparent, they often appear colored. In principle, light radiation is absorbed in this group of materials by two basic mechanisms, which also influence the transmission characteristics of these nonmetals. One of these is electronic polarization (Section 20.4). Absorption by electronic polarization is important only at light frequencies in the vicinity of the relaxation frequency of the constituent atoms. The other mechanism involves valence band-conduction band electron transitions, which depend on the electron energy band structure of the material; band structures for semiconductors and insulators were discussed in Section 17.5.

Absorption of a photon of light may occur by the promotion or excitation of an electron from the nearly filled valence band, across the band gap, and into an empty state within the conduction band, as demonstrated in Figure 20.5a; a

Figure 20.5 (a) Mechanism of photon absorption for nonmetallic materials in which an electron is excited across the band gap, leaving behind a hole in the valence band. The energy of the photon absorbed is ΔE , which is necessarily greater than the band gap energy E_g . (b) Emission of a photon of light by a direct electron transition across the band gap.



free electron in the conduction band and a hole in the valence band are created. Again, the energy of excitation ΔE is related to the absorbed photon frequency through Equation 20.6. These excitations with the accompanying absorption can take place only if the photon energy is greater than that of the band gap E_g —that is, if

$$h\nu > E_g \quad (20.14)$$

or, in terms of wavelength,

$$\frac{hc}{\lambda} > E_g \quad (20.15)$$

The minimum wavelength for visible light, $\lambda(\text{min})$, is about $0.4 \mu\text{m}$, and since $c = 3 \times 10^8 \text{ m/s}$ and $h = 4.13 \times 10^{-15} \text{ eV}\cdot\text{s}$, the maximum band gap energy $E_g(\text{max})$ for which absorption of visible light is possible is just

$$\begin{aligned} E_g(\text{max}) &= \frac{hc}{\lambda(\text{min})} \\ &= \frac{(4.13 \times 10^{-15} \text{ eV}\cdot\text{s})(3 \times 10^8 \text{ m/s})}{4 \times 10^{-7} \text{ m}} \\ &= 3.1 \text{ eV} \end{aligned} \quad (20.16a)$$

Or, no visible light is absorbed by nonmetallic materials having band gap energies greater than about 3.1 eV; these materials, if of high purity, will appear transparent and colorless.

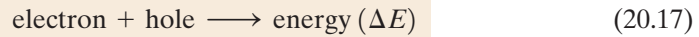
On the other hand, the maximum wavelength for visible light, $\lambda(\text{max})$, is about $0.7 \mu\text{m}$; computation of the minimum band gap energy $E_g(\text{min})$ for which there is absorption of visible light is according to

$$\begin{aligned} E_g(\text{min}) &= \frac{hc}{\lambda(\text{max})} \\ &= \frac{(4.13 \times 10^{-15} \text{ eV}\cdot\text{s})(3 \times 10^8 \text{ m/s})}{7 \times 10^{-7} \text{ m}} = 1.8 \text{ eV} \end{aligned} \quad (20.16b)$$

This result means that all visible light is absorbed by valence band to conduction band electron transitions for those semiconducting materials that have band gap energies less than about 1.8 eV; thus, these materials are opaque. Only a portion of the visible spectrum is absorbed by materials having band gap energies between 1.8 and 3.1 eV; consequently, these materials appear colored.

Every nonmetallic material becomes opaque at some wavelength, which depends on the magnitude of its E_g . For example, diamond, having a band gap of 5.6 eV, is opaque to radiation having wavelengths less than about 0.22 μm .

Interactions with light radiation can also occur in dielectric solids having wide band gaps, involving other than valence band-conduction band electron transitions. If impurities or other electrically active defects are present, electron levels within the band gap may be introduced, such as the donor and acceptor levels (Section 17.11), except that they lie closer to the center of the band gap. Light radiation of specific wavelengths may be emitted as a result of electron transitions involving these levels within the band gap. For example, consider Figure 20.6a, which shows the valence band-conduction band electron excitation for a material that has one such impurity level. Again, the electromagnetic energy that was absorbed by this electron excitation must be dissipated in some manner; several mechanisms are possible. For one, this dissipation may occur via direct electron and hole recombination according to the reaction



which is represented schematically in Figure 20.5b. In addition, multiple-step electron transitions may occur, which involve impurity levels lying within the band gap. One possibility, as indicated in Figure 20.6b, is the emission of two photons; one is emitted as the electron drops from a state in the conduction band to the impurity level, the other as it decays back into the valence band. Alternatively, one of the transitions may involve the generation of a phonon (Figure 20.6c), wherein the associated energy is dissipated in the form of heat.

The intensity of the net absorbed radiation is dependent on the character of the medium as well as the path length within. The intensity of transmitted or

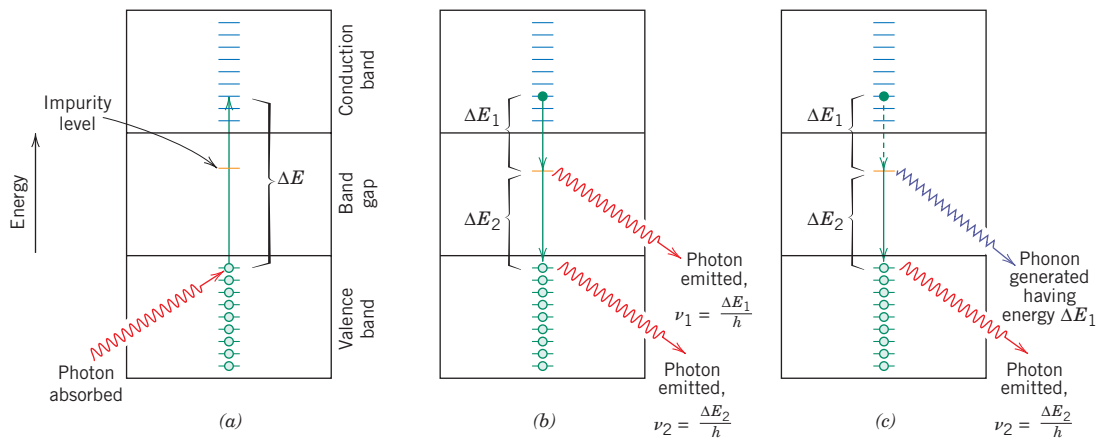


Figure 20.6 (a) Photon absorption via a valence band-conduction band electron excitation for a material that has an impurity level that lies within the band gap. (b) Emission of two photons involving electron decay first into an impurity state, and finally to the ground state. (c) Generation of both a phonon and a photon as an excited electron falls first into an impurity level and finally back to its ground state.

nonabsorbed radiation I_T' continuously decreases with distance x that the light traverses:

$$I_T' = I_0' e^{-\beta x} \quad (20.18)$$

where I_0' is the intensity of the nonreflected incident radiation and β , the *absorption coefficient* (in mm^{-1}), is characteristic of the particular material; furthermore, β varies with wavelength of the incident radiation. The distance parameter x is measured from the incident surface into the material. Materials that have large β values are considered to be highly absorptive.

EXAMPLE PROBLEM 20.1

Computation of the Absorption Coefficient for Glass

The fraction of nonreflected light that is transmitted through a 200 mm thickness of glass is 0.98. Calculate the absorption coefficient of this material.

Solution

This problem calls for us to solve for β in Equation 20.18. We first of all rearrange this expression as

$$\frac{I_T'}{I_0'} = e^{-\beta x}$$

Now taking logarithms of both sides of the above equation leads to

$$\ln\left(\frac{I_T'}{I_0'}\right) = -\beta x$$

And, finally, solving for β , realizing that $I_T'/I_0' = 0.98$ and $x = 200$ mm, yields

$$\begin{aligned} \beta &= -\frac{1}{x} \ln\left(\frac{I_T'}{I_0'}\right) \\ &= -\frac{1}{200 \text{ mm}} \ln(0.98) = 1.01 \times 10^{-4} \text{ mm}^{-1} \end{aligned}$$



Concept Check 20.5

Are the elemental semiconductors silicon and germanium transparent to visible light? Why or why not? *Hint:* you may want to consult Table 17.3.

[The answer may be found in enclosed CD.]

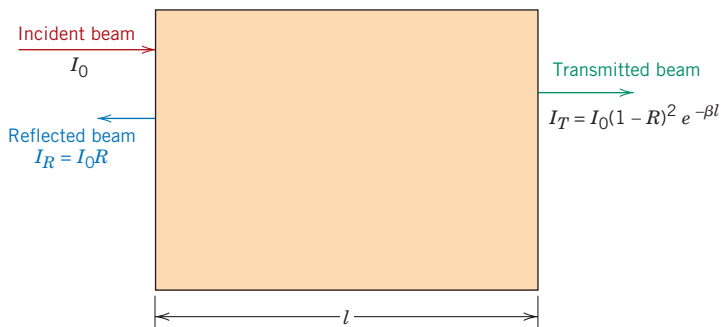
20.8 TRANSMISSION

The phenomena of absorption, reflection, and transmission may be applied to the passage of light through a transparent solid, as shown in Figure 20.7. For an incident beam of intensity I_0 that impinges on the front surface of a specimen of thickness l and absorption coefficient β , the transmitted intensity at the back face I_T is

$$I_T = I_0(1 - R)^2 e^{-\beta l} \quad (20.19)$$

748 • Chapter 20 / Optical Properties

Figure 20.7 The transmission of light through a transparent medium for which there is reflection at front and back faces, as well as absorption within the medium. (Adapted from R. M. Rose, L. A. Shepard, and J. Wulff, *The Structure and Properties of Materials*, Vol. 4, *Electronic Properties*. Copyright © 1966 by John Wiley & Sons, New York. Reprinted by permission of John Wiley & Sons, Inc.)



where R is the reflectance; for this expression, it is assumed that the same medium exists outside both front and back faces. The derivation of Equation 20.19 is left as a homework problem.

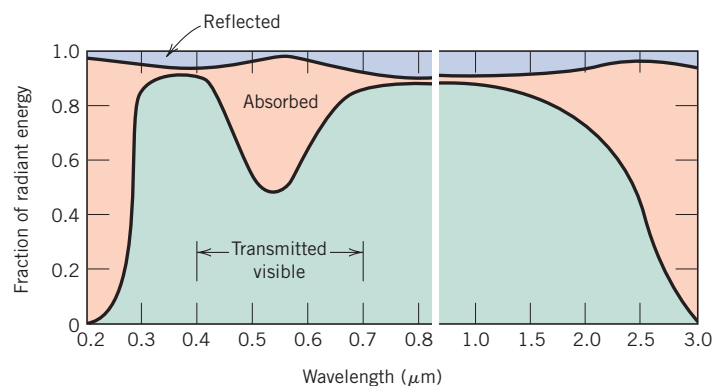
Thus, the fraction of incident light that is transmitted through a transparent material depends on the losses that are incurred by absorption and reflection. Again, the sum of the reflectivity R , absorptivity A , and transmissivity T , is unity according to Equation 20.5. Also, each of the variables R , A , and T depends on light wavelength. This is demonstrated over the visible region of the spectrum for a green glass in Figure 20.8. For example, for light having a wavelength of $0.4 \mu\text{m}$, the fractions transmitted, absorbed, and reflected are approximately 0.90, 0.05, and 0.05, respectively. However, at $0.55 \mu\text{m}$, the respective fractions have shifted to about 0.50, 0.48, and 0.02.

20.9 COLOR

Transparent materials appear colored as a consequence of specific wavelength ranges of light that are selectively absorbed; the **color** discerned is a result of the combination of wavelengths that are transmitted. If absorption is uniform for all visible wavelengths, the material appears colorless; examples include high-purity inorganic glasses and high-purity and single-crystal diamonds and sapphire.

Usually, any selective absorption is by electron excitation. One such situation involves semiconducting materials that have band gaps within the range of photon energies for visible light (1.8 to 3.1 eV). Thus, the fraction of the visible light having energies greater than E_g is selectively absorbed by valence band–conduction band electron transitions. Of course, some of this absorbed radiation is reemitted as the excited electrons drop back into their original, lower-lying energy states. It is not necessary that this reemission occur at the same frequency as that of the absorption. As a result, the color depends on the frequency distribution of both transmitted and reemitted light beams.

Figure 20.8 The variation with wavelength of the fractions of incident light transmitted, absorbed, and reflected through a green glass. (From W. D. Kingery, H. K. Bowen, and D. R. Uhlmann, *Introduction to Ceramics*, 2nd edition. Copyright © 1976 by John Wiley & Sons, New York. Reprinted by permission of John Wiley & Sons, Inc.)



For example, cadmium sulfide (CdS) has a band gap of about 2.4 eV; hence, it absorbs photons having energies greater than about 2.4 eV, which correspond to the blue and violet portions of the visible spectrum; some of this energy is reradiated as light having other wavelengths. Nonabsorbed visible light consists of photons having energies between about 1.8 and 2.4 eV. Cadmium sulfide takes on a yellow-orange color because of the composition of the transmitted beam.

With insulator ceramics, specific impurities also introduce electron levels within the forbidden band gap, as discussed above. Photons having energies less than the band gap may be emitted as a consequence of electron decay processes involving impurity atoms or ions as demonstrated in Figures 20.6b and 20.6c. Again, the color of the material is a function of the distribution of wavelengths that is found in the transmitted beam.

For example, high-purity and single-crystal aluminum oxide or sapphire is colorless. Ruby, which has a brilliant red color, is simply sapphire to which has been added 0.5 to 2% of chromium oxide (Cr_2O_3). The Cr^{3+} ion substitutes for the Al^{3+} ion in the Al_2O_3 crystal structure and, furthermore, introduces impurity levels within the wide energy band gap of the sapphire. Light radiation is absorbed by valence band-conduction band electron transitions, some of which is then reemitted at specific wavelengths as a consequence of electron transitions to and from these impurity levels. The transmittance as a function of wavelength for sapphire and ruby is presented in Figure 20.9. For the sapphire, transmittance is relatively constant with wavelength over the visible spectrum, which accounts for the colorlessness of this material. However, strong absorption peaks (or minima) occur for the ruby, one in the blue-violet region (at about $0.4 \mu\text{m}$), and the other for yellow-green light (at about $0.6 \mu\text{m}$). That nonabsorbed or transmitted light mixed with reemitted light imparts to ruby its deep-red color.

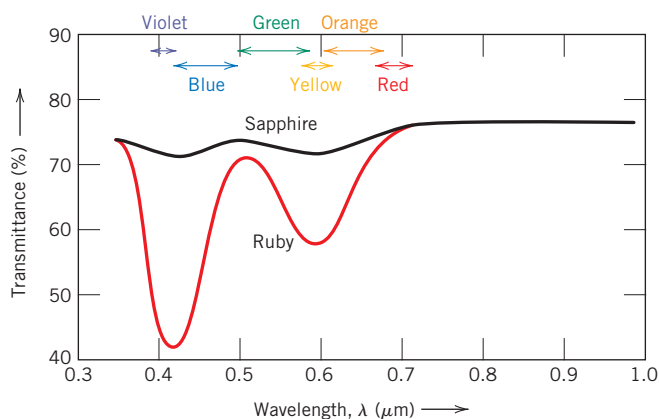
Inorganic glasses are colored by incorporating transition or rare earth ions while the glass is still in the molten state. Representative color-ion pairs include Cu^{2+} , blue-green; Co^{2+} , blue-violet; Cr^{3+} , green; Mn^{2+} , yellow; and Mn^{3+} , purple. These colored glasses are also used as glazes, decorative coatings on ceramic ware.

✓ Concept Check 20.6

Compare those factors that determine the characteristic colors of metals and transparent nonmetals.

[The answer may be found in enclosed CD.]

Figure 20.9 Transmission of light radiation as a function of wavelength for sapphire (single-crystal aluminum oxide) and ruby (aluminum oxide containing some chromium oxide). The sapphire appears colorless, while the ruby has a red tint due to selective absorption over specific wavelength ranges. (Adapted from “The Optical Properties of Materials,” by A. Javan. Copyright © 1967 by Scientific American, Inc. All rights reserved.)



20.10 OPACITY AND TRANSLUCENCY IN INSULATORS

The extent of translucency and opacity for inherently transparent dielectric materials depends to a great degree on their internal reflectance and transmittance characteristics. Many dielectric materials that are intrinsically transparent may be made translucent or even opaque because of interior reflection and refraction. A transmitted light beam is deflected in direction and appears diffuse as a result of multiple scattering events. Opacity results when the scattering is so extensive that virtually none of the incident beam is transmitted, undeflected, to the back surface.

This internal scattering may result from several different sources. Polycrystalline specimens in which the index of refraction is anisotropic normally appear translucent. Both reflection and refraction occur at grain boundaries, which causes a diversion in the incident beam. This results from a slight difference in index of refraction n between adjacent grains that do not have the same crystallographic orientation.

Scattering of light also occurs in two-phase materials in which one phase is finely dispersed within the other. Again, the beam dispersion occurs across phase boundaries when there is a difference in the refractive index for the two phases; the greater this difference, the more efficient is the scattering. Glass-ceramics (Section 12.3), which may consist of both crystalline and residual glass phases, will appear highly transparent if the sizes of the crystallites are smaller than the wavelength of visible light, and when the indices of refraction of the two phases are nearly identical (which is possible by adjustment of composition).

As a consequence of fabrication or processing, many ceramic pieces contain some residual porosity in the form of finely dispersed pores. These pores also effectively scatter light radiation.

Figure 20.10 demonstrates the difference in optical transmission characteristics of single-crystal, fully dense polycrystalline, and porous (~5% porosity) aluminum oxide specimens. Whereas the single crystal is totally transparent, polycrystalline and porous materials are, respectively, translucent and opaque.

For intrinsic polymers (without additives and impurities), the degree of translucency is influenced primarily by the extent of crystallinity. Some scattering of visible light occurs at the boundaries between crystalline and amorphous regions, again as a result of different indices of refraction. For highly crystalline specimens, this degree of scattering is extensive, which leads to translucency, and, in some instances, even opacity. Highly amorphous polymers are completely transparent.

Figure 20.10 Photograph showing the light transmittance of three aluminum oxide specimens. From left to right; single-crystal material (sapphire), which is transparent; a polycrystalline and fully dense (nonporous) material, which is translucent; and a polycrystalline material that contains approximately 5% porosity, which is opaque. (Specimen preparation, P. A. Lessing; photography by S. Tanner.)



Applications of Optical Phenomena

20.11 LUMINESCENCE

Some materials are capable of absorbing energy and then reemitting visible light in a phenomenon called **luminescence**. Photons of emitted light are generated from electron transitions in the solid. Energy is absorbed when an electron is promoted to an excited energy state; visible light is emitted when it falls back to a lower energy state if $1.8 \text{ eV} < h\nu < 3.1 \text{ eV}$. The absorbed energy may be supplied as higher-energy electromagnetic radiation (causing valence band–conduction band transitions, Figure 20.6a) such as ultraviolet light, or other sources such as high energy electrons, or by heat, mechanical, or chemical energy. Furthermore, luminescence is classified according to the magnitude of the delay time between absorption and reemission events. If reemission occurs for times much less than one second, the phenomenon is termed **fluorescence**; for longer times, it is called **phosphorescence**. A number of materials can be made to fluoresce or phosphoresce; these include some sulfides, oxides, tungstates, and a few organic materials. Ordinarily, pure materials do not display these phenomena, and to induce them, impurities in controlled concentrations must be added.

Luminescence has a number of commercial applications. Fluorescent lamps consist of a glass housing, coated on the inside with specially prepared tungstates or silicates. Ultraviolet light is generated within the tube from a mercury glow discharge, which causes the coating to fluoresce and emit white light. The picture viewed on a television screen (cathode ray tube screen) is the product of luminescence. The inside of the screen is coated with a material that fluoresces as an electron beam inside the picture tube very rapidly traverses the screen. Detection of x-rays and γ -rays is also possible; certain phosphors emit visible light or glow when introduced into a beam of the radiation that is otherwise invisible.

20.12 PHOTOCONDUCTIVITY

The conductivity of semiconducting materials depends on the number of free electrons in the conduction band and also the number of holes in the valence band, according to Equation 17.13. Thermal energy associated with lattice vibrations can promote electron excitations in which free electrons and/or holes are created, as described in Section 17.6. Additional charge carriers may be generated as a consequence of photon-induced electron transitions in which light is absorbed; the attendant increase in conductivity is called **photoconductivity**. Thus, when a specimen of a photoconductive material is illuminated, the conductivity increases.

This phenomenon is utilized in photographic light meters. A photoinduced current is measured, and its magnitude is a direct function of the intensity of the incident light radiation, or the rate at which the photons of light strike the photoconductive material. Of course, visible light radiation must induce electronic transitions in the photoconductive material; cadmium sulfide is commonly utilized in light meters.

Sunlight may be directly converted into electrical energy in solar cells, which also employ semiconductors. The operation of these devices is, in a sense, the reverse of that for the light-emitting diode. A p - n junction is used in which photoexcited electrons and holes are drawn away from the junction, in opposite directions, and become part of an external current.

MATERIALS OF IMPORTANCE

Light-Emitting Diodes

In Section 17.15 we discussed semiconductor p - n junctions, and how they may be used as diodes or as rectifiers of an electric current.¹ Furthermore, in some situations, when a forward-biased potential of relatively high magnitude is applied across a p - n junction diode, visible light (or infrared radiation) will be emitted. This conversion of electrical energy into light energy is termed **electroluminescence**, and the device that produces it is termed a **light-emitting diode (LED)**. The forward-biased potential attracts electrons on the n -side toward the junction, where some of them pass into (or are “injected” into) the p -side (Figure 20.11a). Here, the electrons are minority charge carriers, and as such, they “recombine” with, or are annihilated by the holes in the region near the junction, according to Equation 20.17, where the energy is in the form of photons of light (Figure 20.11b). An analogous process occurs on the p -side—i.e., holes travel to the junction, and recombine with the majority electrons on the n -side.

The elemental semiconductors, silicon and germanium, are not suitable for LEDs due to the detailed natures of their band gap structures. Rather, some of the III-V semiconducting compounds such as gallium arsenide (GaAs), indium phosphide (InP), and alloys composed of these materials (i.e., $\text{GaAs}_x\text{P}_{1-x}$, where x is a small number less than unity) are frequently used. Furthermore, the wavelength (i.e., color) of the emitted radiation is related to the band gap of the semiconductor (which is normally the same for both n - and p -sides of the diode). For example, red, orange, and yellow colors are possible for the GaAs–InP system. And, blue and green LEDs have been developed using (Ga, In)N semiconducting alloys. Thus, with this comple-

¹ Schematic diagrams showing electron and hole distributions on both sides of the junction, with no applied electric potential, as well as for both forward and reverse biases are presented in Figure 17.20. In addition, Figure 17.22 shows the current-versus-voltage behavior for a p - n junction.

ment of colors, full-color displays are possible using LEDs.

Several important applications for semiconductor LEDs include digital clocks and illuminated watch displays, optical mice (computer input devices), and film scanners. Electronic remote controls (for televisions, DVD players, etc.) also employ LEDs that emit an infrared beam; this beam transmits coded signals that are picked up by detectors in the receiving devices. In addition, LEDs are now being used for light sources. They are more energy efficient than incandescent lights, generate very little heat, and have much longer lifetimes (since there is no filament that can burn out). Most new traffic control signals use LEDs instead of incandescent lights.

We noted in Section 17.17 that some polymeric materials may be semiconductors (both

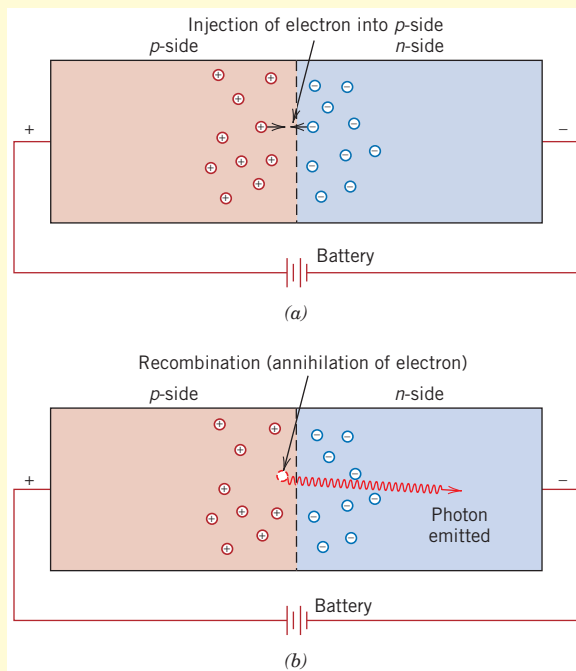


Figure 20.11 Schematic diagram of a forward-biased semiconductor p - n junction showing (a) the injection of an electron from the n -side into the p -side, and (b) the emission of a photon of light as this electron recombines with a hole.

n- and *p*-type). As a consequence, light-emitting diodes made of polymers are possible, of which there are two types: (1) *organic light-emitting diodes* (or *OLEDs*), which have relatively low molecular weights; and (2) the high molecular-weight *polymer light-emitting diodes* (or *PLEDs*). For these LED types, amorphous polymers are used in the form of thin layers that are sandwiched together with electrical contacts (anodes and cathodes). In order for the light to be emitted from the LED, one of the contacts must be transparent. Figure 20.12 is a schematic illustration that shows the components and configuration of an OLED. A wide variety of colors is possible using OLEDs and PLEDs, and, in fact, more than a single color may be produced from each device (such is not possible with semiconductor LEDs)—thus, combining colors makes it possible to generate white light.

Although the semiconductor LEDs currently have longer lifetimes than these organic emitters, OLEDs/PLEDs have distinct advantages. In addition to generating multiple colors, they are easier to fabricate (by “printing” onto their substrates with an ink jet printer), are relatively inexpensive, have slimmer profiles, and can be patterned to give high-resolution and full-color images. OLED displays are currently being mar-

keted for use on digital cameras, cell phones, and car audio components. Potential applications include larger displays for televisions, computers, and bill boards. In addition, using the right combination of materials, these displays can also be flexible. Can you imagine having a computer monitor or television that can be rolled up a like projection screen, or a lighting fixture that is wrapped around an architectural column or is mounted on a room wall to make ever-changing wallpaper?

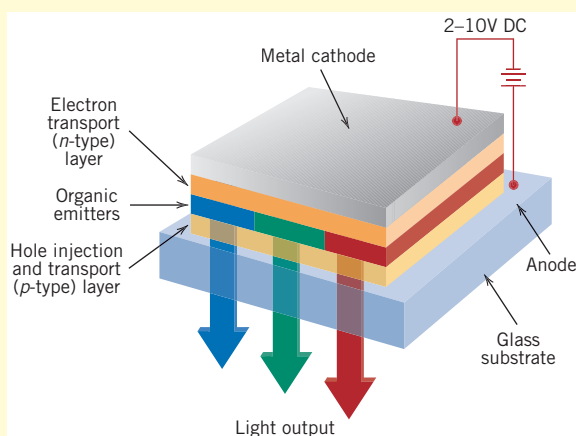


Figure 20.12 Schematic diagram that shows the components and configuration of an organic light-emitting diode (OLED). (Reproduced by arrangement with *Silicon Chip* magazine.)



Photograph showing a very large light-emitting diode video display located at the corner of Broadway and 43rd Street in New York City. (© Stephen Chemin/Getty Images news as Sports Services.)

✓ Concept Check 20.7

Is the semiconductor zinc selenide (ZnSe), which has a band gap of 2.58 eV, photoconductive when exposed to visible light radiation? Why or why not?

[The answer may be found in enclosed CD.]

20.13 LASERS

All the radiative electron transitions heretofore discussed are spontaneous; that is, an electron falls from a high energy state to a lower one without any external provocation. These transition events occur independently of one another and at random times, producing radiation that is incoherent; that is, the light waves are out of phase with one another. With lasers, however, coherent light is generated by electron transitions initiated by an external stimulus; in fact, “**laser**” is just the acronym for *light amplification by stimulated emission of radiation*.

Although there are several different varieties of laser, the principles of operation are explained using the solid-state ruby laser. Ruby is simply a single crystal of Al_2O_3 (sapphire) to which has been added on the order of 0.05% Cr^{3+} ions. As previously explained (Section 20.9), these ions impart to ruby its characteristic red color; more important, they provide electron states that are essential for the laser to function. The ruby laser is in the form of a rod, the ends of which are flat, parallel, and highly polished. Both ends are silvered such that one is totally reflecting and the other partially transmitting.

The ruby is illuminated with light from a xenon flash lamp (Figure 20.13). Before this exposure, virtually all the Cr^{3+} ions are in their ground states; that is, electrons fill the lowest energy levels, as represented schematically in Figure 20.14. However, photons of wavelength $0.56\ \mu\text{m}$ from the xenon lamp excite electrons from the Cr^{3+} ions into higher energy states. These electrons can decay back into their ground state by two different paths. Some fall back directly; associated photon emissions are not part of the laser beam. Other electrons decay into a metastable intermediate state (path *EM*, Figure 20.14), where they may reside for up to 3 ms (milliseconds) before spontaneous emission (path *MG*). In terms of electronic processes, 3 ms is a relatively long time, which means that a large number of these metastable states may become occupied. This situation is indicated in Figure 20.15*b*.

The initial spontaneous photon emission by a few of these electrons is the stimulus that triggers an avalanche of emissions from the remaining electrons in

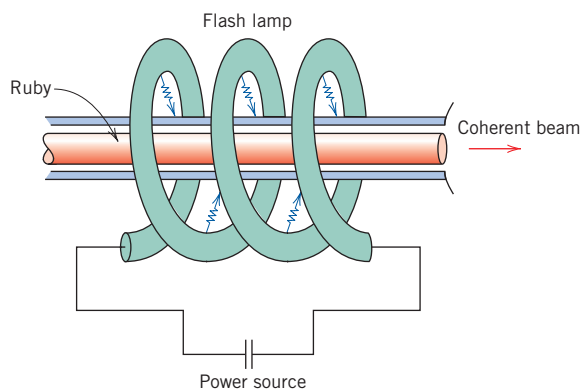


Figure 20.13 Schematic diagram of the ruby laser and xenon flash lamp. (From R. M. Rose, L. A. Shepard, and J. Wulff, *The Structure and Properties of Materials*, Vol. 4, *Electronic Properties*. Copyright © 1966 by John Wiley & Sons, New York. Reprinted by permission of John Wiley & Sons, Inc.)

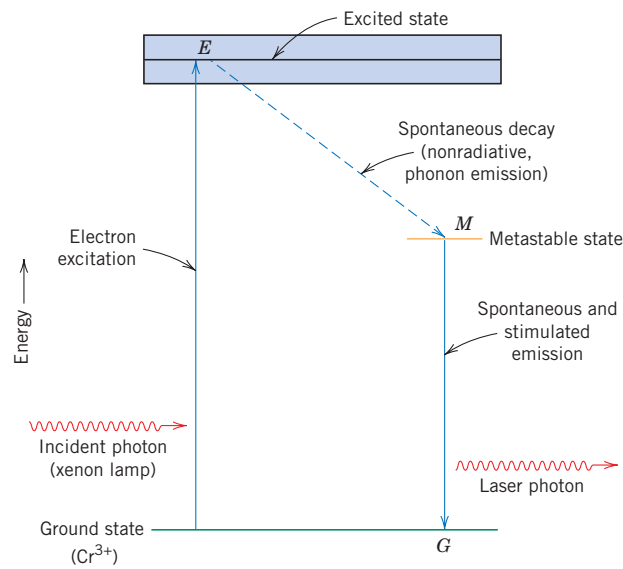


Figure 20.14 Schematic energy diagram for the ruby laser, showing electron excitation and decay paths.

the metastable state (Figure 20.15c). Of the photons directed parallel to the long axis of the ruby rod, some are transmitted through the partially silvered end; others, incident to the totally silvered end, are reflected. Photons that are not emitted in this axial direction are lost. The light beam repeatedly travels back

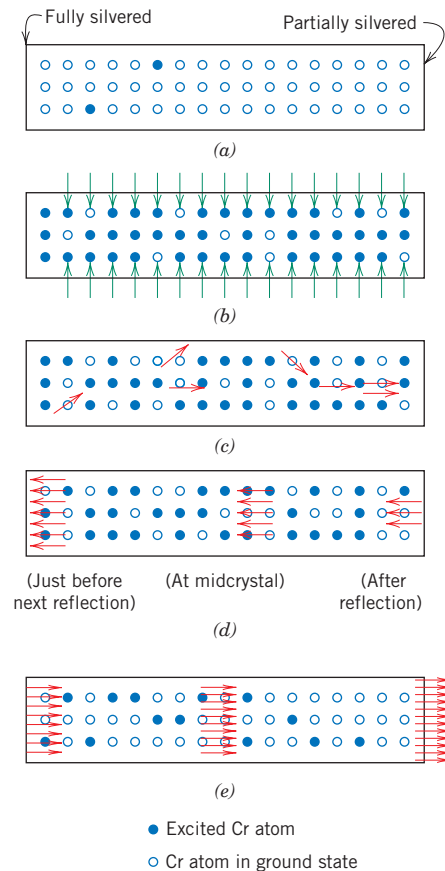


Figure 20.15 Schematic representations of the stimulated emission and light amplification for a ruby laser. (a) The chromium ions before excitation. (b) Electrons in some chromium ions are excited into higher energy states by the xenon light flash. (c) Emission from metastable electron states is initiated or stimulated by photons that are spontaneously emitted. (d) Upon reflection from the silvered ends, the photons continue to stimulate emissions as they traverse the rod length. (e) The coherent and intense beam is finally emitted through the partially silvered end. (From R. M. Rose, L. A. Shepard, and J. Wulff, *The Structure and Properties of Materials*, Vol. 4, *Electronic Properties*. Copyright © 1966 by John Wiley & Sons, New York. Reprinted by permission of John Wiley & Sons, Inc.)

756 • Chapter 20 / Optical Properties

and forth along the rod length, and its intensity increases as more emissions are stimulated. Ultimately, a high intensity, coherent, and highly collimated laser light beam of short duration is transmitted through the partially silvered end of the rod (Figure 20.15e). This monochromatic red beam has a wavelength of $0.6943 \mu\text{m}$.

Semiconducting materials such as gallium arsenide may also be used as lasers that are employed in compact disk players and in the modern telecommunications industry. One requirement of these semiconducting materials is that the wavelength

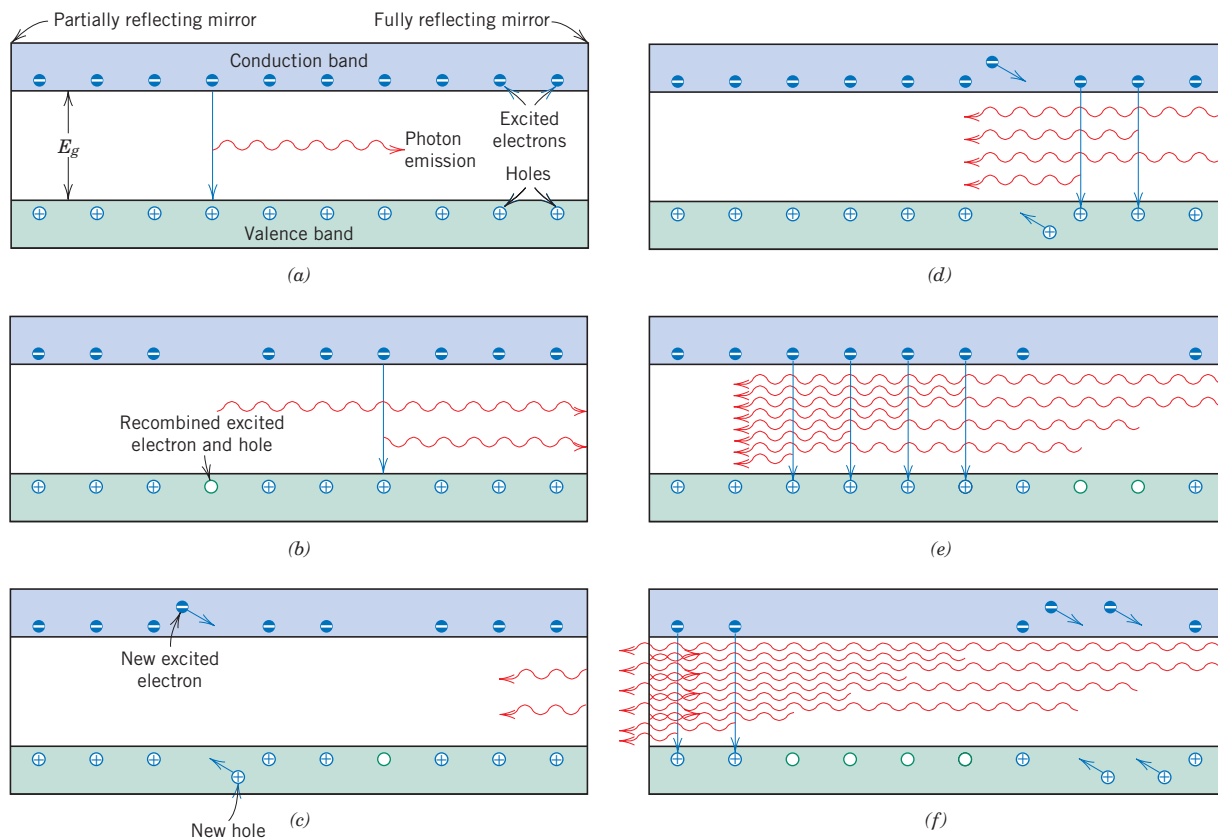


Figure 20.16 For the semiconductor laser, schematic representations of the stimulated recombination of excited electrons in the conduction band with holes in the valence band that gives rise to a laser beam. (a) One excited electron recombines with a hole; the energy associated with this recombination is emitted as a photon of light. (b) The photon emitted in (a) stimulates the recombination of another excited electron and hole resulting in the emission of another photon of light. (c) The two photons emitted in (a) and (b), having the same wavelength and being in phase with one another, are reflected by the fully reflecting mirror, back into the laser semiconductor. In addition, new excited electrons and new holes are generated by a current that passes through the semiconductor. (d) and (e) In proceeding through the semiconductor, more excited electron–hole recombinations are stimulated, which give rise to additional photons of light that also become part of the monochromatic and coherent laser beam. (f) Some portion of this laser beam escapes through the partially reflecting mirror at one end of the semiconducting material. (Adapted from “Photonic Materials,” by J. M. Rowell. Copyright © 1986 by Scientific American, Inc. All rights reserved.)

λ associated with the band gap energy E_g must correspond to visible light. That is, from a modification of Equation 20.3, namely

$$\lambda = \frac{hc}{E_g} \quad (20.20)$$

λ must lie between 0.4 and 0.7 μm . A voltage applied to the material excites electrons from the valence band, across the band gap, and into the conduction band; correspondingly, holes are created in the valence band. This process is demonstrated in Figure 20.16*a*, which shows the energy band scheme over some region of the semiconducting material, along with several holes and excited electrons. Subsequently, a few of these excited electrons and holes spontaneously recombine. For each recombination event, a photon of light having a wavelength given by Equation 20.20 is emitted (Figure 20.16*a*). One such photon will stimulate the recombination of other excited electron–hole pairs, Figure 20.16*b–f*, and the production of additional photons that have the same wavelength and are all in phase with one another and with the original photon; thus, a monochromatic and coherent beam results. As with the ruby laser (Figure 20.15), one end of the semiconductor laser is totally reflecting; at this end, the beam is reflected back into the material so that additional recombinations will be stimulated. The other end of the laser is partially reflecting, which allows for some of the beam to escape. Furthermore, with this type of laser, a continuous beam is produced inasmuch as a constant applied voltage ensures that there is always a steady source of holes and excited electrons.

The semiconductor laser is composed of several layers of semiconducting materials that have different compositions and are sandwiched between a heat sink and a metal conductor; a typical arrangement is represented schematically in Figure 20.17. The compositions of the layers are chosen so as to confine both the excited electrons and holes as well as the laser beam to within the central gallium arsenide layer.

A variety of other substances may be used for lasers, including some gases and glasses. Table 20.2 lists several common lasers and their characteristics. Laser

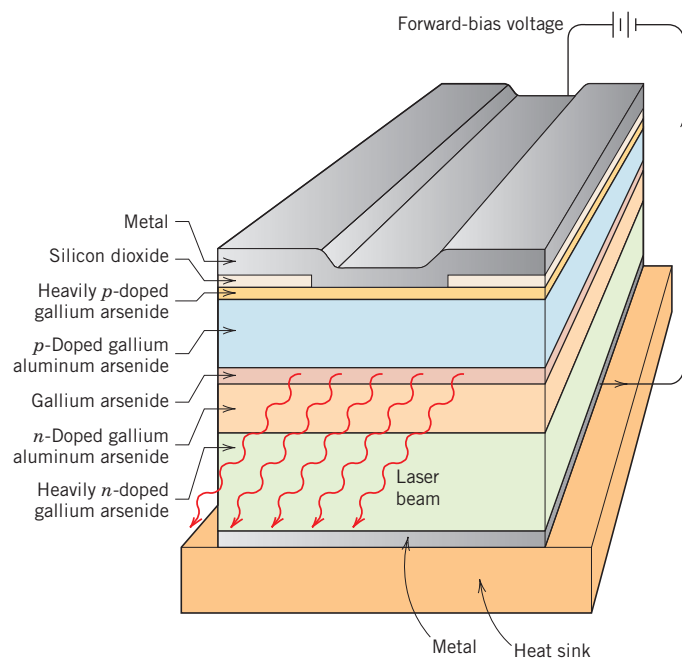


Figure 20.17 Schematic diagram showing the layered cross section of a GaAs semiconducting laser. Holes, excited electrons, and the laser beam are confined to the GaAs layer by the adjacent *n*- and *p*-type GaAlAs layers. (Adapted from “Photonic Materials,” by J. M. Rowell. Copyright © 1986 by Scientific American, Inc. All rights reserved.)

Table 20.2 Characteristics and Applications of Several Types of Lasers

<i>Laser</i>	<i>Type</i>	<i>Common Wavelengths (μm)</i>	<i>Max. Output Power (W)^a</i>	<i>Applications</i>
He–Ne	Gas	0.6328, 1.15, 3.39	0.0005, –0.05 (CW)	Line-of sight communications, recording/playback of holograms
CO ₂	Gas	9.6, 10.6	500–15,000 (CW)	Heat treating, welding, cutting, scribing, marking
Argon	Gas ion	0.488, 0.5145	0.005–20 (CW)	Surgery, distance measurements, holography
HeCd	Metal vapor	0.441, 0.325	0.05–0.1	Light shows, spectroscopy
Dye	Liquid	0.38–1.0	0.01 (CW) 1×10^6 (P)	Spectroscopy, pollution detection
Ruby	Solid state	0.694	(P)	Pulsed holography, hole piercing
Nd–YAG	Solid state	1.06	1000 (CW) 2×10^8 (P)	Welding, hole piercing, cutting
Nd–Glass	Solid state	1.06	5×10^{14} (P)	Pulse Welding, hole piercing
Diode	Semiconductor	0.33–40	0.6 (CW) 100 (P)	Bar-code reading, CDs and DVDs, optical communications

^a “CW” denotes continuous; “P” denotes pulsed.

applications are diverse. Since laser beams may be focused to produce localized heating, they are used in some surgical procedures and for cutting, welding, and machining metals. Lasers are also used as light sources for optical communication systems. Furthermore, because the beam is highly coherent, they may be utilized for making very precise distance measurements.

20.14 OPTICAL FIBERS IN COMMUNICATIONS

The communications field has recently experienced a revolution with the development of optical fiber technology; at present, virtually all telecommunications are transmitted via this medium rather than through copper wires. Signal transmission through a metallic wire conductor is electronic (i.e., by electrons), whereas using optically transparent fibers, signal transmission is *photonic*, meaning that it uses photons of electromagnetic or light radiation. Use of fiber-optic systems has improved speed of transmission, information density, and transmission distance, with a reduction in error rate; furthermore, there is no electromagnetic interference with fiber optics. With regard to speed, optical fibers can transmit, in one second, information equivalent to three episodes of your favorite television program. Or relative to information density, two small optical fibers can transmit the equivalent of 24,000 telephone calls simultaneously. Furthermore, it would require 30,000 kg (33 tons) of copper to transmit the same amount of information as only 0.1 kg ($\frac{1}{4}\text{lb}_m$) of optical fiber material.

The present treatment will center on the characteristics of optical fibers; however, it is thought worthwhile to first briefly discuss the components and operation of the transmission system. A schematic diagram showing these components is presented in Figure 20.18. The information (i.e., telephone conversation) in electronic form must first be digitized into bits, that is, 1's and 0's; this is accomplished in the encoder. It is next necessary to convert this electrical signal into an optical (photonic) one, which takes place in the electrical-to-optical converter (Figure 20.18).

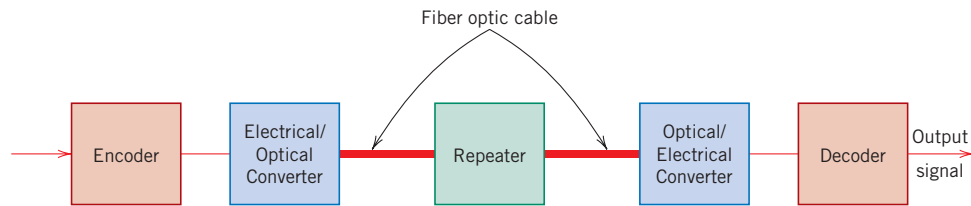


Figure 20.18 Schematic diagram showing the components of an optical fiber communications system.

This converter is normally a semiconductor laser, as described in the previous section, which emits monochromatic and coherent light. The wavelength normally lies between 0.78 and 1.6 μm , which is in the infrared region of the electromagnetic spectrum; absorption losses are low within this range of wavelengths. The output from this laser converter is in the form of pulses of light; a binary 1 is represented by a high-power pulse (Figure 20.19a), whereas a 0 corresponds to a low-power pulse (or the absence of one), Figure 20.19b. These photonic pulse signals are then fed into and carried through the fiber-optical cable (sometimes called a “waveguide”) to the receiving end. For long transmissions, repeaters may be required; these are devices that amplify and regenerate the signal. Finally, at the receiving end the photonic signal is reconverted to an electronic one, and is then decoded (undigitized).

The heart of this communication system is the optical fiber. It must guide these light pulses over long distances without significant signal power loss (i.e., attenuation) and pulse distortion. Fiber components are the core, cladding, and coating; these are represented in the cross-section profile, Figure 20.20. The signal passes through the core, whereas the surrounding cladding constrains the light rays to travel within the core; the outer coating protects core and cladding from damage that might result from abrasion and external pressures.

High-purity silica glass is used as the fiber material; fiber diameters normally range between about 5 and 100 μm . The fibers are relatively flaw free and, thus, remarkably strong; during production the continuous fibers are tested to ensure that they meet minimum strength standards.

Containment of the light to within the fiber core is made possible by total internal reflection; that is, any light rays traveling at oblique angles to the fiber axis are reflected back into the core. Internal reflection is accomplished by varying the index of refraction of the core and cladding glass materials. In this regard, two design

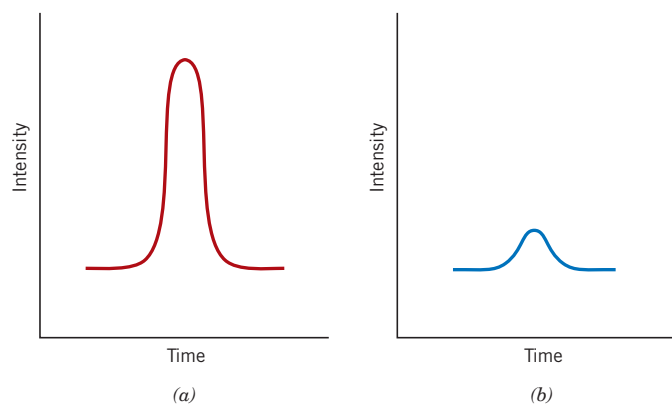


Figure 20.19 Digital encoding scheme for optical communications. (a) A high-power pulse of photons corresponds to a “one” in the binary format. (b) A low-power photon pulse represents a “zero.”

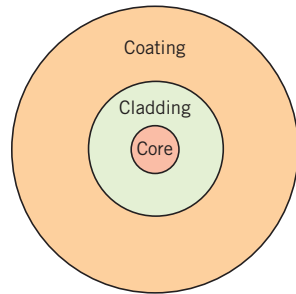


Figure 20.20 Schematic cross section of an optical fiber.

types are employed. With one type (termed “step-index”), the index of refraction of the cladding is slightly lower than that of the core. The index profile and the manner of internal reflection are shown in Figures 20.21*b* and 20.21*d*. For this design, the output pulse will be broader than the input one (Figures 20.21*c* and *e*), a phenomenon that is undesirable since it limits the rate of transmission. Pulse broadening results because various light rays, although being injected at approximately the same instant, arrive at the output at different times; they traverse different trajectories and, thus, have a variety of path lengths.

Pulse broadening is largely avoided by utilization of the other or “graded-index” design. Here, impurities such as boron oxide (B_2O_3) or germanium dioxide (GeO_2) are added to the silica glass such that the index of refraction is made to vary parabolically across the cross section (Figure 20.22*b*). Thus, the velocity of light within the core varies with radial position, being greater at the periphery than the outer periphery of the core travel faster in this lower-index material, and arrive at the output at approximately the same time as undeviated rays that pass through the center portion of the core.

Exceptionally pure and high-quality fibers are fabricated using advanced and sophisticated processing techniques, which will not be discussed here. Impurities and other defects that absorb, scatter, and thus attenuate the light beam must be eliminated. The presence of copper, iron, and vanadium is especially detrimental; their concentrations are reduced to on the order of several parts per billion. Likewise, water and hydroxyl contaminant contents are extremely low. Uniformity of fiber cross-sectional dimensions and core roundness are critical; tolerances of these parameters to within a micrometer over 1 km (0.6 mile) of length are possible. In addition, bubbles within the glass and surface defects have been virtually eliminated. The attenuation

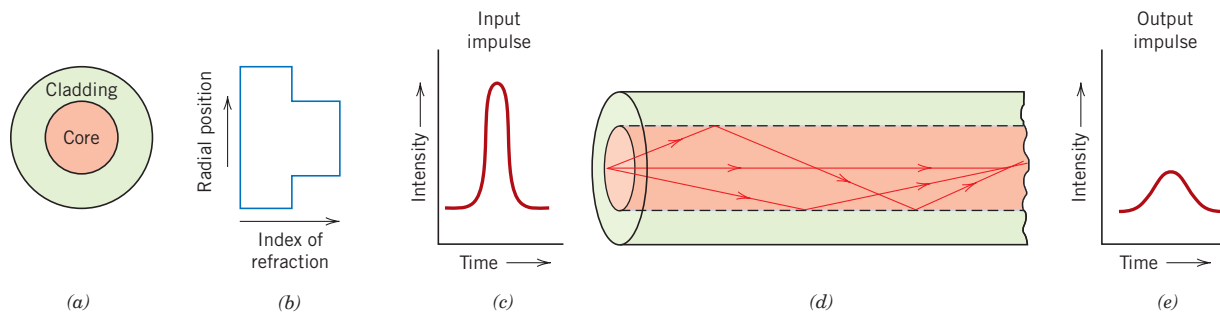


Figure 20.21 Step-index optical fiber design. (a) Fiber cross section. (b) Fiber radial index of refraction profile. (c) Input light pulse. (d) Internal reflection of light rays. (e) Output light pulse. (Adapted from S. R. Nagel, *IEEE Communications Magazine*, Vol. 25, No. 4, p. 34, 1987.)

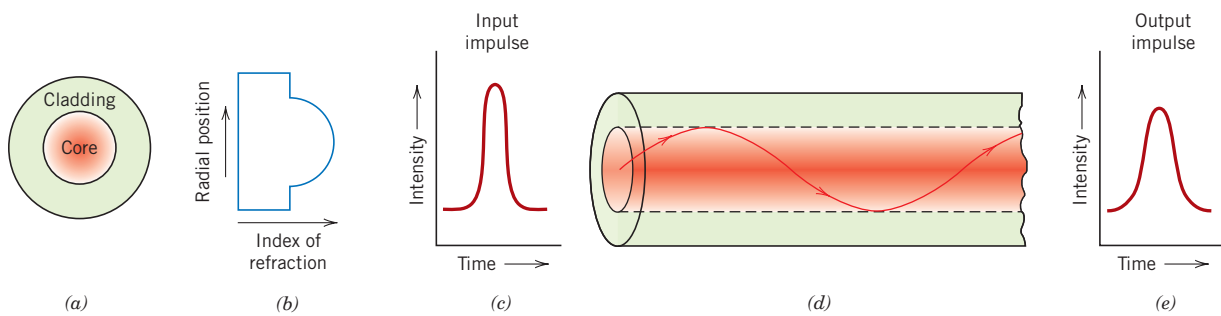


Figure 20.22 Graded-index optical fiber design. (a) Fiber cross section. (b) Fiber radial index of refraction profile. (c) Input light pulse. (d) Internal reflection of a light ray. (e) Output light pulse. (Adapted from S. R. Nagel, *IEEE Communications Magazine*, Vol. 25, No. 4, p. 34, 1987.)

of light in this glass material is imperceptibly small. For example, the power loss through a 16-kilometer (10-mile) thickness of optical fiber glass is equivalent to the power loss through a 25-millimeter (1-inch) thickness of ordinary window glass!

SUMMARY

Electromagnetic Radiation Light Interactions with Solids

The optical behavior of a solid material is a function of its interactions with electromagnetic radiation having wavelengths within the visible region of the spectrum. Possible interactive phenomena include refraction, reflection, absorption, and transmission of incident light.

Optical Properties of Metals

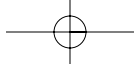
Metals appear opaque as a result of the absorption and then reemission of light radiation within a thin outer surface layer. Absorption occurs via the excitation of electrons from occupied energy states to unoccupied ones above the Fermi energy level. Reemission takes place by decay electron transitions in the reverse direction. The perceived color of a metal is determined by the spectral composition of the reflected light.

Atomic and Electronic Interactions Refraction

Light radiation experiences refraction in transparent materials; that is, its velocity is retarded and the light beam is bent at the interface. Index of refraction is the ratio of the velocity of light in a vacuum to that in the particular medium. The phenomenon of refraction is a consequence of electronic polarization of the atoms or ions, which is induced by the electric field component of the light wave.

Reflection

When light passes from one transparent medium to another having a different index of refraction, some of it is reflected at the interface. The degree of the reflectance depends on the indices of refraction of both media, as well as the angle of incidence.



762 • Chapter 20 / Optical Properties

Absorption

Nonmetallic materials are either intrinsically transparent or opaque. Opacity results in relatively narrow-band gap materials as a result of absorption whereby a photon's energy is sufficient to promote valence band-conduction band electron transitions. Transparent nonmetals have band gaps greater than about 3 eV.

Some light absorption occurs in even transparent materials as a consequence of electronic polarization.

Color

For wide-band gap insulators that contain impurities, decay processes involving excited electrons to states within the band gap are possible with the emission of photons having energies less than the band gap energy. These materials appear colored, and the color depends on the distribution of wavelength ranges in the transmitted beam.

Opacity and Translucency in Insulators

Normally transparent materials may be made translucent or even opaque if the incident light beam experiences interior reflection and/or refraction. Translucency and opacity as a result of internal scattering may occur, (1) in polycrystalline materials that have an anisotropic index of refraction, (2) in two-phase materials, (3) in materials containing small pores, and (4) in highly crystalline polymers.

Luminescence

Photoconductivity

Lasers

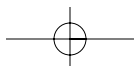
Three other important optical phenomena were discussed: luminescence, photoconductivity, and light amplification by stimulated emission of radiation (lasers). With luminescence, energy is absorbed as a consequence of electron excitations, which is reemitted as visible light. The electrical conductivity of some semiconductors may be enhanced by photoinduced electron transitions, whereby additional free electrons and holes are generated. Coherent and high-intensity light beams are produced in lasers by stimulated electron transitions.

Optical Fibers in Communications

This chapter concluded with a discussion of the use of optical fibers in our modern telecommunications. Using fiber-optic technology, transmission of information is interference free, rapid, and intense.

REFERENCES

- Azaroff, L. V., and J. J. Brophy, *Electronic Processes in Materials*, McGraw-Hill, New York, 1963, Chapter 14. Reprinted by TechBooks, Marietta, OH.
- Javan, A., "The Optical Properties of Materials," *Scientific American*, Vol. 217, No. 3, September 1967, pp. 238–248.
- Kingery, W. D., H. K. Bowen, and D. R. Uhlmann, *Introduction to Ceramics*, 2nd edition, Wiley, New York, 1976, Chapter 13.
- Ralls, K. M., T. H. Courtney, and J. Wulff, *Introduction to Materials Science and Engineering*, Wiley, New York, 1976, Chapter 27.
- Rowell, J. M., "Photonic Materials," *Scientific American*, Vol. 255, No. 4, October 1986, pp. 146–157.



QUESTIONS AND PROBLEMS

Electromagnetic Radiation

- 20.1** Visible light having a wavelength of 5×10^{-7} m appears green. Compute the frequency and energy of a photon of this light.

Light Interactions with Solids

- 20.2** Distinguish between materials that are opaque, translucent, and transparent in terms of their appearance and light transmittance.

Atomic and Electronic Interactions

- 20.3 (a)** Briefly describe the phenomenon of electronic polarization by electromagnetic radiation. **(b)** What are two consequences of electronic polarization in transparent materials?

Optical Properties of Metals

- 20.4** Briefly explain why metals are opaque to electromagnetic radiation having photon energies within the visible region of the spectrum.

Refraction

- 20.5** In ionic materials, how does the size of the component ions affect the extent of electronic polarization?
- 20.6** Can a material have an index of refraction less than unity? Why or why not?
- 20.7** Compute the velocity of light in diamond, which has a dielectric constant ϵ_r of 5.5 (at frequencies within the visible range) and a magnetic susceptibility of -2.17×10^{-5} .
- 20.8** The indices of refraction of fused silica and a polystyrene within the visible spectrum are 1.458 and 1.60, respectively. For each of these materials determine the fraction of the relative dielectric constant at 60 Hz that is due to electronic polarization, using the data of Table 17.5. Neglect any orientation polarization effects.
- 20.9** Using the data in Table 20.1, estimate the dielectric constants for silica glass (fused silica), soda–lime glass, polytetrafluoroethylene, polyethylene, and polystyrene, and compare these values with

those cited in Table 17.5. Briefly explain any discrepancies.

- 20.10** Briefly describe the phenomenon of dispersion in a transparent medium.

Reflection

- 20.11** It is desired that the reflectivity of light at normal incidence to the surface of a transparent medium be less than 5.0%. Which of the following materials in Table 20.1 are likely candidates: soda–lime glass, Pyrex glass, periclase, spinel, polystyrene, and polypropylene? Justify your selections.
- 20.12** Briefly explain how reflection losses of transparent materials are minimized by thin surface coatings.
- 20.13** The index of refraction of quartz is anisotropic. Suppose that visible light is passing from one grain to another of different crystallographic orientation and at normal incidence to the grain boundary. Calculate the reflectivity at the boundary if the indices of refraction for the two grains are 1.544 and 1.553 in the direction of light propagation.

Absorption

- 20.14** Zinc selenide has a band gap of 2.58 eV. Over what range of wavelengths of visible light is it transparent?
- 20.15** Briefly explain why the magnitude of the absorption coefficient (β in Equation 20.18) depends on the radiation wavelength.
- 20.16** The fraction of nonreflected radiation that is transmitted through a 5-mm thickness of a transparent material is 0.95. If the thickness is increased to 12 mm, what fraction of light will be transmitted?

Transmission

- 20.17** Derive Equation 20.19, starting from other expressions given in the chapter.
- 20.18** The transmissivity T of a transparent material 15 mm thick to normally incident light is 0.80. If the index of refraction of this material is 1.5, compute the thickness of material that will yield a transmissivity of 0.70. All reflection losses should be considered.

764 • Chapter 20 / Optical Properties

Color

- 20.19** Briefly explain what determines the characteristic color of (a) a metal and (b) a transparent nonmetal.
- 20.20** Briefly explain why some transparent materials appear colored while others are colorless.

Opacity and Translucency in Insulators

- 20.21** Briefly describe the three absorption mechanisms in nonmetallic materials.
- 20.22** Briefly explain why amorphous polymers are transparent, while predominantly crystalline polymers appear opaque or, at best, translucent.

*Luminescence**Photoconductivity**Lasers*

- 20.23 (a)** In your own words describe briefly the phenomenon of luminescence.

(b) What is the distinction between fluorescence and phosphorescence?

- 20.24** In your own words, briefly describe the phenomenon of photoconductivity.
- 20.25** Briefly explain the operation of a photographic lightmeter.
- 20.26** In your own words, describe how a ruby laser operates.
- 20.27** Compute the difference in energy between metastable and ground electron states for the ruby laser.

Optical Fibers in Communications

- 20.28** At the end of Section 20.14 it was noted that the intensity of light absorbed while passing through a 16-kilometer length of optical fiber glass is equivalent to the light intensity absorbed through for a 25-mm thickness of ordinary window glass. Calculate the absorption coefficient β of the optical fiber glass if the value of β for the window glass is 10^{-4} mm^{-1} .

DESIGN PROBLEM*Atomic and Electronic Interactions*

- 20.D1** Gallium arsenide (GaAs) and gallium phosphide (GaP) are compound semiconductors that have room-temperature band gap energies of 1.42 and 2.25 eV, respectively, and form solid solutions in all proportions. Furthermore, the band gap of the alloy increases approximately linearly with

GaP additions (in mol%). Alloys of these two materials are used for light-emitting diodes wherein light is generated by conduction band-to-valence band electron transitions. Determine the composition of a GaAs–GaP alloy that will emit red light having a wavelength of $0.68 \mu\text{m}$.

Chapter 21 Materials Selection and Design Considerations



Photograph showing the components of an artificial total hip replacement (in exploded perspective). These components are (from left to right) as follows: femoral stem, ball, acetabular cup insert, and acetabular cup. (Photograph courtesy of Zimmer, Inc., Warsaw, IN, USA.)

Learning Objectives

After careful study of this chapter you should be able to do the following:

1. Describe how the strength performance index for a solid cylindrical shaft is determined.
2. Describe the manner in which materials selection charts are employed in the materials selection process.
3. Briefly describe the steps that are used to ascertain whether or not a particular metal alloy is suitable for use in an automobile valve spring.
4. Briefly describe the difference in surface features (as observed in scanning electron micrographs) for a steel alloy that (a) experienced a ductile fracture, and (b) failed in a brittle manner.
5. List and briefly explain six biocompatibility considerations relative to materials that are employed in artificial hip replacements.
6. Name the four components found in the artificial hip replacement, and, for each, list its specific material requirements.
7. Name and briefly define the two factors that are important to consider relative to the suitability of a material for use for chemical protective clothing.
8. Describe the components and their functions for an integrated circuit leadframe.
9. (a) Name and briefly describe the three processes that are carried out during integrated circuit packaging. (b) Note property requirements for each of these processes, and, in addition, cite at least two materials that are employed.

21.1 INTRODUCTION

Virtually the entire book to this point has dealt with the properties of various materials, how the properties of a specific material are dependent on its structure, and, in many cases, how structure may be fashioned by the processing technique that is employed during production. Of late, there has been a trend to emphasize the element of *design* in engineering pedagogy. To a materials scientist or materials engineer, design can be taken in several contexts. First of all, it can mean designing new materials having unique property combinations. Alternatively, design can involve selecting a new material having a better combination of characteristics for a specific application; choice of material cannot be made without consideration of necessary manufacturing processes (i.e., forming, welding, etc.), which also rely on material properties. Or, finally, design might mean developing a process for producing a material having better properties.

One particularly effective technique for teaching design principles is the case study method. With this technique, the solutions to real-life engineering problems are carefully analyzed in detail so that the student may observe the procedures and rationale that are involved in the decision-making process. We have chosen to perform six case studies, which draw upon principles that were introduced in previous chapters. Five of these studies involve materials that are used for the following: (1) a torsionally stressed cylindrical shaft (materials selection); (2) an automobile valve spring; (3) the artificial total hip replacement; (4) chemical protective clothing; and (5) integrated circuit packages. The remaining case study discusses the probable cause of failure of an automobile rear axle.

Materials Selection for a Torsionally Stressed Cylindrical Shaft

We begin by addressing the design process from the perspective of materials selection; that is, for some application, selecting a material having a desirable

21.2 Strength Considerations—Torsionally Stressed Shaft • 767

or optimum property or combination of properties. Elements of this materials selection process involve deciding on the constraints of the problem, and, from these, establishing criteria that can be used in materials selection to maximize performance.

The component or structural element we have chosen to discuss is a solid cylindrical shaft that is subjected to a torsional stress. Strength of the shaft will be considered in detail, and criteria will be developed for the maximization of strength with respect to both minimum material mass and minimum cost. Other parameters and properties that may be important in this selection process are also discussed briefly.

21.2 STRENGTH CONSIDERATIONS— TORSIONALLY STRESSED SHAFT

For this portion of the design problem, we will establish a criterion for selection of light and strong materials for this shaft. It will be assumed that the twisting moment and length of the shaft are specified, whereas the radius (or cross-sectional area) may be varied. We develop an expression for the mass of material required in terms of twisting moment, shaft length, and density and strength of the material. Using this expression, it will be possible to evaluate the performance—that is, maximize the strength of this torsionally stressed shaft with respect to mass and, in addition, relative to material cost.

Consider the cylindrical shaft of length L and radius r , as shown in Figure 21.1. The application of twisting moment (or torque) M_t produces an angle of twist ϕ . Shear stress τ at radius r is defined by the equation

$$\tau = \frac{M_t r}{J} \quad (21.1)$$

Here, J is the polar moment of inertia, which for a solid cylinder is

$$J = \frac{\pi r^4}{2} \quad (21.2)$$

Thus,

$$\tau = \frac{2M_t}{\pi r^3} \quad (21.3)$$

A safe design calls for the shaft to be able to sustain some twisting moment without fracture. In order to establish a materials selection criterion for a light and strong material, we replace the shear stress in Equation 21.3 with the shear strength of the material τ_f divided by a factor of safety N , as

$$\frac{\tau_f}{N} = \frac{2M_t}{\pi r^3} \quad (21.4)$$

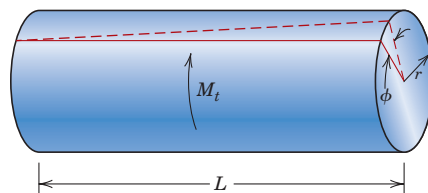


Figure 21.1 A solid cylindrical shaft that experiences an angle of twist ϕ in response to the application of a twisting moment M_t .

768 • Chapter 21 / Materials Selection and Design Considerations

It is now necessary to take into consideration material mass. The mass m of any given quantity of material is just the product of its density (ρ) and volume. Since the volume of a cylinder is just $\pi r^2 L$, then

$$m = \pi r^2 L \rho \quad (21.5)$$

or, the radius of the shaft in terms of its mass is just

$$r = \sqrt{\frac{m}{\pi L \rho}} \quad (21.6)$$

Substitution of this r expression into Equation 21.4 leads to

$$\begin{aligned} \frac{\tau_f}{N} &= \frac{2M_t}{\pi \left(\sqrt{\frac{m}{\pi L \rho}} \right)^3} \\ &= 2M_t \sqrt{\frac{\pi L^3 \rho^3}{m^3}} \end{aligned} \quad (21.7)$$

Solving this expression for the mass m yields

$$m = (2NM_t)^{2/3} (\pi^{1/3} L) \left(\frac{\rho}{\tau_f^{2/3}} \right) \quad (21.8)$$

The parameters on the right-hand side of this equation are grouped into three sets of parentheses. Those contained within the first set (i.e., N and M_t) relate to the safe functioning of the shaft. Within the second parentheses is L , a geometric parameter. Finally, the material properties of density and strength are contained within the last set.

The upshot of Equation 21.8 is that the best materials to be used for a light shaft that can safely sustain a specified twisting moment are those having low $\rho/\tau_f^{2/3}$ ratios. In terms of material suitability, it is sometimes preferable to work with what is termed a *performance index*, P , which is just the reciprocal of this ratio; that is,

$$P = \frac{\tau_f^{2/3}}{\rho} \quad (21.9)$$

In this context we want to utilize a material having a large performance index.

At this point it becomes necessary to examine the performance indices of a variety of potential materials. This procedure is expedited by the utilization of what are termed *materials selection charts*.¹ These are plots of the values of one material property versus those of another property. Both axes are scaled logarithmically and usually span about five orders of magnitude, so as to include the properties of virtually all materials. For example, for our problem, the chart of interest is logarithm of strength versus logarithm of density, which is shown in Figure 21.2.² It may be noted on this plot that materials of a particular type (e.g., woods, engineering polymers, etc.) cluster together and are enclosed within an envelope delineated with a bold line. Subclasses within these clusters are enclosed using finer lines.

¹ A comprehensive collection of these charts may be found in M. F. Ashby, *Materials Selection in Mechanical Design*, 2nd edition, Butterworth-Heinemann, Woburn, UK, 2002.

² Strength for metals and polymers is taken as yield strength, for ceramics and glasses, compressive strength, for elastomers, tear strength, and for composites, tensile failure strength.

21.2 Strength Considerations—Torsionally Stressed Shaft • 769

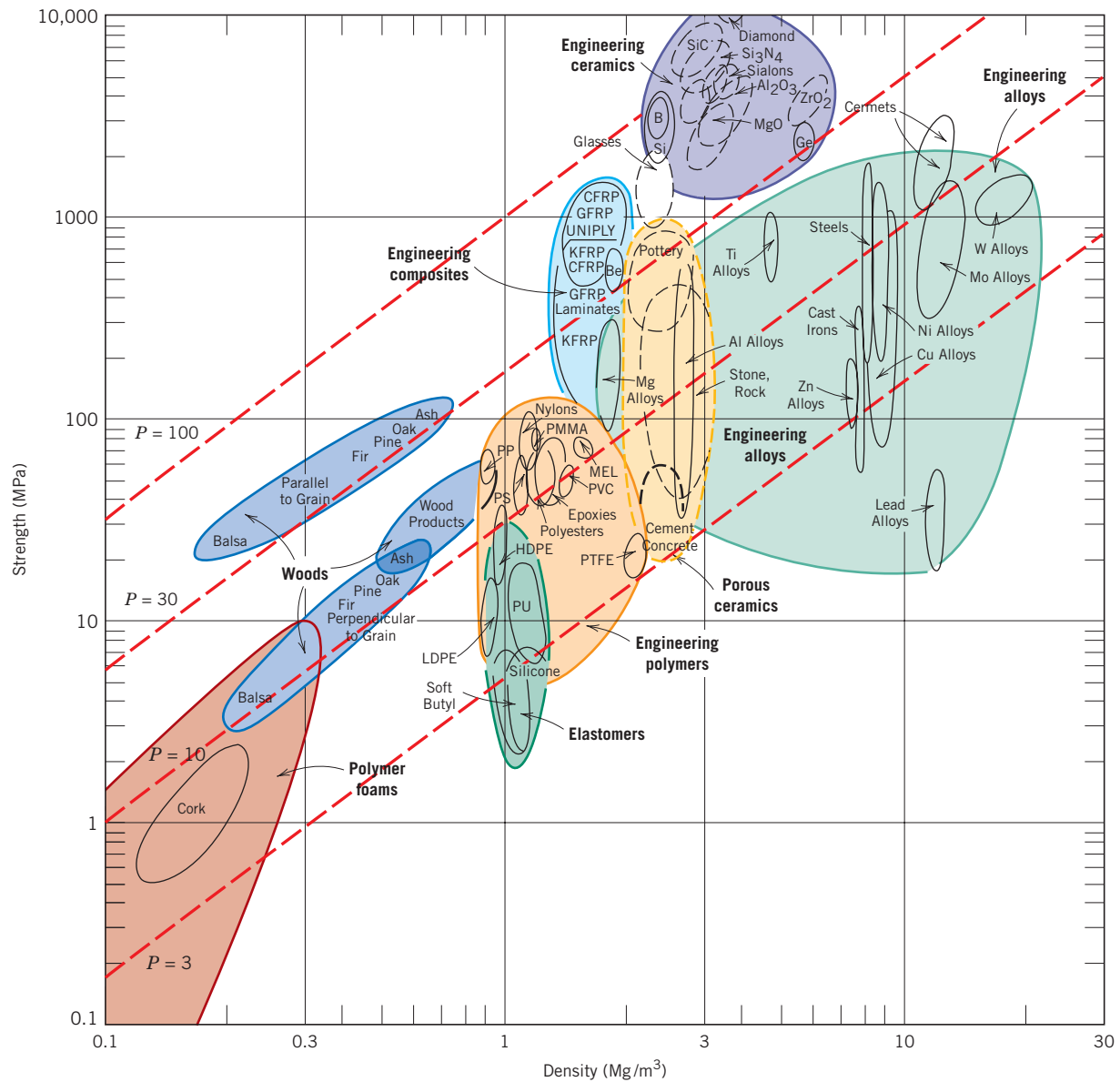


Figure 21.2 Strength versus density materials selection chart. Design guidelines for performance indices of 3, 10, 30, and 100 $(\text{MPa})^{2/3}\text{m}^3/\text{Mg}$ have been constructed, all having a slope of $\frac{3}{2}$. (Adapted from M. F. Ashby, *Materials Selection in Mechanical Design*. Copyright © 1992. Reprinted by permission of Butterworth-Heinemann Ltd.)

Now, taking the logarithm of both sides of Equation 21.9 and rearranging yields

$$\log \tau_f = \frac{3}{2} \log \rho + \frac{3}{2} \log P \quad (21.10)$$

This expression tells us that a plot of $\log \tau_f$ versus $\log \rho$ will yield a family of straight and parallel lines all having a slope of $\frac{3}{2}$; each line in the family corresponds to a different performance index, P . These lines are termed *design guidelines*, and four have been included in Figure 21.2 for P values of 3, 10, 30, and 100 $(\text{MPa})^{2/3}\text{m}^3/\text{Mg}$. All materials that lie on one of these lines will perform equally well in terms of

770 • Chapter 21 / Materials Selection and Design Considerations

strength-per-mass basis; materials whose positions lie above a particular line will have higher performance indices, while those lying below will exhibit poorer performances. For example, a material on the $P = 30$ line will yield the same strength with one-third the mass as another material that lies along the $P = 10$ line.

The selection process now involves choosing one of these lines, a “selection line” that includes some subset of these materials; for the sake of argument let us pick $P = 10 \text{ (MPa)}^{2/3} \text{ m}^3/\text{Mg}$, which is represented in Figure 21.3. Materials lying

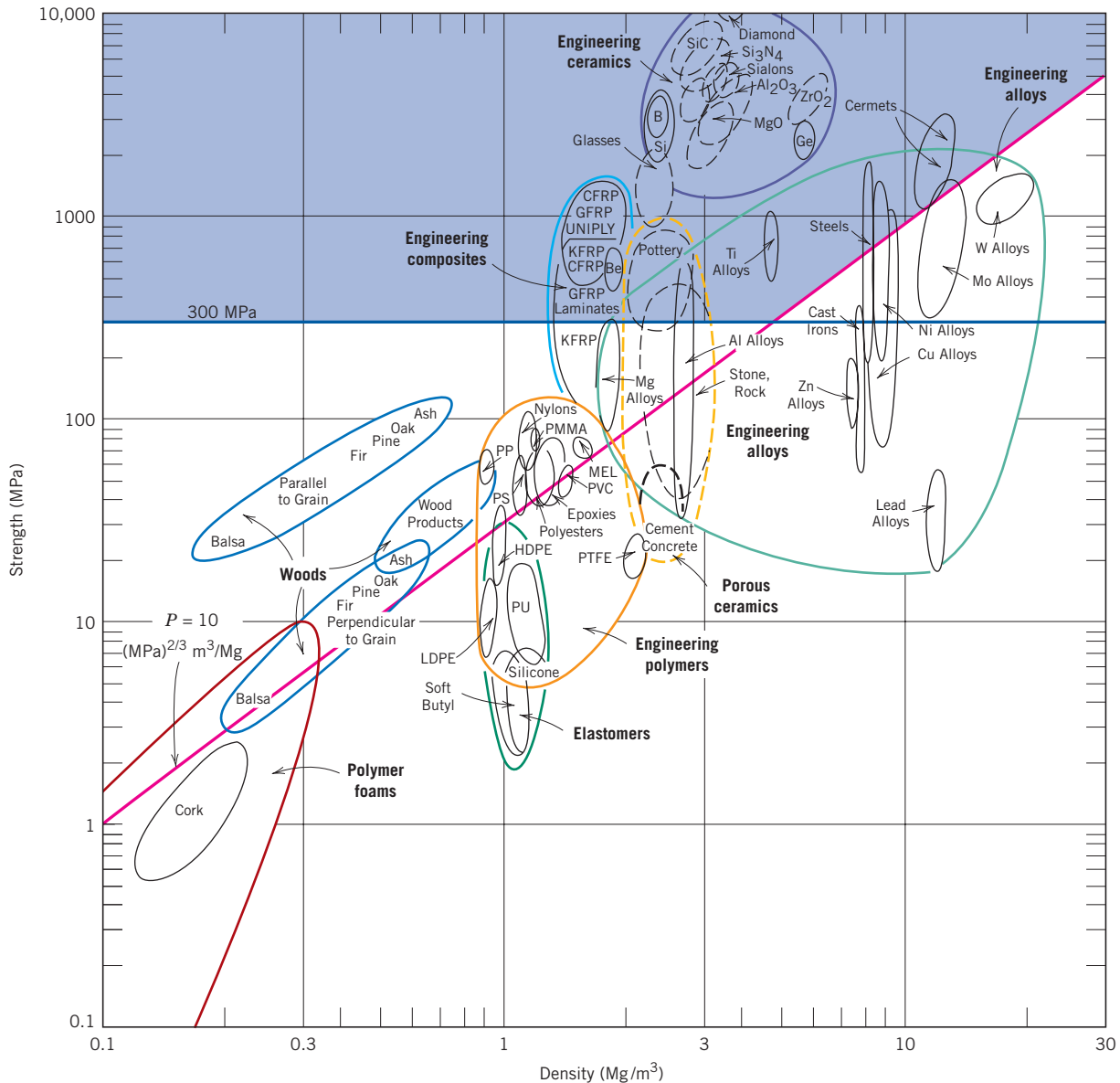


Figure 21.3 Strength versus density materials selection chart. Those materials lying within the shaded region are acceptable candidates for a solid cylindrical shaft that has a mass-strength performance index in excess of $10 \text{ (MPa)}^{2/3} \text{ m}^3/\text{Mg}$, and a strength of at least 300 MPa (43,500 psi). (Adapted from M. F. Ashby, *Materials Selection in Mechanical Design*. Copyright © 1992. Reprinted by permission of Butterworth-Heinemann Ltd.)

21.2 Strength Considerations—Torsionally Stressed Shaft • 771

along this line or above it are in the “search region” of the diagram and are possible candidates for this rotating shaft. These include wood products, some plastics, a number of engineering alloys, the engineering composites, and glasses and engineering ceramics. On the basis of fracture toughness considerations, the engineering ceramics and glasses are ruled out as possibilities.

Let us now impose a further constraint on the problem—namely, that the strength of the shaft must equal or exceed 300 MPa. This may be represented on the materials selection chart by a horizontal line constructed at 300 MPa, Figure 21.3. Now the search region is further restricted to that area above both of these lines. Thus, all wood products, all engineering polymers, other engineering alloys (viz. Mg and some Al alloys), as well as some engineering composites are eliminated as candidates; steels, titanium alloys, high-strength aluminum alloys, and the engineering composites remain as possibilities.

At this point we are in a position to evaluate and compare the strength performance behavior of specific materials. Table 21.1 presents the density, strength, and strength performance index for three engineering alloys and two engineering composites, which were deemed acceptable candidates from the analysis using the materials selection chart. In this table, strength was taken as 0.6 times the tensile yield strength (for the alloys) and 0.6 times the tensile strength (for the composites); these approximations were necessary since we are concerned with strength in torsion and torsional strengths are not readily available. Furthermore, for the two engineering composites, it is assumed that the continuous and aligned glass and carbon fibers are wound in a helical fashion (Figure 15.15), and at a 45° angle referenced to the shaft axis. The five materials in Table 21.1 are ranked according to strength performance index, from highest to lowest: carbon fiber-reinforced and glass fiber-reinforced composites, followed by aluminum, titanium, and 4340 steel alloys.

Material cost is another important consideration in the selection process. In real-life engineering situations, economics of the application often is the overriding issue and normally will dictate the material of choice. One way to determine materials cost is by taking the product of the price (on a per-unit mass basis) and the required mass of material.

Cost considerations for these five remaining candidate materials—steel, aluminum, and titanium alloys, and two engineering composites—are presented in

Table 21.1 Density (ρ), Strength (τ_f), and Performance Index (P) for Five Engineering Materials

<i>Material</i>	ρ (Mg/m ³)	τ_f (MPa)	$\frac{\tau_f^{2/3}}{\rho} = P$ [(MPa) ^{2/3} m ³ /Mg]
Carbon fiber-reinforced composite (0.65 fiber fraction) ^a	1.5	1140	72.8
Glass fiber-reinforced composite (0.65 fiber fraction) ^a	2.0	1060	52.0
Aluminum alloy (2024-T6)	2.8	300	16.0
Titanium alloy (Ti-6Al-4V)	4.4	525	14.8
4340 Steel (oil-quenched and tempered)	7.8	780	10.9

^a The fibers in these composites are continuous, aligned, and wound in a helical fashion at a 45° angle relative to the shaft axis.

772 • Chapter 21 / Materials Selection and Design Considerations

Table 21.2 Tabulation of the $\rho/\tau_f^{2/3}$ Ratio, Relative Cost (\bar{c}), and the Product of $\rho/\tau_f^{2/3}$ and \bar{c} for Five Engineering Materials^a

Material	$\rho/\tau_f^{2/3}$ [$10^{-2}\{Mg/(MPa)^{2/3}m^3\}$]	\bar{c} (\$/\$)	$\bar{c}(\rho/\tau_f^{2/3})$ [$10^{-2} (\$/\$)\{Mg/(MPa)^{2/3}m^3\}$]
4340 Steel (oil-quenched and tempered)	9.2	5	46
Glass fiber-reinforced composite (0.65 fiber fraction) ^b	1.9	40	76
Aluminum alloy (2024-T6)	6.2	15	93
Carbon fiber-reinforced composite (0.65 fiber fraction) ^b	1.4	80	112
Titanium alloy (Ti-6Al-4V)	6.8	110	748

^a The relative cost is the ratio of the prices per-unit mass of the material and low-carbon steel.

^b The fibers in these composites are continuous, aligned, and wound in a helical fashion at a 45° angle relative to the shaft axis.

Table 21.2. In the first column is tabulated $\rho/\tau_f^{2/3}$. The next column lists the approximate relative cost, denoted as \bar{c} ; this parameter is simply the per-unit mass cost of material divided by the per-unit mass cost for low-carbon steel, one of the common engineering materials. The underlying rationale for using \bar{c} is that while the price of a specific material will vary over time, the price ratio between that material and another will, most likely, change more slowly.

Finally, the right-hand column of Table 21.2 shows the product of $\rho/\tau_f^{2/3}$ and \bar{c} . This product provides a comparison of these several materials on the basis of the cost of materials for a cylindrical shaft that would not fracture in response to the twisting moment M_t . We use this product inasmuch as $\rho/\tau_f^{2/3}$ is proportional to the mass of material required (Equation 21.8) and \bar{c} is the relative cost on a per-unit mass basis. Now the most economical is the 4340 steel, followed by the glass fiber-reinforced composite, 2024-T6 aluminum, the carbon fiber-reinforced composite, and the titanium alloy. Thus, when the issue of economics is considered, there is a significant alteration within the ranking scheme. For example, inasmuch as the carbon fiber-reinforced composite is relatively expensive, it is significantly less desirable; in other words, the higher cost of this material may not outweigh the enhanced strength it provides.

21.3 OTHER PROPERTY CONSIDERATIONS AND THE FINAL DECISION

To this point in our materials selection process we have considered only the strength of materials. Other properties relative to the performance of the cylindrical shaft may be important—for example, stiffness, and, if the shaft rotates, fatigue behavior (Sections 11.7 and 11.8). Furthermore, fabrication costs should also be considered; in our analysis they have been neglected.

Relative to stiffness, a stiffness-to-mass performance analysis similar to that above could be conducted. For this case, the stiffness performance index P_s is

$$P_s = \frac{\sqrt{G}}{\rho} \quad (21.11)$$

where G is the shear modulus. The appropriate materials selection chart ($\log G$ versus $\log \rho$) would be used in the preliminary selection process. Subsequently, performance index and per-unit-mass cost data would be collected on specific

candidate materials; from these analyses the materials would be ranked on the basis of stiffness performance and cost.

In deciding on the best material, it may be worthwhile to make a table employing the results of the various criteria that were used. The tabulation would include, for all candidate materials, performance index, cost, etc. for each criterion, as well as comments relative to any other important considerations. This table puts in perspective the important issues and facilitates the final decision process.

Automobile Valve Spring

21.4 MECHANICS OF SPRING DEFORMATION

The basic function of a spring is to store mechanical energy as it is initially elastically deformed and then recoup this energy at a later time as the spring recoils. In this section helical springs that are used in mattresses and in retractable pens and as suspension springs in automobiles are discussed. A stress analysis will be conducted on this type of spring, and the results will then be applied to a valve spring that is utilized in automobile engines.

Consider the helical spring shown in Figure 21.4, which has been constructed of wire having a circular cross section of diameter d ; the coil center-to-center diameter is denoted as D . The application of a compressive force F causes a twisting force, or moment, denoted T , as shown in the figure. A combination of shear stresses result, the sum of which, τ , is

$$\tau = \frac{8FD}{\pi d^3} K_w \quad (21.12)$$

where K_w is a force-independent constant that is a function of the D/d ratio:

$$K_w = 1.60 \left(\frac{D}{d} \right)^{-0.140} \quad (21.13)$$

In response to the force F , the coiled spring will experience deflection, which will be assumed to be totally elastic. The amount of deflection per coil of spring, δ_c , as indicated in Figure 21.5, is given by the expression

$$\delta_c = \frac{8FD^3}{d^4 G} \quad (21.14)$$

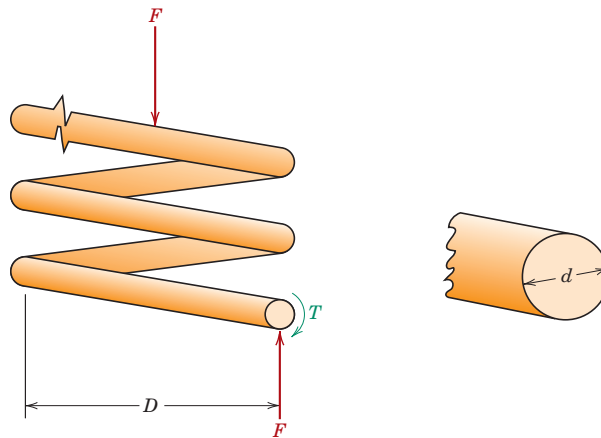


Figure 21.4 Schematic diagram of a helical spring showing the twisting moment T that results from the compressive force F . (Adapted from K. Edwards and P. McKee, *Fundamentals of Mechanical Component Design*. Copyright © 1991 by McGraw-Hill, Inc. Reproduced with permission of The McGraw-Hill Companies.)

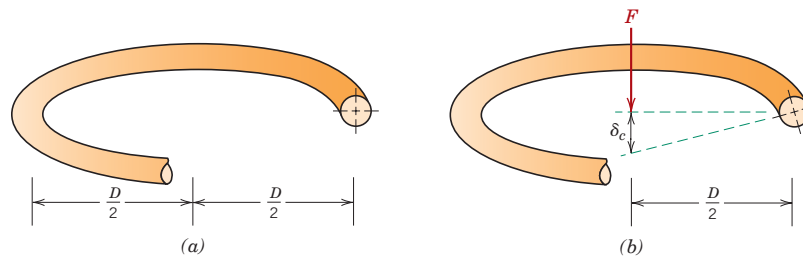


Figure 21.5 Schematic diagrams of one coil of a helical spring, (a) prior to being compressed, and (b) showing the deflection δ_c produced from the compressive force F . (Adapted from K. Edwards and P. McKee, *Fundamentals of Mechanical Component Design*. Copyright © 1991 by McGraw-Hill, Inc. Reproduced with permission of The McGraw-Hill Companies.)

where G is the shear modulus of the material from which the spring is constructed. Furthermore, δ_c may be computed from the total spring deflection, δ_s , and the number of effective spring coils, N_c , as

$$\delta_c = \frac{\delta_s}{N_c} \quad (21.15)$$

Now, solving for F in Equation 21.14 gives

$$F = \frac{d^4 \delta_c G}{8D^3} \quad (21.16)$$

and substituting for F in Equation 21.12 leads to

$$\tau = \frac{\delta_c G d}{\pi D^2} K_w \quad (21.17)$$

Under normal circumstances, it is desired that a spring experience no permanent deformation upon loading; this means that the right-hand side of Equation 21.17 must be less than the shear yield strength τ_y of the spring material, or that

$$\tau_y > \frac{\delta_c G d}{\pi D^2} K_w \quad (21.18)$$

21.5 VALVE SPRING DESIGN AND MATERIAL REQUIREMENTS

We shall now apply the results of the preceding section to an automobile valve spring. A cutaway schematic diagram of an automobile engine showing these springs is presented in Figure 21.6. Functionally, springs of this type permit both intake and exhaust valves to alternately open and close as the engine is in operation. Rotation of the camshaft causes a valve to open and its spring to be compressed, so that the load on the spring is increased. The stored energy in the spring then forces the valve to close as the camshaft continues its rotation. This process occurs for each valve for each engine cycle, and over the lifetime of the engine it occurs many millions of times. Furthermore, during normal engine operation, the temperature of the springs is approximately 80°C (175°F).

21.5 Valve Spring Design and Material Requirements • 775

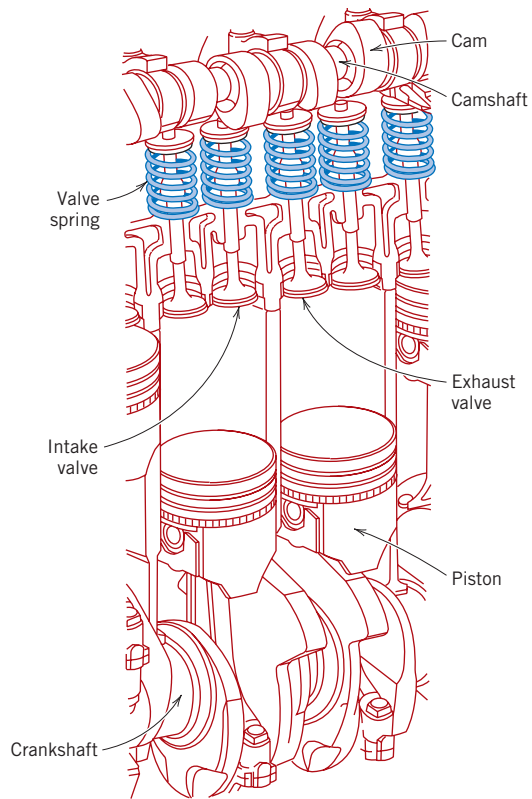


Figure 21.6 Cutaway drawing of a section of an automobile engine in which various components including valves and valve springs are shown.

A photograph of a typical valve spring is shown in Figure 21.7. The spring has a total length of 42 mm, is constructed of wire having a diameter d of 4.3 mm, has six coils (only four of which are active), and has a center-to-center diameter D of 27 mm. Furthermore, when installed and when a valve is completely closed, its spring is compressed a total of 6.0 mm, which, from Equation 21.15, gives an installed



Figure 21.7 Photograph of a typical automobile valve spring.



776 • Chapter 21 / Materials Selection and Design Considerations

deflection per coil δ_{ic} of

$$\delta_{ic} = \frac{0.24 \text{ in.}}{4 \text{ coils}} = 0.060 \text{ in./coil (1.5 mm/coil)}$$

The cam lift is 0.30 in. (7.6 mm), which means that when the cam completely opens a valve, the spring experiences a maximum total deflection equal to the sum of the valve lift and the compressed deflection, namely, 0.30 in. + 0.24 in. = 0.54 in. (13.7 mm). Hence, the maximum deflection per coil, δ_{mc} , is

$$\delta_{mc} = \frac{0.54 \text{ in.}}{4 \text{ coils}} = 0.135 \text{ in./coil (3.4 mm/coil)}$$

Thus, we have available all of the parameters in Equation 21.18 (taking $\delta_c = \delta_{mc}$), except for τ_y , the required shear yield strength of the spring material.

However, the material parameter of interest is really not τ_y inasmuch as the spring is continually stress cycled as the valve opens and closes during engine operation; this necessitates designing against the possibility of failure by fatigue rather than against the possibility of yielding. This fatigue complication is handled by choosing a metal alloy that has a fatigue limit (Figure 11.19a) that is greater than the cyclic stress amplitude to which the spring will be subjected. For this reason, steel alloys, which have fatigue limits, are normally employed for valve springs.

When using steel alloys in spring design, two assumptions may be made if the stress cycle is reversed (if $\tau_m = 0$, where τ_m is the mean stress, or, equivalently, if $\tau_{\max} = -\tau_{\min}$, in accordance with Equation 8.14 and as noted in Figure 21.8). The first of these assumptions is that the fatigue limit of the alloy (expressed as stress amplitude) is 45,000 psi (310 MPa), the threshold of which occurs at about 10^6 cycles. Secondly, for torsion and on the basis of experimental data, it has been found that the fatigue strength at 10^3 cycles is $0.67TS$, where TS is the tensile strength of the material (as measured from a pure tension test). The S - N fatigue diagram (i.e., stress amplitude versus logarithm of the number of cycles to failure) for these alloys is shown in Figure 21.9.

Now let us estimate the number of cycles to which a typical valve spring may be subjected in order to determine whether it is permissible to operate within the fatigue limit regime of Figure 21.9 (i.e., if the number of cycles exceeds 10^6). For the sake of argument, assume that the automobile in which the spring is mounted travels a minimum of 100,000 miles (161,000 km) at an average speed of 40 mph (64.4 km/h), with an average engine speed of 3000 rpm (rev/min). The total time it takes the automobile to travel this distance is 2500 h (100,000 mi/40 mph), or

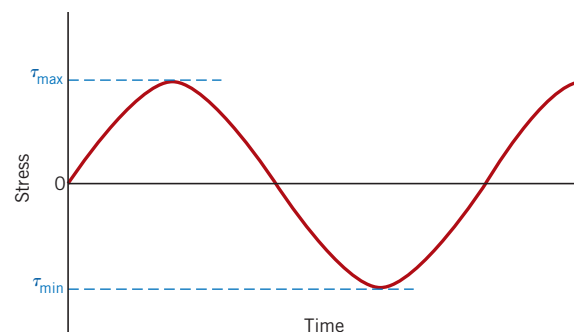


Figure 21.8 Stress versus time for a reversed cycle in shear.

21.6 One Commonly Employed Steel Alloy • 777

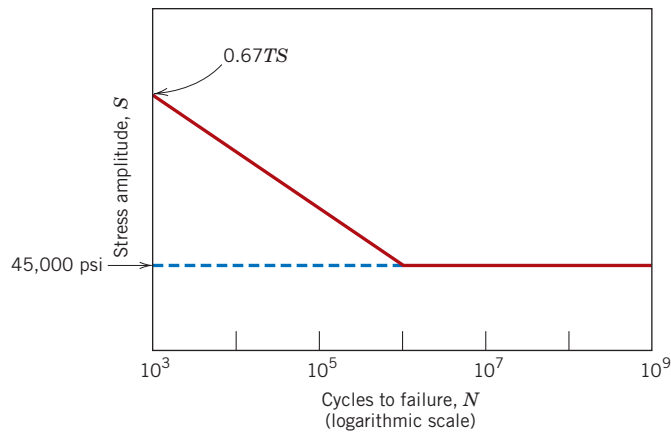


Figure 21.9 Shear stress amplitude versus logarithm of the number of cycles to fatigue failure for typical ferrous alloys.

150,000 min. At 3000 rpm, the total number of revolutions is $(3000 \text{ rev/min})(150,000 \text{ min}) = 4.5 \times 10^8 \text{ rev}$, and since there are 2 rev/cycle, the total number of cycles is 2.25×10^8 . This result means that we may use the fatigue limit as the design stress inasmuch as the limit cycle threshold has been exceeded for the 100,000-mile distance of travel (i.e., since $2.25 \times 10^8 \text{ cycles} > 10^6 \text{ cycles}$).

Furthermore, this problem is complicated by the fact that the stress cycle is not completely reversed (i.e., $\tau_m \neq 0$) inasmuch as between minimum and maximum deflections the spring remains in compression; thus, the 310 MPa fatigue limit is not valid. What we would now like to do is first to make an appropriate extrapolation of the fatigue limit for this $\tau_m \neq 0$ case and then compute and compare with this limit the actual stress amplitude for the spring; if the stress amplitude is significantly below the extrapolated limit, then the spring design is satisfactory.

A reasonable extrapolation of the fatigue limit for this $\tau_m \neq 0$ situation may be made using the following expression (termed Goodman's law):

$$\tau_{al} = \tau_e \left(1 - \frac{\tau_m}{0.67TS} \right) \quad (21.19)$$

where τ_{al} is the fatigue limit for the mean stress τ_m ; τ_e is the fatigue limit for $\tau_m = 0$ [i.e., 310 MPa]; and, again, TS is the tensile strength of the alloy. To determine the new fatigue limit τ_{al} from the above expression necessitates the computation of both the tensile strength of the alloy and the mean stress for the spring.

21.6 ONE COMMONLY EMPLOYED STEEL ALLOY

One common spring alloy is an ASTM 232 chrome–vanadium steel, having a composition of 0.48–0.53 wt% C, 0.80–1.10 wt% Cr, a minimum of 0.15 wt% V, and the balance being Fe. Spring wire is normally cold drawn (Section 23.2) to the desired diameter; consequently, tensile strength will increase with the amount of drawing (i.e., with decreasing diameter). For this alloy it has been experimentally verified that, for the diameter d in inches, the tensile strength is

$$TS \text{ (psi)} = 169,000(d)^{-0.167} \quad (21.20)$$

778 • Chapter 21 / Materials Selection and Design Considerations

Since $d = 0.170$ in. for this spring,

$$\begin{aligned} TS &= (169,000)(0.170 \text{ in.})^{-0.167} \\ &= 227,200 \text{ psi (1570 MPa)} \end{aligned}$$

Computation of the mean stress τ_m is made using Equation 11.14 modified to the shear stress situation as follows:

$$\tau_m = \frac{\tau_{\min} + \tau_{\max}}{2} \quad (21.21)$$

It now becomes necessary to determine the minimum and maximum shear stresses for the spring, using Equation 21.17. The value of τ_{\min} may be calculated from Equations 21.17 and 21.13 inasmuch as the minimum δ_c is known (i.e., $\delta_{ic} = 0.060$ in.). A shear modulus of 11.5×10^6 psi (79 GPa) will be assumed for the steel; this is the room-temperature value, which is also valid at the 80°C service temperature. Thus, τ_{\min} is just

$$\begin{aligned} \tau_{\min} &= \frac{\delta_{ic} G d}{\pi D^2} K_w \quad (21.22a) \\ &= \frac{\delta_{ic} G d}{\pi D^2} \left[1.60 \left(\frac{D}{d} \right)^{-0.140} \right] \\ &= \left[\frac{(0.060 \text{ in.})(11.5 \times 10^6 \text{ psi})(0.170 \text{ in.})}{\pi(1.062 \text{ in.})^2} \right] \left[1.60 \left(\frac{1.062 \text{ in.}}{0.170 \text{ in.}} \right)^{-0.140} \right] \\ &= 41,000 \text{ psi (280 MPa)} \end{aligned}$$

Now τ_{\max} may be determined taking $\delta_c = \delta_{mc} = 0.135$ in. as follows:

$$\begin{aligned} \tau_{\max} &= \frac{\delta_{mc} G d}{\pi D^2} \left[1.60 \left(\frac{D}{d} \right)^{-0.140} \right] \quad (21.22b) \\ &= \left[\frac{(0.135 \text{ in.})(11.5 \times 10^6 \text{ psi})(0.170 \text{ in.})}{\pi(1.062 \text{ in.})^2} \right] \left[1.60 \left(\frac{1.062 \text{ in.}}{0.170 \text{ in.}} \right)^{-0.140} \right] \\ &= 92,200 \text{ psi (635 MPa)} \end{aligned}$$

Now, from Equation 21.21,

$$\begin{aligned} \tau_m &= \frac{\tau_{\min} + \tau_{\max}}{2} \\ &= \frac{41,000 \text{ psi} + 92,200 \text{ psi}}{2} = 66,600 \text{ psi (460 MPa)} \end{aligned}$$

The variation of shear stress with time for this valve spring is noted in Figure 21.10; the time axis is not scaled, inasmuch as the time scale will depend on engine speed.

Our next objective is to determine the fatigue limit amplitude (τ_{al}) for this $\tau_m = 66,600$ psi (460 MPa) using Equation 21.19 and for τ_e and TS values of 45,000 psi (310 MPa) and 227,200 psi (1570 MPa), respectively. Thus,

$$\begin{aligned} \tau_{al} &= \tau_e \left[1 - \frac{\tau_m}{0.67 TS} \right] \\ &= (45,000 \text{ psi}) \left[1 - \frac{66,600 \text{ psi}}{(0.67)(227,200 \text{ psi})} \right] \\ &= 25,300 \text{ psi (175 MPa)} \end{aligned}$$

21.6 One Commonly Employed Steel Alloy • 779

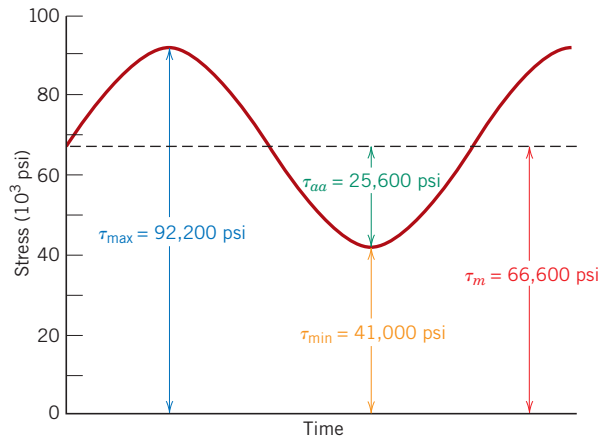


Figure 21.10 Shear stress versus time for an automobile valve spring.

Now let us determine the actual stress amplitude τ_{aa} for the valve spring using Equation 11.16 modified to the shear stress condition:

$$\begin{aligned}\tau_{aa} &= \frac{\tau_{\max} - \tau_{\min}}{2} & (21.23) \\ &= \frac{92,200 \text{ psi} - 41,000 \text{ psi}}{2} = 25,600 \text{ psi (177 MPa)}\end{aligned}$$

Thus, the actual stress amplitude is slightly greater than the fatigue limit, which means that this spring design is marginal.

The fatigue limit of this alloy may be increased to greater than 25,300 psi (175 MPa) by shot peening, a procedure described in Section 11.10. Shot peening involves the introduction of residual compressive surface stresses by plastically deforming outer surface regions; small and very hard particles are projected onto the surface at high velocities. This is an automated procedure commonly used to improve the fatigue resistance of valve springs; in fact, the spring shown in Figure 21.7 has been shot peened, which accounts for its rough surface texture. Shot peening has been observed to increase the fatigue limit of steel alloys in excess of 50% and, in addition, to reduce significantly the degree of scatter of fatigue data.

This spring design, including shot peening, may be satisfactory; however, its adequacy should be verified by experimental testing. The testing procedure is relatively complicated and, consequently, will not be discussed in detail. In essence, it involves performing a relatively large number of fatigue tests (on the order of 1000) on this shot-peened ASTM 232 steel, in shear, using a mean stress of 66,600 psi (460 MPa) and a stress amplitude of 25,600 psi (177 MPa), and for 10^6 cycles. On the basis of the number of failures, an estimate of the survival probability can be made. For the sake of argument, let us assume that this probability turns out to be 0.99999; this means that one spring in 100,000 produced will fail.

Suppose that you are employed by one of the large automobile companies that manufactures on the order of 1 million cars per year, and that the engine powering each automobile is a six-cylinder one. Since for each cylinder there are two valves, and thus two valve springs, a total of 12 million springs would be produced every year. For the above survival probability rate, the total number of spring failures would be approximately 120, which also corresponds to 120 engine failures. As a

practical matter, one would have to weigh the cost of replacing these 120 engines against the cost of a spring redesign.

Redesign options would involve taking measures to reduce the shear stresses on the spring, by altering the parameters in Equations 21.13 and 21.17. This would include either (1) increasing the coil diameter D , which would also necessitate increasing the wire diameter d , or (2) increasing the number of coils N_c .

Failure of an Automobile Rear Axle³

21.7 INTRODUCTION

Subsequent to an accident in which a light pickup truck left the road and overturned, it was noted that one of the rear axes had failed at a point near the wheel mounting flange. This axle was made of a steel that contained approximately 0.3 wt% C. Furthermore, the other axle was intact and did not experience fracture. An investigation was carried out to determine whether the axle failure caused the accident or whether the failure occurred as a consequence of the accident.

Figure 21.11 is a schematic diagram that shows the components of a rear axle assembly of the type used in this pickup truck. The fracture occurred adjacent to the bearing lock nut, as noted in this schematic. A photograph of one end of the failed axle shaft is presented in Figure 21.12a, and Figure 21.12b is an enlarged view of the other fractured piece that includes the wheel mounting flange and the stub end of the failed axle. Here (Figure 21.12b) note that a keyway was present in the area of failure; furthermore, threads for the lock nut were also situated adjacent to this keyway.

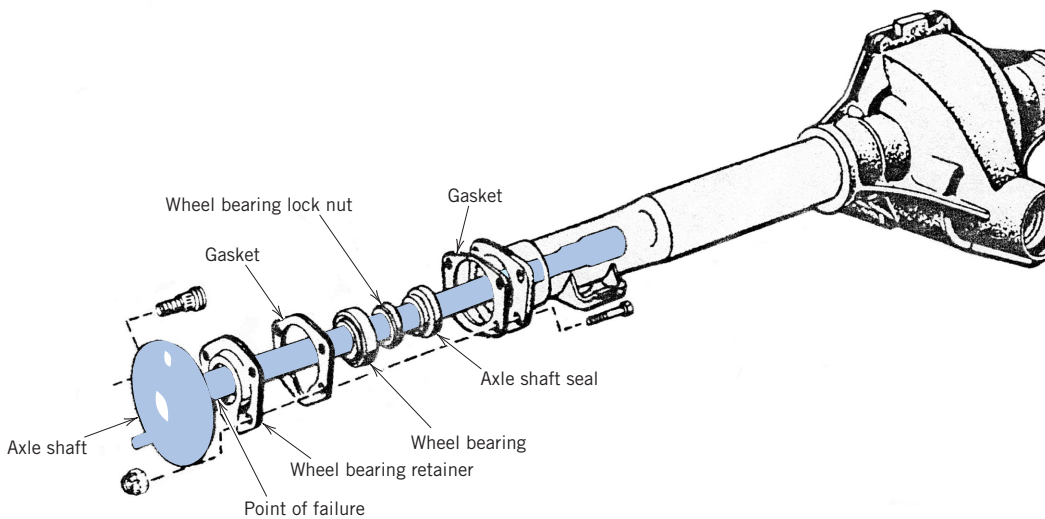


Figure 21.11 Schematic diagram showing typical components of a light truck axle, and the fracture site for the failed axle of this case study. (Reproduced from *MOTOR Auto Repair Manual*, 39th Edition © Copyright 1975. By permission of the Hearst Corporation.)

³ This case study was taken from Lawrence Kashar, "Effect of Strain Rate on the Failure Mode of a Rear Axle," *Handbook of Case Histories in Failure Analysis, Vol. 1*, pp. 74–78, ASM International, Materials Park, OH, 1992.

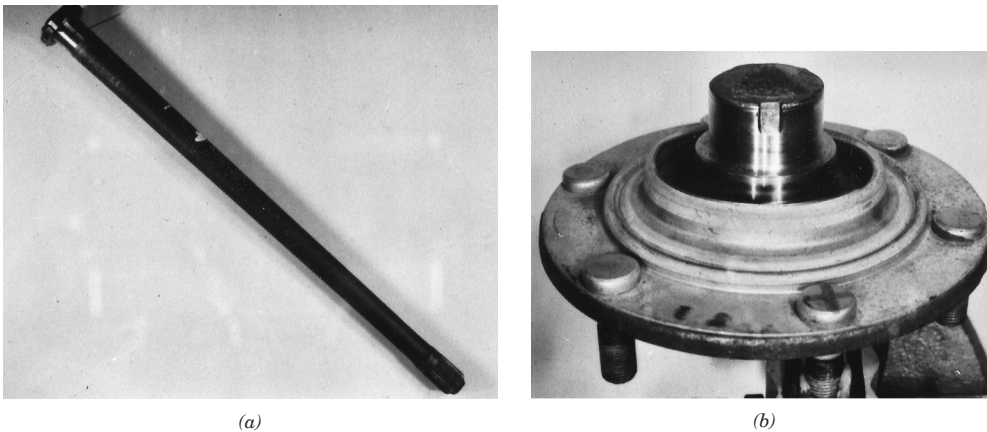


Figure 21.12 (a) Photograph of one section of the failed axle. (b) Photograph showing wheel mounting flange and stub end of failed axle. [Reproduced with permission from *Handbook of Case Studies in Failure Analysis, Vol. 1* (1992), ASM International, Materials Park, OH, 44073-0002.]

Upon examination of the fracture surface it was noted that the region corresponding to the outside shaft perimeter [being approximately 6.4 mm wide] was very flat; furthermore, the center region was rough in appearance.

21.8 TESTING PROCEDURE AND RESULTS

Details of the fracture surface in the vicinity of the keyway are shown in the photograph of Figure 21.13; note that the keyway appears at the bottom of the photograph. Both the flat outer perimeter and rough interior regions may be observed in the photograph. There are chevron patterns that emanate inward from the corners of and parallel to the sides of the keyway; these are barely discernible in the photograph, but indicate the direction of crack propagation.

Fractographic analyses were also conducted on the fracture surface. Figure 21.14 shows a scanning electron micrograph taken near one of the keyway corners. Cleavage features may be noted in this micrograph, whereas any evidence of dimples

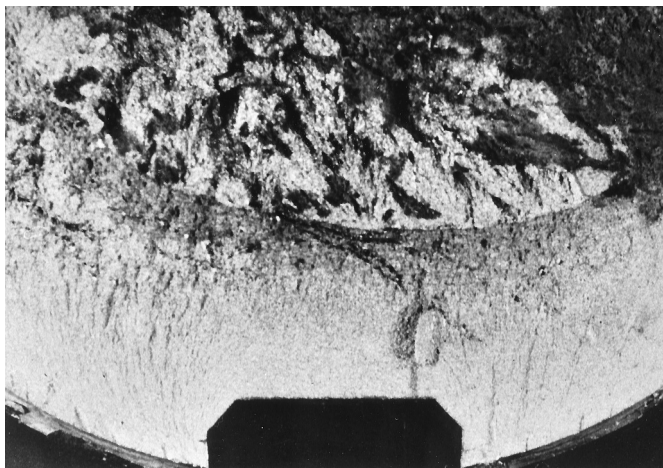


Figure 21.13 Optical micrograph of failed section of axle that shows the keyway (bottom), as well as the flat outer perimeter and rough core regions. [Reproduced with permission from *Handbook of Case Studies in Failure Analysis, Vol. 1* (1992), ASM International, Materials Park, OH, 44073-0002.]

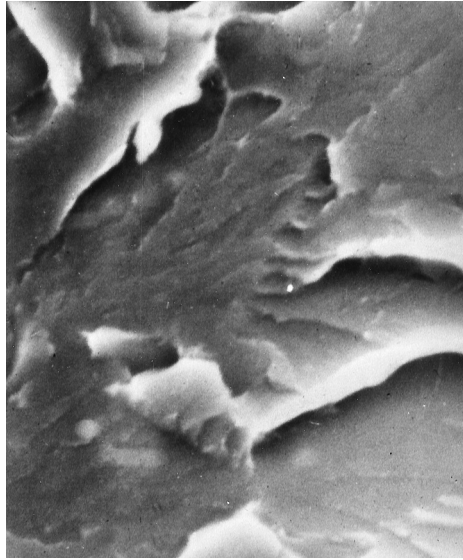


Figure 21.14 Scanning electron micrograph of failed axle outer perimeter region near the keyway, which shows cleavage features. 3500 \times . [Reproduced with permission from *Handbook of Case Studies in Failure Analysis, Vol. 1* (1992), ASM International, Materials Park, OH, 44073-0002.]

and fatigue striations is absent. These results indicate that the mode of fracture within this outer periphery of the shaft was brittle.

An SEM micrograph taken of the rough central region (Figure 21.15) revealed the presence of both brittle cleavage features and also dimples; thus, it is apparent that the failure mode in this central interior region was mixed; that is, it was a combination of both brittle and ductile fracture.

Metallographic examinations were also performed. A transverse cross section of the failed axle was polished, etched, and photographed using the optical microscope. The microstructure of the outer periphery region, as shown in Figure 21.16, consisted of tempered martensite.⁴ On the other hand, in the central region the

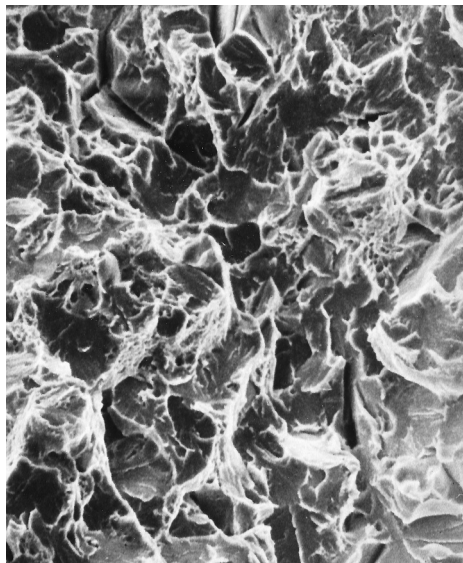


Figure 21.15 Scanning electron micrograph of the failed axle rough central core region, which is composed of mixed cleavage and dimpled regions. 570 \times . [Reproduced with permission from *Handbook of Case Studies in Failure Analysis, Vol. 1* (1992), ASM International, Materials Park, OH, 44073-0002.]

⁴ For a discussion of tempered martensite see Section 8.8.

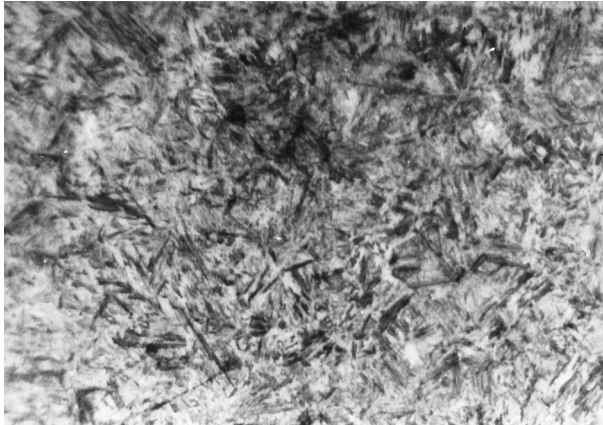
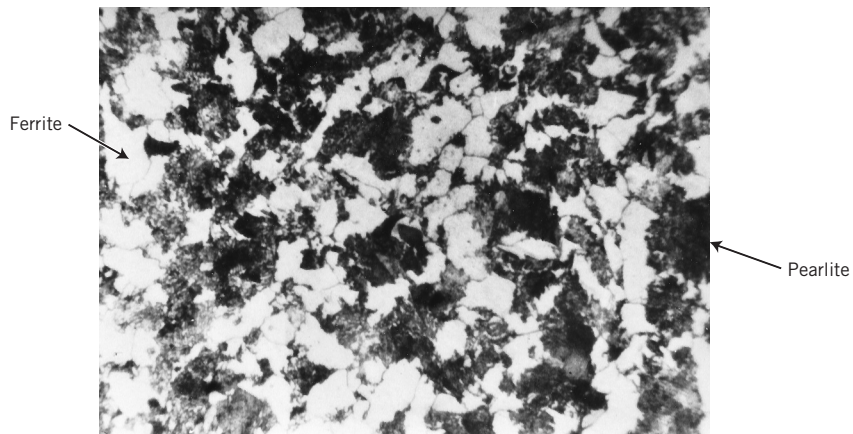


Figure 21.16 Optical photomicrograph of the failed axle outer perimeter region, which is composed of tempered martensite. 500 \times . [Reproduced with permission from *Handbook of Case Studies in Failure Analysis, Vol. 1* (1992), ASM International, Materials Park, OH, 44073-0002.]

microstructure was completely different; from Figure 21.17, a photomicrograph of this region, it may be noted that the microconstituents are ferrite, pearlite, and possibly some bainite.⁵ In addition, transverse microhardness measurements were taken along the cross section; in Figure 21.18 is plotted the resulting hardness profile. Here it may be noted that the maximum hardness of approximately 56 HRC occurred near the surface, and that hardness diminished with radial distance to a hardness of about 20 HRC near the center. On the basis of the observed microstructures and this hardness profile, it was assumed that the axle had been induction hardened.⁶

At this point in the investigation it was not possible to ascertain irrefutably whether the axle fracture caused the accident or whether the accident caused the fracture. The high hardness and, in addition, the evidence of cleavage of the outer surface layer indicated that this region failed in a brittle manner as a result of being overloaded (i.e., as a result of the accident). On the other hand, the evidence of a mixed ductile-brittle mode of fracture in the central region neither supported nor refuted either of the two possible failure scenarios.

Figure 21.17 Optical photomicrograph of the failed axle central core region, which is composed of ferrite and pearlite (and possibly bainite). 500 \times . [Reproduced with permission from *Handbook of Case Studies in Failure Analysis, Vol. 1* (1992), ASM International, Materials Park, OH, 44073-0002.]



⁵ Ferrite, pearlite, and bainite microconstituents are discussed in Sections 8.5 and 8.7.

⁶ With induction hardening, the surface of a piece of medium-carbon steel is rapidly heated using an induction furnace. The piece is then quickly quenched so as to produce an outer surface layer of martensite (which is subsequently tempered), with a mixture of ferrite and pearlite at interior regions.

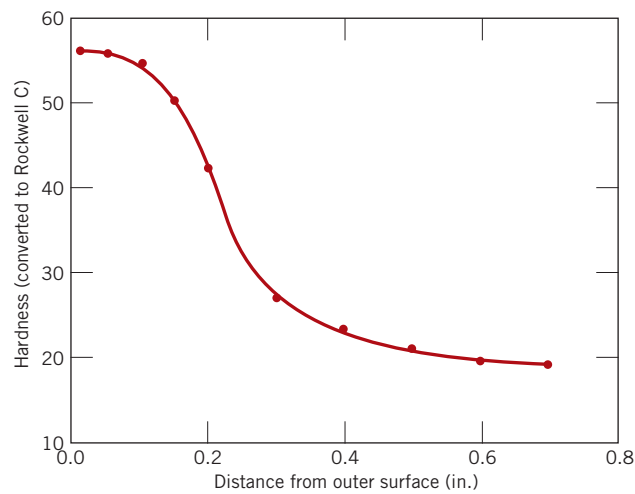


Figure 21.18 Transverse hardness profile across the axle cross section. (Microhardness readings were converted to Rockwell C values). [Reproduced with permission from *Handbook of Case Studies in Failure Analysis, Vol. 1* (1992), ASM International, Materials Park, OH, 44073-0002.]

It was hypothesized that the central core region was strain-rate sensitive to fracture; that is, at high strain rates, as with the truck rollover, the fracture mode would be brittle. By contrast, if failure was due to loads that were applied relatively slowly, as under normal driving conditions, the mode of failure would be more ductile. In light of this reasoning and, also, in order to glean further evidence as to cause of failure, it was decided to fabricate and test both impact and tensile specimens.

Impact Tests

For the impact tests, small [~ 2.5 mm (0.1 in.) wide] Charpy V-notch test specimens were prepared from both outer perimeter and interior areas. Since the hardened outer region was very thin (6.4 mm thick), careful machining of these specimens was required. Impact tests were conducted at room temperature, and it was noted that the energy absorbed by the surface specimen was significantly lower than for the core specimen [4 J (3 ft-lb_f) versus 11 J (8 ft-lb_f)]. Furthermore, the appearances of the fracture surfaces for the two specimens were dissimilar. Very little, if any, deformation was observed for the outer perimeter specimen (Figure 21.19); conversely, the core specimen deformed significantly (Figure 21.20).

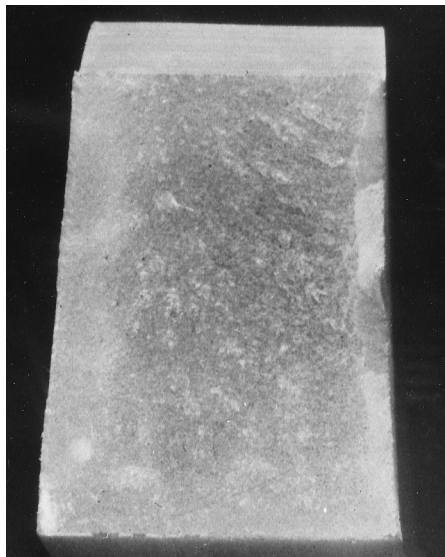


Figure 21.19 Fracture surface of the Charpy impact specimen that was taken from the outer perimeter region. [Reproduced with permission from *Handbook of Case Studies in Failure Analysis, Vol. 1* (1992), ASM International, Materials Park, OH, 44073-0002.]

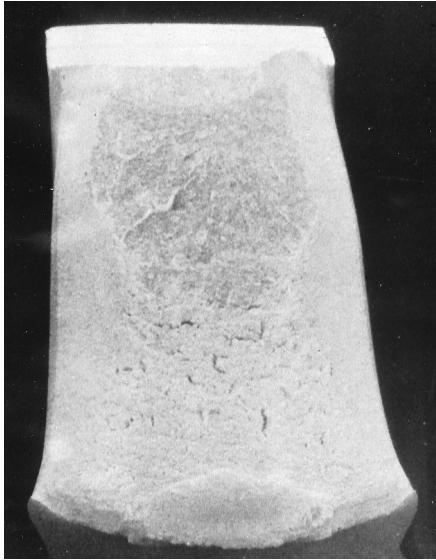
21.8 Testing Procedure and Results • 785

Figure 21.20 Fracture surface of the Charpy impact specimen that was taken from the central core region. [Reproduced with permission from *Handbook of Case Studies in Failure Analysis, Vol. 1* (1992), ASM International, Materials Park, OH, 44073-0002.]

Fracture surfaces of these impact specimens were then subjected to examination using the SEM. Figure 21.21, a micrograph of the outer-periphery specimen that was impact tested, reveals the presence of cleavage features, which indicates that this was a brittle fracture. Furthermore, the morphology of this fracture surface is similar to that of the actual failed axle (Figure 21.14).

For the impact specimen taken from the center-core region the fracture surface had a much different appearance; Figures 21.22a and 21.22b show micrographs for this specimen, which were taken at relatively low and high magnifications, respectively. These micrographs reveal the details of this surface to be composed of interspersed cleavage features and shallow dimples, being similar to the failed axle, as shown in Figure 21.15. Thus, the fracture of this specimen was of the mixed-mode type, having both ductile and brittle components.

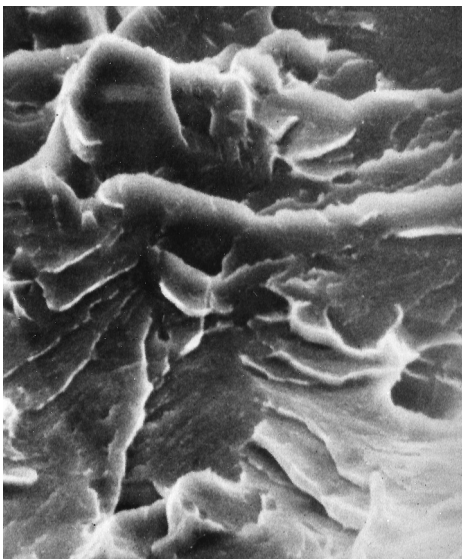


Figure 21.21 Scanning electron micrograph of the fracture surface for the impact specimen prepared from the outer perimeter region of the failed axle. 3000 \times . [Reproduced with permission from *Handbook of Case Studies in Failure Analysis, Vol. 1* (1992), ASM International, Materials Park, OH, 44073-0002.]

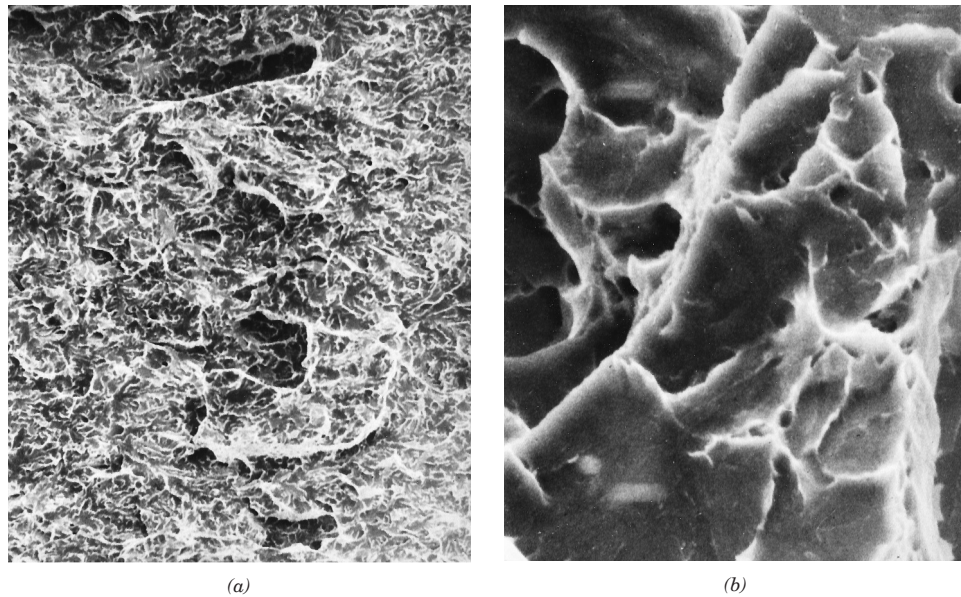


Figure 21.22 (a) Scanning electron micrograph of the fracture surface for the impact specimen prepared from the center-core region of the failed axle. 120 \times . (b) Scanning electron micrograph of the fracture surface for the impact specimen prepared from the center-core region of the failed axle taken at a higher magnification than (a); interspersed cleavage and dimpled features may be noted. 3000 \times . [Reproduced with permission from *Handbook of Case Studies in Failure Analysis, Vol. 1* (1992), ASM International, Materials Park, OH, 44073-0002.]

Tensile Tests

A tensile specimen taken from the center-core region was pulled in tension to failure. The fractured specimen displayed the cup-and-cone configuration, which indicated at least a moderate level of ductility. A fracture surface was examined using the SEM, and its morphology is presented in the micrograph of Figure 21.23. The

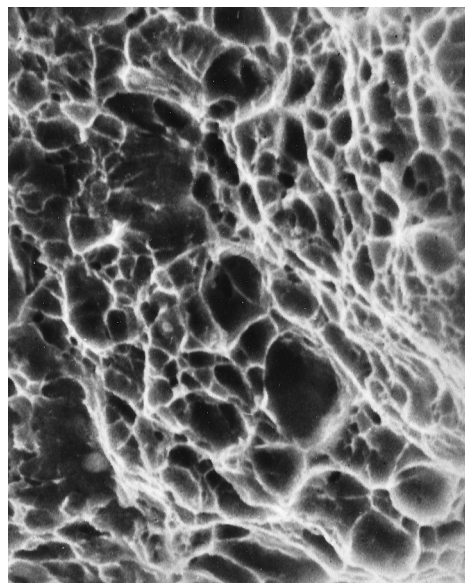


Figure 21.23 Scanning electron micrograph of the fracture surface for the inner-core specimen that was tensile tested; a completely dimpled structure may be noted. Approximately 3500 \times . [Reproduced with permission from *Handbook of Case Studies in Failure Analysis, Vol. 1* (1992), ASM International, Materials Park, OH, 44073-0002.]

surface was composed entirely of dimples, which confirms that this material was at least moderately ductile and that there was no evidence of brittle fracture. Thus, although this center-core material exhibited mixed-mode fracture under impact loading conditions, when the load was applied at a relatively slow rate (as with the tensile test), failure was highly ductile in nature.

21.9 DISCUSSION

In light of the previous discussion it was supposed that the truck rollover was responsible for the axle failure. Reasons for this supposition are as follows:

1. The outer perimeter region of the failed axle shaft failed in a brittle manner, as did also the specimen taken from this region that was impact tested. This conclusion was based on the fact that both fracture surfaces were very flat, and that SEM micrographs revealed the presence of cleavage facets.
2. The fracture behavior of the central core region was strain-rate sensitive, and indicated that axle failure was due to a single high strain-rate incident. Fracture surface features for both the failed axle and impact-tested (i.e., high-strain-rate-tested) specimens taken from this core region were similar: SEM micrographs revealed the presence of features (cleavage features and dimples) that are characteristic of mixed mode (brittle and ductile) fracture.

In spite of evidence supporting the validity of the accident-caused-axle-failure scenario, the plausibility of the other (axle-failure-caused-the-accident) scenario was also explored. This latter scenario necessarily assumes that a fatigue crack or some other slow-crack propagation mechanism initiated the sequence of events that caused the accident. In this case it is important to consider the mechanical characteristics of that portion of the specimen that was last to fail—in this instance, the core region. If failure was due to fatigue, then any increase in loading level of this core region would have occurred relatively slowly, not rapidly as with impact loading conditions. During this gradually increasing load level, fatigue crack propagation would have continued until a critical length was achieved (i.e., until the remaining intact axle cross section was no longer capable of sustaining the applied load); at this time, final failure would have occurred.

On the basis of the tensile tests (i.e., slow strain-rate tests) performed on this core region, the appearance of the axle fracture surface would be entirely ductile (i.e., dimpled, as per the SEM micrograph of Figure 21.23). Inasmuch as this core region of the failed shaft exhibited mixed (ductile and brittle) mode fracture features (both cleavage features and dimples, Figure 21.15), and not exclusively dimples, the axle-failure-caused-the-accident scenario was rejected.

Artificial Total Hip Replacement

21.10 ANATOMY OF THE HIP JOINT

As a prelude to discussing the artificial hip, let us first briefly address some of the anatomical features of joints in general and the hip joint in particular. The joint is an important component of the skeletal system. It is located at bone junctions, where loads may be transmitted from bone to bone by muscular action; this is normally accompanied by some relative motion of the component bones. Bone tissue is a complex natural composite consisting of soft and strong protein collagen and brittle hydroxyapatite, which has a density between 1.6 and 1.7 g/cm³. Bone is an anisotropic

Table 21.3 Mechanical Characteristics of Human Long Bone Both Parallel and Perpendicular to the Bone Axis

<i>Property</i>	<i>Parallel to Bone Axis</i>	<i>Perpendicular to Bone Axis</i>
Elastic modulus, GPa (psi)	17.4 (2.48×10^6)	11.7 (1.67×10^6)
Ultimate strength, tension, MPa (ksi)	135 (19.3)	61.8 (8.96)
Ultimate strength, compression, MPa (ksi)	196 (28.0)	135 (19.3)
Elongation at fracture	3–4%	—

Source: From D. F. Gibbons, “Biomedical Materials,” pp. 253–254, in *Handbook of Engineering in Medicine and Biology*, D. G. Fleming and B. N. Feinberg, CRC Press, Boca Raton, FL, 1976. With permission.

material with mechanical properties that differ in the longitudinal (axial) and transverse (radial) directions (Table 21.3). The articulating (or connecting) surface of each joint is coated with cartilage, which consists of body fluids that lubricate and provide an interface with a very low coefficient of friction that facilitates the bone-sliding movement.

The human hip joint (Figure 21.24) occurs at the junction between the pelvis and the upper leg (thigh) bone, or femur. A relatively large range of rotary motion is permitted at the hip by a ball-and-socket type of joint; the top of the femur terminates in a ball-shaped head that fits into a cup-like cavity (the acetabulum) within the pelvis. An X-ray of a normal hip joint is shown in Figure 21.25a.

This joint is susceptible to fracture, which normally occurs at the narrow region just below the head. An x-ray of a fractured hip is shown in Figure 21.25b; the arrows show the two ends of the fracture line through the femoral neck. Furthermore, the hip may become diseased (osteoarthritis); in such a case small lumps of bone form on the rubbing surfaces of the joint, which causes pain as the head rotates in the acetabulum. Damaged and diseased hip joints have been replaced with artificial or prosthetic ones, with moderate success, beginning in the late 1950s. Total hip

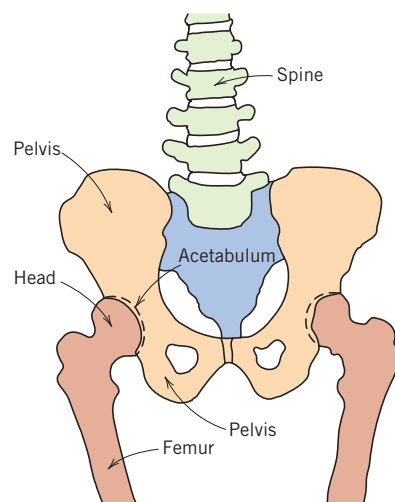
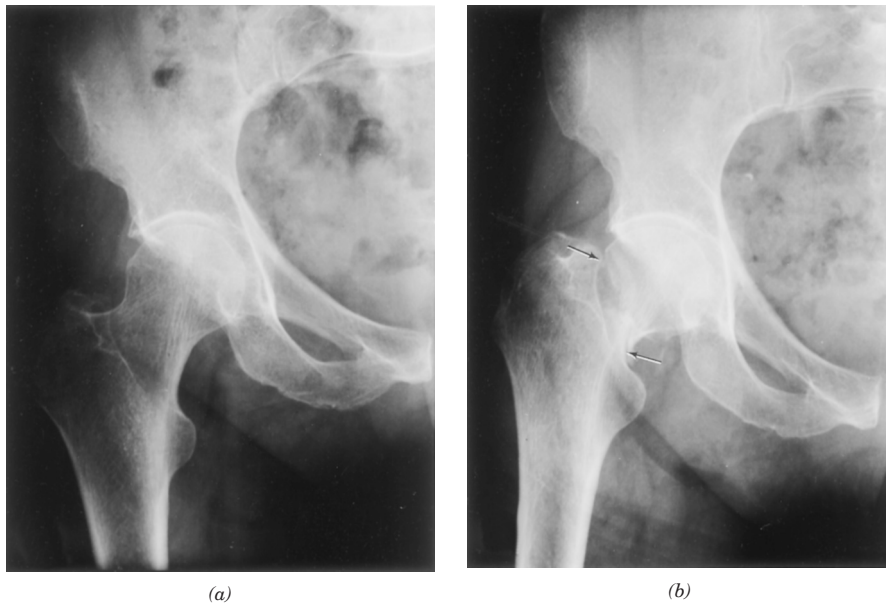


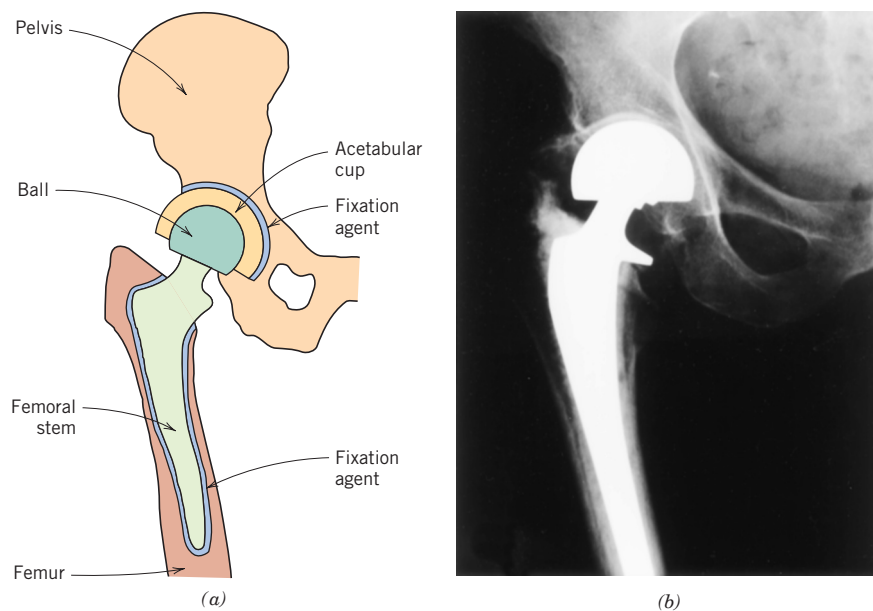
Figure 21.24 Schematic diagram of human hip joints and adjacent skeletal components.

Figure 21.25 X-rays of (a) a normal hip joint and (b) a fractured hip joint. The arrows in (b) show the two ends of the fracture line through the femoral neck.



replacement surgery involves the removal of the head and the upper portion of the femur, and some of the bone marrow at the top of the remaining femur segment. Into this hole within the center of the femur a metal anchorage stem is secured that has the ball portion of the joint at its other end. In addition, the replacement cup socket must be attached to the pelvis. This is accomplished by removal of the old cup and its surrounding bone tissue. The new socket is affixed into this recess. A schematic diagram of the artificial hip joint is presented in Figure 21.26a; Figure 21.26b shows an X-ray of a total hip replacement. In the remainder of this section we discuss material constraints and those materials that have been used with the greatest degree of success for the various artificial hip components.

Figure 21.26 (a) Schematic diagram and (b) x-ray of an artificial total hip replacement.



21.11 MATERIAL REQUIREMENTS

In essence, there are four basic components to the artificial hip: (1) the femoral stem, (2) the ball that attaches to this stem, (3) the acetabular cup that is affixed to the pelvis, and (4) a fixation agent that secures the stem into the femur and the cup to the pelvis. The property constraints on the materials to be used for these elements are very stringent because of the chemical and mechanical complexity of the hip joint. Some of the requisite material characteristics will now be discussed.

Whenever any foreign material is introduced into the body environment, rejection reactions occur. The magnitude of rejection may range from mild irritation or inflammation to death. Any implant material must be *biocompatible*, that is, it must produce a minimum degree of rejection. Products resulting from reactions with body fluids must be tolerated by the surrounding body tissues such that normal tissue function is unimpaired. Biocompatibility is a function of the location of the implant, as well as its chemistry and shape.

Body fluids consist of an aerated and warm solution containing approximately 1 wt% NaCl in addition to other salts and organic compounds in relatively minor concentrations. Thus, body fluids are very corrosive, which for metal alloys can lead not only to uniform corrosion but also to crevice attack and pitting and, when stresses are present, to fretting,⁷ stress corrosion cracking, and corrosion fatigue. It has been estimated that the maximum tolerable corrosion rate for implant metal alloys is about 0.01 mil per year (2.5×10^{-4} mm per year).

Another adverse consequence of corrosion is the generation of corrosion products that are either toxic or interfere with normal body functions. These substances are rapidly transported throughout the body; some may segregate in specific organs. Even though others may be excreted from the body, they may nevertheless still persist in relatively high concentrations because of the ongoing corrosion process.

The bones and replacement components within the hip joint must support forces that originate from outside the body, such as those due to gravity; in addition, they must transmit forces that result from muscular action such as walking. These forces are complex in nature and fluctuate with time in magnitude, in direction, and in rate of application. Thus, mechanical characteristics such as modulus of elasticity, yield strength, tensile strength, fatigue strength, fracture toughness, and ductility are all important considerations relative to the materials of choice for the prosthetic hip. For example, the material used for the femoral stem should have minimum yield and tensile strengths of approximately 500 MPa (72,500 psi) and 650 MPa (95,000 psi), respectively, and a minimum ductility of about 8% EL. In addition, the fatigue strength (for bending stresses that are fully reversed [Figure 11.17a]) should be at least 400 MPa (60,000 psi) at 10^7 cycles. For the average person, the load on the hip joint fluctuates on the order of 10^6 times per year. Ideally the modulus of elasticity of the prosthetic material should match that of bone. A significant difference can lead to deterioration of the surrounding bone tissue and implant failure, which requires a second surgery and another prosthetic implant.

Furthermore, since the ball-and-cup articulating surfaces rub against one another, wear of these surfaces is minimized by using very hard materials. Excessive and uneven wear can lead to a change in shape of the articulating surfaces and cause the prosthesis to malfunction. In addition, particulate debris will be generated as the articulating surfaces wear against one another; accumulation of this debris in the surrounding tissues can also lead to inflammation.

⁷ Fretting is a combination of corrosion and wear in which corrosion produces small debris (generally oxide particles) that increases the friction and induces greater abrasion.

Frictional forces at these rubbing counterfaces should also be minimized to prevent loosening of the femoral stem and acetabular cup assembly from their positions secured by the fixation agent. If these components do become loose over time, the hip joint will experience premature degradation that may require it to be replaced.

Three final important material factors are density, property reproducibility, and cost. It is highly desirable that lightweight components be used, that material properties from prosthesis to prosthesis remain consistent over time, and, of course, that the cost of the prosthesis components be reasonable.

Ideally, an artificial hip that has been surgically implanted should function satisfactorily for the life of the recipient and not require replacement. For current designs, lifetimes range between 15 and 25 years. While this is a substantial improvement from the previous five to ten year figures, longer lifetimes are still desirable.

Several final comments are in order relative to biocompatibility assessment. Biocompatibility of materials is usually determined empirically; that is, tests are conducted wherein materials are implanted in laboratory animals and the biocompatibility of each material is judged on the basis of rejection reactions, level of corrosion, generation of toxic substances, etc. This procedure is then repeated on humans for those materials that were found to be relatively biocompatible in animals. It is difficult to *a priori* predict the biocompatibility of a material. For example, mercury, when ingested into the body, is poisonous; however, dental amalgams, which have high mercury contents, have generally been found to be very biocompatible. Because of this biocompatibility assessment issue, most manufacturers select only materials that have been approved for biomedical use.

One final requirement for implant materials is that they be nonmagnetic [i.e., not exhibit ferromagnetic or ferromagnetic behavior (Chapter 18)]. A frequently used medical diagnostic tool is MRI (magnetic resonance imaging) spectroscopy, a medical test in which the patient is subjected to a very strong magnetic field. The presence of any ferromagnetic/ferromagnetic materials implanted in the patient will disrupt the applied magnetic field, and render MRI spectroscopy unusable. In addition, the magnitudes of these magnetic fields are such that significant forces may be brought to bear on any magnetic implant materials, which forces may loosen the implant and/or harm the patient. Ferromagnetic materials that should be avoided for implant applications include some ferrous alloys (i.e., ferritic and martensitic stainless steels), and alloys having high contents of nickel and/or cobalt.

21.12 MATERIALS EMPLOYED

Femoral Stem and Ball

Early prosthetic hip designs called for both the femoral stem and ball to be of the same material—a stainless steel. Subsequent improvements have been introduced, including the utilization of materials other than stainless steel and, in addition, constructing the stem and ball from different materials. Indeed, stainless steel is rarely used in current implant designs. The chapter-opening photograph for this chapter shows one hip replacement design.

Currently, the femoral stem is constructed from a metal alloy of which there are two primary types: cobalt–chromium–molybdenum and titanium. Some models still use 316L stainless steel, which has a very low sulfur content (<0.002 wt%); its composition is given in Table 9.4. The principal disadvantages of this alloy are its susceptibility to crevice corrosion and pitting and its relatively low fatigue strength. As a result its use has decreased.

Table 21.4 Mechanical and Corrosion Characteristics of Three Metals Alloys That Are Commonly Used for the Femoral Stem Component of the Prosthetic Hip

Alloy	Elastic Modulus [GPa (psi)]	0.2% Yield Strength [MPa (ksi)]	Tensile Strength [MPa (ksi)]	Elongation at Fracture (%)	Fatigue Strength or Limit, 10^7 Cycles [MPa (ksi)]	Corrosion Rate (mpy) ^a
316L Stainless Steel (cold worked, ASTM F138)	200 (29.0×10^6)	689 (100)	862 (125)	12	383 (55.5)	0.001–0.002
Co–28Cr–6Mo (cast, ASTM F75)	210 (30.0×10^6)	483 (70)	772 (112)	8	300 (43.4)	0.003–0.009
Ti–6Al–4V (hot forged, ASTM F620)	120 (17.4×10^6)	827 (120)	896 (130)	10	580 (84.1)	0.007–0.04

^a mpy means mils per year, or 0.001 in./yr

Sources: From Gladus Lewis, *Selection of Engineering Materials*, © 1990, p. 189. Adapted by permission of Prentice Hall, Englewood Cliffs, NJ; and D. F. Gibbons, “Materials for Orthopedic Joint Prostheses,” Ch. 4, p. 116, in *Biocompatibility of Orthopedic Implants*, Vol. I, D. F. Williams, CRC Press, Boca Raton, FL, 1982. With permission.

Various Co–Cr–Mo alloys are used for artificial hip prostheses. One that has been found to be especially suitable, designated F75, is a cast alloy that has a composition of 66 wt% Co, 28 wt% Cr, and 6 wt% Mo. Its mechanical properties and corrosion rate range are listed in Table 21.4. The corrosion and fatigue characteristics of this alloy are excellent.

Of those metal alloys that are implanted for prosthetic hip joints, probably the most biocompatible is the titanium alloy Ti–6Al–4V; its composition is 90 wt% Ti, 6 wt% Al, and 4 wt% V. The optimal properties for this material are produced by hot forging; any subsequent deformation and/or heat treatment should be avoided to prevent the formation of microstructures that are deleterious to its bioperformance. The properties of this alloy are also listed in Table 21.4.

Recent improvements for this prosthetic device include using a ceramic material for the ball component rather than any of the aforementioned metal alloys. The ceramics of choice are a high-purity and polycrystalline aluminum oxide or zirconium oxide, which are harder and more wear resistant than metals, and generate lower frictional stresses at the joint. However, the elastic moduli of these ceramics are large and the fracture toughness of alumina is relatively low. Hence, the femoral stem, is still fabricated from one of the above alloys, and is then attached to the ceramic ball; this femoral stem–ball component thus becomes a two-piece unit.

The materials selected for use in an orthopedic implant come after years of research into the chemical and physical properties of a host of different candidate materials. Ideally, the material(s) of choice will not only be biocompatible but will also have mechanical properties that match the biomaterial being replaced—bone. However, no man-made material is both biocompatible and possesses the property combination of bone and the natural hip joint—low modulus of elasticity, relatively high strength and fracture toughness, low coefficient of friction, and excellent wear resistance. Consequently, material property compromises and trade-offs must be made. For example, recall that the modulus of elasticity of bone and femoral stem materials should be closely matched such that accelerated deterioration of the bone tissue adjacent to the implant is avoided. Unfortunately, man-made materials that are both biocompatible and relatively strong also have high moduli of elasticity. Thus, for this application, it was decided to trade off a low modulus for biocompatibility and strength.

Acetabular Cup

Some acetabular cups are made from one of the biocompatible alloys or aluminum oxide. More commonly, however, ultrahigh molecular weight polyethylene (Section 14.19) is used. This material is virtually inert in the body environment and has excellent wear-resistance characteristics; furthermore, it has a very low coefficient of friction when in contact with the materials used for the ball component of the socket. A two-component cup assembly is shown for the total hip implant in the chapter-opening photograph for this chapter. It consists of an ultrahigh molecular weight polyethylene insert that fits within the cup; this cup is fabricated from one of the metal alloys listed in Table 21.4, which, after implantation, becomes bonded to the pelvis.

Fixation

Successful performance of the artificial hip joint calls for the secure attachment of both the femoral stem to the femur and the acetabular cup to the pelvis. Insecure attachment of either component ultimately leads to a loosening of that component and the accelerated degradation of the joint. A fixation agent is sometimes used to bond these two prosthetic components to their surrounding bone structures. The most commonly used fixation agent is a poly(methyl methacrylate) (acrylic) bone cement that

is polymerized *in situ* during surgery. This reaction must be carefully controlled because the heat released during polymerization can lead to damage to the bone tissue.

This acrylic bond cement has, in some cases, contributed to femoral stem loosening because it is brittle and does not bond well with the metallic implant and bone tissue. It has been found that a more secure implant–bone bond is formed when the stem and cup are coated with a porous surface layer consisting of a sintered metal powder. After implantation, bone tissue grows into the three-dimensional pore network and thereby fixates the implant to the bone. Such a coating has been applied to the upper stem and outer acetabular cup regions of the hip replacement shown in the chapter-opening photograph for this chapter.

Chemical Protective Clothing

21.13 INTRODUCTION

There are a number of commercially important chemicals that, when exposed to the human body, can produce undesirable reactions; these reactions may range from mild skin irritation, to organ damage, or, in the extreme case, death. Anyone who risks exposure to these chemicals should wear chemical protective clothing (CPC) to prevent direct skin contact and contamination. Protective clothing includes at least gloves, but in some instances boots, suits, and/or respirators may be required. This case study involves the assessment of chemical protective glove materials for exposure to methylene chloride.

The choice of a suitable glove material should include consideration of several important factors. The first of these is *breakthrough time*—i.e., the length of time (in minutes) until first detection of the toxic chemical species inside the glove. Another key factor is the *exposure rate*—that is, how much of the toxic chemical passes through the glove per unit time. Consideration of both breakthrough time and exposure rate is important. Other relevant material factors include material degradability, flexibility, and puncture resistance. Trade-offs of these several characteristics may be necessary. For example, a thick glove may have a longer breakthrough time and lower exposure rate, but be less flexible than a thin glove.

Common commercially available glove materials include natural rubber, nitrile rubber, poly(vinyl chloride), neoprene rubber, and poly(vinyl alcohol) (PVA). Some gloves are *multilayered*, that is, composed of layers of two different materials that take advantage of the desirable features of each. For example, PVA is highly impermeable to many organic solvents, but is soluble in water; any exposure to water can soften (and ultimately dissolve) the glove. To counteract this liability, CPC materials that consist of a thin layer of PVA sandwiched between two layers of a nonpolar polymer such as polyethylene have been developed. The PVA layer impedes the diffusion of nonpolar materials (i.e., many of the organic solvents), whereas the polyethylene layers shield the PVA from water and inhibit the permeation of polar solvents (i.e., water and alcohols).

21.14 ASSESSMENT OF CPC GLOVES MATERIALS TO PROTECT AGAINST EXPOSURE TO METHYLENE CHLORIDE

Let us consider the selection of a glove material for use with methylene chloride (CH_2Cl_2), a common ingredient in paint removers. Methylene chloride is a skin irritant, and, furthermore, may also be absorbed into the body through skin; studies

21.14 Assessment of CPC Glove Materials to Project Against Exposure to Methylene Chloride • 795

suggest that its presence in the body may cause cancer as well as birth defects. Computations of breakthrough time and exposure rate for methylene chloride that is in contact with potential glove materials are possible. In light of the hazardous nature of CH_2Cl_2 , for these calculations any assumptions we make are conservative, and overestimate the inherent dangers.

The breakthrough time t_b is related to the diffusion coefficient of methylene chloride in the glove material (D) and the glove thickness (ℓ) according to the following equation:

$$t_b = \frac{\ell^2}{6D} \quad (21.24)$$

Values of D , ℓ , and t_b (computed using the above expression) for several commercially available CPC glove materials are provided in Table 21.5. Breakthrough times can also be measured directly using appropriate equipment; these measured values are in good agreement with the calculated ones presented in the table.

For exposure rate computations, we assume that a condition of steady-state diffusion has been achieved, and also that concentration profile is linear [Figure 6.4(b)]. In actual fact, at the outset of exposure to methylene chloride, its diffusion through the glove is nonsteady-state, and the accompanying diffusion rates are lower than those calculated for conditions of steady state. For steady-state diffusion, the diffusion flux J is according to Equation 6.3 as

$$J = -D \frac{dC}{dx} \quad (21.25)$$

And for a linear concentration profile, this equation takes the form

$$J = -D \frac{C_A - C_B}{x_A - x_B} \quad (21.26)$$

We arbitrarily take the A and B subscripts to denote glove surfaces in contact with the methylene chloride and with the hand, respectively. In addition, the glove thickness $\ell = x_B - x_A$, such that the above equation now takes the form

$$J = D \frac{C_A - C_B}{\ell} \quad (21.27)$$

Now, the exposure rate r_e is equal to the product of the diffusion flux and total glove surface area (A)—that is

$$r_e = JA = \frac{DA}{\ell}(C_A - C_B) \quad (21.28)$$

An average size pair of gloves has an inside surface area of about 800 cm^2 . Furthermore, the surface concentration of methylene chloride (i.e., C_A) is equal to its solubility in that polymer (which we denote as S_A); solubility values for the several glove materials are also included in Table 21.5. Now, if we assume that all methylene chloride, upon contact, is immediately absorbed by the skin and swept away by the blood stream, then C_B takes on a value of 0 g/cm^3 .⁸ Thus, upon making the above

⁸ In most practical situations, $C_B > 0 \text{ g/cm}^3$ since not all of the methylene chloride that passes through the glove will immediately be absorbed into the skin and removed from the hand by the blood stream. Thus, the values of r_e we calculate will be greater than the actual exposure rates that the hands experience.

Table 21.5 Characteristics and Costs for Commercially Available Chemical Protective Glove Materials That May Be Used With Methylene Chloride

Material	Diffusion Coefficient, D (10^{-8} cm ² /s)	Glove Thickness, ℓ (cm)	Breakthrough Time, t_b (min)	Surface Concentration, S_A (g/cm ³)	Exposure Rate, r_e (g/h)	Cost (US\$/pair)
Multilayer ^a	0.0095	0.007	1430	11.1	0.43	4.19
Poly(vinyl alcohol)	4.46	0.075	350	0.68	1.15	24.00
Viton rubber	3.0	0.025	58	0.10	0.35	72.00
Butyl rubber	110	0.090	20	0.44	15.5	58.00
Neoprene rubber	92	0.075	17	3.53	125	3.35
Poly(vinyl chloride)	176	0.070	8	1.59	115	3.21
Nitrile rubber	157	0.040	2.8	2.68	303	1.56

^a Silver Shield™**Sources:** Manufacturers' data sheets.

21.14 Assessment of CPC Glove Materials to Project Against Exposure to Methylene Chloride • 797

substitutions for C_A and C_B into Equation 21.28, we obtain the following expression for r_e :

$$r_e = \frac{DAS_A}{\ell} \quad (21.29)$$

Table 21.5 also includes, for these several glove materials, values of r_e that were determined using Equation 21.29.

At this point, a key question is: What is an acceptable and safe exposure rate? Based on airborne exposure limits set by the Occupational Safety and Health Administration (OSHA) of the US, the maximum allowable r_e to methylene chloride is approximately 1 g/h.

Now let us examine and compare computed breakthrough times and exposure rates for the several glove materials, as listed in Table 21.5. First of all, with regard to exposure rate, two of the seven materials meet or exceed the standard set by OSHA (viz., 1 g/h)—viz. multilayer (Silver Shield™) and Viton™ rubber (with r_e values of 0.43 and 0.35 g/h, respectively). Relative to breakthrough time, the multilayer material has the longer t_b (24 hr versus about 6h for the Viton rubber). Furthermore, the multilayer gloves are considerably less inexpensive (at \$US4.19 per pair compared to \$US72.00 for Viton rubber, Table 21.5).

Therefore, of these two glove materials, other relevant characteristics/properties being equal, the one of choice for this application is multilayer Silver Shield. It has a significantly longer breakthrough time and is much less costly than the Viton rubber material, whereas there is very little difference between their exposure rates. The photograph of Figure 21.27 shows a pair of Silver Shield gloves.

It should be noted that calculated breakthrough time values presented in Table 21.5 assumed the glove material had no previous exposure to methylene chloride. For a second application, some of the methylene chloride that dissolved in the glove during the first exposure probably remains; thus, the breakthrough time will be much shorter than predicted for an unused glove. For this reason, CPC gloves are often discarded after one usage.

One final comment is in order: one should always consult an industrial hygiene specialist when selecting chemical protection clothing. These specialists are experts as to what materials are suitable for exposure to specific toxic chemical substances,



Figure 21.27 Photograph of Silver Shield multilayer chemical protective gloves. (Photograph courtesy of North Safety Products, Anjou, Quebec, Canada.)

and also with regard to other factors to include material degradability, flexibility, grip, puncture resistance, etc.

Materials for Integrated Circuit Packages

21.15 INTRODUCTION

The microelectronic circuitry, including the integrated circuits that are used in our modern computers, calculators, and other electronic devices, was briefly discussed in Section 17.15. The heart of the integrated circuit (abbreviated *IC*) is the *chip*, a small rectangular substrate of high-purity and single-crystal silicon (or more recently gallium arsenide) onto which literally thousands of circuit elements are imprinted. Circuit elements (i.e., transistors, resistors, diodes, etc.) are created by selectively adding controlled concentrations of specific impurities to extremely minute and localized regions near the surface of the semiconducting material using involved photolithographic techniques. The chips are small in size, with the largest on the order of 6 mm ($\frac{1}{4}$ in.) on each side and approximately 0.4 mm (0.015 in.) thick. Photographs of a typical chip are shown in Figure 17.27.

Furthermore, chips are very fragile inasmuch as silicon is a relatively brittle material and gallium arsenide is even more brittle. It is also necessary to fabricate conducting circuit paths over the surface of the chip to facilitate the passage of current from device to device; on silicon ICs the metal conductor used is aluminum or an aluminum–silicon alloy (99 wt% Al, 1 wt% Si) that is metallized onto the chip surface to form a very thin film. The chip design also calls for these circuit paths to terminate at contact pads on the chip periphery, at which points electrical connections may be made with the macroscopic world. It should be obvious that a functioning microelectronic chip is a very sophisticated electronic entity, that materials requirements are very stringent, and that elegant processing techniques are involved in its fabrication.

A large number of IC chips are fabricated onto a circular thin wafer of single-crystal Si, as shown in the photograph in Figure 21.28. Single crystals of Si having

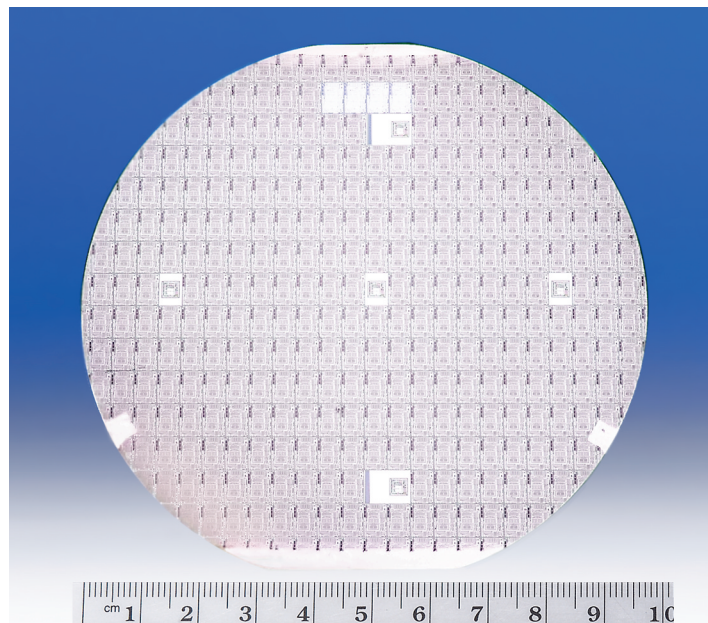


Figure 21.28

Photograph of a 100-mm-diameter (4-in.-diameter) silicon wafer. Each of the small rectangles shown is an individual IC chip or die. (Photography by S. Tanner.)

diameters as large as 200 mm are routinely grown. The small rectangular ICs arrayed in the manner shown in the photograph are collectively referred to as *dice*. Each IC or **die** (singular of dice) is first tested for functionality, after which it is removed from the wafer in a meticulous sawing or “scribe and break” operation. Next, the die is mounted in some type of *package*. The packaged IC may then be bonded to a printed circuit board. The purpose of this section is to discuss the material requirements and some of the materials that are used for the various IC package components.

Some of the functions that an integrated circuit package must perform include the following:

1. To permit electrical contact between the devices on the chip and the macroscopic world. The contact pads on the surface of the IC are so minuscule and numerous that accommodation of macroscopic wiring is simply not possible.
2. To dissipate excess heat. While in operation, the many electronic devices generate significant quantities of heat, which must be dissipated away from the chip.
3. To protect delicate electrical connections on the chip from chemical degradation and contamination.
4. To provide mechanical support so that the small and fragile chip may be handled.
5. To provide an adequate electrical interface such that the performance of the IC itself is not significantly degraded by the package design.

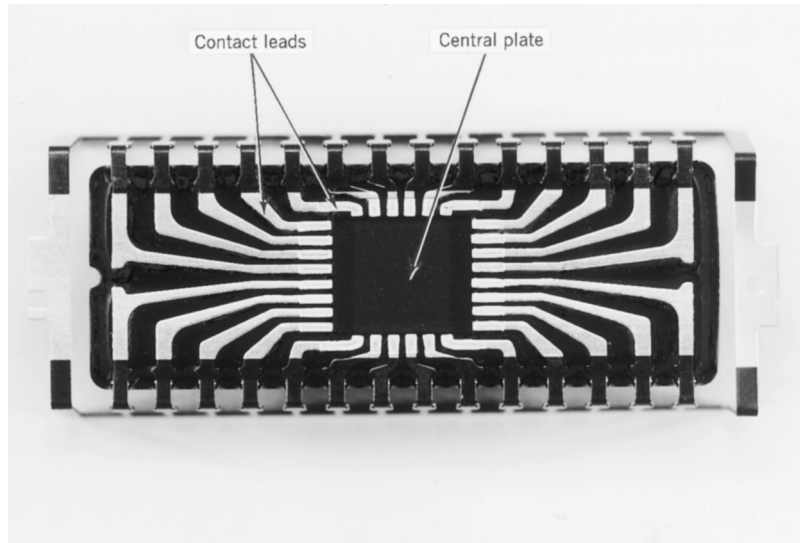
Thus, IC packaging also poses a host of material demands that are very challenging. In fact, it has been noted that the performance of some ICs is limited, not by the characteristics of the semiconducting materials or by the metallization process, but rather by the quality of the package. There are a number of different package designs used by the various IC manufacturers. For one of the common designs, the *leadframe*, we have elected to discuss the various components and, for each component, the materials that are employed along with their property limitations. This package design is popular with digital IC manufacturers primarily because its production can be highly automated.

21.16 LEADFRAME DESIGN AND MATERIALS

The leadframe, as the name suggests, is a frame to which electrical leads may be made from the IC chip. A photograph of a leadframe-type package is shown in Figure 21.29. In essence, the leadframe consists of a central plate onto which the die is mounted, and an array of contact leads to which wire connections may be made from the contact pads on the chip. Some leadframe designs also call for a substrate onto which the die is mounted; this substrate is, in turn, bonded to the central plate. During the packaging process, and after the chip has been attached to the central plate (a procedure termed *die bonding*), the contact pads on the IC chip are cleaned, wires are attached to both the contact pads and the leadframe leads (called *wire bonding*), and, finally, this package is encapsulated in a protective enclosure to seal out moisture, dust, and other contaminants. This procedure is called *hermetic sealing*.

There are some rather stringent requirements on the properties of the material to be used for the leadframe; these are as follows: (1) The leadframe material must have a high electrical conductivity because there will be current passage through its leads. (2) The leadframe, the die attach central plate, substrate (if present),

Figure 21.29
 Photograph of a
 leadframe on which
 the central plate and
 contact leads are
 labeled. 2×.
 (Leadframe supplied
 by National
 Semiconductor
 Corporation.
 Photograph by
 Dennis Haynes.)



and die-bonding adhesive must also be thermally conductive to facilitate the dissipation of heat generated by the IC. (3) A coefficient of thermal expansion comparable to that of Si is highly desirable; a thermal expansion mismatch could destroy the integrity of the bond between the IC and the central plate as a result of thermal cycling during normal operation. (4) The leadframe material and substrate must also adhere to the die-bonding adhesive, and the adhesive and substrate must also be electrically conductive. (5) A secure and electrically conductive joint between the leadframe and the connecting wires must be possible. (6) The leadframe must be resistant to oxidation and retain its mechanical strength during any thermal cycling that may accompany the die-bonding and encapsulation procedures. (7) The leadframe must also withstand corrosive environments at high temperatures and high humidities. (8) It must be possible to mass produce the leadframes economically. Normally, they are stamped from thin metal sheets.

Several alloys have been used for the leadframe with varying degrees of success. The most commonly used materials are copper-based alloys; the compositions, electrical and thermal conductivities, and coefficients of thermal expansion for two of the most popular ones (C19400 and C19500) are listed in Table 21.6. For the most part, they satisfy the criteria listed in the preceding paragraph. Also listed in the table are the compositions of two other alloys (Kovar and Alloy 42) that have been used extensively in leadframes. The desirability of these latter two alloys lies in their relatively low coefficients of thermal expansion, which are closely matched to that of Si [i.e., $2.5 \times 10^{-6} (\text{°C})^{-1}$]. However, from Table 21.6 it may also be noted that both electrical and thermal conductivities for Kovar and Alloy 42 are inferior to the conductivity values for the C19400 and C19500 alloys.

21.17 DIE BONDING

The die-bonding operation consists of attaching the IC chip to the central supporting leadframe plate. For the copper alloys noted in Table 21.6, attachment may be made using a gold–silicon eutectic solder; however, melting of the solder requires heating the assembly to 500°C (900°F).

Another adhesive possibility is an epoxy bonding agent, which is normally filled with metal particles (frequently Ag) so as to provide both a thermally and

Table 21.6 Designations, Compositions, Electrical and Thermal Conductivities, and Coefficients of Thermal Expansion for Common IC Leadframe Alloys

Alloy Designation	Composition (wt%)				Electrical Conductivity [$10^6(\Omega\text{-m})^{-1}$]	Thermal Conductivity (W/m-K)	Coefficient of Thermal Expansion ^a [$10^{-6}(\text{°C})^{-1}$]
	Fe	Ni	Co	Cu			
C19400	2.35			Balance	39.4	260	16.3
C19500	1.5		0.8	Balance	29.1	200	16.9
Kovar (ASTM F15)	54	29	17		2.0	17	5.1
Alloy 42 (ASTM F30)	58	42			1.4	12	4.9

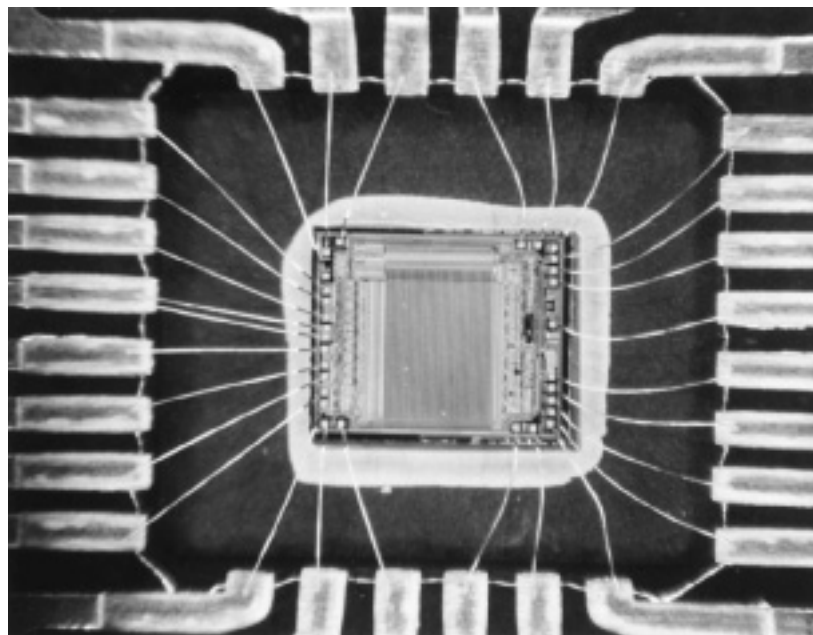
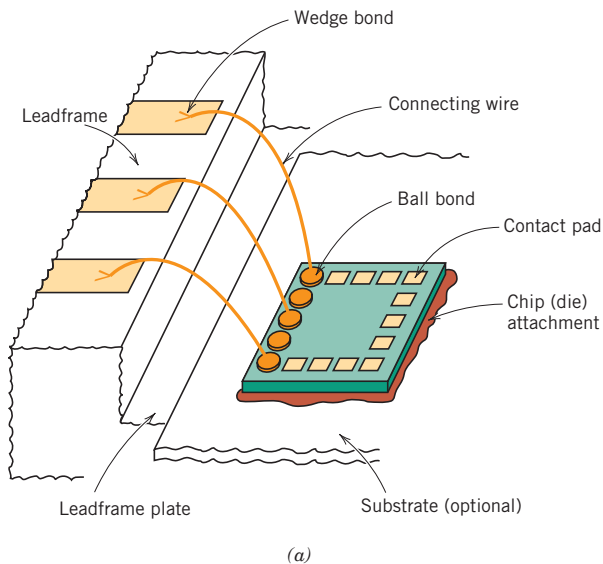
^a Coefficient of thermal expansion values are averages measured between 20°C and 300°C.

802 • Chapter 21 / Materials Selection and Design Considerations

electrically conductive path between the chip and the leadframe. Curing of the epoxy is carried out at temperatures between 60°C (140°F) and 350°C (660°F) depending on the application. Since the amounts of thermal expansion are different for the Cu alloy leadframe plate and Si chip, the epoxy adhesive must be capable of absorbing any thermal strains produced during temperature changes such that the mechanical integrity of the junction is maintained. Figure 21.30a shows a schematic diagram of a chip that is bonded to a substrate layer that is, in turn, bonded to the leadframe plate. Figure 21.30b is a photograph of a chip, its leadframe, and the connecting wires.

Figure 21.30

(a) Schematic diagram showing the IC chip, its attachment to the substrate (or leadframe plate), and the connecting wires that run to the leadframe contact leads. (b) Photograph showing a portion of a leadframe package. Included is the IC chip along with its connecting wires. One end of each wire is bonded to a chip pad; the other wire extremity is bonded to a leadframe contact lead. $7\frac{1}{2}\times$. [Figure (a) adapted from *Electronic Materials Handbook*, Vol. 1, *Packaging*, C. A. Dostal, editor, ASM International, 1989, p. 225. The photograph in (b) courtesy of National Semiconductor Corporation.]



(b)

21.18 WIRE BONDING

The next step in the packaging process involves making electrical connections between the metallized chip pads and the leadframe; this is accomplished using connecting wires (Figures 21.29a and 21.29b). A wire-bonding procedure is normally carried out using a microjoining operation, since very fine wires are used to make the connections. Wire bonding is the slow step in the packaging process because several hundred wires may need to be installed; this procedure is usually automated.

Several important considerations must be taken into account relative to the choice of wire alloy. Of course, a high electrical conductivity is the prime prerequisite. In addition, consideration must be given to the ability of the alloy to bond, by welding or brazing, with both the Al alloy at the chip pad and the Cu alloy on the leadframe; the formation of a microjoint that is both mechanically and electrically stable is an absolute necessity.

The most commonly used wire material is gold—actually a gold alloy containing a small amount of beryllium—copper that is added to inhibit grain growth. Gold wires are round and have diameters that are typically 18 μm , 25 μm , or 50 μm . Less costly Cu and Al have also been employed for contact wires. Prior to making the microjoint, regions of the chip pad and leadframe surfaces at which the junctions are to be made may be coated with Au to improve bondability. During the actual microjoining process, one wire end is brought into the vicinity of one of the joint regions using a special tool. This wire end is then melted with a spark or flame heat source.

Two different types of microjoints are possible: ball and wedge. Figure 21.31 is a schematic diagram showing a connecting wire having a ball microjoint at its contact pad end and a wedge microjoint at the leadframe connection. Ball joints are possible for gold wires since the melted wire end forms into a small ball because of the high surface tension of gold. Bonding of this molten ball with the contact pad or leadframe is accomplished by making mechanical contact with the bonding surface while both wire and surface are subjected to ultrasonic vibrations. A scanning electron micrograph of a ball microjoint is shown in Figure 21.32a. This type of microjoint is especially desirable since, after the first of the two microjoints for each wire has been made (usually on the IC contact pad), the wire may then be bent in any direction in preparation for the microjoining of its other extremity.

The ends of copper and aluminum wires do not form balls upon melting. They are wedge microjoined by positioning the wire between a vibrating probe and the contact pad or leadframe surface; the vibrations loosen and remove surface contaminants, which results in intimate contact of the two surfaces. An electric current is then applied through the probe, which welds the wire to the surface.

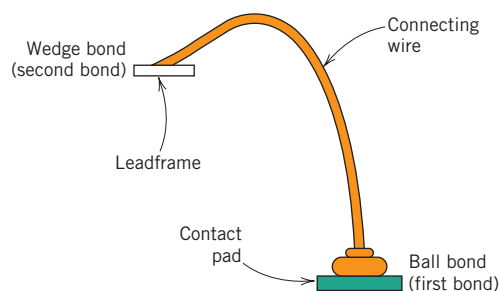


Figure 21.31 Schematic diagram showing a connecting wire that is ball bonded to the IC contact pad and wedge bonded to the leadframe. [Adapted from *Electronic Materials Handbook*, Vol. 1, *Packaging*, C. A. Dostal (Editor), ASM International, 1989, p. 225.]

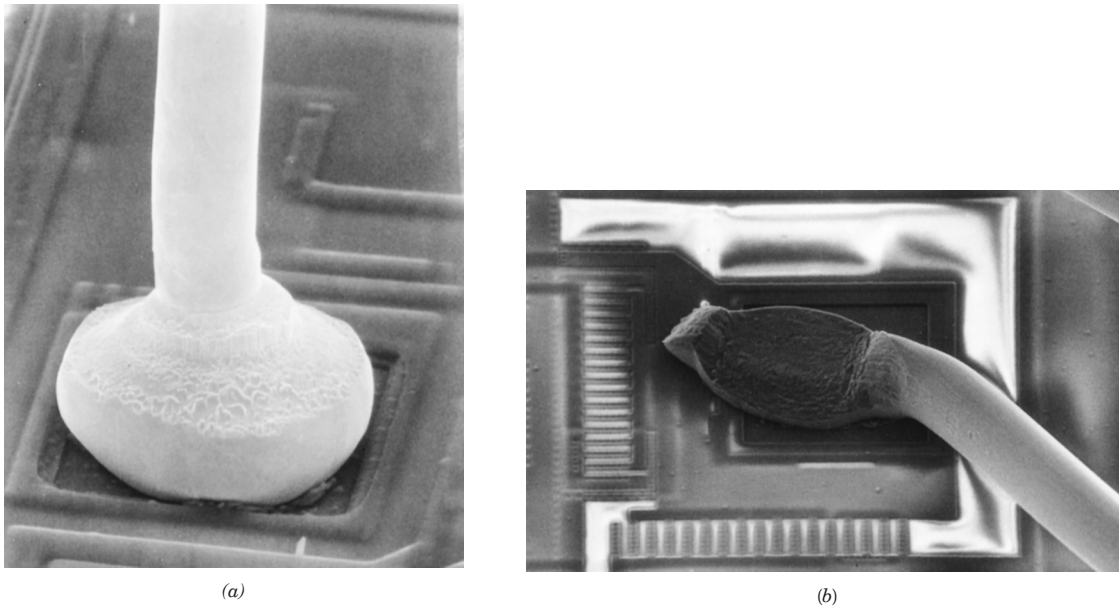


Figure 21.32 Scanning electron micrographs of (a) a ball bond (475 \times), and (b) a wedge bond (275 \times). (Photographs courtesy of National Semiconductor Corporation.)

Unfortunately, the bending motion of wedge-bonded wires is restricted to a single direction. Gold wires may also be bonded using wedge microjoints. Figure 21.32b is a scanning electron micrograph of a wedge microjoint.

There are other considerations relative to wire bonding that deserve mentioning. Microjunction alloy combinations that form intermetallic phases should be avoided because these phases are normally brittle and yield microjoints lacking long-term mechanical stability. For example, Au and Al may react at elevated temperatures to form AuAl_2 , termed the “purple plague”; this compound is not only very brittle (and purple), but also highly electrically resistive. Furthermore, mechanical integrity at each microjoint is important to (1) withstand vibrations that the package may experience, and (2) survive thermal stresses that are generated as the packaging materials change temperature.

21.19 PACKAGE ENCAPSULATION

The microelectronic package, as now constituted, must be provided some type of protection from corrosion, contamination, and damage during handling and while in service. The wire interconnection microjunctions are extremely fragile and may be easily damaged. Especially vulnerable to corrosion are the narrow Al circuit paths that have been metallized onto the surface of the IC chip; even the slightest corrosion of these elements will impair the operation of the chip. These Al-metallized layers experience corrosion when atmospheric moisture in which even minute concentrations of ionic contaminants are dissolved (especially chlorine and phosphorus) condenses on the chip surface. Furthermore, the corrosive reactions are accelerated as a consequence of electric currents that pass through these circuit paths. In addition, any sodium (as Na^+) that gets on the chip surface will eventually diffuse into the chip and destroy its operation.

The material used to encapsulate the package should:

1. Be electrically insulating
2. Be easily molded to the desired shape around the chip die and its wire leads
3. Be highly impervious to the penetration of moisture and contaminants
4. Be able to form strong adhesive bonds with the chip surface, wires, and other leadframe components
5. Exhibit mechanical and chemical stability for the expected lifetime of the package
6. Not require exposure to excessively high temperatures during installation
7. Have a coefficient of thermal expansion similar to those of other package components to avoid thermal stresses capable of fracturing the wire leads

Figure 21.33 shows a schematic diagram of an encapsulated IC package.

Both ceramic and polymeric materials are used to encapsulate IC packages; of course each of these material types has its own set of assets and liabilities. Ceramics are extremely resistant to moisture penetration and are chemically stable and chemically inert. Glasses are the most commonly utilized ceramic materials. The principal disadvantage of glass is the requirement that it be heated to moderately high temperatures to lower its viscosity to the point where it will flow around and make intimate contact with all of the wires that are microjoined to the chip surface. Some common glass constituents should be avoided (notably Na_2O and K_2O) since volatile cation species (Na^+ and K^+) may be emitted from the molten glass. These species are notorious in accelerating corrosion reactions, and the ions will degrade the chip performance.

Polymeric materials are used in the largest volume for packaging encapsulation because they are not as costly as the ceramics, and they may be produced in a low-viscosity state at lower temperatures. Epoxies and polyurethanes are commonly used, with the former being the most common. However, these materials have a tendency to absorb water and do not form moisture-tight bonds with the lead wires. Some of these polymers require curing at a temperature on the order of 150°C , and during cooling to room temperature will shrink more than other package components to which they are attached. This difference in amounts of contraction can give rise to mechanical strains of sufficient magnitude to damage the connecting wires as well as other electronic components. The addition of appropriate fillers (such as fine silica or alumina particles) to the polymer can alleviate this problem but often has undesirable electrical

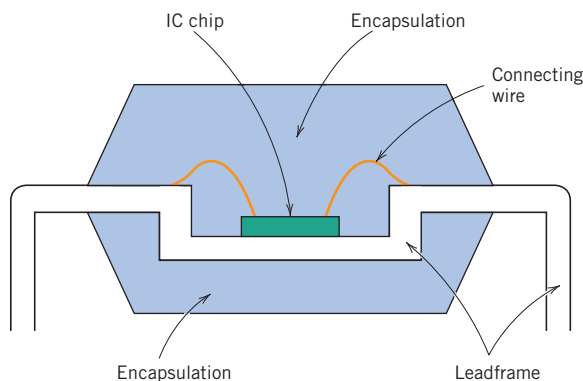


Figure 21.33 Schematic diagram showing an encapsulated IC leadframe package. [Adapted from *Electronic Materials Handbook*, Vol. 1. *Packaging*, C. A. Dostal (Editor), ASM International, 1989, p. 241.]

Table 21.7 Property Comparisons of Four Classes of Polymers Used for IC Package Encapsulation

	<i>Epoxy Resins</i>	<i>Silicones</i>	<i>Polyurethanes</i>	<i>Polysulphides</i>
Dielectric strength	Good	Good	Good	Good
Elastic modulus	High	Low	Wide range	Low
Tensile strength	High	Low	Wide range	—
Precursor viscosity	Low	Low	Low	High
Adhesion to package	Excellent	Poor (to ceramics)	Good	Good
Moisture diffusion rate	High	High	Low	Very low

Source: From C. R. M. Grovenor, *Microelectronic Materials*. Copyright © 1989 by Institute of Physics Publishing, Bristol, England.

consequences. A comparison of the important encapsulation characteristics of four different polymer types is given in Table 21.7.

21.20 TAPE AUTOMATED BONDING

Another packaging design, tape automated bonding (or *TAB*), a variation of the leadframe discussed above, has found widespread use by virtue of its low cost. The tape-bonded package consists of a thin and flexible polyimide polymer backing film substrate; onto this substrate surface is patterned an array of copper “finger” high-conductivity conduction paths similar in configuration to the contact leads for the conventional leadframe. A schematic diagram of a tape-bonded film leadframe is shown in Figure 21.34.

Mechanical support for the assembly is provided by the polyimide film, onto which the die is bonded using an adhesive. Polyimide strip widths are typically 35 mm (1.38 in.), and sprocket holes are incorporated along opposing edges to facilitate movement and positioning of the *TAB* leadframes. Literally thousands of these individual units, attached end to end, are spooled onto reels in preparation for automated processing.

Figure 21.34
Schematic diagram of a complete tape-bonded (*TAB*) leadframe. [From *Electronic Materials Handbook*, Vol. 1, *Packaging*, C. A. Dostal (Editor), ASM International, 1989, p. 233.]

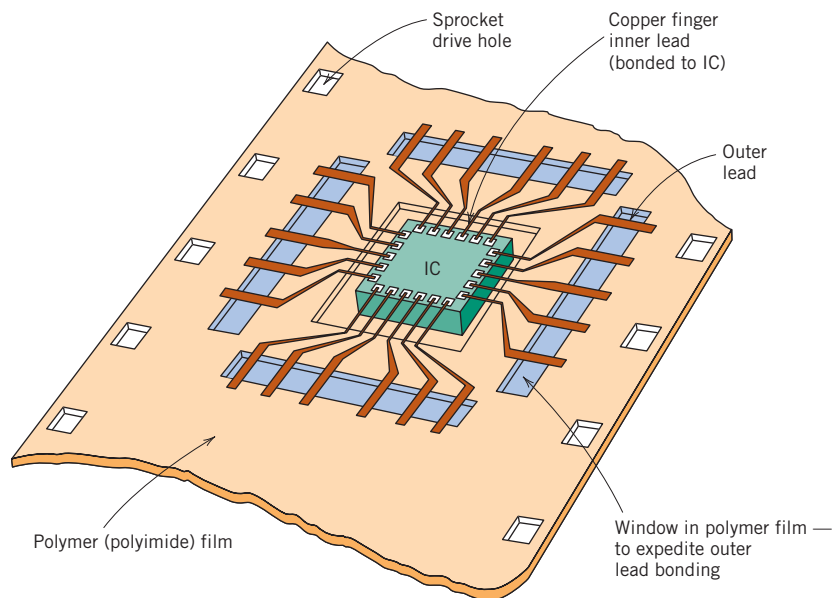
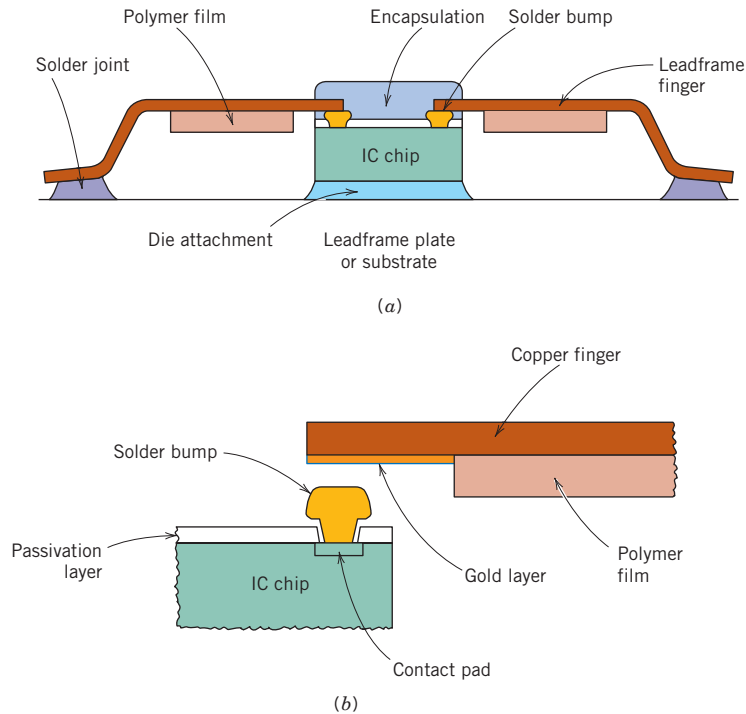


Figure 21.35
Schematic diagrams showing (a) the cross section of an encapsulated TAB leadframe package, and (b) how bonding between the IC chip and a copper finger is achieved with a solder bump.
[Adapted from *Electronic Materials Handbook*, Vol. 1, *Packaging*, C. A. Dostal (Editor), ASM International, 1989, pp. 233, 234.]



The copper fingers are extremely narrow and positioned close together. Separation distances of the inner contact leads are on the order of $50\ \mu\text{m}$, which is much smaller than is possible for the stamped leadframe. Furthermore, each die chip contact pad is microjoined directly to one of these copper fingers, which eliminates the need for any connecting wires. The copper fingers are very thin, so that, for this direct bonding to be achieved, the chip pad bonding sites must be raised above the metallized coating. This is accomplished using “solder bumps,” which are normally layers of gold (or gold-plated copper) approximately $25\ \mu\text{m}$ thick. Schematic representations illustrating this attachment design are presented in Figure 21.35. The finger contacts are bonded to these raised bumps by soldering using a thermal-compression bonding tool. This tape-bonding design is fully automated in that all of the hundred or so microjoints can be made in a single step, a feature not possible with leadframes that require multiple wire-bonding operations.

The packaging operation for the TAB leadframe is completed, as with the stamped leadframe, by encapsulation of the assembly (i.e., tape leadframe and its attached chip) within a fluid polymeric material that subsequently cures to form a protective shield. Protruding from this package are the copper finger conducting paths to which external electrical connections are made. Furthermore, excess heat generated by the chip must be dissipated along these copper fingers since the polymer tape backing does not provide an effective thermal conduction path because of its low thermal conductivity.

The ultimate design goal of the IC package is to allow for the proper electrical operation of the packaged device. As frequencies and computing speeds creep ever higher, the mechanical and electrical design considerations of the package design must become more and more integrated. The overall electrical performance of the package is as important to the end user as the overall reliability.

SUMMARY

Materials Selection for a Torsionally Stressed Cylindrical Shaft

In this chapter, we have illustrated the protocol of materials selection using six diverse examples. For the first case, a torsionally stressed cylindrical shaft, an expression for strength performance index was derived; then, using the appropriate materials selection chart, a preliminary candidate search was conducted. From the results of this search, several candidate engineering materials were ranked on both strength-per-unit mass and cost bases. Other factors that are relevant to the decision-making process were also discussed.

Automobile Valve Spring

A stress analysis was next performed on a helical spring, which was then extended to an automobile valve spring. It was noted that the possibility of fatigue failure was crucial to the performance of this spring application. The shear stress amplitude was computed, the magnitude of which was almost identical to the calculated fatigue limit for a chrome–vanadium steel that is commonly used for valve springs. It was noted that the fatigue limit of valve springs is often enhanced by shot peening. Finally, a procedure was suggested for assessing the economic feasibility of this spring design incorporating the shot-peened chrome–vanadium steel.

Failure of an Automobile Rear Axle

The next case study was devoted to a failure analysis, which detailed an investigation conducted on a failed rear axle of a light pickup truck that had overturned; the problem was to determine whether the accident resulted from this failure, or vice versa. Impact and tensile specimens were fabricated from outer perimeter and interior regions of the axle, which were subsequently tested. On the basis of scanning electron and metallographic examinations of the actual failed axle surface, as well as the surfaces of these test specimens, it was concluded that the accident caused the axle failure.

Artificial Total Hip Replacement

For the fourth case study, the artificial total hip replacement was explored. The hip anatomy was first presented, which was followed by a discussion of the components and material requirements for the artificial replacement. Implant materials must be biocompatible with body tissues and fluids, must be corrosion resistant, and must also be mechanically compatible with interfacing replacement/body components. The femoral stem and ball are normally made of a cold-worked stainless steel, a cast Co–Cr–Mo alloy, or a hot-forged titanium alloy. Some recent designs call for a polycrystalline aluminum oxide or zirconium oxide ball. Ultrahigh molecular weight polyethylene is commonly used for the acetabular cup, whereas acrylic bone cement is normally the fixation agent for attachment of the femoral stem (to the femur) and acetabular cup (to the pelvis).

Chemical Protective Clothing

The fifth materials case study was concerned with materials to be used for chemical protective clothing—specifically, glove materials to protect against exposure to

methylene chloride, a common ingredient in paint removers. Important parameters relative to the suitability of a chemical protective material are breakthrough time and exposure rate. Equations were provided that allow computation of these parameters, and values were determined for seven common protective glove materials. Only two materials {multilayered [poly(vinyl alcohol)/polyethylene] and Viton rubber} were deemed satisfactory for this application.

Materials for Integrated Circuit Packages

Materials utilized for the integrated circuit package incorporating the leadframe design were the topic of the final case study. An IC chip is bonded to the leadframe plate using either a eutectic solder or an epoxy resin. The leadframe material must be both electrically and thermally conductive, and, ideally, have a coefficient of thermal expansion that matches the IC chip material (i.e., silicon or gallium arsenide); copper alloys are commonly used leadframe materials. Very thin wires (preferably of gold, but often of copper or aluminum) are used to make electrical connections from the microscopic IC chip contact pads to the leadframe. Ultrasonic microjoining welding/brazing techniques are used where each connection joint may be in the form of either a ball or wedge. The final step is package encapsulation, wherein this leadframe–wire–chip assembly is encased in a protective enclosure. Ceramic glasses and polymeric resins are the most common encapsulation materials. Resins are less expensive than glasses and require lower encapsulation temperatures; however, glasses normally offer a higher level of protection.

REFERENCES

General

- Ashby, M. F., *CES4 EduPack—Cambridge Engineering Selector*, Granta Design Ltd., Cambridge, UK, <http://www.grantadesign.com>.
- Ashby, M. F., *Materials Selection in Mechanical Design*, 2nd edition, Butterworth-Heinemann, Woburn, UK, 2002.
- Budinski, K. G. and M. K. Budinski, *Engineering Materials: Properties and Selection*, 8th edition, Pearson Prentice Hall, Upper Saddle River, NJ, 2005.
- Dieter, G. E., *Engineering Design, A Materials and Processing Approach*, 3rd edition, McGraw-Hill, New York, 1999.
- Manganon, P. L., *The Principles of Materials Selection for Engineering Design*, Pearson Prentice Hall, Upper Saddle River, NJ, 1999.

Optimization of Strength

- Ashby, M. F. and D. R. H. Jones, *Engineering Materials 1, An Introduction to Their Properties and Applications*, 3rd edition, Butterworth-Heinemann, Woburn, UK, 2005.

Spring Design

- Juvinall, R. C. and K. M. Marshek, *Fundamentals of Machine Component Design*, 4th edition, Chapter 12, John Wiley & Sons, Hoboken, NJ, 2005.
- Shigley, J., C. Mischke, and R. Budynas, *Mechanical Engineering Design*, 7th edition, Chapter 10, McGraw-Hill Companies, New York, 2004.

Artificial Total Hip Replacement

- Black, J. and G. Hastings (Editors), *Handbook of Biomaterial Properties*, Chapman & Hall, London, 1998.
- Davis, J. R., *Handbook of Materials for Medical Devices*, ASM International, Materials Park, OH, 2003.

Materials for Integrated Circuit Packages

- Electronic Materials Handbook*, Vol. I, Packaging, ASM International, Materials Park, OH, 1989.
- Grovenor, C. R. M. *Microelectronic Materials*, Institute of Physics Publishing, Bristol, 1989. Reprinted by Adam Hilger, Ltd., Bristol, UK.

DESIGN QUESTIONS AND PROBLEMS

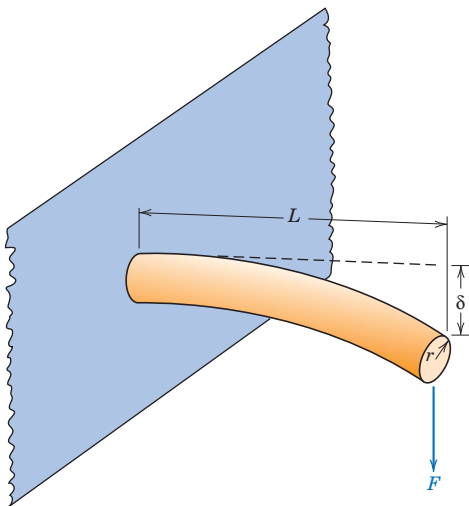
Solving of some problems in this chapter may be expedited by using the “Engineering Materials Properties” component of VMSE found in enclosed CD. We have noted these specific problems by inclusion of the following icon in one of the margins by the problem statement:



Materials Selection Using Performance Indices

21.D1 (a) Using the procedure as outlined in Section 21.2 ascertain which of the metal alloys listed in Appendix B have torsional strength performance indices greater than 10.0 (for τ_f and ρ in units of MPa and g/cm^3 , respectively), and, in addition, shear strengths greater than 350 MPa. **(b)** Also using the cost database (Appendix C), conduct a cost analysis in the same manner as Section 21.2. For those materials that satisfy the criteria noted in part a, and, on the basis of this cost analysis, which material would you select for a solid cylindrical shaft? Why?

21.D2 In a manner similar to the treatment of Section 21.2, perform a stiffness-to-mass performance analysis on a solid cylindrical shaft that is subjected to a torsional stress. Use the same engineering materials that are listed in Table 21.1. In addition, conduct a material cost analysis. Rank these materials both on the basis of mass of ma-



terial required and material cost. For glass and carbon fiber-reinforced composites, assume that the shear moduli are 8.6 and 9.2 GPa, respectively.

21.D3 (a) A cylindrical cantilever beam is subjected to a force F , as indicated in the figure below. Derive strength and stiffness performance index expressions analogous to Equations 21.9 and 21.11 for this beam. The stress imposed on the unfixed end σ is

$$\sigma = \frac{FLr}{I} \quad (21.30)$$

L , r , and I are, respectively, the length, radius, and moment of inertia of the beam. Furthermore, the beam-end deflection δ is

$$\delta = \frac{FL^3}{3EI} \quad (21.31)$$

where E is the modulus of elasticity of the beam.



(b) From the properties database presented in Appendix B, select those metal alloys with stiffness performance indices greater than 3.0 (for E and ρ in units of GPa and g/cm^3 , respectively).



(c) Also using the cost database (Appendix C), conduct a cost analysis in the same manner as Section 21.2. Relative to this analysis and that in part b, which alloy would you select on a stiffness-per-mass basis?



(d) Now select those metal alloys having strength performance indices greater than 14.0 (for σ_y and ρ in units of MPa and g/cm^3 , respectively), and rank them from highest to lowest P .



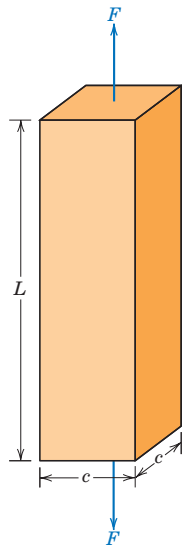
(e) And, using the cost database, rank the materials in part d from least to most costly. Relative to this analysis and that in part d, which alloy would you select on a strength-per-mass basis?

(f) Which material would you select if both stiffness and strength are to be considered relative to this application? Justify your choice.

21.D4 (a) Using the expression developed for stiffness performance index in Problem 21.D3(a) and data contained in Appendix B, determine stiffness performance indices for the following polymeric materials: high-density polyethylene, polypropylene, poly(vinyl chloride), polystyrene, polycarbonate, poly(methyl methacrylate), poly(ethylene terephthalate), polytetrafluoroethylene, and nylon 6,6. How do these values compare with those of the metallic materials? (*Note:* In Appendix B, where ranges of values are given, use average values.)

(b) Now, using the cost database (Appendix C), conduct a cost analysis in the same manner as Section 21.2. Use cost data for the raw forms of these polymers.

(c) Using the expression developed for strength performance index in Problem 21.D3(a) and data contained in Appendix B, determine strength performance indices for these same polymeric materials.



21.D5 (a) A bar specimen having a square cross section of edge length c is subjected to a uniaxial tensile force F , as shown in the following figure. Derive strength and stiffness performance index expressions analogous to Equations 21.9 and 21.11 for this bar.



(b) From the properties database presented in Appendix B, select those metal alloys with stiffness performance indices greater than 26.0 (for E and ρ in units of Gpa and g/cm^3 , respectively).



(c) Also using the cost database (Appendix C), conduct a cost analysis in the same manner as Section 21.2. Relative to this analysis and that in part b, which alloy would you select on a stiffness-per-mass basis?



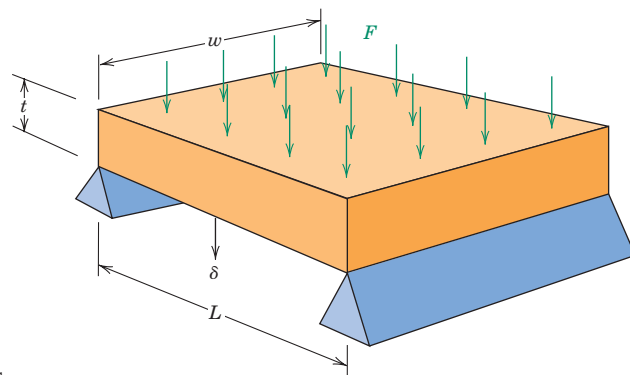
(d) Now select those metal alloys having strength performance indices greater than 120 (for σ_y and ρ in units of MPa and g/cm^3 , respectively), and rank them from highest to lowest P .



(e) And, using the cost database, rank the materials in part d from least to most costly. Relative to this analysis and that in part d, which alloy would you select on a strength-per-mass basis?

(f) Which material would you select if both stiffness and strength are to be considered relative to this application? Justify your choice.

21.D6 Consider the plate shown below that is supported at its ends and subjected to a force F that is uniformly distributed over the upper face as indicated. The deflection δ at the $L/2$ position is given by the expression



$$\delta = \frac{5 FL^3}{32 Ewt^3} \quad (21.32)$$

Furthermore, the tensile stress at the un-

812 • Chapter 21 / Materials Selection and Design Considerations

derside and also at the $L/2$ location is equal to

$$\sigma = \frac{3FL}{4wt^2} \quad (21.33)$$

(a) Derive stiffness and strength performance index expressions analogous to Equations 21.9 and 21.11 for this plate (*Hint*: solve for t in these two equations, and then substitute the resulting expressions into the mass equation, as expressed in terms of density and plate dimensions.)



(b) From the properties database in Appendix B, select those metal alloys with stiffness performance indices greater than 1.40 (for E and ρ in units of GPa and g/cm^3 , respectively).



(c) Also using the cost database (Appendix C), conduct a cost analysis in the same manner as Section 21.2. Relative to this analysis and that in part b, which alloy would you select on a stiffness-per-mass basis?



(d) Now select those metal alloys having strength performance indices greater than 5.0 (for σ_y and ρ in units of MPa and g/cm^3 , respectively), and rank them from highest to lowest P .



(e) And, using the cost database, rank the materials in part d from least to most costly. Relative to this analysis and that in part d, which alloy would you select on a strength-per-mass basis?

(f) Which material would you select if both stiffness and strength are to be considered relative to this application? Justify your choice.

Design and Materials Selection for Springs

21.D7 A spring having a center-to-center diameter of 20 mm (0.8 in.) is to be constructed of cold-drawn and annealed 316 stainless steel wire that is 2.5 mm (0.10 in.) in diameter; this spring design calls for eight coils.

(a) What is the maximum tensile load that may be applied such that the total spring deflection will be no more than 6.5 mm (0.26 in.)?

(b) What is the maximum tensile load that may be applied without any permanent deformation of the spring wire? Assume that the shear yield strength is $0.6\sigma_y$, where σ_y is the yield strength in tension.

21.D8 You have been asked to select a material for a spring that is to be stressed in tension. It is to consist of 10 coils, and the coil-to-coil diameter called for is 15 mm; furthermore, the diameter of the spring wire must be 2.0 mm. Upon application of a tensile force of 35 N, the spring is to experience a deflection of no more than 12 mm, and not plastically deform.

(a) From those materials included in the database in Appendix B, make a list of those candidate materials that meet the above criteria. Assume that the shear yield strength is $0.6\sigma_y$, where σ_y is the yield strength in tension, and that the shear modulus is equal to $0.4E$, E being the modulus of elasticity.

(b) Now, from this list of candidate materials, select the one you would use for this spring application. In addition to the above criteria, the material must be relatively corrosion resistant, and, of course, capable of being fabricated into wire form. Justify your decision.

21.D9 A spring having 7 coils and a coil-to-coil diameter of 0.5 in. is to be made of cold-drawn steel wire. When a tensile load of 15 lb_f is applied the spring is to deflect no more than 0.60 in. The cold drawing operation will, of course, increase the shear yield strength of the wire, and it has been observed that τ_y (in ksi) depends on wire diameter d (in in.) according to

$$\tau_y = \frac{63}{d^{0.2}} \quad (21.34)$$

If the shear modulus for this steel is 11.5×10^6 psi, calculate the minimum wire diameter required such that the spring will not plastically deform when subjected to the above load.

21.D10 A helical spring is to be constructed from a 4340 steel. The design calls for 5 coils, a coil-to-coil diameter of 12 mm, and a wire

diameter of 3 mm. Furthermore, a maximum total deflection of 5.0 mm is possible without any plastic deformation. Specify a heat treatment for this 4340 steel wire in order for the spring to meet the above criteria. Assume a shear modulus of 80 GPa for this steel alloy, and that $\tau_y = 0.6\sigma_y$. *Note:* heat treatment of the 4340 steel is discussed in Section 10.8.

Materials for Integrated Circuit Packages

21.D11 You have been asked to select a metal alloy to be used as leadframe plate in an integrated circuit package that is to house a silicon chip.



(a) Using the database in Appendix B list those materials that are electrically conductive [$\sigma > 10 \times 10^6 (\Omega\text{-m})^{-1}$] have linear coefficients of thermal expansion of between 2×10^{-6} and $10 \times 10^{-6} (\text{°C})^{-1}$, and thermal conductivities of greater than 100 W/m-K. On the bases of properties and cost, would you consider any of these materials in preference to those listed in Table 21.6? Why or why not?



(b) Repeat this procedure for potential insulating leadframe plate materials that must have electrical conductivities less than $10^{-10} (\Omega\text{-m})^{-1}$, as well as coefficients of thermal expansion between 2×10^{-6} and $10 \times 10^{-6} (\text{°C})^{-1}$, and thermal conductivities of greater than 30 W/m-K. On the bases of properties and cost (Appendix C), would you consider any of the materials listed in Appendix B in preference to aluminum oxide? Why or why not?

Design Questions

21.D12 Perform a case study on material usage for the compact disc, after the manner of those studies described in this chapter. Begin with a brief description of the mechanism by which sounds are stored and then reproduced. Then, cite all of the requisite material properties for this application; finally, note which material is most commonly utilized, and the rationale for its use.

21.D13 One of the critical components of our modern video cassette recorders (VCRs) is the magnetic recording/playback head. Write an essay in which you address the following issues: (1) the mechanism by which the head records and plays back video/audio signals; (2) the requisite properties for the material from which the head is manufactured; then (3) present at least three likely candidate materials, and the property values for each that make it a viable candidate.

21.D14 The transdermal patch has recently become popular as a mechanism for delivering drugs into the human body.

(a) Cite at least one advantage of this drug-delivery system over oral administration using pills and caplets.

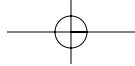
(b) Note the limitations on drugs that are administered by transdermal patches.

(c) Make a list of the characteristics required of materials (other than the delivery drug) that are incorporated in the transdermal patch.

Chapter 22 Economic, Environmental, and Societal Issues in Materials Science and Engineering



Photograph showing beverage cans that are made of an aluminum alloy (left) and a steel alloy (right). The steel beverage can has corroded significantly, and, therefore, is biodegradable and nonrecyclable. Conversely, the aluminum can is non-biodegradable and recyclable inasmuch as it experienced very little corrosion.



Learning Objectives

After careful study of this chapter you should be able to do the following:

1. List and briefly discuss three factors over which an engineer has control that affect the cost of a product.
2. Diagram the total materials cycle, and briefly discuss relevant issues that pertain to each stage of this cycle.
3. List the two inputs and five outputs for the life cycle analysis/assessment scheme.
4. Cite issues that are relevant to the "green design" philosophy of product design.
5. Discuss recyclability/disposability issues relative to (a) metals, (b) glass, (c) plastics and rubber, and (d) composite materials.

22.1 INTRODUCTION

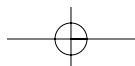
In previous chapters, we dealt with a variety of materials science and materials engineering issues to include criteria that may be employed in the materials selection process. Many of these selection criteria relate to material properties or property combinations—mechanical, electrical, thermal, corrosion, etc.; the performance of some component will depend on the properties of the material from which it is made. Processability or ease of fabrication of the component may also play a role in the selection process. Virtually all of this book, in one way or another, has addressed these property and fabrication issues.

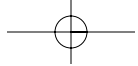
In engineering practice there are other important criteria that must be considered in the development of a marketable product. Some of these are economic in nature, which, to some degree, are unrelated to scientific principles and engineering practice, and yet are significant if a product is to be competitive in the commercial marketplace. Other criteria that should be addressed involve environmental and societal issues such as pollution, disposal, recycling, and energy. This final chapter offers relatively brief overviews of economic, environmental, and societal considerations that are important in engineering practice.

Economic Considerations

It goes without saying that engineering practice involves utilizing scientific principles to design components and systems that perform reliably and satisfactorily. Another critical driving force in engineering practice is that of economics; simply stated, the company or institution must realize a profit from the products that it manufactures and sells. The engineer might design the perfect component; however, as manufactured, it must be offered for sale at a price that is attractive to the consumer and, in addition, return a suitable profit to the company. Only a brief overview of important economic considerations as they apply to the materials engineer will be provided. The student may want to consult references provided at the end of this chapter that address engineering economics in detail.

There are three factors over which the materials engineer has control and that affect the cost of a product; they are (1) component design, (2) the material(s) used, and (3) the manufacturing technique(s) that are employed. These factors are interrelated in that component design may affect which material is used, and both component design and the material used will influence the choice of manufacturing technique(s). Economic considerations for each of these factors is now briefly discussed.





22.2 COMPONENT DESIGN

Some fraction of the cost of a component is associated with its design. In this context, component design is the specification of size, shape, and configuration, which will affect in-service component performance. For example, if mechanical forces are present, then stress analyses may be required. Detailed drawings of the component must be prepared; computers are normally employed, using software that has been generated for this specific function.

It is often the case that a single component is part of a complex device or system consisting of a large number of components (i.e., the television, automobile, DVD player/recorder, etc.). Thus, design must take into consideration each component's contribution to the efficient operation of the complete system.

Component design is a highly iterative process that involves many compromises and trade-offs. The engineer should keep in mind that an optimal component design may not be possible due to system constraints.

22.3 MATERIALS

In terms of economics, we want to select the material or materials with the appropriate combination(s) of properties that are the least expensive. Once a family of materials has been selected that satisfy the design constraints, cost comparisons of the various candidate materials may be made on the basis of cost per part. Material price is usually quoted per unit mass. The part volume may be determined from its dimensions and geometry, which is then converted into mass using the density of the material. In addition, during manufacturing there ordinarily is some unavoidable material waste, which should also be taken into account in these computations. Current prices for a wide variety of engineering materials are contained in Appendix C.

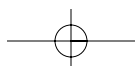
22.4 MANUFACTURING TECHNIQUES

As already stated, the choice of manufacturing process will be influenced by both the material selected and part design. The entire manufacturing process will normally consist of primary and secondary operations. Primary operations are those that convert the raw material into a recognizable part (i.e., casting, plastic forming, powder compaction, molding, etc.), whereas secondary ones are those subsequently employed to produce the finished part (i.e., heat treatments, welding, grinding, drilling, painting, decorating). The major cost considerations for these processes include capital equipment, tooling, labor, repairs, machine downtime, and waste. Of course, within this cost analysis, rate of production is an important consideration. If this particular part is one component of a system, then assembly costs must also be addressed. Finally, there will undoubtedly be costs associated with inspection and packaging of the final product.

As a sidelight, there are also other factors not directly related to design, material, or manufacturing that figure into the product selling price. These factors include labor fringe benefits, supervisory and management labor, research and development, property and rent, insurance, profit, taxes, and so on.

Environmental and Societal Considerations

Our modern technologies and the manufacturing of their associated products impact our societies in a variety of ways—some are positive, others are adverse



Furthermore, these impacts are economic and environmental in type, and international in scope inasmuch as (1) the resources required for a new technology often come from many different countries, (2) the economic prosperity resulting from technological development is global in extent, and (3) environmental impacts may extend beyond the boundaries of a single country.

Materials play a crucial role in this technology-economy-environment scheme. A material that is utilized in some end product and then discarded passes through several stages or phases; these stages are represented in Figure 22.1, which is sometimes termed the “total materials cycle” or just “materials cycle,” and represents the “cradle-to-grave” life circuit of a material. Beginning on the far left side of Figure 22.1, raw materials are extracted from their natural earthly habitats by mining, drilling, harvesting, and so on. These raw materials are then purified, refined, and converted into bulk forms such as metals, cements, petroleum, rubber, and fibers. Further synthesis and processing results in products that are what may be termed “engineered materials”; examples include metal alloys, ceramic powders, glass, plastics, composites, semiconductors, and elastomers. Next, these engineered materials are further shaped, treated, and assembled into products, devices, and appliances that are ready for the consumer—this constitutes the “product design, manufacture, assembly” stage of Figure 22.1. The consumer purchases these products and uses them (the “applications” stage) until they wear out or become obsolete, and are discarded. At this time the product constituents may either be recycled/reused (whereby they reenter the materials cycle) or disposed of as waste, normally being either incinerated or dumped as solid waste in municipal land-fills—as such, they return to the earth and complete the materials cycle.

It has been estimated that worldwide, on the order of 15 billion tons of raw materials are extracted from the earth every year; some of these are renewable and some are not. Over time, it is becoming more apparent that the earth is virtually a

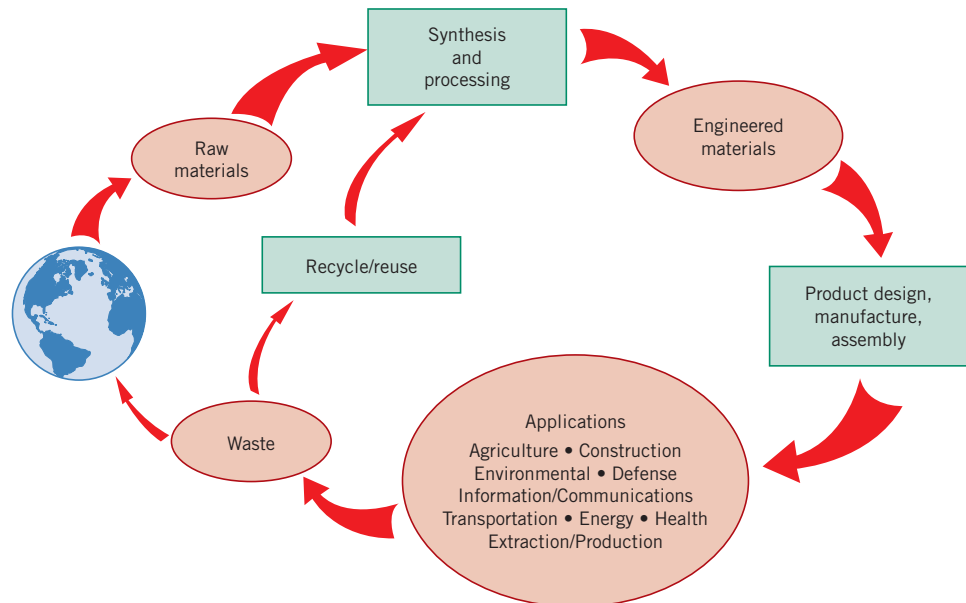
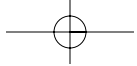


Figure 22.1 Schematic representation of the total materials cycle. (Adapted from M. Cohen, *Advanced Materials & Processes*, Vol. 147, No. 3, p. 70, 1995. Copyright © 1995 by ASM International. Reprinted by permission of ASM International, Materials Park, OH.)

**818 • Chapter 22 / Economic, Environmental, and Societal Issues in Materials Science**

closed system relative to its constituent materials and that its resources are finite. In addition, as our societies mature and populations increase, the available resources become scarcer, and greater attention must be paid to more effective utilization of these resources relative to this materials cycle.

Furthermore, energy must be supplied at each cycle stage; in the United States it has been estimated that approximately one-half of the energy consumed by manufacturing industries goes to produce and fabricate materials. Energy is a resource that, to some degree, is limited in supply, and measures must be taken to conserve and more effectively utilize it in the production, application, and disposal of materials.

Finally, there are interactions with and impacts on the natural environment at all stages of the materials cycle. The condition of the earth's atmosphere, water, and land depends to a large extent on how carefully we traverse this materials cycle. Some ecological damage and landscape spoilage undoubtedly result during the extraction of raw materials phase. Pollutants may be generated that are expelled into the air and water during the synthesis and processing stage; in addition, any toxic chemicals that are produced need to be disposed of or discarded. The final product, device, or appliance should be designed so that during its lifetime, any impact on the environment is minimal; furthermore, that at the end of its life, provision is made for recycling of its component materials, or at least for their disposal with little ecological degradation (i.e., it should be biodegradable).

Recycling of used products rather than disposing of them as waste is a desirable approach for several reasons. First of all, using recycled material obviates the need to extract raw materials from the earth, and thus conserves natural resources and eliminates any associated ecological impact from the extraction phase. Second, energy requirements for the refinement and processing of recycled materials are normally less than for their natural counterparts; for example, approximately 28 times as much energy is required to refine natural aluminum ores as to recycle aluminum beverage can scrap. Finally, there is no need to dispose of recycled materials.

Thus, this materials cycle (Figure 22.1) is really a system that involves interactions and exchanges among materials, energy, and the environment.

In many countries, environmental problems and issues are being addressed by the establishment of standards that are mandated by governmental regulatory agencies. Furthermore, from an industrial perspective, it becomes incumbent for engineers to propose viable solutions to existing and potential environmental concerns.

Correcting any environmental problems associated with manufacturing will influence product price. That is, manufacturing cost is normally greater for a "green" (or "environmentally friendly") product than for its equivalent that is produced under conditions wherein environmental issues are minimized. Thus, a company must confront the dilemma of this potential economic-environmental trade-off and then decide the relative importance of economics and of environmental impact.

One approach that is being implemented by industry to improve the environmental performance of products is termed *life cycle analysis/assessment*. With this approach to product design, consideration is given to the cradle-to-grave environmental assessment of the product, from material extraction to product manufacture to product use, and, finally, to recycling and disposal; sometimes this approach is also labeled "green design." One important phase of this approach is to quantify the various inputs (i.e., materials and energy) and outputs (i.e., wastes) for each phase of the life cycle; this is represented schematically in Figure 22.2. In addition, an assessment is conducted relative to the impact on both global and local environments in terms of the effects on the ecology, human health, and resource reserves.

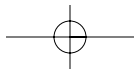
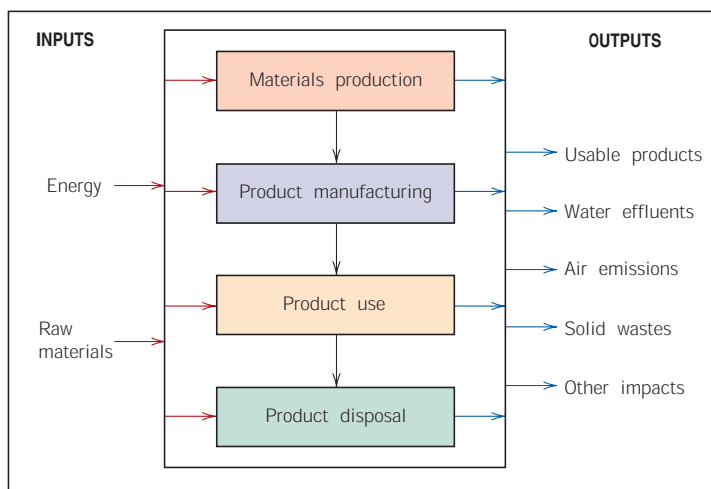


Figure 22.2 Schematic representation of an input/output inventory for the life-cycle assessment of a product. (Adapted from J. L. Sullivan and S. B. Young, *Advanced Materials & Processes*, Vol. 147, No. 2, p. 38, 1995. Copyright © 1995 by ASM International. Reprinted by permission of ASM International, Materials Park, OH.)



22.5 RECYCLING ISSUES IN MATERIALS SCIENCE AND ENGINEERING

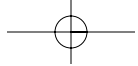
Important stages in the materials cycle where materials science and engineering plays a significant role are recycling and disposal. The issues of recyclability and disposability are important when new materials are being designed and synthesized. Furthermore, during the materials selection process, the ultimate disposition of the materials employed should be an important criterion. Let us conclude this section by briefly discussing several of these recyclability/disposability issues.

From an environmental perspective, the ideal material should be either totally recyclable or completely biodegradable. Recyclable means that a material, after having completed its life cycle in one component, could be reprocessed, could reenter the materials cycle, and could be reused in another component—a process that could be repeated an indefinite number of times. By completely biodegradable, we mean that, by interactions with the environment (natural chemicals, microorganisms, oxygen, heat, sunlight, etc.), the material deteriorates and returns to virtually the same state in which it existed prior to the initial processing. Engineering materials exhibit varying degrees of recyclability and biodegradability.

Metals

Most metal alloys (i.e., Fe, Cu), to one degree or another experience corrosion and are also biodegradable. However, some metals (i.e., Hg, Pb) are toxic and, when land-filled, may present health hazards. Furthermore, alloys of most metals are recyclable; on the other hand it is not feasible to recycle all alloys of every metal. In addition, the quality of alloys that are recycled tends to diminish with each cycle.

Product designs should allow for the dismantling of components composed of different alloys. Another of the problems of recycling involves separation of various alloys types (i.e., aluminum from ferrous alloys) after dismantling and shredding; in this regard, some rather ingenious separation techniques have been devised (i.e., magnetic and gravity). Joining of dissimilar alloys presents contamination problems; for example, if two similar alloys are to be joined, welding is preferred over bolting or riveting. Coatings (paints, anodized layers, claddings, etc.) may also act as contaminants, and render the material nonrecyclable.



820 • Chapter 22 / Economic, Environmental, and Societal Issues in Materials Science

Aluminum alloys are very corrosion resistant and, therefore, nonbiodegradable. Fortunately, however, they may be recycled; in fact, aluminum is the most important recyclable nonferrous metal. Since aluminum is not easily corroded, it may be totally reclaimed. A low ratio of energy is required to refine recycled aluminum relative to its primary production. In addition, there are a large number of commercially available alloys that have been designed to accommodate impurity contamination. The primary sources of recycled aluminum are used beverage cans and scrapped automobiles.

Glass

The one ceramic material that is consumed by the general public in the greatest quantities is glass, in the form of containers. Glass is a relatively inert material, and, as such, it does not decompose; thus, it is not biodegradable. A significant proportion of municipal land-fills consists of waste glass; so also does incinerator residue.

In addition, there is not a significant economic driving force for recycling glass. Its basic raw materials (sand, soda ash, and limestone) are inexpensive and readily available. Furthermore, salvaged glass (also called “cullet”) must be sorted by color (clear, amber, and green), by type (plate versus container), and by composition (lime, lead, and borosilicate [or Pyrex]); these sorting procedures are time-consuming and expensive. Therefore, scrap glass has a low market value, which diminishes its recyclability. Advantages of utilizing recycled glass include more rapid and increased production rates and a reduction in pollutant emissions.

Plastics and Rubber

One of the reasons that synthetic polymers (including rubber) are so popular as engineering materials lies with their chemical and biological inertness. On the down side, this characteristic is really a liability when it comes to waste disposal. Polymers are not biodegradable, and, as such, they constitute a significant land-fill component; major sources of waste are from packaging, junk automobiles, automobile tires, and domestic durables. Biodegradable polymers have been synthesized, but they are relatively expensive to produce. On the other hand, since some polymers are combustible and do not yield appreciable toxic or polluting emissions, they may be disposed of by incineration.

Thermoplastic polymers, specifically poly(ethylene terephthalate), polyethylene, and polypropylene, are those most amenable to reclamation and recycling, since they may be reformed upon heating. Sorting by type and color is necessary. In some countries, type sorting of packaging materials is facilitated using a number identification code; for example, a “1” denotes high-density polyethylene (HDPE). Table 22.1 presents these recycling code numbers and their associated materials. Also included in the table are uses of virgin and recycled materials. Plastics recycling is complicated by the presence of fillers (Section 14.21) that were added to modify the original properties. The recycled plastic is less costly than the original material, and quality and appearance are generally degraded with each recycle. Typical applications for recycled plastics include shoe soles, tool handles, and industrial products such as pallets.

The recycling of thermoset resins is much more difficult since these materials are not easily remolded or reshaped due to their crosslinked or network structures. Some thermosets are ground up and added to the virgin molding material prior to processing; as such, they are recycled as filler materials.

Rubber materials present some disposal and recycling challenges. When vulcanized, they are thermoset materials, which makes chemical recycling difficult. In

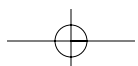


Table 22.1 Recycle Codes, Uses of the Virgin Material, and Recycled Products for Several Commercial Polymers

<i>Recycle Code</i>	<i>Polymer Name</i>	<i>Uses of Virgin Material</i>	<i>Recycled Products</i>
1	Poly(ethylene terephthalate) (PET or PETE)	Plastic beverage containers, mouthwash jars, peanut butter and salad dressing bottles	Liquid-soap bottles, strapping, fiberfill for winter coats, surfboards, paint brushes, fuzz on tennis balls, soft-drink bottles, film, egg cartons, skis, carpets, boats
2	High-density polyethylene (HDPE)	Milk, water and juice containers, grocery bags, toys, liquid detergent bottles	Soft-drink bottle base caps, flower pots, drain pipes, signs, stadium seats, trash cans, recycling bins, traffic-barrier cones, golf bag liners, detergent bottles, toys
3	Poly(vinyl chloride) or vinyl (V)	Clear food packaging, shampoo bottles	Floor mats, pipes, hose, mud flaps
4	Low-density polyethylene (LDPE)	Bread bags, frozen-food bags, grocery bags	Garbage can liners, grocery bags, multipurpose bags
5	Polypropylene (PP)	Ketchup bottles, yogurt containers and margarine tubs, medicine bottles	Manhole steps, paint buckets, videocassette storage cases, ice scrapers, fast food trays, lawn mower wheels, automobile battery parts
6	Polystyrene (PS)	Videocassette cases, compact disc jackets, coffee cups; knives, spoons, and forks; cafeteria trays, grocery store meat trays, and fast-food sandwich containers	License plate holders, golf course and septic tank drainage systems, desktop accessories, hanging files, food service trays, flower pots, trash cans, videocassettes

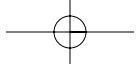
Source: American Plastics Council.

addition, they may also contain a variety of fillers. The major source of rubber scrap in the United States is discarded automobile tires, which are highly nonbiodegradable. Scrap tires have been utilized as a fuel for some industrial applications (i.e., cement plants), but yield dirty emissions. Recycled rubber tires that have been split and reshaped are used in a variety of applications such as automotive bumper guards, mud flaps, door mats, and conveyor rollers; and, of course, used tires may also be recapped. In addition, rubber tires may be ground into small chunks that are then recombined into the desired shape using some type of adhesive; the resulting material may be used in a number of nondemanding applications such as place mats and rubber toys.

The most viable recyclable alternatives to the traditional rubber materials are the thermoplastic elastomers (Section 14.19). Being thermoplastic in nature they are not chemically crosslinked and, thus, are easily reshaped. Furthermore, production energy requirements are lower than for the thermoset rubbers since a vulcanization step is not required in their manufacture.

Composite Materials

Composites are inherently difficult to recycle because they are multiphase in nature. The two or more phases/materials that constitute the composite are normally intermixed on a very fine scale and trying to separate them complicates the recycling process. However, some techniques have been developed, with modest success,



822 • Chapter 22 / Economic, Environmental, and Societal Issues in Materials Science

for recycling polymer–matrix composites. Recycling technologies will differ only slightly for thermoset–matrix and thermoplastic–matrix composite materials.

The first step in recycling both thermoset– and thermoplastic–matrix composites is shredding/grinding, wherein the components are reduced in size to relatively small particles. In some instances, these ground particles are used as filler materials that are blended with a polymer (and perhaps other fillers) before fabrication (usually using some type of molding technique) into postconsumer products. Other recycling processes allow for separating of the fibers and/or matrix materials. With some techniques the matrix is volatilized; with others it is recovered as a monomer. Of course, the recovered fibers have short lengths, as a result of the shredding/grinding process. In addition, fibers will experience a reduction of mechanical strength, the degree of which will depend on the specific recovery process as well as fiber type.

SUMMARY

Economic Considerations

The economics of engineering is very important in product design and manufacturing. To minimize product cost, materials engineers must take into account component design, what materials are used, and manufacturing processes. Other significant economic factors include fringe benefits, labor, insurance, profit, etc.

Environmental and Societal Considerations

Environmental and societal impacts of production are becoming significant engineering issues. In this regard, the material cradle-to-grave life cycle is an important consideration; this cycle consists of extraction, synthesis/processing, product design/manufacture, application, and disposal stages. Materials, energy, and environmental interactions/exchanges are important factors in the efficient operation of the materials cycle. The earth is a closed system in that its materials resources are finite; to some degree, the same may be said of energy resources. Environmental issues involve ecological damage, pollution, and waste disposal. Recycling of used products and the utilization of green design obviate some of these environmental problems.

Recycling Issues in Materials Science and Engineering

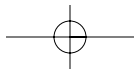
Recyclability and disposability issues were addressed in the context of materials science and engineering. Ideally, a material should be at best recyclable, and at least biodegradable or disposable. The recyclability and disposability of metal alloys, glasses, polymers, and composites were also discussed.

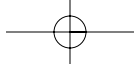
REFERENCES

Engineering Economics

Park, C. S., *Fundamentals of Engineering Economics*, Pearson Education, Upper Saddle River, NJ, 2004.

White, J. A., K. E. Case, D. B. Pratt, and M. H. Agee, *Principles of Engineering Economics Analysis*, 4th edition, John Wiley & Sons, New York, 1998.





Societal

Cohen, M., “Societal Issues in Materials Science and Technology,” *Materials Research Society Bulletin*, September, 1994, pp. 3–8.

Environmental

Ackerman, F., *Why Do We Recycle?: Markets, Values, and Public Policy*, Island Press, Washington, D.C., 1997

Azapagic, A., A Emsley, and I. Hamerton, *Polymers, the Environment and Sustainable*

Development, John Wiley & Sons, West Sussex, UK, 2003.

Landreth, R. E. and P. E. Rebers (Editors), *Municipal Solid Wastes—Problems and Solutions*, CRC Press, Boca Raton, FL, 1997.

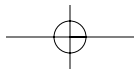
Porter, R. C., *The Economics of Waste*, Resources for the Future Press, Washington, D.C., 2002.

Salvato, J. A., N. L. Nemerow, and F. J. Agardy, *Environmental Engineering*, 5th edition, John Wiley & Sons, Hoboken, NJ, 2003.

DESIGN QUESTION

22.D1 Glass, aluminum, and various plastic materials are utilized for containers (the chapter-opening photograph for Chapter 1). Make a list of the advantages and disadvantages of

using each of these three material types; include such factors as cost, recyclability, and energy consumption for container production.



Chapter 23 Processing of Engineering Materials



This photograph shows the aluminum beverage can in various stages of production. The can is formed from a single sheet of an aluminum alloy. Production operations include drawing, dome forming, trimming, cleaning, decorating, and neck and flange forming. (PEPSI is a registered trademark of PepsiCo, Inc. Used by permission.)

Learning Objectives

After careful study of this chapter you should be able to do the following:

1. Name and describe four forming operations and five casting techniques used to shape metal alloys
2. Define *hardenability* and generate a hardness profile for a cylindrical steel specimen that has been austenitized and then quenched, given the hardenability curve for the specific alloy, as well as quenching rate-versus-bar diameter information.
3. Name and describe four forming methods that are used to fabricate glass pieces.
4. Briefly describe processes that occur during the drying and firing of clay-based ceramic ware.
5. Briefly describe/diagram the sintering process of powder particle aggregates.
6. Name and briefly describe five fabrication techniques used for plastic polymers.
7. Name and briefly describe three production processes used for fiber-reinforced composites.

23.1 INTRODUCTION

Solid materials have been conveniently grouped into three basic classifications: metals, ceramics and polymers. This scheme is based primarily on chemical makeup and atomic structure (Chapter 4), and most materials fall into one distinct grouping or another. In addition, there are the composites, combinations of two or more of the above three basic material classes. With regard to mechanical characteristics, metallic materials are relatively stiff and strong, yet are ductile (Chapter 9), and are resistant to fracture (Chapters 10 and 11). Ceramic materials are relatively stiff and strong, typically very hard but are extremely brittle and are highly susceptible to fracture (Chapter 12). Polymers are not as stiff nor as strong as metals and ceramics, but are extremely ductile and pliable (i.e. plastic), which means they are easily formed into complex shapes (Chapter 14). A composite, by design, possesses a combination of properties that is not displayed by any single material, and incorporates the best characteristics of each of the component materials. For example, fiberglass is relatively stiff and strong (due to the relatively strong and stiff, but also brittle, glass fibers) as well as flexible and ductile (due to the ductile, but weak and flexible, polymer matrix). Several types of synthetic (or man-made) composites were explained in Chapter 15.

Often a materials problem is really one of selecting the material that has the right combination of characteristics for a specific application (Chapter 21). Materials selection decisions may also be influenced by the ease with which engineering materials may be manufactured into useful shapes. This chapter provides a brief overview of fabrication processes for metals, ceramics, polymers and composites. Material properties are altered by manufacturing processes and several examples were explained in the earlier chapters. Further, property alterations in metallic alloys, specially steels, may be induced by the employment of appropriate heat treatments. Therefore, in the early portion of this chapter we consider the details of some heat treatments of steel. Annealing procedures (Section 9.4) and precipitation hardening (Section 10.14) are other examples of heat treatment. The processing of glass, clay products and ceramic powders are explained. This is followed by a brief description of fabrication of different types of polymeric materials like thermoplastics, thermosetting polymers (Section 14.20) and elastomers. The processes by which polymer fibers and film are formed from bulk polymer material is described briefly.

In the end of this chapter we discuss briefly several techniques by which useful products of continuous fiber-reinforced plastics, a good example of fiber-reinforced composites, are processed.

Fabrication of Metals

Metal fabrication techniques are normally preceded by refining, alloying, and often heat-treating processes that produce alloys with the desired characteristics. The classifications of fabrication techniques include various metal-forming methods, casting, powder metallurgy, welding, and machining; often two or more of them must be used before a piece is finished. The methods chosen depend on several factors; the most important are the properties of the metal, the size and shape of the finished piece, and, of course, cost. The metal fabrication techniques we discuss are classified according to the scheme illustrated in Figure 23.1.

23.2 FORMING OPERATIONS

Forming operations are those in which the shape of a metal piece is changed by plastic deformation; for example, forging, rolling, extrusion, and drawing are common forming techniques. Of course, the deformation must be induced by an external force or stress, the magnitude of which must exceed the yield strength of the material. Most metallic materials are especially amenable to these procedures, being at least moderately ductile and capable of some permanent deformation without cracking or fracturing.

When deformation is achieved at a temperature above that at which recrystallization occurs, the process is termed **hot working** (Section 10.12); otherwise, it is cold working. With most of the forming techniques, both hot- and cold-working procedures are possible. For hot-working operations, large deformations are possible, which may be successively repeated because the metal remains soft and ductile. Also, deformation energy requirements are less than for cold working. However, most metals experience some surface oxidation, which results in material loss and a poor final surface finish. **Cold working** produces an increase in strength with the attendant decrease in ductility, since the metal strain hardens; advantages over hot working include a higher quality surface finish, better mechanical properties and a greater variety of them, and closer dimensional control of the finished piece. On occasion, the total deformation is accomplished in a series of steps in which the piece is successively cold worked a small amount and

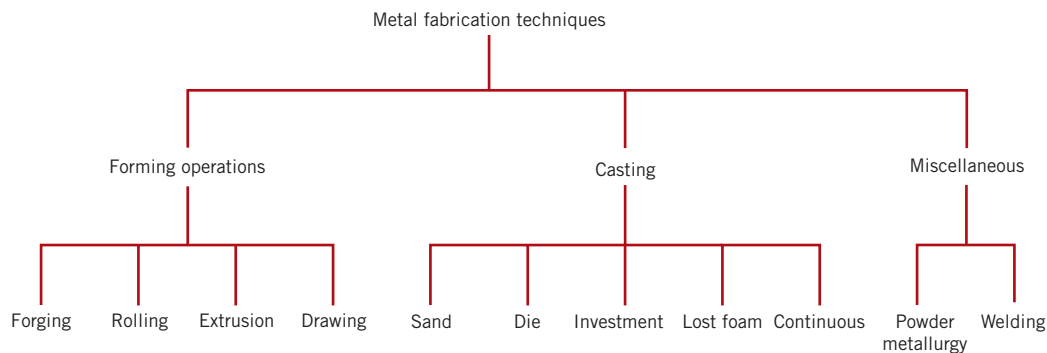
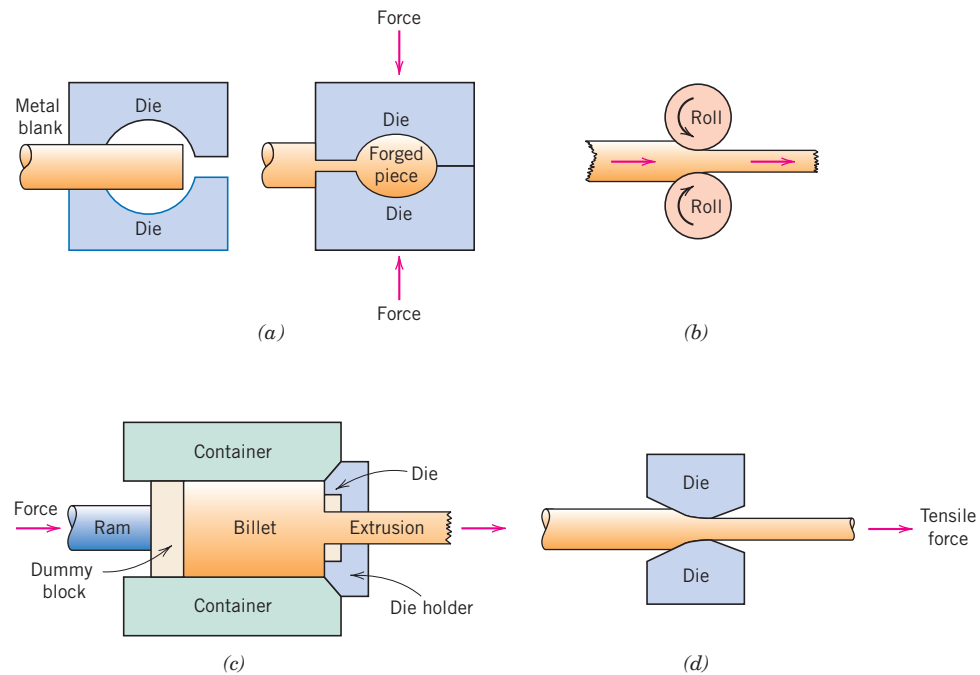


Figure 23.1 Classification scheme of metal fabrication techniques discussed in this chapter.

Figure 23.2 Metal deformation during (a) forging, (b) rolling, (c) extrusion, and (d) drawing.



then process annealed (Section 9.4); however, this is an expensive and inconvenient procedure.

The forming operations to be discussed are illustrated schematically in Figure 23.2.

Forging

Forging is mechanically working or deforming a single piece of a normally hot metal; this may be accomplished by the application of successive blows or by continuous squeezing. Forgings are classified as either closed or open die. For closed die, a force is brought to bear on two or more die halves having the finished shape such that the metal is deformed in the cavity between them (Figure 23.2a). For open die, two dies having simple geometric shapes (e.g., parallel flat, semicircular) are employed, normally on large workpieces. Forged articles have outstanding grain structures and the best combination of mechanical properties. Wrenches, and automotive crankshafts and piston connecting rods are typical articles formed using this technique.

Rolling

Rolling, the most widely used deformation process, consists of passing a piece of metal between two rolls; a reduction in thickness results from compressive stresses exerted by the rolls. Cold rolling may be used in the production of sheet, strip, and foil with high quality surface finish. Circular shapes as well as I-beams and railroad rails are fabricated using grooved rolls.

Extrusion

For **extrusion**, a bar of metal is forced through a die orifice by a compressive force that is applied to a ram; the extruded piece that emerges has the desired shape and a reduced cross-sectional area. Extrusion products include rods and tubing that

828 • Chapter 23 / Processing of Engineering Materials

have rather complicated cross-sectional geometries; seamless tubing may also be extruded.

Drawing

Drawing is the pulling of a metal piece through a die having a tapered bore by means of a tensile force that is applied on the exit side. A reduction in cross section results, with a corresponding increase in length. The total drawing operation may consist of a number of dies in a series sequence. Rod, wire, and tubing products are commonly fabricated in this way.

23.3 CASTING

Casting is a fabrication process whereby a totally molten metal is poured into a mold cavity having the desired shape; upon solidification, the metal assumes the shape of the mold but experiences some shrinkage. Casting techniques are employed when (1) the finished shape is so large or complicated that any other method would be impractical, (2) a particular alloy is so low in ductility that forming by either hot or cold working would be difficult, and (3) in comparison to other fabrication processes, casting is the most economical. Furthermore, the final step in the refining of even ductile metals may involve a casting process. A number of different casting techniques are commonly employed, including sand, die, investment, lost foam, and continuous casting. Only a cursory treatment of each of these is offered.

Sand Casting

With sand casting, probably the most common method, ordinary sand is used as the mold material. A two-piece mold is formed by packing sand around a pattern that has the shape of the intended casting. Furthermore, a *gating system* is usually incorporated into the mold to expedite the flow of molten metal into the cavity and to minimize internal casting defects. Sand-cast parts include automotive cylinder blocks, fire hydrants, and large pipe fittings.

Die Casting

In die casting, the liquid metal is forced into a mold under pressure and at a relatively high velocity, and allowed to solidify with the pressure maintained. A two-piece permanent steel mold or die is employed; when clamped together, the two pieces form the desired shape. When complete solidification has been achieved, the die pieces are opened and the cast piece is ejected. Rapid casting rates are possible, making this an inexpensive method; furthermore, a single set of dies may be used for thousands of castings. However, this technique lends itself only to relatively small pieces and to alloys of zinc, aluminum, and magnesium, which have low melting temperatures.

Investment Casting

For investment (sometimes called lost-wax) casting, the pattern is made from a wax or plastic that has a low melting temperature. Around the pattern is poured a fluid slurry, which sets up to form a solid mold or investment; plaster of paris is usually used. The mold is then heated, such that the pattern melts and is burned out, leaving behind a mold cavity having the desired shape. This technique is employed when high dimensional accuracy, reproduction of fine detail, and an excellent finish are required—for example, in jewelry and dental crowns and inlays. Also, blades for gas turbines and jet engine impellers are investment cast.

Lost Foam Casting

A variation of investment casting is *lost foam* (or *expendable pattern*) casting. Here the expendable pattern is a foam that can be formed by compressing polystyrene beads into the desired shape and then bonding them together by heating. Alternatively, pattern shapes can be cut from sheets and assembled with glue. Sand is then packed around the pattern to form the mold. As the molten metal is poured into the mold, it replaces the pattern which vaporizes. The compacted sand remains in place, and, upon solidification, the metal assumes the shape of the mold.

With lost foam casting, complex geometries and tight tolerances are possible. Furthermore, in comparison to sand casting, lost foam is a simpler, quicker, and less expensive process, and there are fewer environmental wastes. Metal alloys that most commonly use this technique are cast irons and aluminum alloys; furthermore, applications include automobile engine blocks, cylinder heads, crankshafts, marine engine blocks, and electric motor frames.

Continuous Casting

At the conclusion of extraction processes, many molten metals are solidified by casting into large ingot molds. The ingots are normally subjected to a primary hot-rolling operation, the product of which is a flat sheet or slab; these are more convenient shapes as starting points for subsequent secondary metal-forming operations (i.e., forging, extrusion, drawing). These casting and rolling steps may be combined by a *continuous casting* (sometimes also termed “strand casting”) process. Using this technique, the refined and molten metal is cast directly into a continuous strand that may have either a rectangular or circular cross section; solidification occurs in a water-cooled die having the desired cross-sectional geometry. The chemical composition and mechanical properties are more uniform throughout the cross sections for continuous castings than for ingot-cast products. Furthermore, continuous casting is highly automated and more efficient.

23.4 MISCELLANEOUS TECHNIQUES

Powder Metallurgy

Yet another fabrication technique involves the compaction of powdered metal, followed by a heat treatment to produce a more dense piece. The process is appropriately called **powder metallurgy**, frequently designated as P/M. Powder metallurgy makes it possible to produce a virtually nonporous piece having properties almost equivalent to the fully dense parent material. Diffusional processes during the heat treatment are central to the development of these properties. This method is especially suitable for metals having low ductilities, since only small plastic deformation of the powder particles need occur. Metals having high melting temperatures are difficult to melt and cast, and fabrication is expedited using P/M. Furthermore, parts that require very close dimensional tolerances (e.g., bushings and gears) may be economically produced using this technique.

Concept Check 23.1

(a) Cite two advantages of powder metallurgy over casting. (b) Cite two disadvantages.

[The answer may be found in enclosed CD.]

Welding

In a sense, welding may be considered to be a fabrication technique. In **welding**, two or more metal parts are joined to form a single piece when one-part fabrication is expensive or inconvenient. Both similar and dissimilar metals may be welded. The joining bond is metallurgical (involving some diffusion) rather than just mechanical, as with riveting and bolting. A variety of welding methods exist, including arc and gas welding, as well as brazing and soldering.

During arc and gas welding, the workpieces to be joined and the filler material (i.e., welding rod) are heated to a sufficiently high temperature to cause both to melt; upon solidification, the filler material forms a fusion joint between the workpieces. Thus, there is a region adjacent to the weld that may have experienced microstructural and property alterations; this region is termed the *heat-affected zone* (sometimes abbreviated *HAZ*). Possible alterations include the following:

1. If the workpiece material was previously cold worked, this heat-affected zone may have experienced recrystallization and grain growth, and thus a diminishment of strength, hardness, and toughness. The *HAZ* for this situation is represented schematically in Figure 23.3.
2. Upon cooling, residual stresses may form in this region that weaken the joint.
3. For steels, the material in this zone may have been heated to temperatures sufficiently high so as to form austenite. Upon cooling to room temperature, the microstructural products that form depend on cooling rate and alloy composition. For plain carbon steels, normally pearlite and a proeutectoid phase will be present. However, for alloy steels, one microstructural product may be martensite, which is ordinarily undesirable because it is so brittle.
4. Some stainless steels may be “sensitized” during welding, which renders them susceptible to intergranular corrosion, as explained in Section 16.7.

A relatively modern joining technique is that of laser beam welding, wherein a highly focused and intense laser beam is used as the heat source. The laser beam melts the parent metal, and, upon solidification, a fusion joint is produced; often a filler material need not be used. Some of the advantages of this technique are as follows: (1) it is a noncontact process, which eliminates mechanical distortion of the workpieces; (2) it can be rapid and highly automated; (3) energy input to the workpiece is low, and therefore the heat-affected zone size is minimal; (4) welds may be small in size

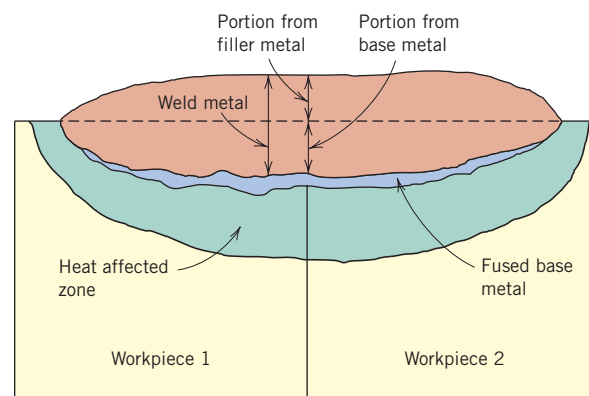


Figure 23.3 Schematic cross-sectional representation showing the zones in the vicinity of a typical fusion weld. [From *Iron Castings Handbook*, C. F. Walton and T. J. Opar (Editors), 1981.]

and very precise; (5) a large variety of metals and alloys may be joined using this technique; and (6) porosity-free welds with strengths equal to or in excess of the base metal are possible. Laser beam welding is used extensively in the automotive and electronic industries where high quality and rapid welding rates are required.

Concept Check 23.2

What are the principal differences between welding, brazing, and soldering? You may need to consult another reference.

[The answer may be found in enclosed CD.]

23.5 HEAT TREATMENT OF STEELS

Conventional heat treatment procedures for producing martensitic steels ordinarily involve continuous and rapid cooling of an austenitized specimen in some type of quenching medium, such as water, oil, or air. The optimum properties of a steel that has been quenched and then tempered can be realized only if, during the quenching heat treatment, the specimen has been converted to a high content of martensite; the formation of any pearlite and/or bainite will result in other than the best combination of mechanical characteristics. During the quenching treatment, it is impossible to cool the specimen at a uniform rate throughout—the surface will always cool more rapidly than interior regions. Therefore, the austenite will transform over a range of temperatures, yielding a possible variation of microstructure and properties with position within a specimen.

The successful heat treating of steels to produce a predominantly martensitic microstructure throughout the cross section depends mainly on three factors: (1) the composition of the alloy, (2) the type and character of the quenching medium, and (3) the size and shape of the specimen. The influence of each of these factors is now addressed.

Hardenability

The influence of alloy composition on the ability of a steel alloy to transform to martensite for a particular quenching treatment is related to a parameter called **hardenability**. For every different steel alloy there is a specific relationship between the mechanical properties and the cooling rate. “Hardenability” is a term that is used to describe the ability of an alloy to be hardened by the formation of martensite as a result of a given heat treatment. Hardenability is not “hardness,” which is the resistance to indentation; rather, hardenability is a qualitative measure of the rate at which hardness drops off with distance into the interior of a specimen as a result of diminished martensite content. A steel alloy that has a high hardenability is one that hardens, or forms martensite, not only at the surface but to a large degree throughout the entire interior.

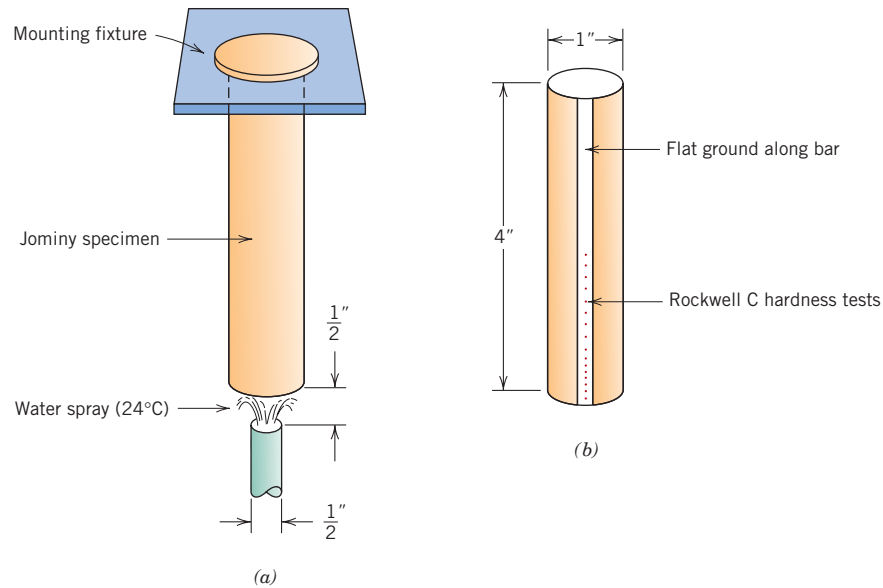
The Jominy End-Quench Test

One standard procedure that is widely utilized to determine hardenability is the **Jominy end-quench test**.¹ With this procedure, except for alloy composition, all

¹ ASTM Standard A 255, “Standard Test Method for End-Quench Test for Hardenability of Steel.”

832 • Chapter 23 / Processing of Engineering Materials

Figure 23.4
Schematic diagram
of Jominy end-
quench specimen
(a) mounted during
quenching and
(b) after hardness
testing from the
quenched end along
a ground flat.
(Adapted from A. G.
Guy, *Essentials of
Materials Science*.
Copyright 1978 by
McGraw-Hill Book
Company, New
York.)



factors that may influence the depth to which a piece hardens (i.e., specimen size and shape, and quenching treatment) are maintained constant. A cylindrical specimen 25.4 mm (1.0 in.) in diameter and 100 mm (4 in.) long is austenitized at a prescribed temperature for a prescribed time. After removal from the furnace, it is quickly mounted in a fixture as diagrammed in Figure 23.4a. The lower end is quenched by a jet of water of specified flow rate and temperature. Thus, the cooling rate is a maximum at the quenched end and diminishes with position from this point along the length of the specimen. After the piece has cooled to room temperature, shallow flats 0.4 mm (0.015 in.) deep are ground along the specimen length and Rockwell hardness measurements are made for the first 50 mm (2 in.) along each flat (Figure 23.4b); for the first 12.8 mm ($\frac{1}{2}$ in.), hardness readings are taken at 1.6 mm ($\frac{1}{16}$ in.) intervals, and for the remaining 38.4 mm ($1\frac{1}{2}$ in.), every 3.2 mm ($\frac{1}{8}$ in.). A hardenability curve is produced when hardness is plotted as a function of position from the quenched end.

Hardenability Curves

A typical hardenability curve is represented in Figure 23.5. The quenched end is cooled most rapidly and exhibits the maximum hardness; 100% martensite is the

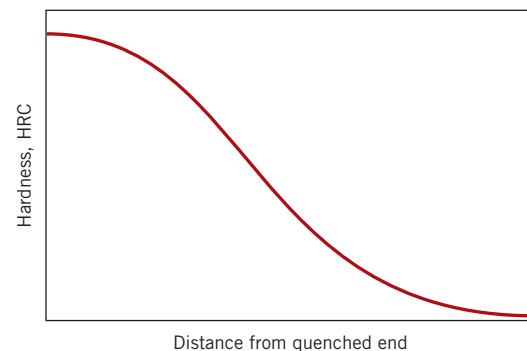


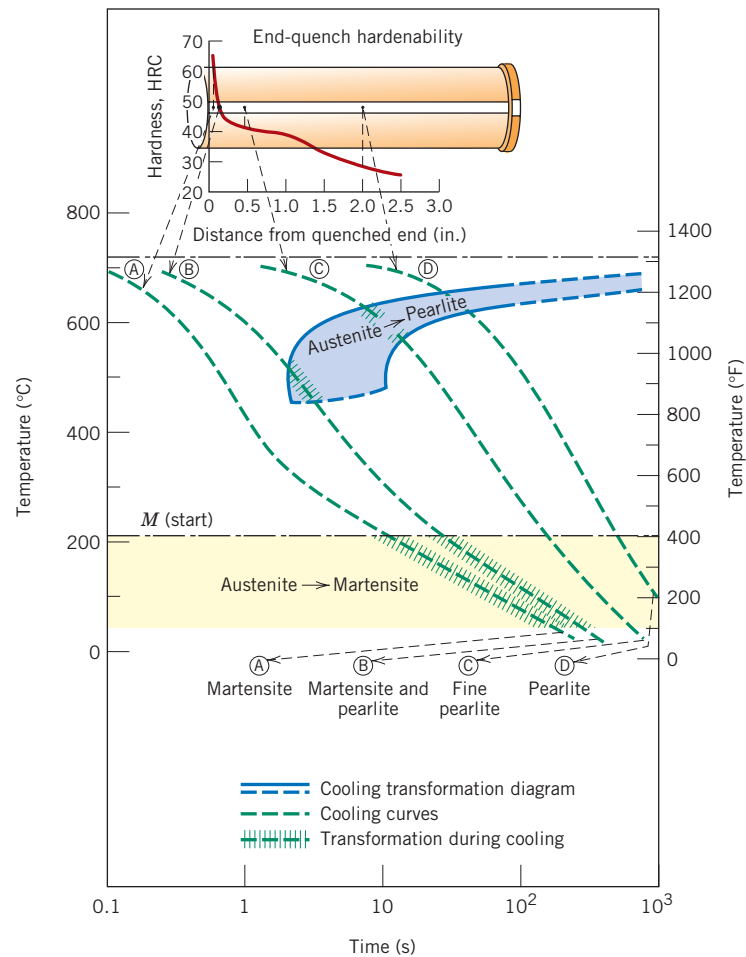
Figure 23.5 Typical hardenability plot of Rockwell C hardness as a function of distance from the quenched end.

product at this position for most steels. Cooling rate decreases with distance from the quenched end, and the hardness also decreases, as indicated in the figure. With diminishing cooling rate more time is allowed for carbon diffusion and the formation of a greater proportion of the softer pearlite, which may be mixed with martensite and bainite. Thus, a steel that is highly hardenable will retain large hardness values for relatively long distances; a low hardenable one will not. Also, each steel alloy has its own unique hardenability curve.

Sometimes, it is convenient to relate hardness to a cooling rate rather than to the location from the quenched end of a standard Jominy specimen. Cooling rate [taken at 700°C (1300°F)] is ordinarily shown on the upper horizontal axis of a hardenability diagram; this scale is included with the hardenability plots presented here. This correlation between position and cooling rate is the same for plaincarbon and many alloy steels because the rate of heat transfer is nearly independent of composition. On occasion, cooling rate or position from the quenched end is specified in terms of Jominy distance, one Jominy distance unit being 1.6 mm ($\frac{1}{16}$ in.).

A correlation may be drawn between position along the Jominy specimen and continuous cooling transformations. For example, Figure 23.6 is a continuous cooling transformation diagram for a eutectoid iron–carbon alloy onto which are

Figure 23.6
Correlation of hardenability and continuous cooling information for an iron–carbon alloy of eutectoid composition. [Adapted from H. Boyer (Editor), *Atlas of Isothermal Transformation and Cooling Transformation Diagrams*, American Society for Metals, 1977, p. 376.]



834 • Chapter 23 / Processing of Engineering Materials

superimposed the cooling curves at four different Jominy positions, and corresponding microstructures that result for each. The hardenability curve for this alloy is also included.

The hardenability curves for five different steel alloys all having 0.40 wt% C, yet differing amounts of other alloying elements, are shown in Figure 23.7. One specimen is a plain carbon steel (1040); the other four (4140, 4340, 5140, and 8640) are alloy steels. The compositions of the four alloy steels are included with the figure. The significance of the alloy designation numbers (e.g., 1040) is explained in Section 9.2. Several details are worth noting from this figure. First, all five alloys have identical hardnesses at the quenched end (57 HRC); this hardness is a function of carbon content only, which is the same for all these alloys.

Probably the most significant feature of these curves is shape, which relates to hardenability. The hardenability of the plain carbon 1040 steel is low because the hardness drops off precipitously (to about 30 HRC) after a relatively short Jominy distance (6.4 mm, $\frac{1}{4}$ in.). By way of contrast, the decreases in hardness for the other four alloy steels are distinctly more gradual. For example, at a Jominy distance of 50 mm (2 in.), the hardnesses of the 4340 and 8640 alloys are approximately 50 and 32 HRC, respectively; thus, of these two alloys, the 4340 is more hardenable. A water-quenched specimen of the 1040 plain carbon steel would harden only to a shallow depth below the surface, whereas for the other four alloy steels the high quenched hardness would persist to a much greater depth.

The hardness profiles in Figure 23.7 are indicative of the influence of cooling rate on the microstructure. At the quenched end, where the quenching rate is approximately $600^{\circ}\text{C}/\text{s}$, 100% martensite is present for all five alloys. For cooling rates less than about $70^{\circ}\text{C}/\text{s}$ or Jominy distances greater than about 6.4 mm ($\frac{1}{4}$ in.), the microstructure of the 1040 steel is predominantly pearlitic, with some proeutectoid ferrite. However, the microstructures of the four alloy steels consist primarily of a mixture of martensite and bainite; bainite content increases with decreasing cooling rate.

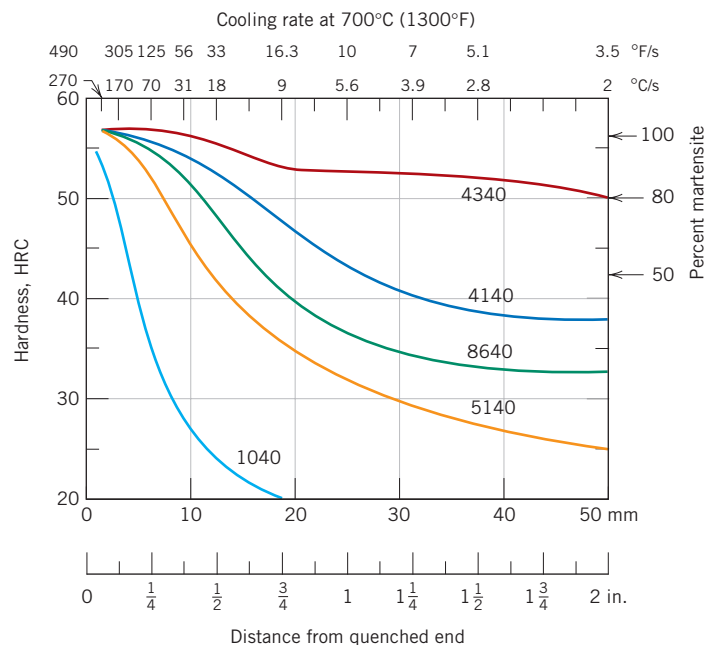


Figure 23.7
Hardenability curves for five different steel alloys, each containing 0.4 wt% C. Approximate alloy compositions (wt%) are as follows: 4340–1.85 Ni, 0.80 Cr, and 0.25 Mo; 4140–1.0 Cr and 0.20 Mo; 8640–0.55 Ni, 0.50 Cr, and 0.20 Mo; 5140–0.85 Cr; and 1040 is an unalloyed steel. (Adapted from figure furnished courtesy Republic Steel Corporation.)

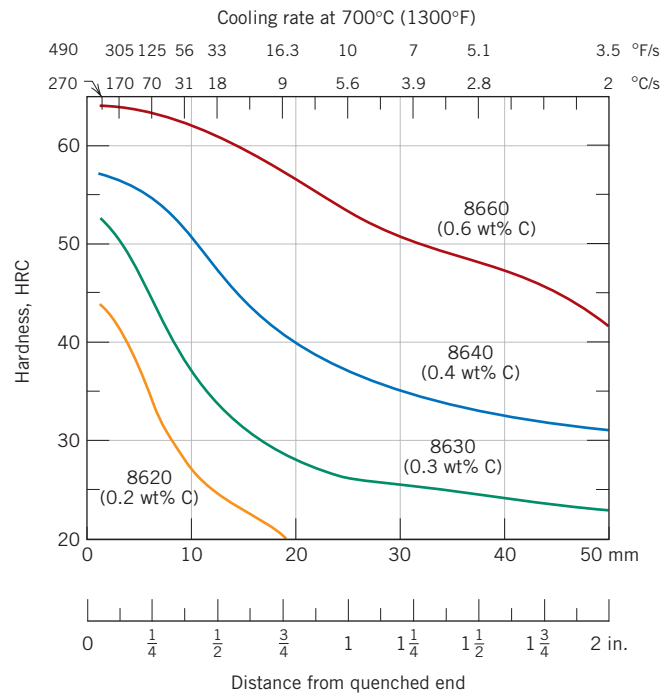


Figure 23.8 Hardenability curves for four 8600 series alloys of indicated carbon content. (Adapted from figure furnished courtesy Republic Steel Corporation.)

This disparity in hardenability behavior for the five alloys in Figure 23.7 is explained by the presence of nickel, chromium, and molybdenum in the alloy steels. These alloying elements delay the austenite-to-pearlite and/or bainite reactions, as explained above; this permits more martensite to form for a particular cooling rate, yielding a greater hardness. The right-hand axis of Figure 23.7 shows the approximate percentage of martensite that is present at various hardnesses for these alloys.

The hardenability curves also depend on carbon content. This effect is demonstrated in Figure 23.8 for a series of alloy steels in which only the concentration of carbon is varied. The hardness at any Jominy position increases with the concentration of carbon.

Also, during the industrial production of steel, there is always a slight, unavoidable variation in composition and average grain size from one batch to another. This variation results in some scatter in measured hardenability data, which frequently are plotted as a band representing the maximum and minimum values that would be expected for the particular alloy. Such a hardenability band is plotted in Figure 23.9 for an 8640 steel. An H following the designation specification for an alloy (e.g., 8640H) indicates that the composition and characteristics of the alloy are such that its hardenability curve will lie within a specified band.

Influence of Quenching Medium, Specimen Size, and Geometry

The preceding treatment of hardenability discussed the influence of both alloy composition and cooling or quenching rate on the hardness. The cooling rate of a specimen depends on the rate of heat energy extraction, which is a function of the characteristics of the quenching medium in contact with the specimen surface, as well as the specimen size and geometry.

836 • Chapter 23 / Processing of Engineering Materials

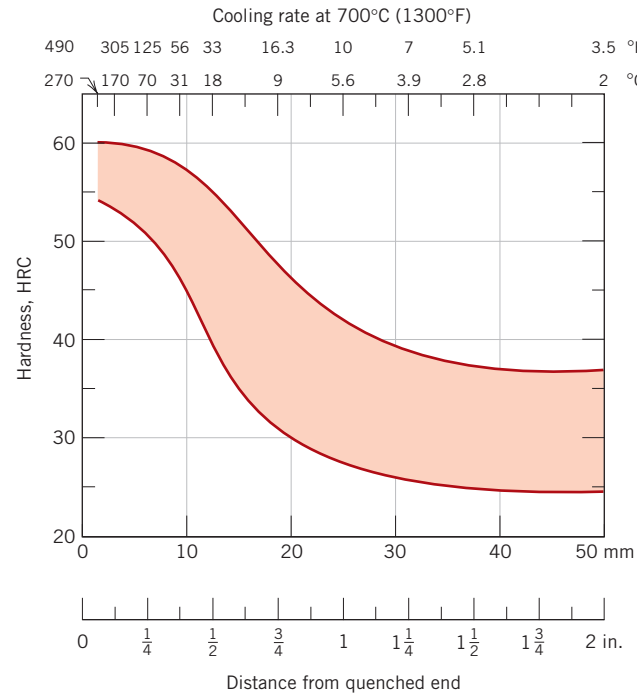


Figure 23.9 The hardenability band for an 8640 steel indicating maximum and minimum limits. (Adapted from figure furnished courtesy Republic Steel Corporation.)

“Severity of quench” is a term often used to indicate the rate of cooling; the more rapid the quench, the more severe the quench. Of the three most common quenching media—water, oil, and air—water produces the most severe quench, followed by oil, which is more effective than air.² The degree of agitation of each medium also influences the rate of heat removal. Increasing the velocity of the quenching medium across the specimen surface enhances the quenching effectiveness. Oil quenches are suitable for the heat treating of many alloy steels. In fact, for higher-carbon steels, a water quench is too severe because cracking and warping may be produced. Air cooling of austenitized plain carbon steels ordinarily produces an almost totally pearlitic structure.

During the quenching of a steel specimen, heat energy must be transported to the surface before it can be dissipated into the quenching medium. As a consequence, the cooling rate within and throughout the interior of a steel structure varies with position and depends on the geometry and size. Figures 23.10a and 23.10b show the quenching rate at 700°C as a function of diameter for cylindrical bars at four radial positions (surface, three-quarters radius, midradius, and center). Quenching is in mildly agitated water (Figure 23.10a) and oil (Figure 23.10b); cooling rate is also expressed as equivalent Jominy distance, since these data are often used in conjunction with hardenability curves. Diagrams similar to those in Figure 23.10 have also been generated for geometries other than cylindrical (e.g., flat plates).

² Aqueous polymer quenchants {solutions composed of water and a polymer [normally poly(alkylene glycol) or PAG]} have recently been developed that provide quenching rates between those of water and oil. The quenching rate can be tailored to specific requirements by changing polymer concentration and quench bath temperature.

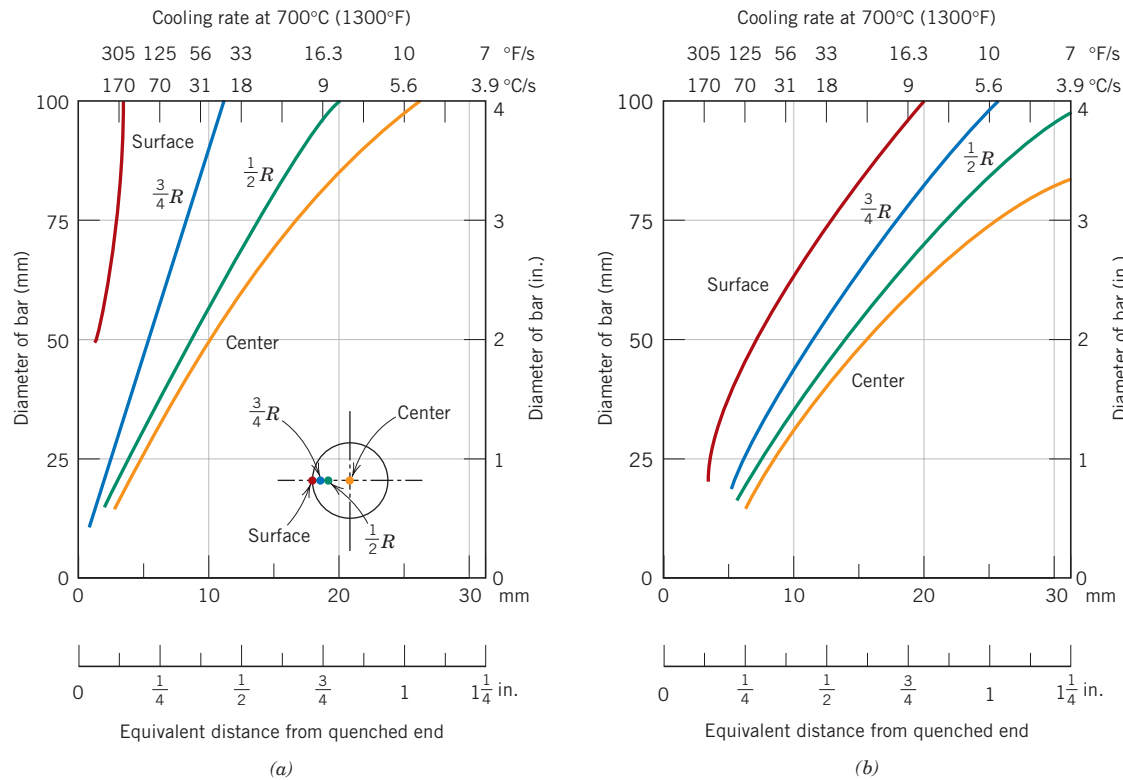


Figure 23.10 Cooling rate as a function of diameter at surface, three-quarters radius ($\frac{3}{4}R$), midradius ($\frac{1}{2}R$), and center positions for cylindrical bars quenched in mildly agitated (a) water and (b) oil. Equivalent Jominy positions are included along the bottom axes. [Adapted from *Metals Handbook: Properties and Selection: Irons and Steels*, Vol. 1, 9th edition, B. Bardes (Editor), American Society for Metals, 1978, p. 492.]

One utility of such diagrams is in the prediction of the hardness traverse along the cross section of a specimen. For example, Figure 23.11a compares the radial hardness distributions for cylindrical plain carbon (1040) and alloy (4140) steel specimens; both have a diameter of 50 mm (2 in.) and are water quenched. The difference in hardenability is evident from these two profiles. Specimen diameter also influences the hardness distribution, as demonstrated in Figure 23.11b, which plots the hardness profiles for oil-quenched 4140 cylinders 50 and 75 mm (2 and 3 in.) in diameter. Example Problem 23.1 illustrates how these hardness profiles are determined.

As far as specimen shape is concerned, since the heat energy is dissipated to the quenching medium at the specimen surface, the rate of cooling for a particular quenching treatment depends on the ratio of surface area to the mass of the specimen. The larger this ratio, the more rapid will be the cooling rate and, consequently, the deeper the hardening effect. Irregular shapes with edges and corners have larger surface-to-mass ratios than regular and rounded shapes (e.g., spheres and cylinders) and are thus more amenable to hardening by quenching.

There are a multitude of steels that are responsive to a martensitic heat treatment, and one of the most important criteria in the selection process is hardenability. Hardenability curves, when utilized in conjunction with plots such as those in Figure 23.10 for various quenching media, may be used to ascertain the

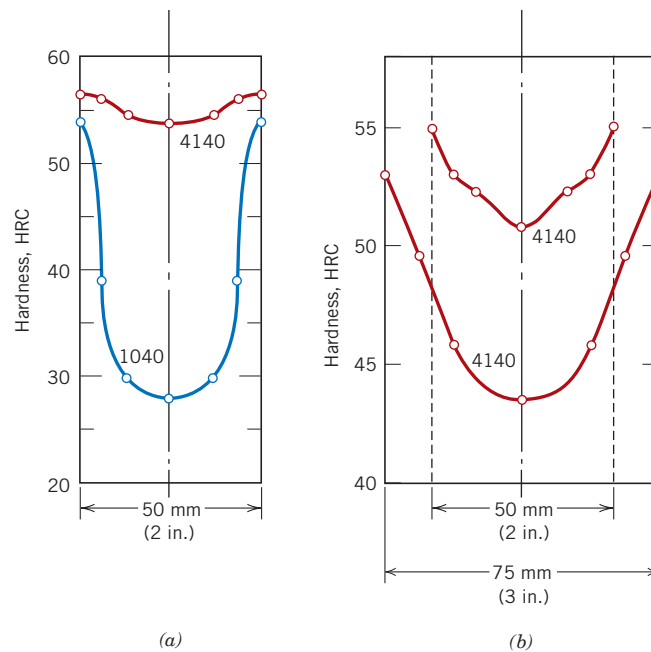


Figure 23.11 Radial hardness profiles for (a) 50 mm diameter cylindrical 1040 and 4140 steel specimens quenched in mildly agitated water, and (b) 50 and 75 mm diameter cylindrical specimens of 4140 steel quenched in mildly agitated oil.

suitability of a specific steel alloy for a particular application. Or, conversely, the appropriateness of a quenching procedure for an alloy may be determined. For parts that are to be involved in relatively high stress applications, a minimum of 80% martensite must be produced throughout the interior as a consequence of the quenching procedure. Only a 50% minimum is required for moderately stressed parts.

Concept Check 23.3

Name the three factors that influence the degree to which martensite is formed throughout the cross section of a steel specimen. For each, tell how the extent of martensite formation may be increased.

[The answer may be found in enclosed CD.]

EXAMPLE PROBLEM 23.1

Determination of Hardness Profile for Heat-Treated 1040 Steel

Determine the radial hardness profile for a 50 mm diameter cylindrical specimen of 1040 steel that has been quenched in moderately agitated water.

Solution

First, evaluate the cooling rate (in terms of the Jominy end-quench distance) at center, surface, mid-, and three-quarter radial positions of the cylindrical

specimen. This is accomplished using the cooling rate-versus-bar diameter plot for the appropriate quenching medium, in this case, Figure 23.10a. Then, convert the cooling rate at each of these radial positions into a hardness value from a hardenability plot for the particular alloy. Finally, determine the hardness profile by plotting the hardness as a function of radial position.

This procedure is demonstrated in Figure 23.12, for the center position. Note that for a water-quenched cylinder of 50 mm (2 in.) diameter, the cooling rate at the center is equivalent to that approximately 9.5 mm ($\frac{3}{8}$ in.) from the Jominy specimen quenched end (Figure 23.12a). This corresponds to a hardness of about 28 HRC, as noted from the hardenability plot for the 1040 steel alloy (Figure 23.12b). Finally, this data point is plotted on the hardness profile in Figure 23.12c.

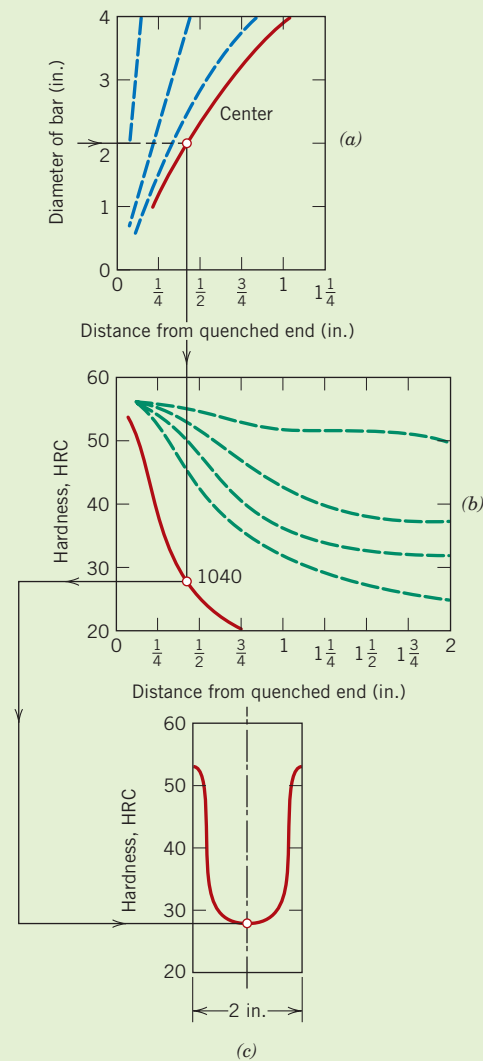
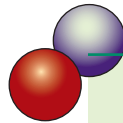


Figure 23.12 Use of hardenability data in the generation of hardness profiles. (a) The cooling rate at the center of a water-quenched 50 mm (2 in.) diameter specimen is determined. (b) The cooling rate is converted into an HRC hardness for a 1040 steel. (c) The Rockwell hardness is plotted on the radial hardness profile.

Surface, midradius, and three-quarter radius hardnesses would be determined in a similar manner. The complete profile has been included, and the data that were used are tabulated below.

<i>Radial Position</i>	<i>Equivalent Distance from Quenched End [mm (in.)]</i>	<i>Hardness (HRC)</i>
Center	9.5 ($\frac{3}{8}$)	28
Midradius	8 ($\frac{5}{16}$)	30
Three-quarters radius	4.8 ($\frac{3}{16}$)	39
Surface	1.6 ($\frac{1}{16}$)	54



DESIGN EXAMPLE 23.1

Steel Alloy and Heat Treatment Selection

It is necessary to select a steel alloy for a gearbox output shaft. The design calls for a 1-in. diameter cylindrical shaft having a surface hardness of at least 38 HRC and a minimum ductility of 12% EL. Specify an alloy and treatment that meet these criteria.

Solution

First of all, cost is also most likely an important design consideration. This would probably eliminate relatively expensive steels, such as stainless and those that are precipitation hardenable. Therefore, let us begin by examining plain-carbon and low-alloy steels, and what treatments are available to alter their mechanical characteristics.

It is unlikely that merely cold working one of these steels would produce the desired combination of hardness and ductility. For example, from Figure 9.25, a hardness of 38 HRC corresponds to a tensile strength of 1200 MPa. The tensile strength as a function of percent cold work for a 1040 steel is represented in Figure 10.19*b*. Here it may be noted that at 50% CW, a tensile strength of only about 900 MPa is achieved; furthermore, the corresponding ductility is approximately 10% EL (Figure 10.19*c*). Hence, both of these properties fall short of those specified in the design; furthermore, cold working other plain-carbon or low-alloy steels would probably not achieve the required minimum values.

Another possibility is to perform a series of heat treatments in which the steel is austenitized, quenched (to form martensite), and finally tempered. Let us now examine the mechanical properties of various plain-carbon and low-alloy steels that have been heat treated in this manner. To begin, the surface hardness of the quenched material (which ultimately affects the tempered hardness) will depend on both alloy content and shaft diameter, as discussed in the previous two sections. For example, the degree to which surface hardness decreases with diameter is represented in Table 23.1 for a 1060 steel that was oil quenched. Furthermore, the tempered surface hardness will also depend on tempering temperature and time.

Table 23.1 Surface Hardnesses for Oil-Quenched Cylinders of 1060 Steel Having Various Diameters

Diameter (in.)	Surface Hardness (HRC)
0.5	59
1	34
2	30.5
4	29

As-quenched and tempered hardness and ductility data were collected for one plain-carbon (AISI/SAE 1040) and several common and readily available low-alloy steels, data for which are presented in Table 23.2. The quenching medium (either oil or water) is indicated, and tempering temperatures were 540°C (1000°F), 595°C (1100°F), and 650°C (1200°F). As may be noted, the only alloy-heat treatment combinations that meet the stipulated criteria are 4150/oil-540°C temper, 4340/oil-540°C temper, and 6150/oil-540°C temper; data for these alloys/heat treatments are boldfaced in the table. The costs of these three materials are probably comparable; however, a cost analysis should be conducted. Furthermore, the 6150 alloy has the highest ductility (by a narrow margin), which would give it a slight edge in the selection process.

Table 23.2 Rockwell C Hardness (Surface) and Percent Elongation Values for 1-in. Diameter Cylinders of Six Steel Alloys, in the As-Quenched Condition and for Various Tempering Heat Treatments

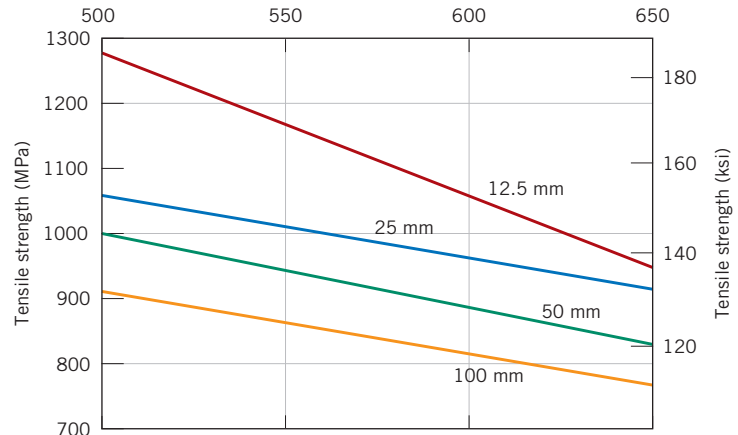
Alloy Designation/ Quenching Medium	As-Quenched	Tempered at 540°C (1000°F)		Tempered at 595°C (1100°F)		Tempered at 650°C (1200°F)	
	Hardness (HRC)	Hardness (HRC)	Ductility (%EL)	Hardness (HRC)	Ductility (%EL)	Hardness (HRC)	Ductility (%EL)
1040/oil	23	(12.5) ^a	26.5	(10) ^a	28.2	(5.5) ^a	30.0
1040/water	50	(17.5) ^a	23.2	(15) ^a	26.0	(12.5) ^a	27.7
4130/water	51	31	18.5	26.5	21.2	—	—
4140/oil	55	33	16.5	30	18.8	27.5	21.0
4150/oil	62	38	14.0	35.5	15.7	30	18.7
4340/oil	57	38	14.2	35.5	16.5	29	20.0
6150/oil	60	38	14.5	33	16.0	31	18.7

^a These hardness values are only approximate because they are less than 20 HRC.

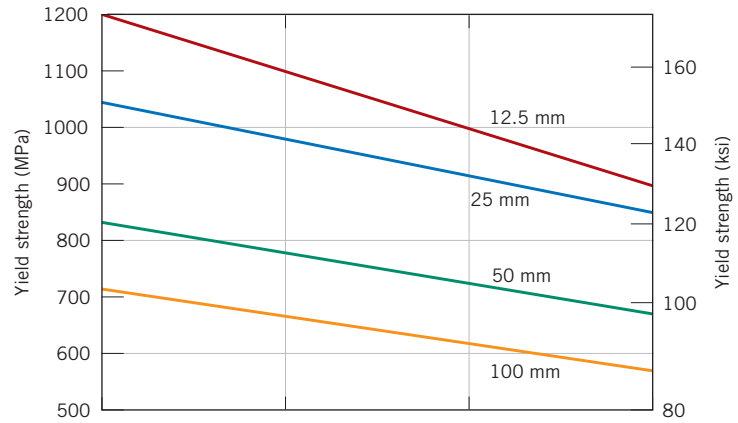
As the previous section notes, for cylindrical steel alloy specimens that have been quenched, surface hardness depends, not only upon alloy composition and quenching medium, but also upon specimen diameter. Likewise, the mechanical characteristics of steel specimens that have been quenched and subsequently tempered will also be a function of specimen diameter. This phenomenon is illustrated in Figure 23.13, which plots for an oil-quenched 4140 steel, tensile strength, yield strength, and ductility (%EL) versus tempering temperature for four diameters—viz. 12.5 mm (0.5 in.), 25 mm (1 in.), 50 mm (2 in.), and 100 mm (4 in.).

842 • Chapter 23 / Processing of Engineering Materials

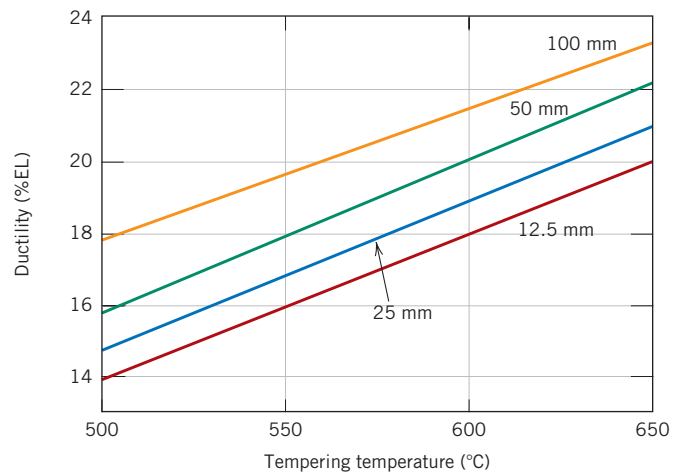
Figure 23.13 For cylindrical specimens of an oil-quenched 4140 steel, (a) tensile strength, (b) yield strength, and (c) ductility (percent elongation) versus tempering temperature for diameters of 12.5 mm, 25 mm, 50 mm, and 100 mm.



(a)



(b)



(c)

Fabrication and Processing of Ceramics

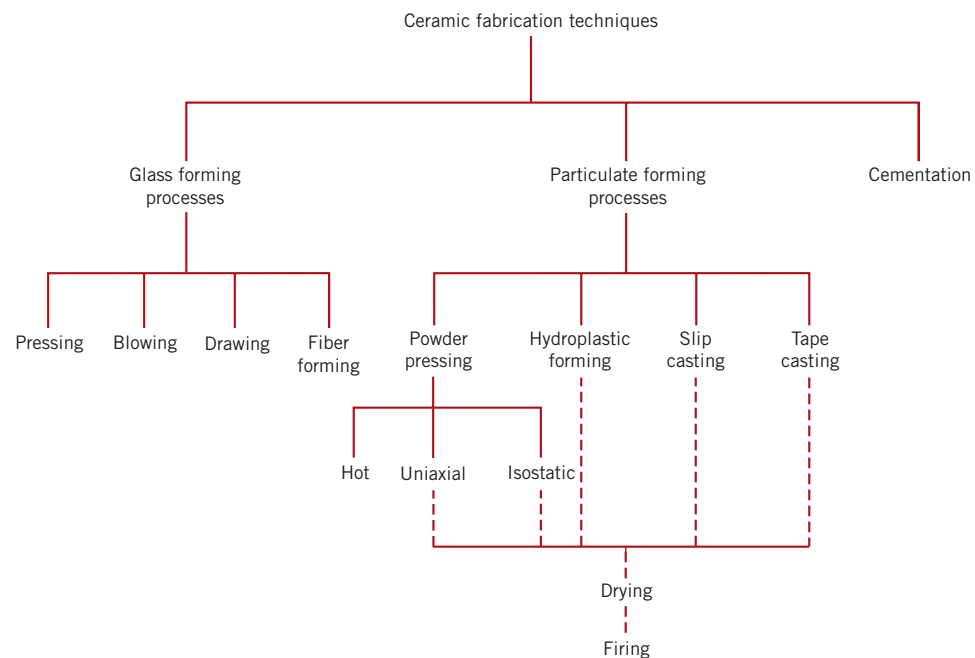
One chief concern in the application of ceramic materials is the method of fabrication. Many of the metal-forming operations discussed in this chapter rely on casting and/or techniques that involve some form of plastic deformation. Since ceramic materials have relatively high melting temperatures, casting them is normally impractical. Furthermore, in most instances the brittleness of these materials precludes deformation. Some ceramic pieces are formed from powders (or particulate collections) that must ultimately be dried and fired. Glass shapes are formed at elevated temperatures from a fluid mass that becomes very viscous upon cooling. Cements are shaped by placing into forms a fluid paste that hardens and assumes a permanent set by virtue of chemical reactions. A taxonomical scheme for the several types of ceramic-forming techniques is presented in Figure 23.14.

23.6 GLASS FORMING

Glass is produced by heating the raw materials to an elevated temperature above which melting occurs. Most commercial glasses are of the silica-soda-lime variety; the silica is usually supplied as common quartz sand, whereas Na_2O and CaO are added as soda ash (Na_2CO_3) and limestone (CaCO_3). For most applications, especially when optical transparency is important, it is essential that the glass product be homogeneous and pore free. Homogeneity is achieved by complete melting and mixing of the raw ingredients. Porosity results from small gas bubbles that are produced; these must be absorbed into the melt or otherwise eliminated, which requires proper adjustment of the viscosity of the molten material.

Four different forming methods are used to fabricate glass products: pressing, blowing, drawing, and fiber forming. Pressing is used in the fabrication of relatively

Figure 23.14 A classification scheme for the ceramic-forming techniques discussed in this chapter.



844 • Chapter 23 / Processing of Engineering Materials

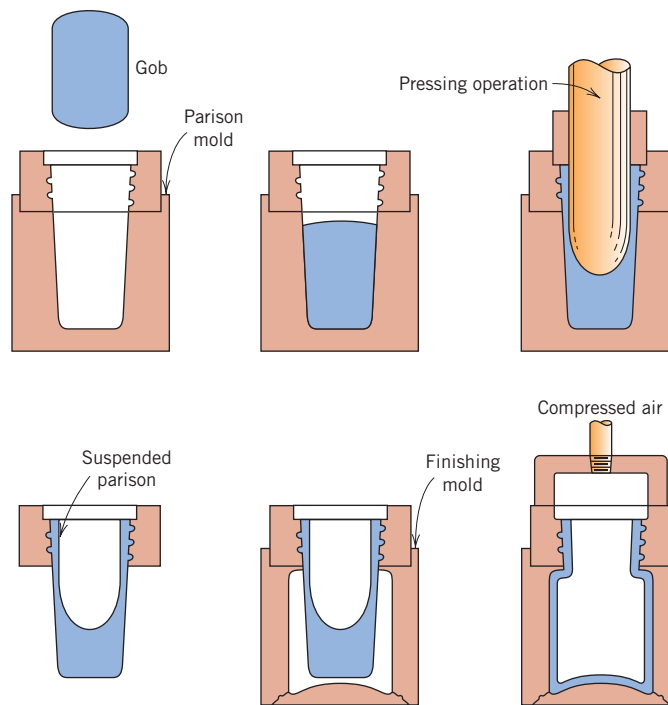


Figure 23.15 The press-and-blow technique for producing a glass bottle. (Adapted from C. J. Phillips, *Glass: The Miracle Maker*. Reproduced by permission of Pitman Publishing Ltd., London.)

thick-walled pieces such as plates and dishes. The glass piece is formed by pressure application in a graphite-coated cast iron mold having the desired shape; the mold is ordinarily heated to ensure an even surface.

Although some glass blowing is done by hand, especially for art objects, the process has been completely automated for the production of glass jars, bottles, and light bulbs. The several steps involved in one such technique are illustrated in Figure 23.15. From a raw gob of glass, a *parison*, or temporary shape, is formed by mechanical pressing in a mold. This piece is inserted into a finishing or blow mold and forced to conform to the mold contours by the pressure created from a blast of air.

Drawing is used to form long glass pieces such as sheet, rod, tubing, and fibers, which have a constant cross section. One process by which sheet glass is formed is illustrated in Figure 23.16; it may also be fabricated by hot rolling. Flatness and the surface finish may be improved significantly by floating the sheet on a bath of molten tin at an elevated temperature; the piece is slowly cooled and subsequently heat treated by annealing.

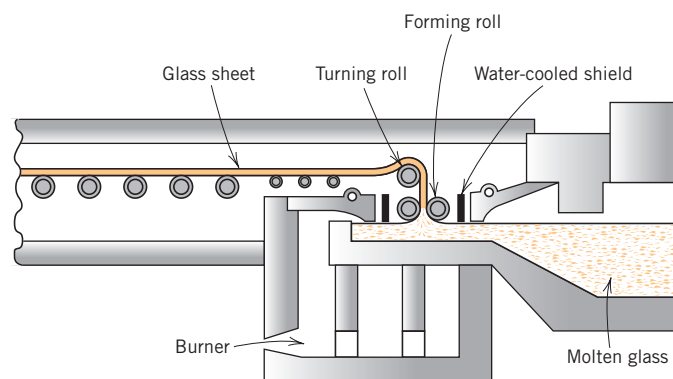


Figure 23.16 A process for the continuous drawing of sheet glass. (From W. D. Kingery, *Introduction to Ceramics*. Copyright © 1960 by John Wiley & Sons, New York. Reprinted by permission of John Wiley & Sons, Inc.)

Continuous glass fibers are formed in a rather sophisticated drawing operation. The molten glass is contained in a platinum heating chamber. Fibers are formed by drawing the molten glass through many small orifices at the chamber base. The glass viscosity, which is critical, is controlled by chamber and orifice temperatures.

23.7 FABRICATION AND PROCESSING OF CLAY PRODUCTS

As Section 12.4 noted, this class of materials includes the structural clay products and the whitewares. In addition to clay, many of these products also contain other ingredients. After having been formed, pieces most often must be subjected to drying and firing operations; each of the ingredients influences the changes that take place during these processes and the characteristics of the finished piece.

The Characteristics of Clay

The clay minerals play two very important roles in ceramic bodies. First, when water is added, they become very plastic, a condition termed *hydroplasticity*. This property is very important in forming operations, as discussed below. In addition, clay fuses or melts over a range of temperatures; thus, a dense and strong ceramic piece may be produced during firing without complete melting such that the desired shape is maintained. This fusion temperature range, of course, depends on the composition of the clay.

Clays are aluminosilicates, being composed of alumina (Al_2O_3) and silica (SiO_2), that contain chemically bound water. They have a broad range of physical characteristics, chemical compositions, and structures; common impurities include compounds (usually oxides) of barium, calcium, sodium, potassium, and iron, and also some organic matter. Crystal structures for the clay minerals are relatively complicated; however, one prevailing characteristic is a layered structure. The most common clay minerals that are of interest have what is called the kaolinite structure. Kaolinite clay $[\text{Al}_2(\text{Si}_2\text{O}_5)(\text{OH})_4]$ has the crystal structure shown in Figure 4.23. When water is added, the water molecules fit in between these layered sheets and form a thin film around the clay particles. The particles are thus free to move over one another, which accounts for the resulting plasticity of the water–clay mixture.

Compositions of Clay Products

In addition to clay, many of these products (in particular the whitewares) also contain some nonplastic ingredients; the nonclay minerals include flint, or finely ground quartz, and a flux such as feldspar.³ The quartz is used primarily as a filler material, being inexpensive, relatively hard, and chemically unreactive. It experiences little change during high-temperature heat treatment because it has a high melting temperature; when melted, however, quartz has the ability to form a glass.

When mixed with clay, a flux forms a glass that has a relatively low melting point. The feldspars are some of the more common fluxing agents; they are a group of aluminosilicate materials that contain K^+ , Na^+ , and Ca^{2+} ions.

As would be expected, the changes that take place during drying and firing processes, and also the characteristics of the finished piece, are influenced by the proportions of these three constituents: clay, quartz, and flux. A typical porcelain might contain approximately 50% clay, 25% quartz, and 25% feldspar.

³ Flux, in the context of clay products, is a substance that promotes the formation of a glassy phase during the firing heat treatment.

Fabrication Techniques

The as-mined raw materials usually have to go through a milling or grinding operation in which particle size is reduced; this is followed by screening or sizing to yield a powdered product having a desired range of particle sizes. For multicomponent systems, powders must be thoroughly mixed with water and perhaps other ingredients to give flow characteristics that are compatible with the particular forming technique. The formed piece must have sufficient mechanical strength to remain intact during transporting, drying, and firing operations. Two common shaping techniques are utilized for forming clay-based compositions: **hydroplastic forming** and **slip casting**.

Hydroplastic Forming

As mentioned above, clay minerals, when mixed with water, become highly plastic and pliable and may be molded without cracking; however, they have extremely low yield strengths. The consistency (water–clay ratio) of the hydroplastic mass must give a yield strength sufficient to permit a formed ware to maintain its shape during handling and drying.

The most common hydroplastic forming technique is extrusion, in which a stiff plastic ceramic mass is forced through a die orifice having the desired cross-sectional geometry; it is similar to the extrusion of metals (Figure 23.2c). Brick, pipe, ceramic blocks, and tiles are all commonly fabricated using hydroplastic forming. Usually the plastic ceramic is forced through the die by means of a motor-driven auger, and often air is removed in a vacuum chamber to enhance the density. Hollow internal columns in the extruded piece (e.g., building brick) are formed by inserts situated within the die.

Slip Casting

Another forming process used for clay-based compositions is slip casting. A slip is a suspension of clay and/or other nonplastic materials in water. When poured into a porous mold (commonly made of plastic or paris), water from the slip is absorbed into the mold, leaving behind a solid layer on the mold wall the thickness of which depends on the time. This process may be continued until the entire mold cavity becomes solid (solid casting), as demonstrated in Figure 23.17a. Or it may be terminated when the solid shell wall reaches the desired thickness, by inverting the mold and pouring out the excess slip; this is termed drain casting (Figure 23.17b). As the cast piece dries and shrinks, it will pull away (or release) from the mold wall; at this time the mold may be disassembled and the cast piece removed.

The nature of the slip is extremely important; it must have a high specific gravity and yet be very fluid and pourable. These characteristics depend on the solid-to-water ratio and other agents that are added. A satisfactory casting rate is an essential requirement. In addition, the cast piece must be free of bubbles, and it must have a low drying shrinkage and a relatively high strength.

The properties of the mold itself influence the quality of the casting. Normally, plaster of paris, which is economical, relatively easy to fabricate into intricate shapes, and reusable, is used as the mold material. Most molds are multipiece items that must be assembled before casting. Also, the mold porosity may be varied to control the casting rate. The rather complex ceramic shapes that may be produced by means of slip casting include sanitary lavatory ware, art objects, and specialized scientific laboratory ware such as ceramic tubes.

23.7 Fabrication and Processing of Clay Products • 847

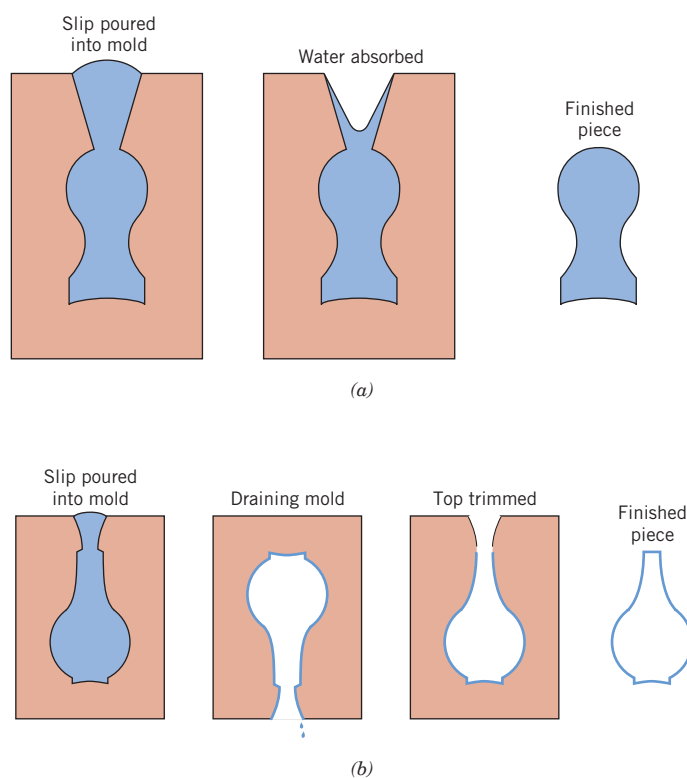


Figure 23.17 The steps in (a) solid and (b) drain slip casting using a plaster of paris mold. (From W. D. Kingery, *Introduction to Ceramics*. Copyright © 1960 by John Wiley & Sons, New York. Reprinted by permission of John Wiley & Sons, Inc.)

Drying and Firing

A ceramic piece that has been formed hydroplastically or by slip casting retains significant porosity and insufficient strength for most practical applications. In addition, it may still contain some liquid (e.g., water), which was added to assist in the forming operation. This liquid is removed in a drying process; density and strength are enhanced as a result of a high-temperature heat treatment or firing procedure. A body that has been formed and dried but not fired is termed **green**. Drying and firing techniques are critical inasmuch as defects that ordinarily render the ware useless (e.g., warpage, distortion, and cracks) may be introduced during the operation. These defects normally result from stresses that are set up from nonuniform shrinkage.

Drying

As a clay-based ceramic body dries, it also experiences some shrinkage. In the early stages of drying the clay particles are virtually surrounded by and separated from one another by a thin film of water. As drying progresses and water is removed, the interparticle separation decreases, which is manifested as shrinkage (Figure 23.18). During drying it is critical to control the rate of water removal. Drying at interior regions of a body is accomplished by the diffusion of water molecules to the surface where evaporation occurs. If the rate of evaporation is greater than the rate of diffusion, the surface will dry (and as a consequence shrink) more rapidly than the interior, with a high probability of the formation of the aforementioned defects. The rate of surface evaporation should be diminished to, at most, the rate of water diffusion; evaporation rate may be controlled by temperature, humidity, and the rate of airflow.

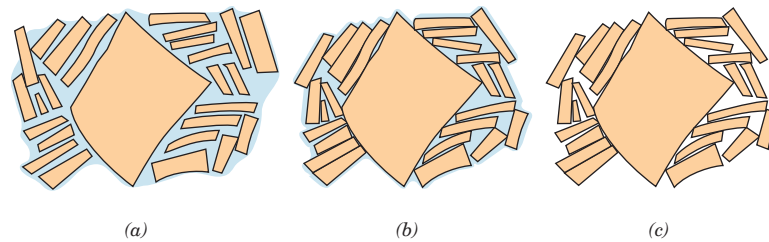


Figure 23.18 Several stages in the removal of water from between clay particles during the drying process. (a) Wet body. (b) Partially dry body. (c) Completely dry body. (From W. D. Kingery, *Introduction to Ceramics*. Copyright © 1960 by John Wiley & Sons, New York. Reprinted by permission of John Wiley & Sons, Inc.)

Other factors also influence shrinkage. One of these is body thickness; nonuniform shrinkage and defect formation are more pronounced in thick pieces than in thin ones. Water content of the formed body is also critical: the greater the water content, the more extensive the shrinkage. Consequently, the water content is ordinarily kept as low as possible. Clay particle size also has an influence; shrinkage is enhanced as the particle size is decreased. To minimize shrinkage, the size of the particles may be increased, or nonplastic materials having relatively large particles may be added to the clay.

Microwave energy may also be used to dry ceramic wares. One advantage of this technique is that the high temperatures used in conventional methods are avoided; drying temperatures may be kept to below 50°C (120°F). This is important because the drying of some temperature-sensitive materials should be kept as low as possible.

Concept Check 23.4

Thick ceramic wares are more likely to crack upon drying than thin wares. Why is this so?

[The answer may be found in enclosed CD.]

Firing

After drying, a body is usually fired at a temperature between 900 and 1400°C; the firing temperature depends on the composition and desired properties of the finished piece. During the firing operation, the density is further increased (with an attendant decrease in porosity) and the mechanical strength is enhanced.

When clay-based materials are heated to elevated temperatures, some rather complex and involved reactions occur. One of these is **vitrification**, the gradual formation of a liquid glass that flows into and fills some of the pore volume. The degree of vitrification depends on firing temperature and time, as well as the composition of the body. The temperature at which the liquid phase forms is lowered by the addition of fluxing agents such as feldspar. This fused phase flows around the remaining unmelted particles and fills in the pores as a result of surface tension forces (or capillary action); shrinkage also accompanies this process. Upon cooling, this fused phase forms a glassy matrix that results in a dense, strong body. Thus, the final microstructure consists of the vitrified phase, any unreacted quartz particles,

23.7 Fabrication and Processing of Clay Products • 849

and some porosity. Figure 23.19 is a scanning electron micrograph of a fired porcelain in which may be seen these microstructural elements.

The degree of vitrification, of course, controls the room-temperature properties of the ceramic ware; strength, durability, and density are all enhanced as it increases. The firing temperature determines the extent to which vitrification occurs; that is, vitrification increases as the firing temperature is raised. Building bricks are ordinarily fired around 900°C (1650°F) and are relatively porous. On the other hand, firing of highly vitrified porcelain, which borders on being optically translucent, takes place at much higher temperatures. Complete vitrification is avoided during firing, since a body becomes too soft and will collapse.

✓ Concept Check 23.5

Explain why a clay, once having been fired at an elevated temperature, loses its hydroplasticity.

[The answer may be found in enclosed CD.]

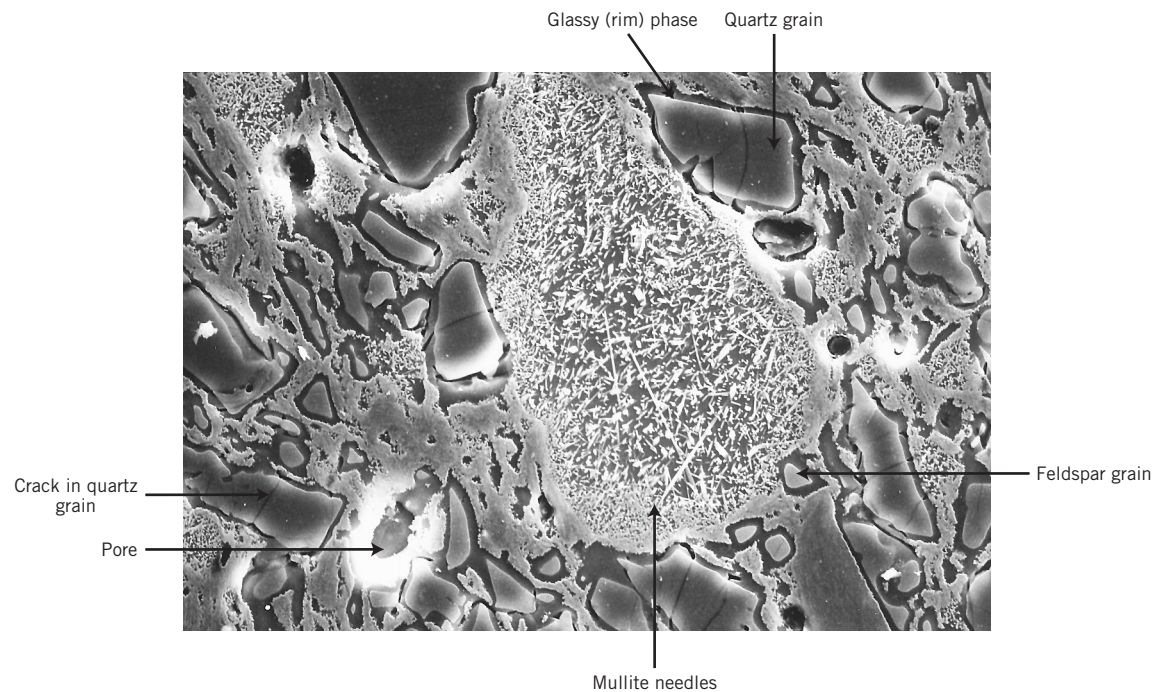


Figure 23.19 Scanning electron micrograph of a fired porcelain specimen (etched 15 s, 5°C, 10% HF) in which may be seen the following features: quartz grains (large dark particles), which are surrounded by dark glassy solution rims; partially dissolved feldspar regions (small unfeatured areas); mullite needles; and pores (dark holes with white border regions). Also, cracks within the quartz particles may be noted, which were formed during cooling as a result of the difference in shrinkage between the glassy matrix and the quartz. 1500×. (Courtesy of H. G. Brinkies, Swinburne University of Technology, Hawthorn Campus, Hawthorn, Victoria, Australia.)

23.8 POWDER PRESSING

Several ceramic-forming techniques have already been discussed relative to the fabrication of glass and clay products. Another important and commonly used method that warrants a brief treatment is powder pressing. Powder pressing, the ceramic analogue to powder metallurgy, is used to fabricate both clay and nonclay compositions, including electronic and magnetic ceramics as well as some refractory brick products. In essence, a powdered mass, usually containing a small amount of water or other binder, is compacted into the desired shape by pressure. The degree of compaction is maximized and fraction of void space is minimized by using coarse and fine particles mixed in appropriate proportions. There is no plastic deformation of the particles during compaction, as there may be with metal powders. One function of the binder is to lubricate the powder particles as they move past one another in the compaction process.

There are three basic powder-pressing procedures: uniaxial, isostatic (or hydrostatic), and hot pressing. For uniaxial pressing, the powder is compacted in a metal die by pressure that is applied in a single direction. The formed piece takes on the configuration of die and platens through which the pressure is applied. This method is confined to shapes that are relatively simple; however, production rates are high and the process is inexpensive. The steps involved in one technique are illustrated in Figure 23.20.

For isostatic pressing, the powdered material is contained in a rubber envelope and the pressure is applied by a fluid, isostatically (i.e., it has the same magnitude in all directions). More complicated shapes are possible than with uniaxial pressing; however, the isostatic technique is more time consuming and expensive.

For both uniaxial and isostatic procedures, a firing operation is required after the pressing operation. During firing the formed piece shrinks, and experiences a reduction of porosity and an improvement in mechanical integrity. These changes occur by the coalescence of the powder particles into a more dense mass in a process termed

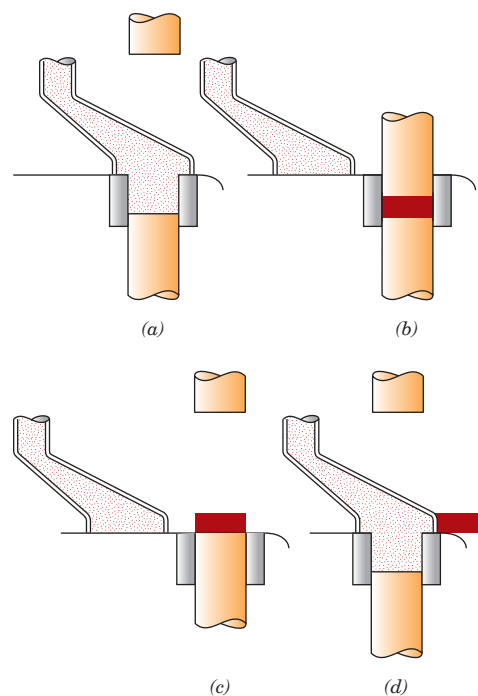


Figure 23.20 Schematic representation of the steps in uniaxial powder pressing. (a) The die cavity is filled with powder. (b) The powder is compacted by means of pressure applied to the top die. (c) The compacted piece is ejected by rising action of the bottom punch. (d) The fill shoe pushes away the compacted piece, and the fill step is repeated. (From W. D. Kingery, Editor, *Ceramic Fabrication Processes*, MIT Press. Copyright © 1958 by the Massachusetts Institute of Technology.)

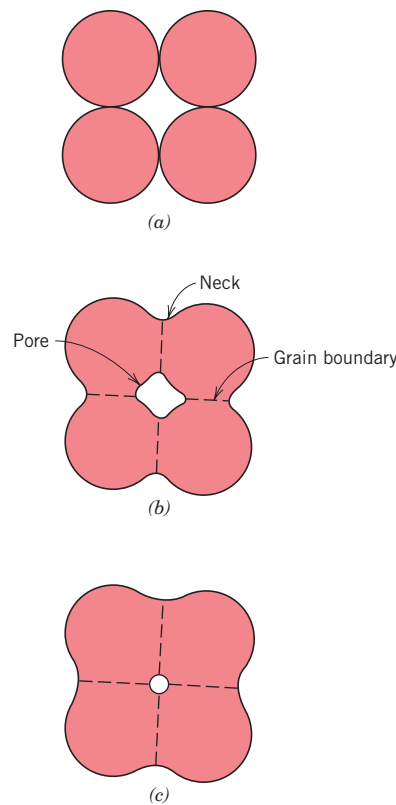


Figure 23.21 For a powder compact, microstructural changes that occur during firing. (a) Powder particles after pressing. (b) Particle coalescence and pore formation as sintering begins. (c) As sintering proceeds, the pores change size and shape.

sintering. The mechanism of sintering is schematically illustrated in Figure 23.21. After pressing, many of the powder particles touch one another (Figure 23.21a). During the initial sintering stage, necks form along the contact regions between adjacent particles; in addition, a grain boundary forms within each neck, and every interstice between particles becomes a pore (Figure 23.21b). As sintering progresses, the pores become smaller and more spherical in shape (Figure 23.21c). A scanning electron micrograph of a sintered alumina material is shown in Figure 23.22. The driving force for sintering is the reduction in total particle surface area; surface energies are larger in magnitude than grain boundary energies. Sintering is carried out below the melting temperature so that a liquid phase is normally not present. Mass transport necessary to effect the changes shown in Figure 23.21 is accomplished by atomic diffusion from the bulk particles to the neck regions.

With hot pressing, the powder pressing and heat treatment are performed simultaneously—the powder aggregate is compacted at an elevated temperature. The procedure is used for materials that do not form a liquid phase except at very high and impractical temperatures; in addition, it is utilized when high densities without appreciable grain growth are desired. This is an expensive fabrication technique that has some limitations. It is costly in terms of time, since both mold and die must be heated and cooled during each cycle. In addition, the mold is usually expensive to fabricate and ordinarily has a short lifetime.

23.9 TAPE CASTING

An important ceramic fabrication technique, tape casting, will now be briefly discussed. As the name implies, thin sheets of a flexible tape are produced by means of a casting process. These sheets are prepared from slips, in many respects similar

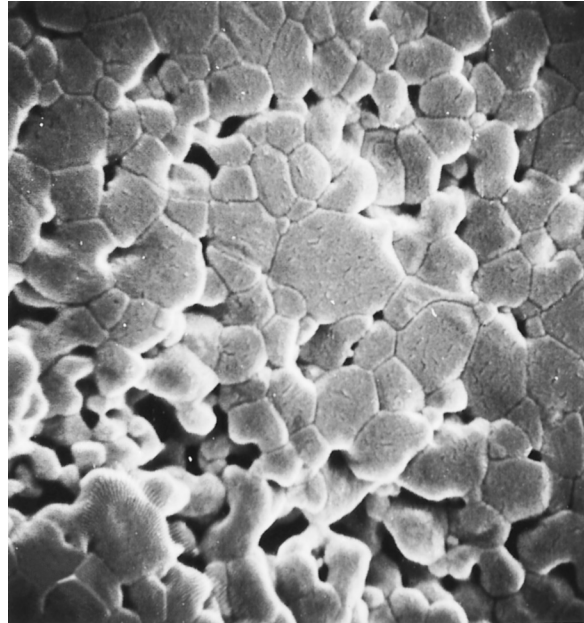


Figure 23.22 Scanning electron micrograph of an aluminum oxide powder compact that was sintered at 1700°C for 6 min. 5000 \times . (From W. D. Kingery, H. K. Bowen, and D. R. Uhlmann, *Introduction to Ceramics*, 2nd edition, p. 483. Copyright © 1976 by John Wiley & Sons, New York. Reprinted by permission of John Wiley & Sons, Inc.)

to those that are employed for slip casting (Section 23.7). This type of slip consists of a suspension of ceramic particles in an organic liquid that also contains binders and plasticizers that are incorporated to impart strength and flexibility to the cast tape. De-airing in a vacuum may also be necessary to remove any entrapped air or solvent vapor bubbles, which may act as crack-initiation sites in the finished piece. The actual tape is formed by pouring the slip onto a flat surface (of stainless steel, glass, a polymeric film, or paper); a doctor blade spreads the slip into a thin tape of uniform thickness, as shown schematically in Figure 23.23. In the drying process, volatile slip components are removed by evaporation; this green product is a flexible tape that may be cut or into which holes may be punched prior to a firing operation. Tape thicknesses normally range between 0.1 and 2 mm. Tape casting is widely used in the production of ceramic substrates that are used for integrated circuits and for multilayered capacitors.

Cementation is also considered to be a ceramic fabrication process (Figure 23.14). The cement material, when mixed with water, forms a paste that, after being fashioned into a desired shape, subsequently hardens as a result of complex chemical reactions. Cements and the cementation process were discussed briefly in Section 12.17.

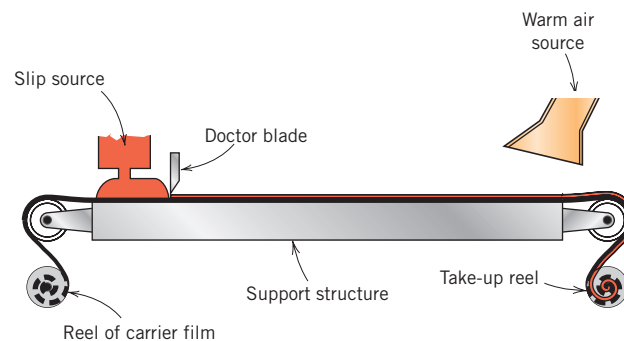


Figure 23.23 Schematic diagram showing the tape-casting process using a doctor blade. (From D. W. Richerson, *Modern Ceramic Engineering*, 2nd edition, Marcel Dekker, Inc., NY, 1992. Reprinted from *Modern Ceramic Engineering*, 2nd edition, p. 472 by courtesy of Marcel Dekker, Inc.)

Processing of Plastics

23.10 FORMING TECHNIQUES FOR PLASTICS

Quite a variety of different techniques are employed in the forming of polymeric materials. The method used for a specific polymer depends on several factors: (1) whether the material is thermoplastic or thermosetting; (2) if thermoplastic, the temperature at which it softens; (3) the atmospheric stability of the material being formed; and (4) the geometry and size of the finished product. There are numerous similarities between some of these techniques and those utilized for fabricating metals and ceramics.

Fabrication of polymeric materials normally occurs at elevated temperatures and often by the application of pressure. Thermoplastics are formed above their glass transition temperatures, if amorphous, or above their melting temperatures, if semicrystalline. An applied pressure must be maintained as the piece is cooled so that the formed article will retain its shape. One significant economic benefit of using thermoplastics is that they may be recycled; scrap thermoplastic pieces may be remelted and reformed into new shapes.

Fabrication of thermosetting polymers is ordinarily accomplished in two stages. First comes the preparation of a linear polymer (sometimes called a prepolymer) as a liquid, having a low molecular weight. This material is converted into the final hard and stiff product during the second stage, which is normally carried out in a mold having the desired shape. This second stage, termed “curing,” may occur during heating and/or by the addition of catalysts, and often under pressure. During curing, chemical and structural changes occur on a molecular level: a crosslinked or a network structure forms. After curing, thermoset polymers may be removed from a mold while still hot, since they are now dimensionally stable. Thermosets are difficult to recycle, do not melt, are usable at higher temperatures than thermoplastics, and are often more chemically inert.

Molding is the most common method for forming plastic polymers. The several molding techniques used include compression, transfer, blow, injection, and extrusion molding. For each, a finely pelletized or granulated plastic is forced, at an elevated temperature and by pressure, to flow into, fill, and assume the shape of a mold cavity.

Compression and Transfer Molding

For compression molding, the appropriate amounts of thoroughly mixed polymer and necessary additives are placed between male and female mold members, as illustrated in Figure 23.24. Both mold pieces are heated; however, only one is movable. The mold is closed, and heat and pressure are applied, causing the plastic to become viscous and flow to conform to the mold shape. Before molding, raw materials may be mixed and cold pressed into a disc, which is called a preform. Preheating of the preform reduces molding time and pressure, extends the die lifetime, and produces a more uniform finished piece. This molding technique lends itself to the fabrication of both thermoplastic and thermosetting polymers; however, its use with thermoplastics is more time-consuming and expensive than the more commonly used extrusion or injection molding techniques discussed below.

In transfer molding, a variation of compression molding, the solid ingredients are first melted in a heated transfer chamber. As the molten material is injected into the mold chamber, the pressure is distributed more uniformly over all surfaces. This process is used with thermosetting polymers and for pieces having complex geometries.

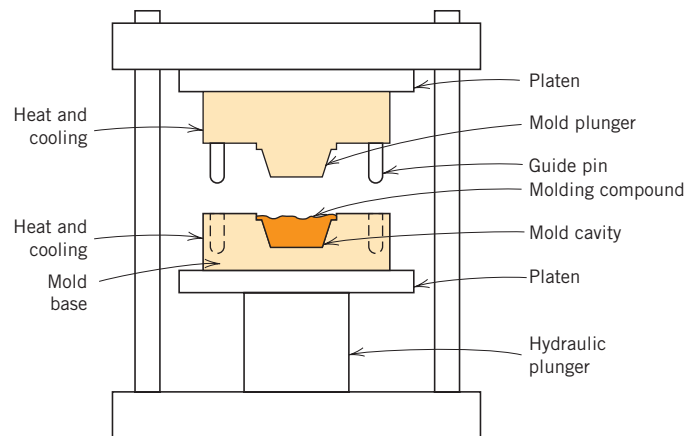


Figure 23.24 Schematic diagram of a compression molding apparatus. (From F. W. Billmeyer, Jr., *Textbook of Polymer Science*, 3rd edition. Copyright © 1984 by John Wiley & Sons, New York. Reprinted by permission of John Wiley & Sons, Inc.)

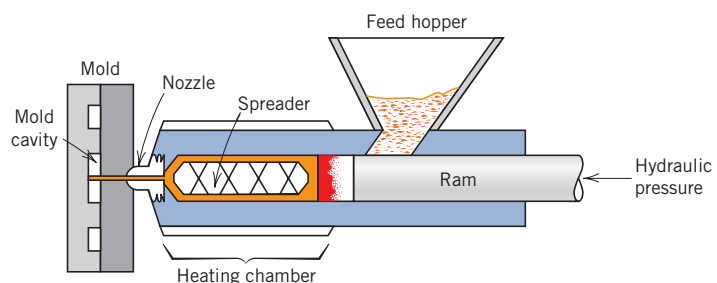
Injection Molding

Injection molding, the polymer analogue of die casting for metals, is the most widely used technique for fabricating thermoplastic materials. A schematic cross section of the apparatus used is illustrated in Figure 23.25. The correct amount of pelletized material is fed from a feed hopper into a cylinder by the motion of a plunger or ram. This charge is pushed forward into a heating chamber where it is forced around a spreader so as to make better contact with the heated wall. As a result, the thermoplastic material melts to form a viscous liquid. Next, the molten plastic is impelled, again by ram motion, through a nozzle into the enclosed mold cavity; pressure is maintained until the molding has solidified. Finally, the mold is opened, the piece is ejected, the mold is closed, and the entire cycle is repeated. Probably the most outstanding feature of this technique is the speed with which pieces may be produced. For thermoplastics, solidification of the injected charge is almost immediate; consequently, cycle times for this process are short (commonly within the range of 10 to 30 s). Thermosetting polymers may also be injection molded; curing takes place while the material is under pressure in a heated mold, which results in longer cycle times than for thermoplastics. This process is sometimes termed reaction injection molding (RIM) and is commonly used for materials such as polyurethane.

Extrusion

The extrusion process is the molding of a viscous thermoplastic under pressure through an open-ended die, similar to the extrusion of metals (Figure 23.2c). A mechanical screw or auger propels through a chamber the pelletized material, which is successively compacted, melted, and formed into a continuous charge of viscous

Figure 23.25 Schematic diagram of an injection molding apparatus. (Adapted from F. W. Billmeyer, Jr., *Textbook of Polymer Science*, 2nd edition. Copyright © 1971 by John Wiley & Sons, New York. Reprinted by permission of John Wiley & Sons, Inc.)



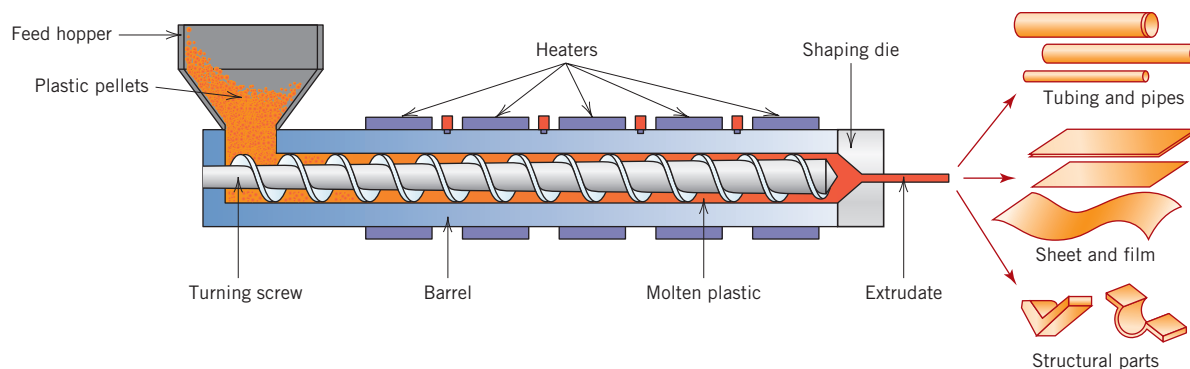


Figure 23.26 Schematic diagram of an extruder. (Reprinted with permission from *Encyclopædia Britannica*, © 1997 by Encyclopædia Britannica, Inc.)

fluid (Figure 23.26). Extrusion takes place as this molten mass is forced through a die orifice. Solidification of the extruded length is expedited by blowers, a water spray, or bath. The technique is especially adapted to producing continuous lengths having constant cross-sectional geometries—for example, rods, tubes, hose channels, sheets, and filaments.

Blow Molding

The blow-molding process for the fabrication of plastic containers is similar to that used for blowing glass bottles, as represented in Figure 23.15. First, a parison, or length of polymer tubing, is extruded. While still in a semimolten state, the parison is placed in a two-piece mold having the desired container configuration. The hollow piece is formed by blowing air or steam under pressure into the parison, forcing the tube walls to conform to the contours of the mold. Of course the temperature and viscosity of the parison must be carefully regulated.

Casting

Like metals, polymeric materials may be cast, as when a molten plastic material is poured into a mold and allowed to solidify. Both thermoplastic and thermosetting plastics may be cast. For thermoplastics, solidification occurs upon cooling from the molten state; however, for thermosets, hardening is a consequence of the actual polymerization or curing process, which is usually carried out at an elevated temperature.

23.11 FABRICATION OF ELASTOMERS

Techniques used in the actual fabrication of rubber parts are essentially the same as those discussed for plastics as described above—that is, compression molding, extrusion, and so on. Furthermore, most rubber materials are vulcanized (Section 14.9) and some are reinforced with carbon black (Section 15.2).

Concept Check 23.6

For a rubber component that, in its final form is to be vulcanized, should vulcanization be carried out prior to or subsequent to the forming operation? Why? *Hint:* you may want to consult Section 14.9.

[The answer may be found in enclosed CD.]

23.12 FABRICATION OF FIBERS AND FILMS

Fibers

The process by which fibers are formed from bulk polymer material is termed **spinning**. Most often, fibers are spun from the molten state in a process called melt spinning. The material to be spun is first heated until it forms a relatively viscous liquid. Next, it is pumped through a plate called a spinneret, which contains numerous small, typically round holes. As the molten material passes through each of these orifices, a single fiber is formed, which is rapidly solidified by cooling with air blowers or a water bath.

The crystallinity of a spun fiber will depend on its rate of cooling during spinning. The strength of fibers is improved by a postforming process called drawing, as discussed in Section 14.8. Again, drawing is simply the permanent mechanical elongation of a fiber in the direction of its axis. During this process the molecular chains become oriented in the direction of drawing (Figure 14.13*d*), such that the tensile strength, modulus of elasticity, and toughness are improved. The cross section of melt spun, drawn fibers is nearly circular, and the properties are uniform throughout the cross section.

Two other techniques that involve producing fibers from solutions of dissolved polymers are *dry spinning* and *wet spinning*. For dry spinning the polymer is dissolved in a volatile solvent. The polymer-solvent solution is then pumped through a spinneret into a heated zone; here the fibers solidify as the solvent evaporates. In wet spinning, the fibers are formed by passing a polymer-solvent solution through a spinneret directly into a second solvent that causes the polymer fiber to come out of (i.e., precipitate from) the solution. For both of these techniques, a skin first forms on the surface of the fiber. Subsequently, some shrinkage occurs such that the fiber shrivels up (like a raisin); this leads to a very irregular cross-section profile, which causes the fiber to become stiffer (i.e., increases the modulus of elasticity).

Films

Many films are simply extruded through a thin die slit; this may be followed by a rolling (calendering) or drawing operation that serves to reduce thickness and improve strength. Alternatively, film may be blown: continuous tubing is extruded through an annular die; then, by maintaining a carefully controlled positive gas pressure inside the tube and by drawing the film in the axial direction as it emerges from the die, the material expands around this trapped air bubble like a balloon (Figure 23.27). As a result the wall thickness is continuously reduced to produce a thin cylindrical film which can be sealed at the end to make garbage bags, or which may be cut and laid flat to make a film. This is termed a biaxial drawing process and produces films that are strong in both stretching directions. Some of the newer films are produced by coextrusion; that is, multilayers of more than one polymer type are extruded simultaneously.

Processing of Composites

23.13 PROCESSING OF FIBER-REINFORCED COMPOSITES

To fabricate continuous fiber-reinforced plastics that meet design specifications, the fibers should be uniformly distributed within the plastic matrix and, in most in-

23.13 Processing of Fiber-Reinforced Composites • 857

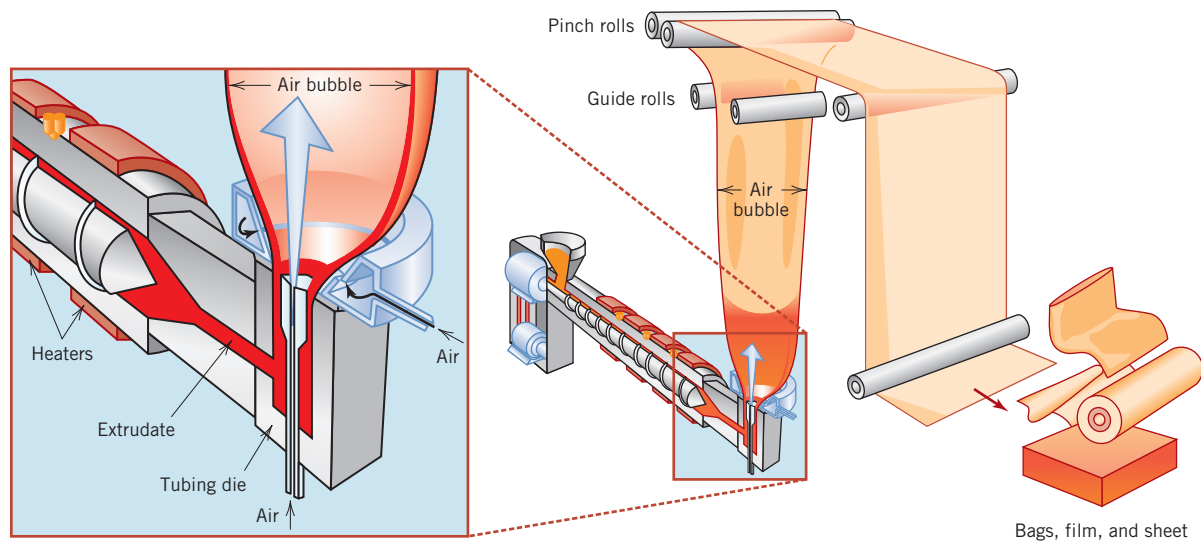


Figure 23.27 Schematic diagram of an apparatus that is used to form thin polymer films. (Reprinted with permission from *Encyclopædia Britannica*, © 1997 by Encyclopædia Britannica, Inc.)

stances, all oriented in virtually the same direction. In this section several techniques (pultrusion, filament winding, and prepreg production processes) by which useful products of these materials are manufactured will be discussed.

Pultrusion

Pultrusion is used for the manufacture of components having continuous lengths and a constant cross-sectional shape (i.e., rods, tubes, beams, etc.). With this technique, illustrated schematically in Figure 23.28, continuous fiber *rovings*, or *tows*,⁴ are first impregnated with a thermosetting resin; these are then pulled through a steel die that preforms to the desired shape and also establishes the resin/fiber ratio. The stock then passes through a curing die that is precision machined so as to impart the final shape; this die is also heated to initiate curing of the resin matrix. A pulling device draws the stock through the dies and also determines the production speed.

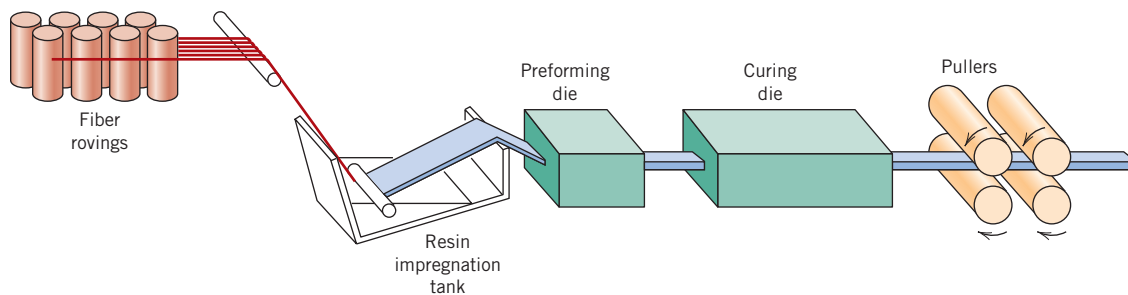


Figure 23.28 Schematic diagram showing the pultrusion process.

⁴ A roving, or tow, is a loose and untwisted bundle of continuous fibers that are drawn together as parallel strands.

Tubes and hollow sections are made possible by using center mandrels or inserted hollow cores. Principal reinforcements are glass, carbon, and aramid fibers, normally added in concentrations between 40 and 70 vol%. Commonly used matrix materials include polyesters, vinyl esters, and epoxy resins.

Pultrusion is a continuous process that is easily automated; production rates are relatively high, making it very cost effective. Furthermore, a wide variety of shapes are possible, and there is really no practical limit to the length of stock that may be manufactured.

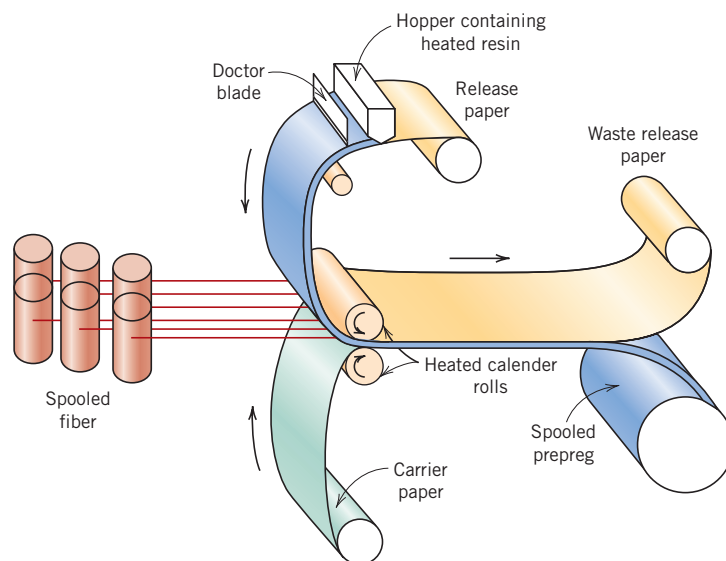
Prepreg Production Processes

Prepreg is the composite industry's term for continuous fiber reinforcement preimpregnated with a polymer resin that is only partially cured. This material is delivered in tape form to the manufacturer, who then directly molds and fully cures the product without having to add any resin. It is probably the composite material form most widely used for structural applications.

The prepregging process, represented schematically for thermoset polymers in Figure 23.29, begins by collimating a series of spool-wound continuous fiber tows. These tows are then sandwiched and pressed between sheets of release and carrier paper using heated rollers, a process termed “calendering.” The release paper sheet has been coated with a thin film of heated resin solution of relatively low viscosity so as to provide for its thorough impregnation of the fibers. A “doctor blade” spreads the resin into a film of uniform thickness and width. The final prepreg product—the thin tape consisting of continuous and aligned fibers embedded in a partially cured resin—is prepared for packaging by winding onto a cardboard core. As shown in Figure 23.29, the release paper sheet is removed as the impregnated tape is spooled. Typical tape thicknesses range between 0.08 and 0.25 mm, tape widths range between 25 and 1525 mm, whereas resin content usually lies between about 35 and 45 vol%.

At room temperature the thermoset matrix undergoes curing reactions; therefore, the prepreg is stored at 0°C or lower. Also, the time in use at room temperature (or “out-time”) must be minimized. If properly handled, thermoset prepregs have a lifetime of at least six months and usually longer.

Figure 23.29
Schematic diagram illustrating the production of prepreg tape using a thermoset polymer.



23.13 Processing of Fiber-Reinforced Composites • 859

Both thermoplastic and thermosetting resins are utilized; carbon, glass, and aramid fibers are the common reinforcements.

Actual fabrication begins with the “lay-up”—laying of the prepreg tape onto a tooled surface. Normally a number of plies are laid up (after removal from the carrier backing paper) to provide the desired thickness. The lay-up arrangement may be unidirectional, but more often the fiber orientation is alternated to produce a cross-ply or angle-ply laminate. Final curing is accomplished by the simultaneous application of heat and pressure.

The lay-up procedure may be carried out entirely by hand (hand lay-up), wherein the operator both cuts the lengths of tape and then positions them in the desired orientation on the tooled surface. Alternately, tape patterns may be machine cut, then hand laid. Fabrication costs can be further reduced by automation of prepreg lay-up and other manufacturing procedures (e.g., filament winding, as discussed below), which virtually eliminates the need for hand labor. These automated methods are essential for many applications of composite materials to be cost effective.

Filament Winding

Filament winding is a process by which continuous reinforcing fibers are accurately positioned in a predetermined pattern to form a hollow (usually cylindrical) shape. The fibers, either as individual strands or as tows, are first fed through a resin bath and then are continuously wound onto a mandrel, usually using automated winding equipment (Figure 23.30). After the appropriate number of layers have been applied, curing is carried out either in an oven or at room temperature, after which the mandrel is removed. As an alternative, narrow and thin prepregs (i.e., tow pregs) 10 mm or less in width may be filament wound.

Various winding patterns are possible (i.e., circumferential, helical, and polar) to give the desired mechanical characteristics. Filament-wound parts have very high strength-to-weight ratios. Also, a high degree of control over winding uniformity and orientation is afforded with this technique. Furthermore, when automated, the

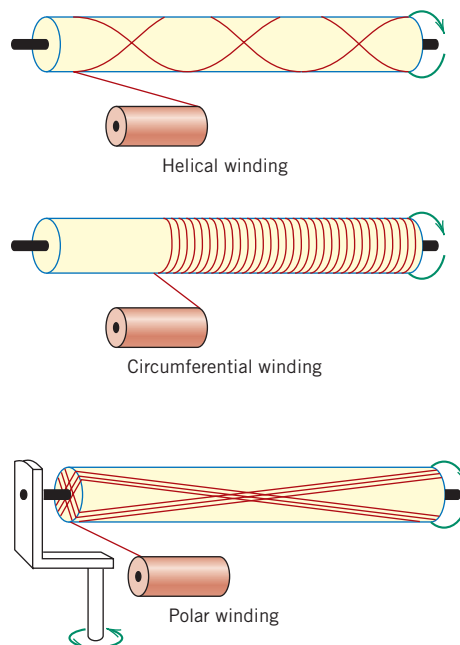


Figure 23.30 Schematic representations of helical, circumferential, and polar filament winding techniques. [From N. L. Hancox, (Editor), *Fibre Composite Hybrid Materials*, The Macmillan Company, New York, 1981.]

860 • Chapter 23 / Processing of Engineering Materials

process is most economically attractive. Common filament-wound structures include rocket motor casings, storage tanks and pipes, and pressure vessels.

Manufacturing techniques are now being used to produce a wide variety of structural shapes that are not necessarily limited to surfaces of revolution (e.g., I-beams). This technology is advancing very rapidly because it is very cost effective.

SUMMARY

Fabrication of Metals

Forming operations are those in which a metal piece is shaped by plastic deformation. When deformation is carried out above the recrystallization temperature, it is termed hot working; otherwise, it is cold working. Forging, rolling, extrusion, and drawing are four of the more common forming techniques. Depending on the properties and shape of the finished piece, casting may be the most desirable and economical fabrication process; sand, die, investment, lost foam, and continuous casting methods were also treated. Additional fabrication procedures, including powder metallurgy and welding, may be utilized alone or in combination with other methods.

Heat Treatment of Steels

For high-strength steels, the best combination of mechanical characteristics may be realized if a predominantly martensitic microstructure is developed over the entire cross section; this is converted to tempered martensite during a tempering heat treatment. Hardenability is a parameter used to ascertain the influence of composition on the susceptibility to the formation of a predominantly martensitic structure for some specific heat treatment. Determination of hardenability is accomplished by the standard Jominy end-quench test, from which hardenability curves are generated.

Other factors also influence the extent to which martensite will form. Of the common quenching media, water is the most efficient, followed by oil and air, in that order. The relationships between cooling rate and specimen size and geometry for a specific quenching medium frequently are expressed on empirical charts; two were introduced for cylindrical specimens. These may be used in conjunction with hardenability data to generate cross-sectional hardness profiles.

Glass Forming

Four of the more common glass-forming techniques—pressing, blowing, drawing, and fiber forming—were discussed briefly.

Fabrication and Processing of Clay Products

For clay products, two fabrication techniques that are frequently utilized are hydroplastic forming and slip casting. After forming, a body must be first dried and then fired at an elevated temperature to reduce porosity and enhance strength. Shrinkage that is excessive or too rapid may result in cracking and/or warping, and a worthless piece. Densification during firing is accomplished by vitrification, the formation of a glassy bonding phase.

Powder Pressing

Tape Casting

Some ceramic pieces are formed by powder compaction; uniaxial and isostatic techniques are possible. Densification of pressed pieces takes place by a sintering

mechanism during a high-temperature firing procedure. Hot pressing is also possible in which pressing and sintering operations are carried out simultaneously.

Thin ceramic substrate layers are often fabricated by tape casting.

Forming Techniques for Plastics

Fabrication of plastic polymers is usually accomplished by shaping the material in molten form at an elevated temperature, using at least one of several different molding techniques—compression, transfer, injection, and blow. Extrusion and casting are also possible.

Fabrication of Fibers and Films

Some fibers are spun from a viscous melt, after which they are plastically elongated during a drawing operation, which improves the mechanical strength. Films are formed by extrusion and blowing, or by calendering.

Processing of Fiber-Reinforced Composites

Several composite processing techniques have been developed that provide a uniform fiber distribution and a high degree of alignment. With pultrusion, components of continuous length and constant cross section are formed as resin-impregnated fiber tows are pulled through a die. Composites utilized for many structural applications are commonly prepared using a lay-up operation (either hand or automated), wherein prepreg tape plies are laid down on a tooled surface and are subsequently fully cured by the simultaneous application of heat and pressure. Some hollow structures may be fabricated using automated filament winding procedures, whereby resin-coated strands or tows or prepreg tape are continuously wound onto a mandrel, followed by a curing operation.

REFERENCES

- ASM Handbook*, Vol. 4, *Heat Treating*, ASM International, Materials Park, OH, 1991.
- ASM Handbook*, Vol. 6, *Welding, Brazing and Soldering*, ASM International, Materials Park, OH, 1993.
- ASM Handbook*, Vol. 14, *Forming and Forging*, ASM International, Materials Park, OH, 1988.
- ASM Handbook*, Vol. 15, *Casting*, ASM International, Materials Park, OH, 1988.
- ASM Handbook*, Vol. 21, *Composites*, ASM International, Materials Park, OH, 2001.
- Brooks, C. R., *Principles of the Heat Treatment of Plain Carbon and Low Alloy Steels*, ASM International, Materials Park, OH, 1995.
- Chawla, K. K., *Composite Materials Science and Engineering*, 2nd edition, Springer-Verlag, New York, 1998.
- Engineered Materials Handbook*, Vol. 2, *Engineering Plastics*, ASM International, Metals Park, OH, 1988.
- Engineered Materials Handbook*, Vol. 4, *Ceramics and Glasses*, ASM International, Materials Park, OH, 1991.
- Heat Treater's Guide: Standard Practices and Procedures for Irons and Steels*, 2nd edition, ASM International, Materials Park, OH, 1995.
- Kalpakjian, S. and S. R. Schmid, *Manufacturing Processes for Engineering Materials*, 4th edition, Pearson Education, Upper Saddle River, NJ, 2003.
- Krauss, G., *Steels: Heat Treatment and Processing Principles*, ASM International, Materials Park, OH, 1990.
- Mallick, P. K., *Fiber-Reinforced Composites, Materials, Manufacturing, and Design*, 2nd edition, Marcel Dekker, New York, 1993.
- McCrum, N. G., C. P. Buckley, and C. B. Bucknall, *Principles of Polymer Engineering*, 2nd edition, Oxford University Press, Oxford, 1997. Chapters 7–8.

862 • Chapter 23 / Processing of Engineering Materials

Muccio, E. A., *Plastic Part Technology*, ASM International, Materials Park, OH, 1991.

Muccio, E. A., *Plastics Processing Technology*, ASM International, Materials Park, OH, 1994.

Powell, P. C., and A. J. Housz, *Engineering with Polymers*, 2nd edition, Nelson Thornes, Cheltenham, UK, 1998.

Reed, J. S., *Principles of Ceramic Processing*, 2nd edition, Wiley, New York, 1995.

Richerson, D. W., *Modern Ceramic Engineering*, 2nd edition, Marcel Dekker, New York, 1992.

Strong, A. B., *Plastics: Materials and Processing*, 3rd edition, Prentice Hall PTR, Paramus, IL, 2006.

Tooley, F. V. (Editor), *Handbook of Glass Manufacture*, Ashlee, New York, 1985. In two volumes.

Upadhyaya, G.S. and A. Upadhyaya, *Materials Science and Engineering*, Viva Books, New Delhi, 2006.

QUESTIONS AND PROBLEMS

Forming Operations

- 23.1** Cite advantages and disadvantages of hot working and cold working.
- 23.2 (a)** Cite advantages of forming metals by extrusion as opposed to rolling. **(b)** Cite some disadvantages.

Casting

- 23.3** List four situations in which casting is the preferred fabrication technique.
- 23.4** Compare sand, die, investment, lost foam, and continuous casting techniques.

Miscellaneous Techniques

- 23.5** If it is assumed that, for steel alloys, the average cooling rate of the heat-affected zone in the vicinity of a weld is 10°C/s , compare the microstructures and associated properties that will result for 1080 (eutectoid) and 4340 alloys in their HAZs.
- 23.6** Describe one problem that might exist with a steel weld that was cooled very rapidly.

Heat Treatment of Steels

- 23.7** Briefly explain the difference between hardness and hardenability.
- 23.8** What influence does the presence of alloying elements (other than carbon) have on the shape of a hardenability curve? Briefly explain this effect.
- 23.9** How would you expect a decrease in the austenite grain size to affect the hardenability of a steel alloy? Why?
- 23.10** Name two thermal properties of a liquid medium that will influence its quenching effectiveness.

- 23.11** Construct radial hardness profiles for the following:

(a) A 75-mm diameter cylindrical specimen of an 8640 steel alloy that has been quenched in moderately agitated oil

(b) A 50-mm diameter cylindrical specimen of a 5140 steel alloy that has been quenched in moderately agitated oil

(c) A 90-mm diameter cylindrical specimen of an 8630 steel alloy that has been quenched in moderately agitated water

(d) A 100-mm diameter cylindrical specimen of an 8660 steel alloy that has been quenched in moderately agitated water

- 23.12** Compare the effectiveness of quenching in moderately agitated water and oil, by graphing on a single plot radial hardness profiles for 75-mm diameter cylindrical specimens of an 8640 steel that have been quenched in both media.

Fabrication and Processing of Clay Products

- 23.13** Cite the two desirable characteristics of clay minerals relative to fabrication processes.
- 23.14** From a molecular perspective, briefly explain the mechanism by which clay minerals become hydroplastic when water is added.
- 23.15 (a)** What are the three main components of a whiteware ceramic such as porcelain?
(b) What role does each component play in the forming and firing procedures?
- 23.16 (a)** Why is it so important to control the rate of drying of a ceramic body that has been hydroplastically formed or slip cast?
(b) Cite three factors that influence the rate of drying, and explain how each affects the rate.

- 23.17** Cite one reason why drying shrinkage is greater for slip cast or hydroplastic products that have smaller clay particles.
- 23.18 (a)** Name three factors that influence the degree to which vitrification occurs in clay-based ceramic wares.
- (b)** Explain how density, firing distortion, strength, corrosion resistance, and thermal conductivity are affected by the extent of vitrification.

Powder Pressing

- 23.19** Some ceramic materials are fabricated by hot isostatic pressing. Cite some of the limitations and difficulties associated with this technique.

Forming Techniques for Plastics

- 23.20** Cite four factors that determine what fabrication technique is used to form polymeric materials.

- 23.21** Contrast compression, injection, and transfer molding techniques that are used to form plastic materials.

Fabrication of Fibers and Films

- 23.22** Why must fiber materials that are melt spun and then drawn be thermoplastic? Cite two reasons.
- 23.23** Which of the following polyethylene thin films would have the better mechanical characteristics: (1) formed by blowing, or (2) formed by extrusion and then rolled? Why?

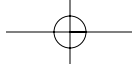
Processing of Fiber-Reinforced Composites

- 23.24** Briefly describe pultrusion, filament winding, and prepreg production fabrication processes; cite the advantages and disadvantages of each.

DESIGN PROBLEMS

Heat Treatment of Steels

- 23.D1** A cylindrical piece of steel 38 mm ($1\frac{1}{2}$ in.) in diameter is to be quenched in moderately agitated oil. Surface and center hardnesses must be at least 50 and 40 HRC, respectively. Which of the following alloys will satisfy these requirements: 1040, 5140, 4340, 4140, and 8640? Justify your choice(s).
- 23.D2** A cylindrical piece of steel 57 mm ($2\frac{1}{4}$ in.) in diameter is to be austenitized and quenched such that a minimum hardness of 45 HRC is to be produced throughout the entire piece. Of the alloys 8660, 8640, 8630, and 8620, which will qualify if the quenching medium is **(a)** moderately agitated water, and **(b)** moderately agitated oil? Justify your choice(s).
- 23.D3** A cylindrical piece of steel 44 mm ($1\frac{3}{4}$ in.) in diameter is to be austenitized and quenched such that a microstructure consisting of at least 50% martensite will be produced throughout the entire piece. Of the alloys 4340, 4140, 8640, 5140, and 1040, which will qualify if the quenching medium is **(a)** moderately agitated oil and **(b)** moderately agitated water? Justify your choice(s).
- 23.D4** A cylindrical piece of steel 50 mm (2 in.) in diameter is to be quenched in moderately agitated water. Surface and center hardnesses must be at least 50 and 40 HRC, respectively. Which of the following alloys will satisfy these requirements: 1040, 5140, 4340, 4140, 8620, 8630, 8640, and 8660? Justify your choice(s).
- 23.D5** A cylindrical piece of 4140 steel is to be austenitized and quenched in moderately agitated oil. If the microstructure is to consist of at least 80% martensite throughout the entire piece, what is the maximum allowable diameter? Justify your answer.
- 23.D6** A cylindrical piece of 8660 steel is to be austenitized and quenched in moderately agitated oil. If the hardness at the surface of the piece must be at least 58 HRC, what is the maximum allowable diameter? Justify your answer.

**864 • Chapter 23 / Processing of Engineering Materials**

23.D7 Is it possible to temper an oil-quenched 4140 steel cylindrical shaft 25 mm in diameter so as to give a minimum yield strength of 950 MPa and a minimum ductility of 17%EL? If so, specify a tempering temperature. If this is not possible, then explain why.

23.D8 Is it possible to temper an oil-quenched 4140 steel cylindrical shaft 50 mm in diameter so as to give a minimum tensile strength of 900 MPa and a minimum ductility of 20%EL? If so, specify a tempering temperature. If this is not possible, then explain why.

